

Molecular Mechanisms of Learning, Memory and Aging

Moleculaire mechanismen van leren, geheugen en
veroudering

Proefschrift

Ter verkrijging van de graad van doctor aan de
Erasmus Universiteit Rotterdam
op gezag van de
rector magnificus

prof. dr. H. G. Schmidt

en volgens besluit van het College voor Promoties.

De openbare verdediging zal plaatsvinden op

Woensdag 19 januari 2011 om 11:30 uur

door

Cornelis Herman Zuiderveen Borgesius

geboren te Ede



Promotiecommissie

Promotor: Prof. dr. Y. Elgersma

Overige leden: Prof. dr. J. G. G. Borst
Prof. dr. S. A. Kushner
Prof. dr. J. C. Verhaagen

Table of contents

Chapter 1	General introduction	10
1	What is aging?	11
1.1	An evolutionary view on aging	
1.2	A molecular view on aging	
1.2.1	Oxidative damage	
1.2.2	Repairing (oxidative) DNA damage	
1.2.3	Telomere shortening	
2	Aging of the brain	21
2.1	Age-related memory impairment	
2.1.1	Spatial memory	
2.1.2	Working memory	
2.1.3	Associative memory	
2.2	Age-related molecular and cellular changes	
2.2.1	Age-related changes in synaptic plasticity	
2.2.2	Cell morphology	
2.2.3	Transcription	
3	Aging of the peripheral nervous system	29
3.1	Age-related hearing loss	
3.2	Age-related vision loss	
4	Conclusion	30
5	Scope of this thesis	30
Chapter 2	Accelerated age-related cognitive decline caused by deficient DNA repair	53
	<i>Manuscript in preparation</i>	
Chapter 3	Age-related loss of hearing and vision in the DNA repair deficient <i>Ercc1</i>^{Δ/-} mouse	85
	<i>Manuscript in preparation</i>	
Chapter 4	Age-related motor neuron degeneration in DNA repair deficient <i>Ercc1</i> mice	111
	<i>Published in Acta Neuropathol. 2010 Jul; 120(4):461-475</i>	

Chapter 5	βCaMKII play a non-enzymatic role in hippocampal synaptic plasticity and learning by targeting αCaMKII to synapses	143
	<i>Under review</i>	
Chapter 6	Functional requirement of CA3 αCaMKII in long-term potentiation	165
	<i>Manuscript in preparation</i>	
Chapter 7	General discussion	179
Addendum		191
	Summary	193
	Samenvatting	195
	Publications	198
	Curriculum vitae	200
	Portfolio	202
	Dankwoord	204

Chapter 1

Introduction

Aging, or rather, how to avoid it, has intrigued mankind from the earliest times. It has been a quest comparable to the alchemists' search for a way to turn lead into gold. Just as the alchemists spawned chemistry the quest for the fountain of youth has led to a large body of research into aging. Among the many theories on the nature of aging the oxidative stress hypothesis is the most plausible one. This theory states that the lifelong accumulation of oxidative damage to biological macromolecules such as proteins, DNA and lipids is the mechanism underlying aging. Considering that DNA contains all the information needed to build and maintain a cell, it is surmised that (oxidative) damage to DNA is the predominant contributor to aging. In support of this idea are the accelerated segmental aging phenotypes of humans and mice with defects in DNA repair mechanisms [1-10].

The somatic cells of an organism can be divided into two classes, mitotic and post-mitotic cells. The way these cells age differs. Despite this difference in cellular aging they both contribute to organismal aging. In mitotic cells, approximately half of the macromolecules are renewed every time the cell divides. Moreover, in mitotic tissues defective cells can be eliminated. In these ways aging can be slowed down. However, during DNA replication, errors can be introduced and this would be expected to speed up aging. Regardless, post-mitotic cells are expected to be more vulnerable to oxidative stress. Elimination of defective cells is not an option in post-mitotic tissues and their DNA has got to last an entire lifetime.

The brain is particularly vulnerable to oxidative stress since its neurons are post-mitotic, it exhibits one of the highest oxygen metabolisms in the body, has abundant lipid content and a relative paucity of antioxidant levels compared to other organs [11-13]. Moreover, the brain is one of the most active organs at the transcriptional level [14]. Therefore, neurons may be especially prone to DNA lesions resulting from oxidative stress and accumulate unrepaired DNA lesions throughout life, which eventually may alter transcription, trigger DNA damage responses and ultimately cause neuronal degeneration. Some of the most common, but nonetheless devastating age-related impairments are associated with the nervous system, like cognitive decline, loss of vision and hearing.

Considering the ever-increasing life expectancy of the human population, a greater understanding of aging and age-related impairments is of great significance. Consequently, we wanted to investigate the role of DNA damage in aging of the nervous system. To be able to study age-related perturbations of the nervous system it is also necessary to understand the normal processes. One of the most devastating consequences

of aging is loss of memory, which at present we are unable to treat. A central molecule in learning and memory is the CaMKII protein. Therefore, we also examined the role of CaMKII in synaptic plasticity to better understand learning and memory. In the future this can help investigations into age-related cognitive decline.

1 What is aging?

What is aging? Aging is recognized instantly by all and seems to be an inevitable part of life. However, a good definition is presently lacking. A real definition of aging should be accompanied by quantifiable parameters. Preferably, it would also offer a mechanistic explanation of how the process of aging takes place. Furthermore, a distinction should be made between normal aging and age-related diseases. For example, in sporadic Alzheimer's disease (AD) age is the biggest risk factor. However, not everybody that grows old suffers from AD and therefore AD should not be considered as part of normal aging. Surprisingly, aging may not be an inevitable consequence of life. Prokaryotic organisms do not seem to age. So, why do we age at all? Theories on both proximate (mechanistic) and ultimate (evolutionary) causes of aging will be discussed. For now the definition of aging will be the random, passive deterioration of the ability to maintain homeostasis, thereby decreasing life expectancy with age.

1.1 An evolutionary view on aging

What possible use can it have to die from an evolutionary point of view? The whole notion of aging is a general decline of Darwinian fitness. So why has evolution not selected more efficiently against it? One of the most obvious arguments is that with most species in the wild individuals die of extrinsic factors long before they show signs of aging. However, even species that experience very little predatorial pressure, like turtles and naked mole rats, age. The general idea underlying evolutionary theories of aging is that the force of natural selection declines with age in natural populations that have overlapping generations [15]. The group of older individuals will become smaller and smaller and therefore their offspring as well. As a consequence the force of natural selection declines because of extrinsic mortality. There are two evolutionary models that incorporate this that explain aging, first the Mutation Accumulation theory and second the Antagonistic Pleiotropy theory.

The Mutation Accumulation theory states that late acting detrimental genes arising from de novo germ line mutations would hardly be selected against. Thus, these genes would rise to substantial frequencies within populations and thereby contribute to

aging [15, 16]. The Antagonistic Pleiotropy theory is based on the idea that some genes have pleiotropic, i.e. multiple, effects. If these genes are beneficial early in life and have adverse effects later on, when selection is weak, these would be very strongly selected for. Some types of pleiotropic genes that would fit into the Antagonistic Pleiotropy theory are worth mentioning on their own. This has resulted in a sub-theory that is called the Disposable Soma theory

The Disposable Soma theory is based on the fact that resources are limited and that allocating energy to one process means the organism cannot provide that energy to the other process. Two processes that are very important to Darwinian fitness and metabolically costly are reproduction and somatic maintenance. The tradeoff between these two will result in maintaining the body for as long as it takes to raise offspring, within the restraints of the life expectancy under pressure of extrinsic mortality [15, 16]. Unlike the Mutation Accumulation and the Antagonistic Pleiotropy theory, the Disposable Soma theory makes specific predictions about the biology of aging. (i) Aging is the result of the lifelong accumulation of molecular and cellular damage. This damage is not repaired because of limitations evolved into the repair mechanisms. (ii) The genes that control life span will be genes involved in somatic maintenance and repair functions. (iii) The molecular and cellular mechanisms underlying aging are stochastic. This would explain the complexity and great variability of the aging phenotype. (iv) It is likely that there are multiple kinds of damage underlying aging. Thus, there will be complex network of maintenance and repair functions [16]. In conclusion, the only theory on the ultimate cause for aging that can make predictions about the proximate causes for aging is the Disposable Soma theory.

1.2 A molecular view on aging

When looking for proximate causes of aging one has to turn to molecular biology and biochemistry. A complicating matter is that there are many different tissues and organs that all age in different ways and at different rates. One division that can be made between cells is between mitotic and post-mitotic cells. Mitotic cells are cells that continuously divide, such as epithelium cells. Post-mitotic cells are part of tissues that do not renew themselves and thus have to last for the duration of a lifetime, like neurons or skeletal muscle cells.

The Disposable Soma theory predicts that the proximate cause for aging will be a lifelong accumulation of molecular and cellular damage [15, 16]. The most influential targets for the damage accumulation will be macromolecules, i.e. DNA, proteins and

membrane lipids. This damage will not be repaired completely because of limitations evolved into the repair mechanisms. However, there are other suggested molecular causes for aging such as telomere shortening. DNA damage will likely contribute most to aging, as it does not have the same turnover rate as proteins and membrane lipids. Moreover, in post-mitotic cells, such as neurons, there is no turnover of DNA. Consequently, DNA repair mechanisms are the only processes counteracting the accumulation of damage to DNA in post-mitotic cells.

1.2.1 Oxidative damage

The oxidative stress hypothesis of aging states that the accumulation of macromolecular damage caused by Reactive Oxygen Species (ROS) causes the deterioration of cellular physiological function and thus aging [17-20]. The vast majority of cellular ROS can be traced back to the mitochondria [21]. This proximate cause of aging is in line with the Disposable Soma theory. The oxidative stress hypothesis also relates to the rate of living theory by Raymond Pearl from 1928 [22]. According to this theory the life span of an organism depends on two things, first the rate of energy consumption (metabolic rate), second, a genetically determined maximum amount of energy consumed during adult life (metabolic potential). The first support for this theory came from life span extension of poikilothermic organisms such as *Drosophila melanogaster* by cooling their environment [23]. Another way of expanding life span is caloric restriction, which has been shown to be effective in a wide range of species from yeast to Rhesus monkeys [24-27]. The life span extension effect of caloric restriction is most likely due to reduced oxidative stress and increased maintenance of macromolecules [18, 28-34].

The integrity of the genomic information is of course a critical factor in the ability to function normally and maintain homeostasis for the cell, and consequently for the whole organism. Eukaryotic cells have two genomes to maintain, the nuclear and the mitochondrial genome.

Approximately 90% of the ROS is produced by the mitochondria [21]. Therefore, damage to the mitochondrial genome, which is so close to this source of ROS, is suggested by some to play a pivotal role in aging. Unlike nuclear DNA (nDNA) mitochondrial DNA (mtDNA) is not protected by histones and DNA binding proteins [35]. Consistently, the mutation rate of mtDNA is about 5 times that of nDNA [36]. Furthermore, the information density of mtDNA is much higher than that of nDNA [35]. Therefore, there is an increased chance that a mutation has deleterious consequences.

Although they are not part of the progeria syndromes, human syndromes caused by reduced mtDNA repair show a few aging phenotypes such as hearing loss, sarcopenia and neurodegeneration [37-40]. Two knock-in mouse mutants have been created that expresses a proofreading deficient version of Pol- γ -A, the nucleus encoded catalytic subunit of mtDNA polymerase [41, 42], thereby disabling the DNA repair mechanism base excision repair (BER) specifically in the mitochondria. BER is the only DNA repair pathway that is certain to be present in mitochondria [43]. This leads to an increase in point mutations and deletions of mtDNA and some age-related phenotypes, although these seem to be mostly related to tissues with rapid cellular turnover and overlap with phenotypes seen in nDNA repair deficient mice [42, 44].

A much stronger case can be made for the role of nDNA damage in aging. There is a strong correlation between age and amount of nDNA damage [29, 45-49] and in contrast to the several thousands of mitochondrial genomes the nuclear genome is merely diploid [6]. Therefore, the chance of a mutation in nDNA hindering cellular function is bigger. Furthermore, all accelerated aging syndromes are caused by mutations in genes involved in nuclear genome maintenance; the severity of the phenotype is related to the level of remaining nDNA repair capacity, and the more severe syndromes show a more extended overlap with the natural aging phenotype than the mtDNA repair defects [1, 50-54]. Moreover, there is also a correlation between level of nDNA repair activity and life span when species are compared [55-57]. Even the experimental enhancement or reduction of nDNA repair can increase or shorten the life span of *Drosophila melanogaster* [58]. Finally, the fact that numerous DNA repair mechanisms in the nucleus have evolved while there is only one in the mitochondria suggests that nDNA integrity is more important (see paragraph 1.2.2).

Not only (ribo)nucleotides incorporated in DNA or RNA strands can be damaged. The deoxyribonucleotide triphosphate (dNTP) pool can also be subject to ROS induced damage [59-64]. Moreover, owing to their location and that they are single nucleotides, as opposed to single or double strands, the dNTP pool is more susceptible to oxidative damage than DNA or RNA [62]. Furthermore, the oxidized dNTP pool is an importance source of 8-oxoG in DNA and RNA and greatly contributes to transcriptional and translational errors and mutagenesis in Mis Match Repair (MMR) deficient cells [60, 61, 63, 64]. What is more, accumulation of 8-oxoG in cytosolic RNA from or in the dNTP pool has been observed in age-related neurodegenerative diseases such as Alzheimer's and Parkinson's disease [64].

In mammals, enzymatic hydrolysis of 8-oxodGTP by MTH1, the mammalian

homologue of MutT of the bacteria *Escherichia coli* has been shown [62]. MTH1 is also present in humans [59, 61-63]. Furthermore, it is capable of hydrolyzing nucleosides, not only 8-oxodGTP but also 8-oxodATP and 2-hydroxy(-OH)dATP to their respective dNMTPs and PPi [62-64]. Moreover, it also hydrolyses the ribonucleotides 2-OH-ATP, 8-oxoATP and 8-oxoGTP [64]. MTH1 is mostly located in the cytoplasm [64]. There are no known human deficiencies of MTH1. However increased expression of MTH1 and accumulation of 8-oxo-ribonucleotides and -nucleosides have been observed in Alzheimer's and Parkinson's disease [64].

Accumulation of oxidative damage to macromolecules other than DNA such as lipids, proteins and RNA is also suggested to play a role in aging. However, this implies that there is either an age-related increase in ROS production, reduction of antioxidant mechanisms or increased half-life of these potential targets. The possibility of degrading and replacing an affected molecule besides the continuous turnover is in sharp contrast to the necessity of restoring damaged nDNA, which has no turnover. Even though deficiencies in lipid, protein or RNA metabolism can have severe consequences, they do not result in accelerated aging syndromes. Nevertheless, oxidative damage to these targets could contribute to aging.

Oxidative damage to RNA has not been studied as much as damage to DNA, most likely because these modifications are not passed on during mitosis and thus not mutagenic. However, although mRNA does not have to maintain the genetic information for as long as DNA, the information it does contain is needed at that moment and the information density is at its highest. Consequently, any damage to mRNA will have an immediate impact on cellular function. Furthermore, mRNA is single stranded and located in the cytosol unprotected by a nuclear envelope or histones, making it more vulnerable to ROS insults. In addition, damage to tRNA and rRNA could lead to dysfunctional protein synthesis [65]. However, RNA is less susceptible to oxidative damage than DNA owing to its 2'-hydroxyl group [66]. Despite this there are some studies that implicate oxidative RNA damage in age-related neurodegenerative disease in humans and age-related memory loss in rats [67-69]. Moreover, there is more oxidatively damaged RNA than DNA in Alzheimers' disease and in memory impaired aged rats [67, 69]. Turnover of mRNA is the most obvious way to counteract oxidative damage. Another, recently discovered way is direct reversal repair, although this does not repair oxidative damage.

Intracellular proteins have been suggested to play a key role in the age-related decline of physiological functions because oxidized proteins often lose their catalytic

function and undergo selective degradation [18, 70]. Oxidative damage to proteins can have secondary consequences, for example, inactivation of DNA repair enzymes, loss of fidelity of DNA polymerases in DNA replication and development of new antigens provoking autoimmune responses [71]. If the damaged protein is a mitochondrial protein involved in the respiratory chain, it could lead to an increased ROS production. An increased ROS production is indeed seen in aging organisms ranging from mammals to insects [35]. Moreover, older animals are more susceptible to oxidative damage [72].

Among cellular macromolecules, polyunsaturated fatty acids exhibit the highest sensitivity to ROS-induced damage. Their sensitivity to oxidation exponentially increases as a function of the number of double bonds per fatty acid molecule [73-75]. Furthermore, it has been shown that longer-lived species have a lower number of double bonds in the mitochondrial phospholipids of their livers [75] and that lipid peroxidation contributes to age-related membrane rigidity [76]. Moreover, lipid peroxidation products have been shown to increase in aging animals [12, 77]. Taken together, these results suggest that oxidative damage to phospholipids could contribute to aging.

All fatty acids are possible targets for ROS. However, under normal circumstances there are not many free fatty acids in the cell. Thus, membrane phospholipids are the predominant target, especially the membrane lipids of the mitochondria owing to their location that exposes them most frequently to ROS. The polyunsaturated fatty acids react with a hydroxyl radical generated by the Fenton reaction to lipid hydroperoxides. These are then reduced by peroxidases to corresponding hydroxy acid. These lipid radicals can participate in long free radical chain reactions in an autocatalytic way [75, 77, 78]. The only mechanisms to stop these autocatalytic chain reactions without detrimental consequences are antioxidants. The chain reaction can also be stopped by an adduction reaction with another molecule like DNA or a protein.

The reactive products of lipid peroxidation can cause oxidative damage to other macromolecules and membrane function deteriorates as a consequence of oxidized lipids. This secondary damage can be even more important for aging than the damage to the lipids themselves. Mitochondrial DNA (mtDNA) is at higher risk than nuclear DNA considering their proximity to membrane lipids. Accordingly, proteins in the membrane such as receptors, ion channels, ion pumps and mitochondrial proteins from the electron transport chain are most at risk. This means that the brain with its high metabolism and high numbers of receptors, ion channels and pumps would be very vulnerable [79]. The use of ROS in signal cascades and the use of lipid second messengers might further enhance the risk.

Yet another secondary effect of lipid peroxidation is the change in membrane characteristics. This will in general be deleterious for cellular functioning. In particular damage to mitochondrial membranes will have serious consequences. It will either result in more ROS production or in an enlarged proton leak and thus a less efficient ATP production [77]. Lipid turnover is the only means to restore membrane characteristics to normal.

1.2.2 Repairing (oxidative) DNA damage

The importance of nuclear genome integrity is highlighted by the numerous nDNA repair systems that have evolved. As mentioned before, deficiency of nDNA repair may cause accelerated segmental aging. There are at least 7 repair mechanisms in the nucleus, some of which have subdivisions. These are (i) nucleotide excision repair (NER), (ii) base excision repair (BER), (iii) homologous recombination (HR), (iv) non-homologous end joining (NHEJ), (v) mismatch repair (MMR), (vi) direct reversal or reversion repair and (vii) interstrand crosslink repair (ICL) [43, 80-83]. The most important repair pathway in ROS induced damage is BER [30, 43, 84-87]. However, all other DNA repair pathways also remove damage induced directly or indirectly by ROS.

Direct damage by ROS may be in the form of base modifications, abasic sites and various other types of lesions [43, 88]. However, direct ROS inflicted damage *in vivo* seems to be limited to abasic sites, base modifications and single strand breaks that can be turned into double strand breaks during DNA replication [82], while over a hundred oxidative modifications have been identified in DNA [82]. These include secondary damage by lipid peroxidation products or through reactions with reducing sugars. It is beyond the scope of this thesis to list all ROS derived types of DNA damage. The most common base modification is 8-oxoguanine (8-oxoG) [35, 43, 88]. This base modification is commonly used as a marker for oxidative damage to DNA.

NER mostly removes helix-distorting, bulky adducts, although it can also remove the same base modifications as BER [82, 89]. It is the most flexible DNA repair pathway, since it is able to remove a wide range of unrelated DNA lesions [89]. The oxidative lesions it repairs are probably the secondary oxidative damage such as the lipid peroxidation adducts and the 10% of the BER substrates that is not repaired by BER [43]. Moreover, the three most well known syndromes caused by NER deficiencies, Cockayne syndrome, xeroderma pigmentosum (XP) and trichothiodystrophy (TTD) display (segmental) accelerated aging [1, 10, 82, 90-92], thereby implying a causal role for nDNA damage in aging. Furthermore, in these syndromes neurodegeneration is one

of the features [1, 10, 54, 82, 89, 90], thus implicating nDNA damage in aging in general and aging of the brain specifically.

NER comprises two distinct pathways: Global Genome NER (GG-NER) and Transcription Coupled NER (TC-NER) [81, 82, 89]. The two pathways are mechanistically essentially the same, except for the initial damage recognition [89]. In GG-NER this is performed by XPC/HHR23B [81, 82, 89]. Other damage recognition factors are the RPA-XPA complex and the two polypeptides DDB1 and DDB2 that belong to the XPE complementation group [81]. There is some debate as to the order in which the XPC/HHR23B and RPA-XPA complex are recruited to DNA lesions and thus to their role in recognition or other processes in NER. In TC-NER damaged DNA is recognized by stalling of RNA polymerase II (RNAPII) [81, 82, 89]. Therefore, TC-NER seems to be capable of repairing every lesion that stalls RNAPII. However, TC-NER is limited to the transcribed strand of active genes. After damage recognition the multi-subunit complex TFIIH is recruited to the lesion, this unwinds and excises the DNA lesion [81, 82, 89]. The unwinding is done by XPB and XPD [81, 89]. The excision at the 5' site is done by XPF-ERCC1; at the 3' site this is done by XPG. The excised strand is around 30 nucleotides long [81, 82, 89]. The DNA gap is filled by Pol- δ and Pol- ϵ and the nick is sealed by DNA ligase I [81, 82, 89].

The BER pathway deals with small, non helix-distorting, chemical modifications of bases mostly originating from endogenous origin, e.g. ROS induced damage [82, 87]. In general, BER is initiated by the action of a glycosylase, which cleaves the glycosidic bond between the damaged base and its sugar [43, 82, 88]. These glycosylases are fairly specific each dealing with a narrow, partially overlapping class of lesions. The abasic site (AP site) is cleaved by AP endonuclease (APE1), creating a 3'-OH and 5'-deoxyribose phosphate groups on either site of the lesion, i.e. a single strand break [43, 82, 88]. DNA polymerase- γ (Pol- γ) catalyses the β -elimination of the 5'-terminal baseless sugar residue and fills the nucleotide gap [43, 82]. In mitochondria Pol- γ is the only known polymerase [41, 42, 88]. In nuclear BER this step is carried out by Pol- β [43, 82]. The nick is sealed by DNA ligase III. This scenario represents the short-patch repair mode. The long-patch mode, which does not exist in mitochondria, involves different DNA-polymerases, i.e. Pol- δ and Pol- ϵ , flap endonuclease (FEN-1) and DNA ligase I.

Double strand breaks are caused by a number of agents like replication of a single strand break, ROS or ionizing radiation [6, 82]. Ionizing radiation causes these distortions by generating a trail of ROS along its route as it travels through our body [6]. However ROS are not the only source of single strand breaks and double strand breaks.

Therefore, it is hard to say to what extent double strand break repair contributes to the elimination of oxidative damage. Since one of the two ways in which double strand breaks are repaired is the only DNA repair mechanism in which genetic information is often lost, even repaired double strand breaks could contribute to aging [6].

Double strand breaks are repaired by either homologous recombination (HR) or non-homologous end joining (NHEJ) [6, 81, 82]. HR is almost only possible during the late S and G2 phase of cell replication since only then the DNA content is 4N and sister chromosomes are aligned. Thus this repair mechanism of double strand breaks is limited to mitotic tissue and within that tissue only to certain time points. However, contrary to NHEJ, HR is error free owing to the presence of the template [6, 82]. NHEJ is not limited to a certain stage in the cell cycle and can therefore be used in post-mitotic tissues. However, NHEJ often fails to restore the full information content of the genome [6, 81, 82]. Typically at least one nucleotide, and often up to 10-20 nucleotides, is lost [6]. Because of this information loss and the fact that NHEJ is the major pathway for double strand break repair it is particularly interesting in the context of aging. The NER protein complex XPF-ERCC1 complex is also involved in double strand break repair [80].

MMR removes mispaired nucleotides and insertion/deletion loops ranging from 1 to 10 or more bases that result from slippage during replication of repetitive sequences or during recombination [82]. Moreover, MMR also removes bases that are mismatched as a consequence of spontaneous and induced base deamination, methylation and oxidation [81]. Furthermore MMR removes various chemically induced DNA lesions, among other things the major ROS induced base modification 8-oxoG [81]. However, MMR deficiency is not associated with accelerated aging syndromes but with hereditary nonpolyposis colorectal cancer [81].

Direct reversal repair is performed by single proteins that do not remove the modified base but the modification of that base [81, 82, 93, 94]. This repair mechanism reverses damage inflicted by alkylating agents [81, 82, 93, 94]. These agents form adducts at all O- and N-atoms in nucleobases [94]. The methyl adduct to the O⁶ position of Guanine (O⁶-meG) is probably the principal mutagenic lesion formed by alkylating agents [94]. O⁶-meG causes damage by mispairing with thymine during replication causing G:C → A:T transitions [93]. The main component of the direct repair family are the alkyltransferase proteins, which remove alkyl groups from the O⁶ position from guanine and to a lesser extent from the O⁴ position from thymine [93].

Interstrand crosslinks are covalent links between the two strands of DNA, as these block replication and transcription they are arguably the most cytotoxic lesions.

Endogenous lipid peroxidation products like malondialdehyde can lead to crosslinks [95-98]. The ICL repair pathway is well understood in *Escherichia coli* and *Saccharomyces cerevisiae* but not completely in mammalian cells. Most likely the repair involves passing through a double strand break phase. It is certain that the NER protein complex XPF-ERCC1 is intimately involved [80, 99-101].

1.2.3 Telomere shortening

One of the first molecular processes recognized to be involved in cellular aging is telomere shortening. Telomeres are the terminal part of eukaryotic chromosomes. They consist of simple repeats that do not code for protein and form complexes with a number of proteins. Their function is to protect the genetic integrity of the chromosome by preventing end-to-end fusion of chromosomes. Normal polymerases cannot replicate telomeres completely. Therefore, the integrity of the telomeres depends on the activity of the telomerase enzyme. Telomerase is normally only present in germline cells and not in somatic cells. Consequently, with each cell division in somatic cells part of the telomeres is lost. Obviously, this cellular aging mechanism is unique to mitotic cells. In post-mitotic cells, such as neurons, telomeres do not shorten as a result of cell division. When cells are cultured they fail to divide after a fixed number of replications. This is called replicative senescence. This state is characterized by irreversible growth inhibition, mostly in G₁, changes in cell morphology, a change in gene-expression and an upregulation of p53 or p21 activity [102]. Presumably, this is due to the fact that the telomeres are shortened to a minimal, threshold length. In this way telomeres would constitute a mitotic clock. However, not only cellular replication shortens the telomere length. Oxidative stress is also a major regulator [102]. Moreover, oxidative damage to the telomere sequence hinders binding of two proteins, telomere repeat binding factors (TRF) 1 and 2, which are crucial to telomere function. Therefore, the telomere system seems to keep track of the amount of damage to and the number of cell divisions of somatic cells and in that way preventing cancer and other deleterious consequences of genomic damage. In humans telomere shortening could explain the age-related decline in divisional capacity seen in many somatic tissues [16].

1.3 Conclusion

In conclusion, one of the most plausible theories on aging, with solid theoretical and experimental basis is the theory of damage accumulation in macromolecules; more specifically, the accumulation of damage induced by ROS. Of the four targets, protein,

lipids, DNA and RNA, DNA seems to be the most influential. Nevertheless, naturally occurring or engineered deficiencies in DNA repair mechanisms only cause segmental aging, suggesting that not all aspects of aging are caused by DNA damage. Moreover, different phenotypes arise when different kinds of lesions accumulate within nDNA, as can be concluded from the progeroid syndromes and their mouse models.

Another conclusion that might be drawn is that the brain, or rather the central nervous system, is especially sensitive to aging caused by ROS. There are a number of arguments that make it tempting to surmise this. Firstly, neurodegeneration is a prominent feature of progeroid syndromes and normal aging. In humans aging is accompanied by cognitive decline and often by neurodegenerative diseases like Parkinson and Alzheimer's disease (AD). Strictly speaking these latter are diseases and therefore not part of normal aging. However, both diseases have been linked to oxidative stress and for AD age is the biggest risk factor. Secondly, the brain is likely to be extra susceptible to ROS induced damage, because of a number of reasons: (i) the brain has a very high glucose metabolism, (ii) almost all neurons are post-mitotic, (iii) it has very low antioxidant levels, (iv) the brain has the second highest lipid content of all tissues and its function greatly depends on membrane function and finally (v) it uses ROS as secondary messengers [11-13, 103]. Furthermore, as the brain is one of the most transcriptionally active organs DNA damage hindering transcription is expected to be especially harmful in the brain [14].

2 Aging of the Brain

What actually constitutes brain aging? This question can and should be answered at multiple levels, ranging from the behavioral through electrophysiological, cellular to the molecular level. An important aspect of the brain that is compromised during aging is plasticity. Declining plasticity is a well-known feature of aging in humans and results in progressive difficulty in storing new memories. More specifically, spatial and declarative memory as stored in the hippocampus is affected in aging. In this thesis age-related decline of learning and memory will be used both as a definition and as a measure of brain aging, although other aspects of the aging nervous system will also be discussed. Consequently, most of the data discussed will be on the hippocampus and its function as this brain structure is important in declarative learning and memory.

2.1 Age-related memory impairment

There is an impressive amount of data that shows age-related memory impairment takes

place. This decline during normal aging is seen in humans and other mammals [79, 104-106]. Most of the data is gathered using rats or mice in hippocampus-dependent learning and memory tasks. In this paragraph a number of these tasks and their results will be discussed.

2.1.1 Spatial memory

Spatial memory is impaired in aged mice, rats, primates and humans [106-117]. The Morris water maze is a hippocampus-dependent spatial memory task where an animal, mouse or rat, is trained to find an invisible, submerged platform in a circular pool of opaque water by using distal, visual cues. During testing the movement of the animal is continuously and automatically monitored and a number of parameters such as path length, latency time and swim speed are determined. Several laboratories have repeatedly found that aged animals perform worse than young or adult animals on this test of spatial memory [67, 106, 112-115, 117-122].

Similar results are obtained with the Barnes circular platform task. In this task a rat or mouse has to remember which of the ± 18 holes on the perimeter of a brightly lit circular platform leads to a dark escape room. Rodents have a natural preference for darkness. The Barnes maze task is very similar to Morris water maze, although not identical. Consistently, aged rats and mice perform worse on this test of spatial memory [106, 113, 123, 124]. Moreover, when animals from the same cohort were tested to compare the two tasks similar age-related impairments were revealed [125]. Importantly, when humans are tested on a virtual water maze task they show a comparable age-related impairment [126, 127].

2.1.2 Working memory

Working memory is dependent on short-term memory. Some forms of this memory depend on the hippocampus and are also impaired in aging. Both working memory and spatial memory can be tested on the radial arm water maze. This test is an adaptation of the Morris water maze. In short, the animal has to learn the location of a submerged platform that is located in one of the ± 12 arms. The test is set up in such a way that it depends on spatial (short-term) memory, i.e. the animal has to use distal visual cues. The first entry in a wrong arm is counted as a spatial memory error. Reentries in previously visited arms count as working memory errors. A similar but dry alternative is the radial arm maze. In this test four out of eight arms are baited with a food reward. After training the food is not replaced and the animals are allowed to search for food again. The animals

are tested relatively shortly after training. This task only tests working memory.

Aged rats and mice show significant working memory impairment, but intact reference memory in these tests [117, 126-133]. The fact that the reference memory is still intact might seem to contradict the findings in the Morris water maze. However, it has been shown that the Morris water maze is harder to solve than a water maze with a limited number of choices such as the radial arm water maze [134].

The novel object recognition task is based upon the tendency of an animal to exhibit more exploratory behavior towards a novel object. Therefore, an animal is first exposed to two objects for several minutes after being habituated to the environment of the test-cage and returned to its home-cage. After a certain time interval the animal is put back in the test-cage with one old and one novel object. Usually, the time interval is up to one hour for testing working memory and 24 hours for reference memory. An animal is expected to explore the unknown object more. Hence, equal time spent exploring both objects is interpreted as memory failure. On this task aged rats showed significantly impaired working memory performance [121, 135-137]. However, the 24-hour memory is often found to be intact in mice and rats [138-140].

In the one-way inhibitory avoidance task the animal is learned to avoid an environment that has its natural preference. The animal is placed in an alley that is divided into an illuminated safe compartment and a dark compartment that is normally preferred. A shock generator is connected to the floor of the dark compartment. In training the animal is placed in the illuminated part. The door of the dark compartment is closed when the animal walks in and a shock is applied. Subsequently, the animal is returned to its home cage. After three hours a retention test is given. The animal is again placed in the apparatus in the illuminated side and the latency time for entering the dark compartment is taken as a measurement of retention. Again aged rats and mice show impaired performance [135, 141-146].

2.1.3 Associative memory

Associative memory refers to the ability to connect two related phenomena. It is a prerequisite for classical conditioning. Associative memory declines with age in humans [147-153]. Associative memory in rodents is usually tested by fear conditioning in which animals are trained to associate a fearful experience to a neutral stimulus. When the neutral stimulus is a multimodal stimulus, like the context of the test cage, performance on the task depends on the hippocampus and amygdala. This is referred to as contextual fear conditioning. When the neutral stimulus is a unimodal stimulus, like a tone, the task

is referred to as cued conditioning. This task does not depend on the hippocampus, only on the amygdala.

In general, age-related impairments have been found using hippocampus dependent fear conditioning tasks [133, 141, 154-157], not when hippocampus independent fear conditioning was tested [154]. Finally a study testing associative learning in rats with two neutral stimuli, like in the human studies, also found an age-related impairment [158]. In conclusion, all but a few studies found age-related impairments of hippocampus-dependent memory in humans, rats, mice and other mammals in wide variety of tests.

2.2 Age-related molecular en cellular changes

Now that we have established that aging results in impaired brain function at the systems level as discussed in the preceding paragraph, the next question arises. What are the electrophysiological, molecular and cellular changes underlying the age-related decline of hippocampus-dependent memory function?

2.2.1 Age-related changes in synaptic plasticity

The putative cellular substrate for hippocampal learning and memory is synaptic plasticity. An activity dependent increase in synaptic efficacy is called long-term potentiation (LTP). Long-term reduction of synaptic transmission is called long-term depression (LTD). Ca^{2+} /calmodulin-dependent kinase II (CaMKII) is pivotal in both LTP and learning. Its activation is both necessary and sufficient for LTP [159], and LTP and learning can be impaired and even abolished by introducing different genetic mutations in knockin mice [160-163]. The early phase of LTP (E-LTP) is protein kinase dependent and lasts for 3-6 hours. The late phase of LTP (L-LTP) is dependent on transcription and translation [164]. Both LTP and its counterpart LTD show age-related changes.

Age-related LTP impairment is not always found when LTP is induced using high-intensity stimulation protocols. However, when non-saturating protocols are used with less intense or fewer stimuli, aged rats do show LTP deficits in Schaffer-collateral LTP (see review [105]). Moreover, in the first hour, i.e. E-LTP, there is often no defect in aged rats [105, 106, 165]. In a number of studies these experimentally evoked phenomena have been correlated with the age-related decline in performance on the aforementioned behavioral memory tasks. Defects in L-LTP have been correlated to poorer performance on the one-way inhibitory avoidance learning task in aged rats [142]. Such a correlation between behavior and L-LTP was also seen in mice [115].

Although L-LTP is generally considered to be affected most by aging, deficits in E-LTP have also been found [154, 166-173]. Moreover, the E-LTP impairment was correlated to impaired trace fear conditioning [154]. Not only is LTP negatively affected by aging, the opposite process LTD is enhanced [118, 122, 174, 175].

What could be the age-related changes underlying the age-related LTP deficits? At the cellular level there are a number of electrophysiological properties capable of influencing plasticity that are in general not changed during aging: (i) resting membrane potential, (ii) input resistance, (iii) amplitude and duration of Na⁺ mediated action potentials (APs), (iv) amplitude of Ca²⁺ mediated APs, (v) firing rates in awake and asleep animals, (vi) EPSP rise time and width and (vii) membrane time constant (see review [105]).

One of the most noticeable changes in Ca²⁺ regulation with a possible connection to synaptic plasticity is the increase of L-VDCC Ca²⁺ currents with age [105, 128, 176-181]. Consistently, with aging the Ca²⁺ influx through voltage dependent calcium channels (VDCCs) of the L-type is increased compared to the NMDA receptor mediated influx during LTP induction [128, 179-181], which likely stems from the age-related increased expression of L-VDCCs [128, 179, 182, 183]. The concomitant increase of CaN could also enlarge the current through the L-VDCCs [184, 185]. Increased L-VDCC currents have been linked to impaired memory performance [105, 176-178].

Another consequence of the increased L-VDCC Ca²⁺ influx is a prolonged afterhyperpolarisation (AHP) [180, 186]. However, this AHP is indirectly caused by the L-VDCCs through the activation of calcium-activated potassium channels [154, 186, 187]. Moreover, these channels also show increased expression with age and are correlated with memory impairment [154]. An increased AHP would decrease the rate of repetitive firing and reduce the chance of coincidence and summation of EPSCs thereby lowering the chance of LTP induction. Consistently, the AHP has been found to correlate with spatial learning ability in aged rats [188] and impaired fear conditioning in aged mice [155]. The age-related increased susceptibility for LTD is partly caused by changes in the properties of intracellular calcium stores (ICS) [175]. Furthermore, the ICS contribute to the age-related increase of the AHP [187]. Additionally, the observed increased susceptibility for LTD is caused by the ICS mediated increase in AHP. Moreover, this actually masks an age-related increase in LTP susceptibility [189].

There are strong indications that in the Ca²⁺ dependent signal cascade underlying LTP oxidizing agents are involved. First, NMDA receptor stimulation activates neuronal

nitric-oxide synthase (nNOS) through the rise in $[Ca^{2+}]_i$ [190]. Moreover, the protein level of nNOS is increased in the aged hippocampus [191]. Furthermore, the consequent protein nitrotyrosine adducts content has also been shown to be increased [191]. Second, ROS have been shown to have a substantial modulatory role in cellular transduction pathways and gene expression in many biological processes [11, 192]. Moreover, there are a number of arguments that implicate ROS in normal functioning and plasticity at the glutamatergic synapse: (i) several enzymes downstream of the NMDAR produce ROS, (ii) superoxide production is increased after NMDA application to neuronal cultures and hippocampal slices, (iii) glutamate is exchanged for ascorbate by the glutamate transporter protein and (iv) the NMDAR has a redox sensitive site that modulates receptor activity by up to 50%. Moreover, NO can also activate this site [192]. Furthermore, calcineurin an important neuronal protein phosphatase is regulated by ROS [119], CaMKII is regulated by H_2O_2 [166], oxidation of calmodulin results in the inability to activate CaMKII, support T286 phosphorylation, prevent 305/6 phosphorylation and support binding to the NR2B subunit of the NMDA receptor [193] and NMDA receptor responses are reduced in aging through a CaMKII and redox state dependent mechanism [194]. This implicates that neurons, or even synapses are exposed to oxidative insults to a greater extent and are thus more inclined to aging by oxidative stress than other cell types. The increased activity of the antioxidant enzymes catalase, superoxide dismutase, glutathione in the aged rat brain adds further weight to this hypothesis [182].

In aged animals that did not show L-LTP, dendritic CaMKII was not upregulated. Moreover, regulation of CaMKII was absent in cell bodies, regardless of the duration of LTP [195]. Another signal transduction enzyme regulated by Ca^{2+} /calmodulin is calcineurin also known as PP2B. This protein phosphatase is involved in regulation of synaptic plasticity [196-198]. Although its role is not completely clear it seems to be involved in LTD and/or depotentiation [197]. One of its functions is to dephosphorylate CREB and thereby inactivating it, thus possibly counteracting L-LTP induction [196]. Calcineurin activity is increased in aged F-344 rats [118, 119]. Another study reports a decreased activity and increased aggregation of calcineurin in aged F344/BNF1 rats [104]. These differences might be explained by the use of a different rat strain and the fact that in the two studies that show upregulation the rats had undergone training and testing on the Morris water maze. However, it does show that the signaling cascade involved in synaptic plasticity is perturbed. Moreover, protein phosphatase 1 (PP1) was found to be increased and CREB was found to be more dephosphorylated and thus less active [119].

All these signal transduction enzymes are part of the Ca^{2+} dependent pathway involved in synaptic plasticity. Furthermore, calcineurin has been shown to selectively enhance L-VDCC Ca^{2+} currents in aged cultured hippocampal neurons [184]. Thus (dys) regulation of Ca^{2+} homeostasis might be involved in brain aging.

2.2.2 Cell morphology

Cell numbers in the hippocampus do not decline significantly with increasing age, i.e. brain aging is not accompanied by sizable loss of hippocampal neurons [199-204]. Therefore, age-related cognitive impairment is not likely to be caused by neuronal loss. However, there are some changes in cell morphology, especially in the structures related to synapses.

There is a significant age-related increase of axonal fragments in hippocampus and amygdala [200]. The decline of the dopaminergic mesolimbic system might be the cause for this [200]. Mice that are haploinsufficient for *trkB*, *trkC* or both of these receptors show similar increase in axonal fragments as aged mice [205]. These tyrosine kinase receptors are the targets for a number of neurotrophins, like BDNF. Additionally, a relation between Morris water maze performance and the number of synaptophysin-positive boutons on dentate gyrus granule cells was found [203] and between spine numbers and length [206, 207] and PSD size [207, 208]. Consistently, the functional connectivity changes with age. In the dentate gyrus the synapses on the granule cells coming from the perforant path are reduced in numbers but increased in strength [105, 209, 210]. The number of synapses on the pyramidal cells in the CA1 region is reduced without becoming stronger [105, 170, 211-214].

2.2.3 Transcription

There are a number of reasons to investigate gene expression in brain aging. First, DNA damage can affect transcription and it increases with age in neurons [29, 45-47]. Second, arguably almost all biological changes should be evident at the transcriptional level. Therefore, investigating the transcriptome using the microarray technique should give some indication of the changes taking place in the aging brain.

A strong confounding factor in comparing microarray studies is the difference in experimental set-up. One of the most important factors is the choice of species that is investigated as highlighted by a study where mice, rhesus monkey and human brains were investigated [215]. Only very few transcripts were regulated in the same direction in all three species. Importantly, the largest category of age-regulated transcripts showed

similar regulation in Rhesus monkeys and humans, but opposite regulation in mice. The anti-oxidant lipid binding protein ApoD was upregulated with age in all three species and two proteins involved in cAMP dependent signaling, CaMKIV and ARPP-21, were downregulated [215]. However, when humans are compared to our closest relative the chimpanzee no correlation was found in the age-related expression changes of the cortex [216]. Together this strongly suggests that validity of transcriptome analyses across species is limited. With this caveat in mind, the murine brain transcriptome has repeatedly been found to show age-related changes indicative of increased inflammation and oxidative stress and reduced synaptic plasticity and transcription [121, 217-224]. Interestingly, some studies report downregulation of genes involved in DNA repair [221, 224, 225] and downregulation of CaMKII [217, 225].

A gene profiling study in the human brain has uncovered a set of genes that is reduced in expression in the cortex past the age of 40 [226]. The microarray data has been confirmed in qPCR experiments. Genes that play a role in synaptic function and plasticity are among those most significantly downregulated. Furthermore, genes involved in vesicular transport/protein trafficking and protein turnover were reduced in expression. Increased expression was found in the BER enzymes 8-oxoguanine DNA glycosylase and uracil DNA glycosylase and other genes involved in counteracting oxidative stress. This last finding led to the most important discovery: the downregulation of genes in the aged human cortex is associated with accelerated oxidative DNA damage. Moreover, specifically the promoter sequences of the downregulated genes are extra susceptible to oxidative damage and are repaired more slowly [226].

In conclusion, these microarray data are very interesting and indicative of the processes that are involved in brain aging. They are in line with the theory of accumulated ROS induced damage to macromolecules as an important cause of brain aging. The increased immune response could contribute to the oxidative damage through the release of ROS and NOS. However, the data are not completely in concordance with one and other, thereby emphasizing the necessity for repeating these investigations in multiple species and inbred lines, before the regulation of certain genes can be used as biomarkers for aging. On the other hand, the data from the study in the human brain provide a very strong indication that ROS induced nDNA damage causes brain aging through downregulation of specific genes. Among the genes that are downregulated and whose promoters are extra sensitive for ROS induced damage are number of Ca²⁺ binding proteins and kinases that are directly involved in LTP like α CaMKII [226]. Moreover, the increased ROS induced damage has been correlated to the reduced expression [226].

3 Aging of the peripheral nervous system

Not only the central nervous system is subject to age-related decline, the peripheral nervous system is too. Here we focus on two forms of sensory perception, vision and hearing. The two most common age-related impairments are hearing loss (ARHL) and loss of vision (ARVL). Their impact on daily life however, is hard to underestimate. Functional decline of the peripheral nervous system is at the root of these age-related impairments, although non-neuronal factors also play a role.

Importantly, patients with progeroid syndromes Cockayne syndrome or XP, both caused by impairment of the DNA repair pathway NER, have accelerated segmental aging accompanied by loss of hearing and vision already at a very young age [10, 90-92, 227]. This suggests that DNA damage could play a causative role in ARHL and ARVL.

3.1 Age-related hearing loss

Age-related hearing loss (ARHL) affects 40% of the population over 65, and 10% of the total population to the extent that hearing aids are required in the USA [228]. Therefore, it can be considered as a major socio-economic burden on society. It is characterized by increasing hearing thresholds, starting at higher frequencies [229-231]. Besides the increase in hearing thresholds, ARHL is characterized by changes in distortion product otoacoustic emissions (DPOAEs). DPOAEs are sounds produced by the ear when stimulated using a pair of primary tones. DPOAEs are generally thought to depend on functional OHCs [232, 233]. This non-invasive method is widely used in clinical and laboratory settings. It has been shown that aging and ARHL are accompanied by a progressive reduction of DPOAE output and a progressive increase in detection threshold starting at higher frequencies, both in humans [234-236] and mice [237-241].

The etiology of ARHL is largely unknown and probably multifactorial. There are however strong indications that DNA damage plays an important role. First, as mentioned above the progeroid syndromes XP and Cockayne syndrome present with hearing loss [10, 90-92, 227]. Second, oxidative metabolism is high in the cochlea [242] as is the normal expression of genes involved in NER, i.e. XPC and XPA [243]. Finally, reducing oxidative stress and DNA damage slows down ARHL [244].

3.2 Age-related vision loss

Everybody will experience age-related deterioration of his or her vision. Most of the time the solution is easy: wear glasses. There are however some more serious age-related optic changes such as increase in density, yellowing and hardening of the lens, the latter

of which leads to insufficient accommodation ability. However, the optic changes that occur with increasing age cannot explain all aspects of age-related vision loss (ARVL). Hence, changes in the retina or the central visual pathways must also play a role [245].

The etiology of ARVL is unknown and probably multicausal. As mentioned before, the human progeroid syndromes XP and Cockayne syndrome are accompanied by a loss of vision, and degeneration of the retina [90-92]. Moreover, a mouse model of Cockayne syndrome showed an age-dependent thinning of the outer nuclear layer (ONL) of the retina due to spontaneous loss of photoreceptors [246]. Finally, loss of photoreceptors or thinning of the ONL is commonly seen in aging humans [247-250], rats [251-255] and mice [256, 257].

These findings suggest that (retinal) DNA damage might play an important role in ARVL. This idea is strengthened by the fact that the retina has high oxidative metabolism [258] and that the retinal pigment epithelium (RPE) has very high antioxidant capacity and high DNA repair capacity [259]. Cataract is the major contributor to age-related visual impairment and age-related macula degeneration (AMD) is the main contributor to blindness over the age of 75 [260]. ROS have been implicated in the etiology of both cataract and AMD [261-266]. Finally, DNA damage has found to be increased and DNA repair decreased in AMD patients [267, 268]. Taken together, these results suggest that in ARVL DNA damage could play a causative role [269].

4 Conclusion

Does oxidative damage to nDNA cause brain aging? The strongest indication that it does comes from a microarray study on human cortices [226]. Here a link is made between the increasing oxidative damage to nDNA during aging and the downregulation of genes involved in synaptic plasticity [226]. It is also clear that there is not one single cause for brain aging, as can be seen from the wide body of research in (brain) aging. Other influential causes seem to be the Ca^{2+} regulation and the subsequent gene expression in the processes of synaptic plasticity. However, it seems to be a valid statement that oxidative damage to nDNA is part of the cause of brain aging.

5 Scope of this Thesis

The scope of this thesis is to elucidate the role of DNA damage in aging of the central and peripheral nervous system. As the average lifespan increases, age-related impairments become a pressing social challenge. Therefore it is important to understand more about the fundamental mechanisms underlying aging and its related impairments. To this end

we have analyzed mice with a targeted disruption of the *Ercc1* gene resulting in deficiency in the DNA repair pathways NER, ICL and double strand break repair. We study the consequences of unrepaired DNA damage on various aspects of neuronal function. In chapter 2 we study synaptic plasticity, learning and memory in the hippocampus, in chapter 3 sensory processing and in chapter 4 the neuromuscular system. As fundamental knowledge of a mechanism is needed to understand its failure, we have also investigated the function of α - and β CaMKII in hippocampal synaptic plasticity in chapter 5 and 6. In future this might help to understand more of the age-related failure of learning and memory.

6 References

1. Andressoo, J.O. and J.H. Hoeijmakers, *Transcription-coupled repair and premature ageing*. Mutat Res, 2005.
2. de Boer, J., et al., *Premature aging in mice deficient in DNA repair and transcription*. Science, 2002. **296**(5571): p. 1276-9.
3. Hasty, P., et al., *Aging and genome maintenance: lessons from the mouse?* Science, 2003. **299**(5611): p. 1355-9.
4. Hoeijmakers, J.H., *DNA damage, aging, and cancer*. N Engl J Med, 2009. **361**(15): p. 1475-85.
5. Bohr, V.A., *Deficient DNA repair in the human progeroid disorder, Werner syndrome*. Mutat Res, 2005.
6. Karanjawala, Z.E. and M.R. Lieber, *DNA damage and aging*. Mech Ageing Dev, 2004. **125**(6): p. 405-16.
7. Lehmann, A.R., *DNA repair-deficient diseases, xeroderma pigmentosum, Cockayne syndrome and trichothiodystrophy*. Biochimie, 2003. **85**(11): p. 1101-11.
8. Niedernhofer, L.J., *Tissue-specific accelerated aging in nucleotide excision repair deficiency*. Mech Ageing Dev, 2008. **129**(7-8): p. 408-15.
9. Niedernhofer, L.J., et al., *A new progeroid syndrome reveals that genotoxic stress suppresses the somatotroph axis*. Nature, 2006. **444**(7122): p. 1038-43.
10. Rapin, I., et al., *Cockayne syndrome and xeroderma pigmentosum*. Neurology, 2000. **55**(10): p. 1442-9.
11. Serrano, F. and E. Klann, *Reactive oxygen species and synaptic plasticity in the aging hippocampus*. Ageing Res Rev, 2004. **3**(4): p. 431-43.
12. Leutner, S., A. Eckert, and W.E. Muller, *ROS generation, lipid peroxidation and antioxidant enzyme activities in the aging brain*. J Neural Transm, 2001. **108**(8-9): p. 955-67.
13. Cai, Q., L. Tian, and H. Wei, *Age-dependent increase of indigenous DNA adducts in rat brain is associated with a lipid peroxidation product*. Exp Gerontol, 1996. **31**(3): p. 373-85.
14. Velculescu, V.E., et al., *Analysis of human transcriptomes*. Nat Genet, 1999. **23**(4): p. 387-8.
15. Hughes, K.A. and R.M. Reynolds, *Evolutionary and mechanistic theories of aging*. Annu Rev Entomol, 2005. **50**: p. 421-45.

16. Kirkwood, T.B., *Understanding the odd science of aging*. Cell, 2005. **120**(4): p. 437-47.
17. Sohal, R.S., *Oxidative stress hypothesis of aging*. Free Radic Biol Med, 2002. **33**(5): p. 573-4.
18. Sohal, R.S., *Role of oxidative stress and protein oxidation in the aging process*. Free Radic Biol Med, 2002. **33**(1): p. 37-44.
19. Sohal, R.S., R.J. Mockett, and W.C. Orr, *Mechanisms of aging: an appraisal of the oxidative stress hypothesis*. Free Radic Biol Med, 2002. **33**(5): p. 575-86.
20. Butterfield, D.A., B.J. Howard, and M.A. LaFontaine, *Brain oxidative stress in animal models of accelerated aging and the age-related neurodegenerative disorders, Alzheimer's disease and Huntington's disease*. Curr Med Chem, 2001. **8**(7): p. 815-28.
21. Balaban, R.S., S. Nemoto, and T. Finkel, *Mitochondria, oxidants, and aging*. Cell, 2005. **120**(4): p. 483-95.
22. Pearl, R., *The rate of living*. 1928, London: London University Press.
23. Miquel, J., et al., *Effects of temperature on the life span, vitality and fine structure of Drosophila melanogaster*. Mech Ageing Dev, 1976. **5**(5): p. 347-70.
24. Klass, M.R., *Aging in the nematode Caenorhabditis elegans: major biological and environmental factors influencing life span*. Mech Ageing Dev, 1977. **6**(6): p. 413-29.
25. Fontana, L., L. Partridge, and V.D. Longo, *Extending healthy life span--from yeast to humans*. Science, 2010. **328**(5976): p. 321-6.
26. Colman, R.J., et al., *Caloric restriction delays disease onset and mortality in rhesus monkeys*. Science, 2009. **325**(5937): p. 201-4.
27. Hosono, R., S. Nishimoto, and S. Kuno, *Alterations of life span in the nematode Caenorhabditis elegans under monoxenic culture conditions*. Exp Gerontol, 1989. **24**(3): p. 251-64.
28. Weindruch, R., et al., *Microarray profiling of gene expression in aging and its alteration by caloric restriction in mice*. J Nutr, 2001. **131**(3): p. 918S-923S.
29. Sohal, R.S., et al., *Effect of age and caloric restriction on DNA oxidative damage in different tissues of C57BL/6 mice*. Mech Ageing Dev, 1994. **76**(2-3): p. 215-24.
30. Cabelof, D.C., et al., *Caloric restriction promotes genomic stability by induction of base excision repair and reversal of its age-related decline*. DNA

- Repair (Amst), 2003. **2**(3): p. 295-307.
31. Gredilla, R. and G. Barja, *The Role of Oxidative Stress in relation to Caloric Restriction and Longevity*. Endocrinology, 2005.
 32. Wei, M., et al., *Life span extension by calorie restriction depends on Rim15 and transcription factors downstream of Ras/PKA, Tor, and Sch9*. PLoS Genet, 2008. **4**(1): p. e13.
 33. Pendergrass, W.R., et al., *Caloric restriction: conservation of cellular replicative capacity in vitro accompanies life-span extension in mice*. Exp Cell Res, 1995. **217**(2): p. 309-16.
 34. Wolf, N.S., et al., *Caloric restriction: conservation of in vivo cellular replicative capacity accompanies life-span extension in mice*. Exp Cell Res, 1995. **217**(2): p. 317-23.
 35. Wei, Y.H., et al., *Oxidative damage and mutation to mitochondrial DNA and age-dependent decline of mitochondrial respiratory function*. Ann N Y Acad Sci, 1998. **854**: p. 155-70.
 36. Browner, W.S., et al., *The genetics of human longevity*. Am J Med, 2004. **117**(11): p. 851-60.
 37. Van Goethem, G., et al., *POLG mutations in neurodegenerative disorders with ataxia but no muscle involvement*. Neurology, 2004. **63**(7): p. 1251-7.
 38. Luoma, P., et al., *Parkinsonism, premature menopause, and mitochondrial DNA polymerase gamma mutations: clinical and molecular genetic study*. Lancet, 2004. **364**(9437): p. 875-82.
 39. Van Goethem, G., et al., *Recessive POLG mutations presenting with sensory and ataxic neuropathy in compound heterozygote patients with progressive external ophthalmoplegia*. Neuromuscul Disord, 2003. **13**(2): p. 133-42.
 40. Mancuso, M., et al., *POLG mutations causing ophthalmoplegia, sensorimotor polyneuropathy, ataxia, and deafness*. Neurology, 2004. **62**(2): p. 316-8.
 41. Trifunovic, A., et al., *Premature ageing in mice expressing defective mitochondrial DNA polymerase*. Nature, 2004. **429**(6990): p. 417-23.
 42. Kujoth, G.C., et al., *Mitochondrial DNA mutations, oxidative stress, and apoptosis in mammalian aging*. Science, 2005. **309**(5733): p. 481-4.
 43. Bohr, V.A., *Repair of oxidative DNA damage in nuclear and mitochondrial DNA, and some changes with aging in mammalian cells*. Free Radic Biol Med, 2002. **32**(9): p. 804-12.
 44. Khrapko, K., et al., *Does premature aging of the mtDNA mutator mouse prove*

- that mtDNA mutations are involved in natural aging?* Aging Cell, 2006. **5**(3): p. 279-82.
45. Dorszewska, J. and Z. Adamczewska-Goncerzewicz, *Oxidative damage to DNA, p53 gene expression and p53 protein level in the process of aging in rat brain.* Respir Physiol Neurobiol, 2004. **139**(3): p. 227-36.
 46. Gedik, C.M., et al., *Effects of age and dietary restriction on oxidative DNA damage, antioxidant protection and DNA repair in rats.* Eur J Nutr, 2005. **44**(5): p. 263-72.
 47. Hamilton, M.L., et al., *Does oxidative damage to DNA increase with age?* Proc Natl Acad Sci U S A, 2001. **98**(18): p. 10469-74.
 48. Singh, N.P., et al., *DNA double-strand breaks in mouse kidney cells with age.* Biogerontology, 2001. **2**(4): p. 261-70.
 49. Bailey, K.J., A.Y. Maslov, and S.C. Pruitt, *Accumulation of mutations and somatic selection in aging neural stem/progenitor cells.* Aging Cell, 2004. **3**(6): p. 391-7.
 50. Shen, J.C., et al., *Werner syndrome protein. I. DNA helicase and dna exonuclease reside on the same polypeptide.* J Biol Chem, 1998. **273**(51): p. 34139-44.
 51. Kamath-Loeb, A.S., et al., *Werner syndrome protein. II. Characterization of the integral 3' --> 5' DNA exonuclease.* J Biol Chem, 1998. **273**(51): p. 34145-50.
 52. Gray, M.D., et al., *The Werner syndrome protein is a DNA helicase.* Nat Genet, 1997. **17**(1): p. 100-3.
 53. Karmakar, P. and V.A. Bohr, *Cellular dynamics and modulation of WRN protein is DNA damage specific.* Mech Ageing Dev, 2005.
 54. Coppede, F. and L. Migliore, *DNA repair in premature aging disorders and neurodegeneration.* Curr Aging Sci, 2010. **3**(1): p. 3-19.
 55. Cortopassi, G.A. and E. Wang, *There is substantial agreement among interspecies estimates of DNA repair activity.* Mech Ageing Dev, 1996. **91**(3): p. 211-8.
 56. Hart, R.W. and R.B. Setlow, *Correlation between deoxyribonucleic acid excision-repair and life-span in a number of mammalian species.* Proc Natl Acad Sci U S A, 1974. **71**(6): p. 2169-73.
 57. Hart, R.W. and R.B. Setlow, *DNA repair and life span of mammals.* Basic Life Sci, 1975. **5B**: p. 801-4.

58. Symphorien, S. and R.C. Woodruff, *Effect of DNA repair on aging of transgenic Drosophila melanogaster: I. mei-41 locus*. J Gerontol A Biol Sci Med Sci, 2003. **58**(9): p. B782-7.
59. Nohmi, T., S.R. Kim, and M. Yamada, *Modulation of oxidative mutagenesis and carcinogenesis by polymorphic forms of human DNA repair enzymes*. Mutat Res, 2005.
60. Colussi, C., et al., *The mammalian mismatch repair pathway removes DNA 8-oxodGMP incorporated from the oxidized dNTP pool*. Curr Biol, 2002. **12**(11): p. 912-8.
61. Ishibashi, T., et al., *Mammalian enzymes for preventing transcriptional errors caused by oxidative damage*. Nucleic Acids Res, 2005. **33**(12): p. 3779-84.
62. Mo, J.Y., H. Maki, and M. Sekiguchi, *Hydrolytic elimination of a mutagenic nucleotide, 8-oxodGTP, by human 18-kilodalton protein: sanitization of nucleotide pool*. Proc Natl Acad Sci U S A, 1992. **89**(22): p. 11021-5.
63. Russo, M.T., et al., *The oxidized deoxynucleoside triphosphate pool is a significant contributor to genetic instability in mismatch repair-deficient cells*. Mol Cell Biol, 2004. **24**(1): p. 465-74.
64. Nakabeppu, Y., et al., *Biological significance of the defense mechanisms against oxidative damage in nucleic acids caused by reactive oxygen species: from mitochondria to nuclei*. Ann N Y Acad Sci, 2004. **1011**: p. 101-11.
65. Rhee, Y., M.R. Valentine, and J. Termini, *Oxidative base damage in RNA detected by reverse transcriptase*. Nucleic Acids Res, 1995. **23**(16): p. 3275-82.
66. Thorp, H.H., *The importance of being r: greater oxidative stability of RNA compared with DNA*. Chem Biol, 2000. **7**(2): p. R33-6.
67. Liu, J., et al., *Memory loss in old rats is associated with brain mitochondrial decay and RNA/DNA oxidation: partial reversal by feeding acetyl-L-carnitine and/or R-alpha -lipoic acid*. Proc Natl Acad Sci U S A, 2002. **99**(4): p. 2356-61.
68. Zhang, J., et al., *Parkinson's disease is associated with oxidative damage to cytoplasmic DNA and RNA in substantia nigra neurons*. Am J Pathol, 1999. **154**(5): p. 1423-9.
69. Nunomura, A., et al., *RNA oxidation is a prominent feature of vulnerable neurons in Alzheimer's disease*. J Neurosci, 1999. **19**(6): p. 1959-64.
70. Agarwal, S. and R.S. Sohal, *Aging and protein oxidative damage*. Mech

- Ageing Dev, 1994. **75**(1): p. 11-9.
71. Cakatay, U., et al., *Relation of aging with oxidative protein damage parameters in the rat skeletal muscle*. Clin Biochem, 2003. **36**(1): p. 51-5.
 72. Agarwal, S. and R.S. Sohal, *Relationship between aging and susceptibility to protein oxidative damage*. Biochem Biophys Res Commun, 1993. **194**(3): p. 1203-6.
 73. Pamplona, R., G. Barja, and M. Portero-Otin, *Membrane fatty acid unsaturation, protection against oxidative stress, and maximum life span: a homeoviscous-longevity adaptation?* Ann N Y Acad Sci, 2002. **959**: p. 475-90.
 74. Pamplona, R., et al., *Modification of the longevity-related degree of fatty acid unsaturation modulates oxidative damage to proteins and mitochondrial DNA in liver and brain*. Exp Gerontol, 2004. **39**(5): p. 725-33.
 75. Portero-Otin, M., et al., *Protein nonenzymatic modifications and proteasome activity in skeletal muscle from the short-lived rat and long-lived pigeon*. Exp Gerontol, 2004. **39**(10): p. 1527-35.
 76. Choe, M., C. Jackson, and B.P. Yu, *Lipid peroxidation contributes to age-related membrane rigidity*. Free Radic Biol Med, 1995. **18**(6): p. 977-84.
 77. Hulbert, A.J., *On the importance of fatty acid composition of membranes for aging*. J Theor Biol, 2005. **234**(2): p. 277-88.
 78. Spiteller, G., *Are changes of the cell membrane structure causally involved in the aging process?* Ann N Y Acad Sci, 2002. **959**: p. 30-44.
 79. Murray, C.A. and M.A. Lynch, *Dietary supplementation with vitamin E reverses the age-related deficit in long term potentiation in dentate gyrus*. J Biol Chem, 1998. **273**(20): p. 12161-8.
 80. Ahmad, A., et al., *ERCC1-XPF endonuclease facilitates DNA double-strand break repair*. Mol Cell Biol, 2008. **28**(16): p. 5082-92.
 81. Christmann, M., et al., *Mechanisms of human DNA repair: an update*. Toxicology, 2003. **193**(1-2): p. 3-34.
 82. Hoeijmakers, J.H., *Genome maintenance mechanisms for preventing cancer*. Nature, 2001. **411**(6835): p. 366-74.
 83. Wood, R.D., *Mammalian nucleotide excision repair proteins and interstrand crosslink repair*. Environ Mol Mutagen, 2010. **51**(6): p. 520-6.
 84. Szczesny, B., et al., *Age-dependent modulation of DNA repair enzymes by covalent modification and subcellular distribution*. Mech Ageing Dev, 2004. **125**(10-11): p. 755-65.

85. Stuart, J.A., et al., *Mitochondrial and nuclear DNA base excision repair are affected differently by caloric restriction*. *Faseb J*, 2004. **18**(3): p. 595-7.
86. Croteau, D.L., R.H. Stierum, and V.A. Bohr, *Mitochondrial DNA repair pathways*. *Mutat Res*, 1999. **434**(3): p. 137-48.
87. Cabelof, D.C., et al., *Induction of DNA polymerase beta-dependent base excision repair in response to oxidative stress in vivo*. *Carcinogenesis*, 2002. **23**(9): p. 1419-25.
88. Mandavilli, B.S., J.H. Santos, and B. Van Houten, *Mitochondrial DNA repair and aging*. *Mutat Res*, 2002. **509**(1-2): p. 127-51.
89. de Boer, J. and J.H. Hoeijmakers, *Nucleotide excision repair and human syndromes*. *Carcinogenesis*, 2000. **21**(3): p. 453-60.
90. Lindenbaum, Y., et al., *Xeroderma pigmentosum/cockayne syndrome complex: first neuropathological study and review of eight other cases*. *Eur J Paediatr Neurol*, 2001. **5**(6): p. 225-42.
91. Robbins, J.H., et al., *Neurological disease in xeroderma pigmentosum. Documentation of a late onset type of the juvenile onset form*. *Brain*, 1991. **114** (Pt 3): p. 1335-61.
92. Weidenheim, K.M., D.W. Dickson, and I. Rapin, *Neuropathology of Cockayne syndrome: Evidence for impaired development, premature aging, and neurodegeneration*. *Mech Ageing Dev*, 2009. **130**(9): p. 619-36.
93. Hansen, W.K. and M.R. Kelley, *Review of mammalian DNA repair and translational implications*. *J Pharmacol Exp Ther*, 2000. **295**(1): p. 1-9.
94. Drablos, F., et al., *Alkylation damage in DNA and RNA--repair mechanisms and medical significance*. *DNA Repair (Amst)*, 2004. **3**(11): p. 1389-407.
95. Marnett, L.J. and J.P. Plataras, *Endogenous DNA damage and mutation*. *Trends Genet*, 2001. **17**(4): p. 214-21.
96. Kadlubar, F.F., et al., *Comparison of DNA adduct levels associated with oxidative stress in human pancreas*. *Mutat Res*, 1998. **405**(2): p. 125-33.
97. Sharma, R.A., et al., *Cyclooxygenase-2, malondialdehyde and pyrimidopurinone adducts of deoxyguanosine in human colon cells*. *Carcinogenesis*, 2001. **22**(9): p. 1557-60.
98. Niedernhofer, L.J., et al., *Malondialdehyde, a product of lipid peroxidation, is mutagenic in human cells*. *J Biol Chem*, 2003. **278**(33): p. 31426-33.
99. Rahn, J.J., G.M. Adair, and R.S. Nairn, *Multiple roles of ERCC1-XPF in mammalian interstrand crosslink repair*. *Environ Mol Mutagen*, 2010. **51**(6): p.

- 567-81.
100. Dronkert, M.L. and R. Kanaar, *Repair of DNA interstrand cross-links*. *Mutat Res*, 2001. **486**(4): p. 217-47.
 101. McHugh, P.J., V.J. Spanswick, and J.A. Hartley, *Repair of DNA interstrand crosslinks: molecular mechanisms and clinical relevance*. *Lancet Oncol*, 2001. **2**(8): p. 483-90.
 102. von Zglinicki, T., *Oxidative stress shortens telomeres*. *Trends Biochem Sci*, 2002. **27**(7): p. 339-44.
 103. Moller, P., et al., *Aging and oxidatively damaged nuclear DNA in animal organs*. *Free Radic Biol Med*, 2010. **48**(10): p. 1275-1285.
 104. Agbas, A., A. Zaidi, and E.K. Michaelis, *Decreased activity and increased aggregation of brain calcineurin during aging*. *Brain Res*, 2005.
 105. Rosenzweig, E.S. and C.A. Barnes, *Impact of aging on hippocampal function: plasticity, network dynamics, and cognition*. *Prog Neurobiol*, 2003. **69**(3): p. 143-79.
 106. Erickson, C.A. and C.A. Barnes, *The neurobiology of memory changes in normal aging*. *Exp Gerontol*, 2003. **38**(1-2): p. 61-9.
 107. Sharma, S., S. Rakoczy, and H. Brown-Borg, *Assessment of spatial memory in mice*. *Life Sci*, 2010.
 108. Uttl, B. and P. Graf, *Episodic spatial memory in adulthood*. *Psychol Aging*, 1993. **8**(2): p. 257-73.
 109. Wilkniss, S.M., et al., *Age-related differences in an ecologically based study of route learning*. *Psychol Aging*, 1997. **12**(2): p. 372-5.
 110. Lai, Z.C., et al., *Executive system dysfunction in the aged monkey: spatial and object reversal learning*. *Neurobiol Aging*, 1995. **16**(6): p. 947-54.
 111. Rapp, P.R., M.T. Kansky, and J.A. Roberts, *Impaired spatial information processing in aged monkeys with preserved recognition memory*. *Neuroreport*, 1997. **8**(8): p. 1923-8.
 112. Barnes, C.A., *Memory deficits associated with senescence: a neurophysiological and behavioral study in the rat*. *J Comp Physiol Psychol*, 1979. **93**(1): p. 74-104.
 113. Markowska, A.L., et al., *Individual differences in aging: behavioral and neurobiological correlates*. *Neurobiol Aging*, 1989. **10**(1): p. 31-43.
 114. Gallagher, M. and P.R. Rapp, *The use of animal models to study the effects of aging on cognition*. *Annu Rev Psychol*, 1997. **48**: p. 339-70.

115. Bach, M.E., et al., *Age-related defects in spatial memory are correlated with defects in the late phase of hippocampal long-term potentiation in vitro and are attenuated by drugs that enhance the cAMP signaling pathway*. Proc Natl Acad Sci U S A, 1999. **96**(9): p. 5280-5.
116. Iaria, G., et al., *Age differences in the formation and use of cognitive maps*. Behav Brain Res, 2009. **196**(2): p. 187-91.
117. Murphy, G.G., N.P. Rahnama, and A.J. Silva, *Investigation of age-related cognitive decline using mice as a model system: behavioral correlates*. Am J Geriatr Psychiatry, 2006. **14**(12): p. 1004-11.
118. Foster, T.C., et al., *Interaction of age and chronic estradiol replacement on memory and markers of brain aging*. Neurobiol Aging, 2003. **24**(6): p. 839-52.
119. Foster, T.C., et al., *Calcineurin links Ca²⁺ dysregulation with brain aging*. J Neurosci, 2001. **21**(11): p. 4066-73.
120. Verbitsky, M., et al., *Altered hippocampal transcript profile accompanies an age-related spatial memory deficit in mice*. Learn Mem, 2004. **11**(3): p. 253-60.
121. Blalock, E.M., et al., *Gene microarrays in hippocampal aging: statistical profiling identifies novel processes correlated with cognitive impairment*. J Neurosci, 2003. **23**(9): p. 3807-19.
122. Foster, T.C. and A. Kumar, *Susceptibility to induction of long-term depression is associated with impaired memory in aged Fischer 344 rats*. Neurobiol Learn Mem, 2007. **87**(4): p. 522-35.
123. Barnes, C.A., *Long-term potentiation and the ageing brain*. Philos Trans R Soc Lond B Biol Sci, 2003. **358**(1432): p. 765-72.
124. Luine, V., D. Bowling, and M. Hearn, *Spatial memory deficits in aged rats: contributions of monoaminergic systems*. Brain Res, 1990. **537**(1-2): p. 271-8.
125. McLay, R.N., et al., *Tests used to assess the cognitive abilities of aged rats: their relation to each other and to hippocampal morphology and neurotrophin expression*. Gerontology, 1999. **45**(3): p. 143-55.
126. Moffat, S.D., W. Elkins, and S.M. Resnick, *Age differences in the neural systems supporting human allocentric spatial navigation*. Neurobiol Aging, 2006. **27**(7): p. 965-72.
127. Driscoll, I., et al., *The aging hippocampus: cognitive, biochemical and structural findings*. Cereb Cortex, 2003. **13**(12): p. 1344-51.
128. Veng, L.M., M.H. Mesches, and M.D. Browning, *Age-related working memory impairment is correlated with increases in the L-type calcium channel protein*

- alpha1D (Cav1.3) in area CA1 of the hippocampus and both are ameliorated by chronic nimodipine treatment.* Brain Res Mol Brain Res, 2003. **110**(2): p. 193-202.
129. Jacobson, L., et al., *Correlation of cellular changes and spatial memory during aging in rats.* Exp Gerontol, 2008. **43**(10): p. 929-38.
130. Bennett, J.C., et al., *Long-term continuous, but not daily, environmental enrichment reduces spatial memory decline in aged male mice.* Neurobiol Learn Mem, 2006. **85**(2): p. 139-52.
131. Chen, G.H., et al., *Age- and sex-related disturbance in a battery of sensorimotor and cognitive tasks in Kunming mice.* Physiol Behav, 2004. **83**(3): p. 531-41.
132. Shukitt-Hale, B., et al., *Effect of age on the radial arm water maze-a test of spatial learning and memory.* Neurobiol Aging, 2004. **25**(2): p. 223-9.
133. Oler, J.A. and E.J. Markus, *Age-related deficits on the radial maze and in fear conditioning: hippocampal processing and consolidation.* Hippocampus, 1998. **8**(4): p. 402-15.
134. Burguiere, E., et al., *Spatial navigation impairment in mice lacking cerebellar LTD: a motor adaptation deficit?* Nat Neurosci, 2005. **8**(10): p. 1292-4.
135. Scali, C., et al., *Effect of metrifonate on extracellular brain acetylcholine and object recognition in aged rats.* Eur J Pharmacol, 1997. **325**(2-3): p. 173-80.
136. Scali, C., et al., *Tacrine administration enhances extracellular acetylcholine in vivo and restores the cognitive impairment in aged rats.* Pharmacol Res, 1997. **36**(6): p. 463-9.
137. Vannucchi, M.G., et al., *Selective muscarinic antagonists differentially affect in vivo acetylcholine release and memory performances of young and aged rats.* Neuroscience, 1997. **79**(3): p. 837-46.
138. Fahlstrom, A., Q. Yu, and B. Ulfhake, *Behavioral changes in aging female C57BL/6 mice.* Neurobiol Aging, 2009.
139. Platano, D., et al., *Long-term visual object recognition memory in aged rats.* Rejuvenation Res, 2008. **11**(2): p. 333-9.
140. de Lima, M.N., et al., *Reversal of age-related deficits in object recognition memory in rats with l-deprenyl.* Exp Gerontol, 2005. **40**(6): p. 506-11.
141. Si, W., et al., *A novel derivative of xanomeline improves fear cognition in aged mice.* Neurosci Lett, 2010. **473**(2): p. 115-9.
142. Hsu, K.S., et al., *Alterations in the balance of protein kinase and phosphatase*

- activities and age-related impairments of synaptic transmission and long-term potentiation.* Hippocampus, 2002. **12**(6): p. 787-802.
143. Huang, A.M., et al., *Expression of integrin-associated protein gene associated with memory formation in rats.* J Neurosci, 1998. **18**(11): p. 4305-13.
144. Riekkinen, P., Jr., et al., *The correlation of passive avoidance deficit in aged rat with the loss of nucleus basalis choline acetyltransferase-positive neurons.* Brain Res Bull, 1990. **25**(3): p. 415-7.
145. Frye, C.A., et al., *3alpha-androstanediol, but not testosterone, attenuates age-related decrements in cognitive, anxiety, and depressive behavior of male rats.* Front Aging Neurosci, 2010. **2**: p. 15.
146. Vasquez, B.J., et al., *Learning and memory in young and aged Fischer 344 rats.* Arch Gerontol Geriatr, 1983. **2**(4): p. 279-91.
147. Overman, A.A. and J.T. Becker, *The associative deficit in older adult memory: Recognition of pairs is not improved by repetition.* Psychol Aging, 2009. **24**(2): p. 501-6.
148. Bastin, C. and M. Van der Linden, *The effects of aging on the recognition of different types of associations.* Exp Aging Res, 2006. **32**(1): p. 61-77.
149. Bender, A.R., M. Naveh-Benjamin, and N. Raz, *Associative deficit in recognition memory in a lifespan sample of healthy adults.* Psychol Aging, 2010.
150. Old, S.R. and M. Naveh-Benjamin, *Differential effects of age on item and associative measures of memory: a meta-analysis.* Psychol Aging, 2008. **23**(1): p. 104-18.
151. Naveh-Benjamin, M., et al., *Adult age differences in episodic memory: further support for an associative-deficit hypothesis.* J Exp Psychol Learn Mem Cogn, 2003. **29**(5): p. 826-37.
152. Naveh-Benjamin, M., et al., *The associative memory deficit of older adults: further support using face-name associations.* Psychol Aging, 2004. **19**(3): p. 541-6.
153. Naveh-Benjamin, M., J. Guez, and S. Shulman, *Older adults' associative deficit in episodic memory: assessing the role of decline in attentional resources.* Psychon Bull Rev, 2004. **11**(6): p. 1067-73.
154. Blank, T., et al., *Small-conductance, Ca²⁺-activated K⁺ channel SK3 generates age-related memory and LTP deficits.* Nat Neurosci, 2003. **6**(9): p. 911-2.

-
155. Kaczorowski, C.C. and J.F. Disterhoft, *Memory deficits are associated with impaired ability to modulate neuronal excitability in middle-aged mice*. Learn Mem, 2009. **16**(6): p. 362-6.
156. Moyer, J.R., Jr. and T.H. Brown, *Impaired trace and contextual fear conditioning in aged rats*. Behav Neurosci, 2006. **120**(3): p. 612-24.
157. Kudo, K., et al., *Age-related disturbance of memory and CREB phosphorylation in CA1 area of hippocampus of rats*. Brain Res, 2005. **1054**(1): p. 30-7.
158. Luu, T.T., E. Pirogovsky, and P.E. Gilbert, *Age-related changes in contextual associative learning*. Neurobiol Learn Mem, 2008. **89**(1): p. 81-5.
159. Pettit, D.L., S. Perlman, and R. Malinow, *Potentiated transmission and prevention of further LTP by increased CaMKII activity in postsynaptic hippocampal slice neurons*. Science, 1994. **266**(5192): p. 1881-5.
160. Elgersma, Y., J.D. Sweatt, and K.P. Giese, *Mouse genetic approaches to investigating calcium/calmodulin-dependent protein kinase II function in plasticity and cognition*. J Neurosci, 2004. **24**(39): p. 8410-5.
161. Lisman, J., H. Schulman, and H. Cline, *The molecular basis of CaMKII function in synaptic and behavioural memory*. Nat Rev Neurosci, 2002. **3**(3): p. 175-90.
162. Lisman, J.E. and C.C. McIntyre, *Synaptic plasticity: a molecular memory switch*. Curr Biol, 2001. **11**(19): p. R788-91.
163. Griffith, L.C., *Calcium/calmodulin-dependent protein kinase II: an unforgettable kinase*. J Neurosci, 2004. **24**(39): p. 8391-3.
164. Bliss, T.V. and G.L. Collingridge, *A synaptic model of memory: long-term potentiation in the hippocampus*. Nature, 1993. **361**(6407): p. 31-9.
165. Pang, P.T. and B. Lu, *Regulation of late-phase LTP and long-term memory in normal and aging hippocampus: role of secreted proteins tPA and BDNF*. Ageing Res Rev, 2004. **3**(4): p. 407-30.
166. Watson, J.B., et al., *Age-related deficits in long-term potentiation are insensitive to hydrogen peroxide: coincidence with enhanced autophosphorylation of Ca²⁺/calmodulin-dependent protein kinase II*. J Neurosci Res, 2002. **70**(3): p. 298-308.
167. Rosenzweig, E.S., et al., *Role of temporal summation in age-related long-term potentiation-induction deficits*. Hippocampus, 1997. **7**(5): p. 549-58.
168. Griffin, R., et al., *The age-related attenuation in long-term potentiation is*

- associated with microglial activation.* J Neurochem, 2006. **99**(4): p. 1263-72.
169. Lynch, M.A. and K.L. Voss, *Membrane arachidonic acid concentration correlates with age and induction of long-term potentiation in the dentate gyrus in the rat.* Eur J Neurosci, 1994. **6**(6): p. 1008-14.
170. Deupree, D.L., J. Bradley, and D.A. Turner, *Age-related alterations in potentiation in the CA1 region in F344 rats.* Neurobiol Aging, 1993. **14**(3): p. 249-58.
171. Moore, C.I., M.D. Browning, and G.M. Rose, *Hippocampal plasticity induced by primed burst, but not long-term potentiation, stimulation is impaired in area CA1 of aged Fischer 344 rats.* Hippocampus, 1993. **3**(1): p. 57-66.
172. Watson, J.B., et al., *Age-dependent modulation of hippocampal long-term potentiation by antioxidant enzymes.* J Neurosci Res, 2006. **84**(7): p. 1564-74.
173. Mothet, J.P., et al., *A critical role for the glial-derived neuromodulator D-serine in the age-related deficits of cellular mechanisms of learning and memory.* Aging Cell, 2006. **5**(3): p. 267-74.
174. Norris, C.M., D.L. Korol, and T.C. Foster, *Increased susceptibility to induction of long-term depression and long-term potentiation reversal during aging.* J Neurosci, 1996. **16**(17): p. 5382-92.
175. Kumar, A. and T.C. Foster, *Intracellular calcium stores contribute to increased susceptibility to LTD induction during aging.* Brain Res, 2005. **1031**(1): p. 125-8.
176. Woodruff-Pak, D.S., et al., *Nimodipine ameliorates impaired eyeblink classical conditioning in older rabbits in the long-delay paradigm.* Neurobiol Aging, 1997. **18**(6): p. 641-9.
177. Quevedo, J., et al., *L-type voltage-dependent calcium channel blocker nifedipine enhances memory retention when infused into the hippocampus.* Neurobiol Learn Mem, 1998. **69**(3): p. 320-5.
178. Wu, W.W., M.M. Oh, and J.F. Disterhoft, *Age-related biophysical alterations of hippocampal pyramidal neurons: implications for learning and memory.* Ageing Res Rev, 2002. **1**(2): p. 181-207.
179. Shankar, S., T.J. Teyler, and N. Robbins, *Aging differentially alters forms of long-term potentiation in rat hippocampal area CA1.* J Neurophysiol, 1998. **79**(1): p. 334-41.
180. Murphy, G.G., et al., *Investigation of age-related cognitive decline using mice as a model system: neurophysiological correlates.* Am J Geriatr Psychiatry,

2006. **14**(12): p. 1012-21.
181. Thibault, O., R. Hadley, and P.W. Landfield, *Elevated postsynaptic [Ca²⁺]_i and L-type calcium channel activity in aged hippocampal neurons: relationship to impaired synaptic plasticity*. J Neurosci, 2001. **21**(24): p. 9744-56.
182. Bhalla, P. and B. Nehru, *Modulatory effects of centrophenoxine on different regions of ageing rat brain*. Exp Gerontol, 2005.
183. Power, J.M., et al., *Age-related enhancement of the slow outward calcium-activated potassium current in hippocampal CA1 pyramidal neurons in vitro*. J Neurosci, 2002. **22**(16): p. 7234-43.
184. Norris, C.M., et al., *Calcineurin enhances L-type Ca(2+) channel activity in hippocampal neurons: increased effect with age in culture*. Neuroscience, 2002. **110**(2): p. 213-25.
185. Norris, C.M., et al., *Hippocampal 'zipper' slice studies reveal a necessary role for calcineurin in the increased activity of L-type Ca(2+) channels with aging*. Neurobiol Aging, 2010. **31**(2): p. 328-38.
186. Sah, P. and J.D. Clements, *Photolytic manipulation of [Ca²⁺]_i reveals slow kinetics of potassium channels underlying the afterhyperpolarization in hippocampal pyramidal neurons*. J Neurosci, 1999. **19**(10): p. 3657-64.
187. Foster, T.C. and A. Kumar, *Calcium dysregulation in the aging brain*. Neuroscientist, 2002. **8**(4): p. 297-301.
188. Tombaugh, G.C., W.B. Rowe, and G.M. Rose, *The slow afterhyperpolarization in hippocampal CA1 neurons covaries with spatial learning ability in aged Fisher 344 rats*. J Neurosci, 2005. **25**(10): p. 2609-16.
189. Kumar, A. and T.C. Foster, *Enhanced long-term potentiation during aging is masked by processes involving intracellular calcium stores*. J Neurophysiol, 2004. **91**(6): p. 2437-44.
190. Rameau, G.A., L.Y. Chiu, and E.B. Ziff, *Bidirectional regulation of neuronal nitric-oxide synthase phosphorylation at serine 847 by the N-methyl-D-aspartate receptor*. J Biol Chem, 2004. **279**(14): p. 14307-14.
191. Sharman, E.H., et al., *Reversal of biochemical and behavioral parameters of brain aging by melatonin and acetyl L-carnitine*. Brain Res, 2002. **957**(2): p. 223-30.
192. Smythies, J., *Redox mechanisms at the glutamate synapse and their significance: a review*. Eur J Pharmacol, 1999. **370**(1): p. 1-7.

193. Robison, A.J., et al., *Oxidation of calmodulin alters activation and regulation of CaMKII*. *Biochem Biophys Res Commun*, 2007. **356**(1): p. 97-101.
194. Bodhinathan, K., A. Kumar, and T.C. Foster, *Intracellular redox state alters NMDA receptor response during aging through Ca²⁺/calmodulin-dependent protein kinase II*. *J Neurosci*, 2010. **30**(5): p. 1914-24.
195. Davis, S., et al., *Dysfunctional regulation of alphaCaMKII and syntaxin 1B transcription after induction of LTP in the aged rat*. *Eur J Neurosci*, 2000. **12**(9): p. 3276-82.
196. Hongpaisan, J., C.A. Winters, and S.B. Andrews, *Calcium-dependent mitochondrial superoxide modulates nuclear CREB phosphorylation in hippocampal neurons*. *Mol Cell Neurosci*, 2003. **24**(4): p. 1103-15.
197. Jouvenceau, A., et al., *Different phosphatase-dependent mechanisms mediate long-term depression and depotentiation of long-term potentiation in mouse hippocampal CA1 area*. *Eur J Neurosci*, 2003. **18**(5): p. 1279-85.
198. Kamsler, A. and M. Segal, *Hydrogen peroxide modulation of synaptic plasticity*. *J Neurosci*, 2003. **23**(1): p. 269-76.
199. Keuker, J.I., et al., *Preservation of hippocampal neuron numbers and hippocampal subfield volumes in behaviorally characterized aged tree shrews*. *J Comp Neurol*, 2004. **468**(4): p. 509-17.
200. von Bohlen und Halbach, O. and K. Unsicker, *Morphological alterations in the amygdala and hippocampus of mice during ageing*. *Eur J Neurosci*, 2002. **16**(12): p. 2434-40.
201. Merrill, D.A., A.A. Chiba, and M.H. Tuszynski, *Conservation of neuronal number and size in the entorhinal cortex of behaviorally characterized aged rats*. *J Comp Neurol*, 2001. **438**(4): p. 445-56.
202. Rapp, P.R. and M. Gallagher, *Preserved neuron number in the hippocampus of aged rats with spatial learning deficits*. *Proc Natl Acad Sci U S A*, 1996. **93**(18): p. 9926-30.
203. Calhoun, M.E., et al., *Hippocampal neuron and synaptophysin-positive bouton number in aging C57BL/6 mice*. *Neurobiol Aging*, 1998. **19**(6): p. 599-606.
204. Rasmussen, T., et al., *Memory impaired aged rats: no loss of principal hippocampal and subicular neurons*. *Neurobiol Aging*, 1996. **17**(1): p. 143-7.
205. von Bohlen und Halbach, O., L. Minichiello, and K. Unsicker, *Haploinsufficiency in *trkB* and/or *trkC* neurotrophin receptors causes structural alterations in the aged hippocampus and amygdala*. *Eur J Neurosci*,

2003. **18**(8): p. 2319-25.
206. von Bohlen und Halbach, O., et al., *Age-related alterations in hippocampal spines and deficiencies in spatial memory in mice*. J Neurosci Res, 2006. **83**(4): p. 525-31.
207. Long, L.H., et al., *Age-related synaptic changes in the CA1 stratum radiatum and spatial learning impairment in rats*. Clin Exp Pharmacol Physiol, 2009. **36**(7): p. 675-81.
208. Nicholson, D.A., et al., *Reduction in size of perforated postsynaptic densities in hippocampal axospinous synapses and age-related spatial learning impairments*. J Neurosci, 2004. **24**(35): p. 7648-53.
209. Barnes, C.A. and B.L. McNaughton, *Physiological compensation for loss of afferent synapses in rat hippocampal granule cells during senescence*. J Physiol, 1980. **309**: p. 473-85.
210. Foster, T.C., et al., *Increase in perforant path quantal size in aged F-344 rats*. Neurobiol Aging, 1991. **12**(5): p. 441-8.
211. Barnes, C.A., et al., *Region-specific age effects on AMPA sensitivity: electrophysiological evidence for loss of synaptic contacts in hippocampal field CA1*. Hippocampus, 1992. **2**(4): p. 457-68.
212. Barnes, C.A., G. Rao, and G. Orr, *Age-related decrease in the Schaffer collateral-evoked EPSP in awake, freely behaving rats*. Neural Plast, 2000. **7**(3): p. 167-78.
213. Potier, B., et al., *NMDA receptor activation in the aged rat hippocampus*. Exp Gerontol, 2000. **35**(9-10): p. 1185-99.
214. Kerr, D.S., et al., *Chronic stress-induced acceleration of electrophysiologic and morphometric biomarkers of hippocampal aging*. J Neurosci, 1991. **11**(5): p. 1316-24.
215. Loerch, P.M., et al., *Evolution of the aging brain transcriptome and synaptic regulation*. PLoS One, 2008. **3**(10): p. e3329.
216. Fraser, H.B., et al., *Aging and gene expression in the primate brain*. PLoS Biol, 2005. **3**(9): p. e274.
217. Rowe, W.B., et al., *Hippocampal expression analyses reveal selective association of immediate-early, neuroenergetic, and myelinogenic pathways with cognitive impairment in aged rats*. J Neurosci, 2007. **27**(12): p. 3098-110.
218. Burger, C., et al., *Changes in transcription within the CA1 field of the hippocampus are associated with age-related spatial learning impairments*.

- Neurobiol Learn Mem, 2007. **87**(1): p. 21-41.
219. Kadish, I., et al., *Hippocampal and cognitive aging across the lifespan: a bioenergetic shift precedes and increased cholesterol trafficking parallels memory impairment*. J Neurosci, 2009. **29**(6): p. 1805-16.
220. Pawlowski, T.L., et al., *Hippocampal gene expression changes during age-related cognitive decline*. Brain Res, 2009. **1256**: p. 101-10.
221. Lee, C.K., R. Weindruch, and T.A. Prolla, *Gene-expression profile of the ageing brain in mice*. Nat Genet, 2000. **25**(3): p. 294-7.
222. Kelly, K.M., et al., *The neurobiology of aging*. Epilepsy Res, 2006. **68 Suppl 1**: p. S5-20.
223. Prolla, T.A., *DNA microarray analysis of the aging brain*. Chem Senses, 2002. **27**(3): p. 299-306.
224. Xu, X., et al., *Gene expression atlas of the mouse central nervous system: impact and interactions of age, energy intake and gender*. Genome Biol, 2007. **8**(11): p. R234.
225. Jiang, C.H., et al., *The effects of aging on gene expression in the hypothalamus and cortex of mice*. Proc Natl Acad Sci U S A, 2001. **98**(4): p. 1930-4.
226. Lu, T., et al., *Gene regulation and DNA damage in the ageing human brain*. Nature, 2004. **429**(6994): p. 883-91.
227. Niedernhofer, L.J., *Nucleotide excision repair deficient mouse models and neurological disease*. DNA Repair (Amst), 2008. **7**(7): p. 1180-9.
228. Ries, P.W., *Prevalence and characteristics of persons with hearing trouble: United States, 1990-91*. Vital Health Stat 10, 1994(188): p. 1-75.
229. Huang, Q. and J. Tang, *Age-related hearing loss or presbycusis*. Eur Arch Otorhinolaryngol, 2010. **267**(8): p. 1179-91.
230. Gates, G.A. and J.H. Mills, *Presbycusis*. Lancet, 2005. **366**(9491): p. 1111-20.
231. Liu, X.Z. and D. Yan, *Ageing and hearing loss*. J Pathol, 2007. **211**(2): p. 188-97.
232. Dallos, P., *The active cochlea*. J Neurosci, 1992. **12**(12): p. 4575-85.
233. Brownell, W.E., *Outer hair cell electromotility and otoacoustic emissions*. Ear Hear, 1990. **11**(2): p. 82-92.
234. Dorn, P.A., et al., *On the existence of an age/threshold/frequency interaction in distortion product otoacoustic emissions*. J Acoust Soc Am, 1998. **104**(2 Pt 1): p. 964-71.
235. Uchida, Y., et al., *The effects of aging on distortion-product otoacoustic*

-
- emissions in adults with normal hearing*. Ear Hear, 2008. **29**(2): p. 176-84.
236. Oeken, J., A. Lenk, and F. Bootz, *Influence of age and presbycusis on DPOAE*. Acta Otolaryngol, 2000. **120**(3): p. 396-403.
237. Varghese, G.I., X. Zhu, and R.D. Frisina, *Age-related declines in distortion product otoacoustic emissions utilizing pure tone contralateral stimulation in CBA/CaJ mice*. Hear Res, 2005. **209**(1-2): p. 60-7.
238. Parham, K., *Distortion product otoacoustic emissions in the C57BL/6J mouse model of age-related hearing loss*. Hear Res, 1997. **112**(1-2): p. 216-34.
239. Parham, K., X.M. Sun, and D.O. Kim, *Distortion product otoacoustic emissions in the CBA/J mouse model of presbycusis*. Hear Res, 1999. **134**(1-2): p. 29-38.
240. Jimenez, A.M., et al., *Age-related loss of distortion product otoacoustic emissions in four mouse strains*. Hear Res, 1999. **138**(1-2): p. 91-105.
241. Zhu, X., et al., *Auditory efferent feedback system deficits precede age-related hearing loss: contralateral suppression of otoacoustic emissions in mice*. J Comp Neurol, 2007. **503**(5): p. 593-604.
242. Kopke, R., et al., *A radical demise. Toxins and trauma share common pathways in hair cell death*. Ann N Y Acad Sci, 1999. **884**: p. 171-91.
243. Guthrie, O.W. and F.A. Carrero-Martinez, *Real-Time Quantification of Xeroderma pigmentosum mRNA From the Mammalian Cochlea*. Ear Hear, 2010.
244. Someya, S., et al., *Age-related hearing loss in C57BL/6J mice is mediated by Bak-dependent mitochondrial apoptosis*. Proc Natl Acad Sci U S A, 2009. **106**(46): p. 19432-7.
245. Spear, P.D., *Neural bases of visual deficits during aging*. Vision Res, 1993. **33**(18): p. 2589-609.
246. Gorgels, T.G., et al., *Retinal degeneration and ionizing radiation hypersensitivity in a mouse model for Cockayne syndrome*. Mol Cell Biol, 2007. **27**(4): p. 1433-41.
247. Gao, H. and J.G. Hollyfield, *Aging of the human retina. Differential loss of neurons and retinal pigment epithelial cells*. Invest Ophthalmol Vis Sci, 1992. **33**(1): p. 1-17.
248. Curcio, C.A., et al., *Aging of the human photoreceptor mosaic: evidence for selective vulnerability of rods in central retina*. Invest Ophthalmol Vis Sci, 1993. **34**(12): p. 3278-96.

249. Aggarwal, P., T.C. Nag, and S. Wadhwa, *Age-related decrease in rod bipolar cell density of the human retina: an immunohistochemical study*. J Biosci, 2007. **32**(2): p. 293-8.
250. Panda-Jonas, S., J.B. Jonas, and M. Jakobczyk-Zmija, *Retinal photoreceptor density decreases with age*. Ophthalmology, 1995. **102**(12): p. 1853-9.
251. Weisse, I., H. Loosen, and H. Peil, *Age-related retinal changes--comparison between albino and pigmented rats*. Lens Eye Toxic Res, 1990. **7**(3-4): p. 717-39.
252. Imai, R. and Z. Tanakamaru, *Visual dysfunction in aged Fischer 344 rats*. J Vet Med Sci, 1993. **55**(3): p. 367-70.
253. O'Steen, W.K., et al., *Analysis of severe photoreceptor loss and Morris water-maze performance in aged rats*. Behav Brain Res, 1995. **68**(2): p. 151-8.
254. Spencer, R.L., W.K. O'Steen, and B.S. McEwen, *Water maze performance of aged Sprague-Dawley rats in relation to retinal morphologic measures*. Behav Brain Res, 1995. **68**(2): p. 139-50.
255. Feng, L., et al., *No age-related cell loss in three retinal nuclear layers of the Long-Evans rat*. Vis Neurosci, 2007. **24**(6): p. 799-803.
256. Bravo-Nuevo, A., N. Walsh, and J. Stone, *Photoreceptor degeneration and loss of retinal function in the C57BL/6-C2J mouse*. Invest Ophthalmol Vis Sci, 2004. **45**(6): p. 2005-12.
257. Sanyal, S. and R.K. Hawkins, *Development and degeneration of retina in rds mutant mice: effects of light on the rate of degeneration in albino and pigmented homozygous and heterozygous mutant and normal mice*. Vision Res, 1986. **26**(8): p. 1177-85.
258. Sickel, W., *Electrical and metabolic manifestations of receptor and higher-order neuron activity in vertebrate retina*. Adv Exp Med Biol, 1972. **24**(0): p. 101-18.
259. Jarrett, S.G., J. Albon, and M. Boulton, *The contribution of DNA repair and antioxidants in determining cell type-specific resistance to oxidative stress*. Free Radic Res, 2006. **40**(11): p. 1155-65.
260. Klaver, C.C., et al., *Age-specific prevalence and causes of blindness and visual impairment in an older population: the Rotterdam Study*. Arch Ophthalmol, 1998. **116**(5): p. 653-8.
261. Vrensen, G.F., *Early cortical lens opacities: a short overview*. Acta Ophthalmol, 2009. **87**(6): p. 602-10.

-
262. Ting, A.Y., T.K. Lee, and I.M. MacDonald, *Genetics of age-related macular degeneration*. *Curr Opin Ophthalmol*, 2009. **20**(5): p. 369-76.
263. Chiu, C.J. and A. Taylor, *Nutritional antioxidants and age-related cataract and maculopathy*. *Exp Eye Res*, 2007. **84**(2): p. 229-45.
264. Sackett, C.S. and S. Schenning, *The age-related eye disease study: the results of the clinical trial*. *Insight*, 2002. **27**(1): p. 5-7.
265. Delcourt, C., et al., *Age-related macular degeneration and antioxidant status in the POLA study*. *POLA Study Group. Pathologies Oculaires Liees a l'Age*. *Arch Ophthalmol*, 1999. **117**(10): p. 1384-90.
266. Delcourt, C., et al., *Associations of antioxidant enzymes with cataract and age-related macular degeneration*. *The POLA Study. Pathologies Oculaires Liees a l'Age*. *Ophthalmology*, 1999. **106**(2): p. 215-22.
267. Wozniak, K., et al., *DNA damage/repair and polymorphism of the hOGG1 gene in lymphocytes of AMD patients*. *J Biomed Biotechnol*, 2009. **2009**: p. 827562.
268. Szaffik, J.P., et al., *DNA damage and repair in age-related macular degeneration*. *Mutat Res*, 2009. **669**(1-2): p. 169-76.
269. Ding, X., M. Patel, and C.C. Chan, *Molecular pathology of age-related macular degeneration*. *Prog Retin Eye Res*, 2009. **28**(1): p. 1-18.

Chapter 2

Accelerated age-related cognitive decline and neurodegeneration caused by deficient DNA repair

Nils Z. Borgesius, Monique C. de Waard, Ingrid van der Pluijm, Azar Omrani, Gerben C. M. Zondag, Gijsbertus T. J. van der Horst, David. W. Melton, Jan H. J. Hoeijmakers, Dick Jaarsma, Ype Elgersma

submitted

Abstract

Age-related cognitive decline and neurodegenerative diseases are a growing challenge for our societies with their aging populations. DNA damage has been shown to accumulate with age, but direct proof that DNA damage results in impaired neuronal plasticity and memory is lacking. Here we show that *Ercc1*^{-/-} mutant mice, which are impaired in the DNA repair pathways nucleotide excision repair, interstrand crosslink repair and double strand break repair, exhibit an age-dependent decrease in neuronal plasticity and neurodegenerative changes. A similar phenotype is observed in mice where the mutation is restricted to excitatory forebrain neurons. Moreover, these mice develop a learning impairment. Taken together, these results show a causal relationship between unrepaired DNA damage and age-dependent cognitive decline and neurodegeneration. Hence, accumulated DNA damage could be an important factor in the onset and progression of age-related cognitive decline and neurodegenerative diseases.

Introduction

Accumulated DNA damage is thought to be an important factor underlying aging [1]. Several studies show that aging is accompanied by accumulation of neuronal DNA damage in rodents and humans [2-5]. The accumulation of this unrepaired DNA damage is greatest in organs with limited cell proliferation such as the brain [6]. Furthermore, the brain is particularly vulnerable to oxidative stress since it exhibits very high oxygen metabolism, has abundant lipid content and relatively low levels of antioxidant compared to other organs [6-9]. Moreover, the human brain is one of the most active organs at the transcriptional level [10]. Therefore neurons may be especially prone to DNA lesions resulting from oxidative stress and accumulate unrepaired DNA lesions throughout life, which eventually may alter transcription, trigger DNA damage responses and ultimately cause neuronal degeneration.

Increased oxidative DNA damage has been observed in subjects with mild cognitive impairments as well as late-Alzheimer's Disease (AD) [11-13] suggesting a correlation between age-related accumulation of DNA damage and cognitive decline. Evidence linking DNA damage to cognitive impairment follows from animals and patients receiving genotoxic chemotherapeutic drugs [14, 15]. In addition, hypomorphic mutations in DNA repair genes may cause neurological impairments and segmental accelerated aging, observed in a variety of progeroid conditions like xeroderma pigmentosum (XP), Cockayne syndrome (CS) and trichothiodystrophy (TTD) [16-18]. XP, CS and TTD patients are defective in nucleotide excision repair and show neurological abnormalities and progressive neurodegeneration [1, 19-22]. However, in above examples, it cannot be ruled out that the cognitive dysfunction is secondary to the large impact of chemotherapy or progeroid syndrome on overall health.

To examine whether unrepaired DNA damage is indeed sufficient to induce age-related neurodegeneration and cognitive decline we made use of a global as well as a neuron-specific mouse mutant with impaired DNA repair function. In both mouse mutants we targeted the excision repair cross-complementing group 1 (*Ercc1*) gene. ERCC1 forms a stable complex with the xeroderma pigmentosum group F protein (XPF) and is involved in multiple DNA repair pathways: nucleotide excision repair for the removal of helix distorting DNA damage [23], interstrand crosslink repair [24, 25] and double strand break repair [26, 27]. As a consequence of the *Ercc1* mutation and the resulting DNA repair defect, complete *Ercc1* knockout animals (*Ercc1*^{-/-}) exhibit various age-related symptoms already at the age of 2-3 weeks including early cessation of growth, ataxia, cachexia, kyphosis, as well as aging of different organs, such as hepatocellular

polyploidization, intra-nuclear inclusions and lipofuscin accumulation in the liver and kidney, and multilineage cytopenia and fatty replacement of bone marrow, which are both hallmarks of normal mouse aging [28-30]. These *Ercc1*^{-/-} knockout animals die prematurely with a maximal lifespan of approximately 8 weeks. Full mouse genome expression analysis of various organs of these DNA repair deficient, progeroid mice revealed significant overlap in expression profile changes observed in normal aging, stressing the parallels between accelerated and natural aging [31, 32].

To study the effect of unrepaired DNA damage in all tissues on neuronal function, we made use of the global *Ercc1*^{Δ/-} mouse mutant, which carries in one allele of the *Ercc1* gene a null mutation. The protein derived from the second allele shows reduced activity, due to a seven amino-acid carboxy-terminal truncation [29]. This hypomorphic mutation results in severely impaired nucleotide excision repair, interstrand crosslink repair [29] and double strand break repair [26]. These animals have the exact same phenotype as the *Ercc1*^{-/-}, but since the mutation is less severe, the aging symptoms arise at a slower pace and the *Ercc1*^{Δ/-} thereby can reach an age of about 25-30 weeks, which makes them an ideal model to study the age-related neurological phenotype in more detail. Recently it was shown that these animals also have age-related neuronal changes in the spinal cord, as well as in neuromuscular junctions [33]. To specifically study the effect of neuronal unrepaired DNA damage in the brain on behavior and neuronal plasticity we generated a conditional knockout model in which the *Ercc1* gene was deleted in post-mitotic excitatory neurons of the forebrain and investigated the hippocampal functioning.

Here we show that both these DNA repair mutants display an age-dependent decline in synaptic plasticity. Moreover, the neuron-specific knockout mice showed an age-dependent decline in cognitive function and we observed an age-dependent increase of astrogliosis and an increased labeling of markers that indicate mild ongoing neuronal degeneration. Taken together, our data supports the notion that accumulation of unrepaired (neuronal) DNA damage can contribute to age-related neuronal dysfunction and cause neurodegeneration and cognitive decline.

Results

***Ercc1*^{Δ/-} mice develop mild neurodegenerative changes**

Ercc1^{Δ/-} mutants and their wild-type littermates were analyzed at 1 and 4 months of age. The age of 4 months was chosen since at this age animals display clear signs of premature aging, without significant mortality. The maximum lifespan of these mice in the genetically homogeneous F1 C57BL/6J-FVB/N hybrid genetic background used

here is approximately 6 months [33].

Macroscopically, the brains of *Ercc1^{Δ/Δ}* mice are smaller, but proportional to their reduced body size. Furthermore, they showed no gross morphological abnormalities in a thionin staining (Figure 1A) indicating that there is no evident developmental perturbation, and that neurons are relatively preserved at both ages, consistent with the largely normal embryonic development. Moreover, 4 month old *Ercc1^{Δ/Δ}* mice did not show reduced immunolabeling of the somato-dendritic marker MAP2 compared to their littermates, again suggesting that there is no overt neuronal loss (Figure 1B left panels). However, immunostaining for glial acidic filament protein (GFAP) showed positive staining throughout the central nervous system in 4 months old *Ercc1^{Δ/Δ}* mice, while at 1 month staining was relatively normal indicating age-dependent reactive astrogliosis (Figure 1A lower panels and 1B middle panels). A silver staining method that selectively labels degenerating neurons and their axons (Figure 1C) showed very few dying neurons in several brain areas of 1 month old *Ercc1^{Δ/Δ}* mice, including the hippocampus and striatum. This was significantly increased in 4 month old mice, while the littermates showed no labeling. Additional evidence for mild neuronal degeneration was obtained by staining brain sections with ATF3, an injury-induced transcription factor expressed in cells afflicted by multiple types of pathology [34] and transcription factor p53, which is activated by several types of DNA damage and implicated in neuronal degeneration [35] (Figure 1D and Figure S1D-E). Already at 1 month of age, *Ercc1^{Δ/Δ}* mice showed neurons with ATF3- and p53-labeled nuclei throughout the brain, and this number was significantly increased at 4 months of age (Figure 1D). Moreover, many of the ATF3-positive neurons showed eccentric nuclei suggestive of poor state (Figure S1D). Double labeling with neuronal marker NeuN showed that >95% of the p53- and ATF3-positive cells are neurons (Figure S1E). In contrast, ATF3 labeling was absent in most brain areas of wild-type mice except for weakly labeled neuronal nuclei in the dentate gyrus, olfactory bulb, and pyriform cortex. In addition, no p53-positive nuclei were observed in wild-type mice.

Immunohistochemistry of activated caspase 3, a final executioner caspase in multiple cell death pathways [36], revealed a low but distinctive number of labeled cells in several brain areas of *Ercc1^{Δ/Δ}* mice, including hippocampus and cortex, (Figure 1D and Figure S1A-C). Most labeled cells showed a neuronal morphology, although caspase 3 immunoreactivity was also observed to be associated with glial cells in both the white and gray matter (Figure S1C). In contrast, wild-type mice did not show any caspase 3 activation. Consistent with findings in other mouse models of neurodegenerative disease

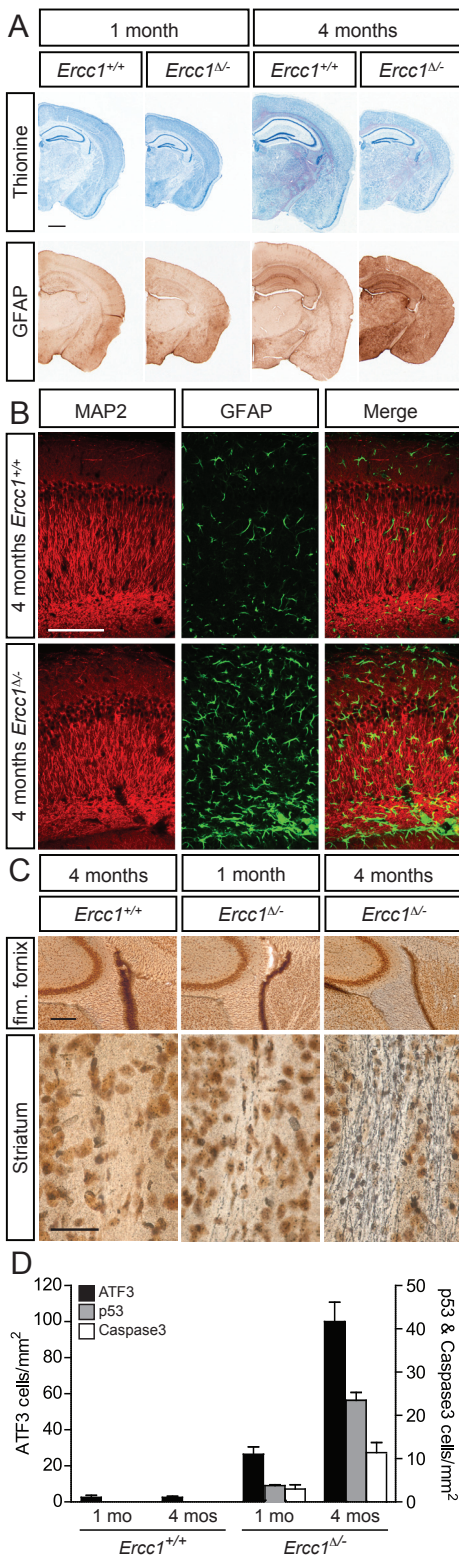


Figure 1. *Ercc1^{Δ/Δ}* mice display mild neuronal degeneration and reactive astrocytosis

(A) Immunostaining of coronal brain slices with thionine showing normal gross morphology in *Ercc1^{Δ/Δ}* mice of the brain. GFAP staining shows increased GFAP expression throughout the brain of 4 months old *Ercc1^{Δ/Δ}* mice. (scale bar 500 μ m)

(B) Confocal immunostaining images of CA1 area in the hippocampus showing normal levels of MAP2 (left panels) and increasing GFAP staining (middle panels) in 4 months old *Ercc1^{Δ/Δ}* mice compared to age-matched littermates. (scale bar 100 μ m)

(C) Silver staining showing age related axonal degeneration in fimbria fornix (upper panels) and in the fibers of the internal capsule of the striatum (lower panels) in *Ercc1^{Δ/Δ}* mice. Low levels of argyrophilic degeneration staining were mostly observed in the gray matter of 4 months old *Ercc1^{Δ/Δ}* mice. (scale bar upper panels 250 μ m; lower panels 50 μ m)

(D) Quantification of cortical cell density positive for ATF3, p53 or caspase 3 (y-axis on left indicates values for ATF3; y-axis on the right indicates values for p53 and caspase 3). All data are reported as mean \pm SEM. Two-way ANOVA revealed a significant effect for genotype, age and their interaction for ATF3 (all $p < 0.0001$), p53 (all $p < 0.0001$) and caspase 3 (all $p < 0.01$).

See also Figure S1

[37], the density of ATF3-labeled cells was higher than the level of caspase 3 positive cells (Figure 1D). Also p53 labeling was much less abundant compared to ATF3-positive nuclei. One explanation is that a degenerating neuron expresses ATF3 for a longer period than p53 or caspase 3 before it is cleared by apoptosis. Alternatively, unrepaired DNA damage may trigger an injury response without concomitant activation of cell death pathways. Taken together, these neuropathological data indicate that 4 month old *Ercc1^{Δ/Δ}* mice show a low number of neurons in the process of dying while a greater number of neurons show signs of genotoxic stress and poor condition.

***Ercc1^{Δ/Δ}* mice show reduction of hippocampal synaptic plasticity**

We investigated basal synaptic transmission properties of *Ercc1^{Δ/Δ}* mice, using field potential measurements. The ratio between the fEPSP slope and the fiber volley, which is a measure of the efficacy of the synapses, did not differ significantly between genotypes at either 1 month or at 4 months of age, suggesting no changes in basal synaptic transmission (Figure S2A and S2B; $F_{1,74}=2.5$, $P = 0.11$; $F_{1,138}=2.0$, $P = 0.16$, one-way ANOVA for 1 month and 4 months old, respectively).

Synaptic plasticity can be assessed *in vitro* by measuring the ability of synaptic connections to become potentiated upon a train of high frequency stimulation, a process known as long-term potentiation (LTP). LTP was induced at the Schaffer-collateral synapse with a 10 Hz stimulus. Although LTP was observed in all groups, 4 months old *Ercc1^{Δ/Δ}* mice showed significantly less LTP as compared with their controls, whereas no significant difference was observed in 1 month old mice, indicating normal initial functioning and accelerated, progressive decline in plasticity (Figure 2A and 2B; $F_{1,24}=0.6$, $P = 0.40$; $F_{1,35}=5.3$, $P < 0.05$, one-way ANOVA for 1 month and 4 months old respectively). A reduction of LTP was also observed when using a strong (100 Hz) stimulus; 4 months old *Ercc1^{Δ/Δ}* mice, but not 1 month old *Ercc1^{Δ/Δ}* mice, displayed significantly reduced LTP compared to age-matched controls (Figure 2C and 2D; $F_{1,27}=2.7$ $P = 0.10$; $F_{1,33}=13.4$, $P < 0.001$, one-way ANOVA for 1 month and 4 months old respectively). These results show that *Ercc1^{Δ/Δ}* mice develop an age-related impairment of synaptic plasticity.

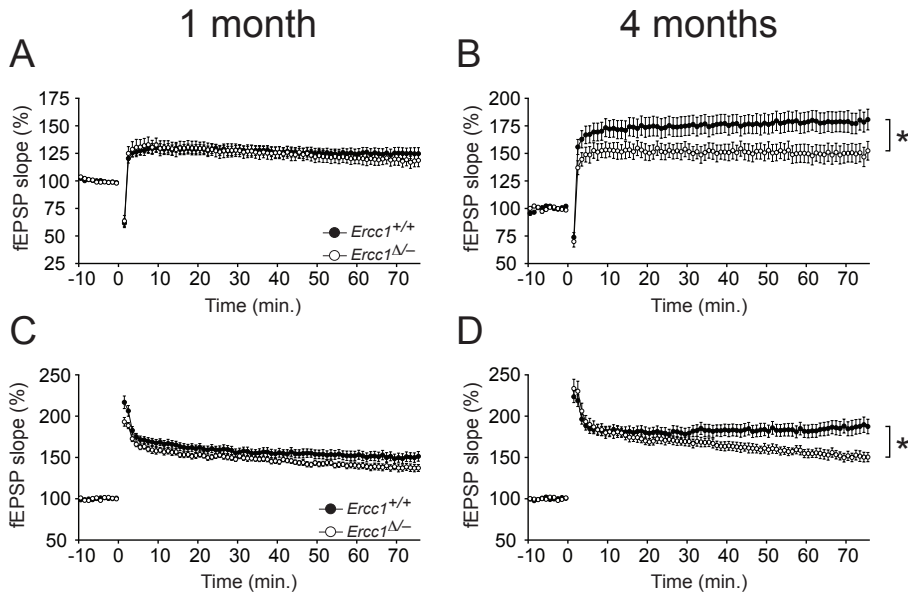


Figure 2. *Ercc1*^{Δ/Δ} mice show reduced synaptic plasticity at 4 months of age

- (A) 10 Hz LTP in 1 month old mice shows no difference between *Ercc1*^{Δ/Δ} and *Ercc1*^{+/+} mice.
 (B) 10 Hz LTP in 4 months old mice shows reduced LTP in *Ercc1*^{Δ/Δ} mice.
 (C) 100 Hz LTP in 1 month old mice shows no difference between *Ercc1*^{Δ/Δ} and *Ercc1*^{+/+} mice.
 (D) 100 Hz LTP in 4 months old mice shows reduced LTP in *Ercc1*^{Δ/Δ} mice.

All data are reported as mean \pm SEM. Significantly different ($P < 0.05$) from age-matched *Ercc1*^{+/+} mice indicated by *. See also Figure S2

Unrepaired DNA damage exclusively in excitatory post-natal forebrain neurons causes gradual neuronal degeneration and reactive astrocytosis

Although the aforementioned results showed that the global *Ercc1*^{Δ/Δ} mutation significantly affects neuronal health and plasticity, it cannot be ruled out that these outcomes are secondary to the reduced fitness of these animals due to liver, kidney and other pathology [28, 29, 33, 38, 39]. To examine the direct effect of unrepaired DNA in neurons, and to rule out possibly confounding effects of systemic aging pathology, we made use of the Cre-loxP system to generate mutant mice with a neuron-specific ablation of *Ercc1*.

Ercc1^{fl/fl} mice containing a floxed *ercc1* gene were crossed with *Ercc1*^{+/-}CaMKII-Cremice, resulting in *Ercc1*^{fl/-}CaMKII-Cre mice (hereinafter referred to as *Ercc1*^{fl/-} mice). *Ercc1*^{fl/-}, which are homozygous *Ercc1* knockouts in α CaMKII-expressing cells (mostly excitatory post-mitotic neurons of the hippocampus and cortex), and heterozygous for *Ercc1* in the rest of their body. As controls we used *Ercc1*^{fl/+}CaMKII-Cre littermates,

which are heterozygous for the *Ercc1* gene in the α CaMKII-expressing cells, and wild-type in the rest of their body (hereinafter *Ercc1^{f/+}*). (See Experimental Procedures for details and origin of mouse lines). Importantly, heterozygosity for *Ercc1* does not result in an obvious phenotype (data not shown) [29]. Indeed the two genotypes were very similar in overall appearance, health and bodyweight (data not shown) and could not be distinguished by eye, in contrast to the global *Ercc1^{Δ/Δ}* and their littermates.

The brains of 2 months old *Ercc1^{f/-}* mice showed no detectable difference in GFAP staining compared to their *Ercc1^{f/+}* controls (Figure S3A). At the age of 4 months GFAP staining was increased mainly in hippocampus and cortex and this increase progressed resulting in further elevated levels of GFAP staining at 6 months (Figures 3A and 3B middle panel). Although this resembles the phenotype of the *Ercc1^{Δ/Δ}* mice, the reactive astrogliosis does not seem as severe as in the 4 months old *Ercc1^{Δ/Δ}* mice. *Ercc1^{f/-}* mice did not show a detectable reduction of the neuronal somato-dendritic marker MAP2 in the hippocampus and cortex between the age of 2 and 6 months (Figure 3B) with levels comparable to *Ercc1^{f/+}* control mice (data not shown). This indicates that, similar to the *Ercc1^{Δ/Δ}* mice, there is no major loss of neurons in *Ercc1^{f/-}* mice. However, silver staining clearly shows some degenerating axons in 6 months old *Ercc1^{f/-}* mice as opposed to age-matched control mice. A low but distinctive number of cells were labeled in hippocampus and cortex and degenerating axons were stained in the fimbria-fornix (Figure 3C and data not shown). Further evidence for neurodegeneration was obtained using stainings for ATF3, p53 and caspase 3 (Figure 3D and Figure S3B-E). Only very few ATF3, p53 and caspase 3 positive cells were observed in 2 months old *Ercc1^{f/-}* and *Ercc1^{f/+}* mice. However, at 4 months of age, the number of ATF3- and p53-positive nuclei was increased in the cortex of *Ercc1^{f/-}* mice and this progressed further resulting in an approximate doubling at 6 months of age (Figure 3D). Of the ATF3- and p53-positive cells >95% are NeuN-positive. The frequency of caspase 3 positive cells was much lower than the abundance of ATF3 and p53 cells, but there was an age-related increase in the number of caspase 3 stained cells from 4 to 6 months of age in *Ercc1^{f/-}* mice, indicating that a low level of apoptosis and neuronal loss is indeed occurring. Together this shows that neuronal degeneration progressively increases in *Ercc1^{f/-}* mice. Furthermore, the lower expression of caspase 3 compared to ATF3 is similar to what we found in *Ercc1^{Δ/Δ}* mice and what has been observed in other models of neurodegenerative disease [37]. In contrast, *Ercc1^{f/+}* control mice showed negligible ATF3, p53 and caspase 3 staining in the cortex at 2, 4 and 6 months of age (Figure 3D and Figure S3C-E).

In conclusion, these immunohistochemistry data show that the *Ercc1^{f/-}* mice have

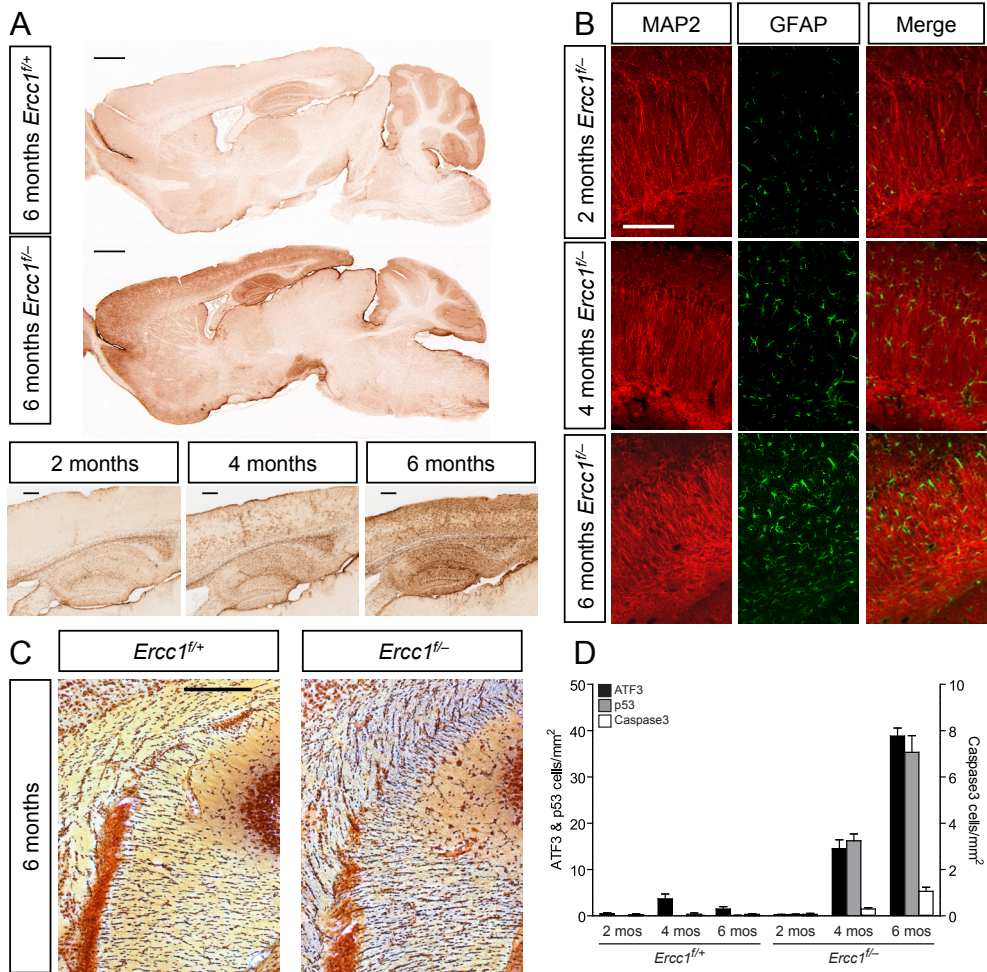


Figure 3. DNA damage accumulation exclusively in neurons causes slow ongoing neuronal degeneration and reactive astrocytosis

(A) GFAP immunostaining indicates increased GFAP expression in sagittal brain slices of 6 months old *Ercc1^{fl/-}* mice, compared to *Ercc1^{fl/+}* mice of the same age. The lower panels show progressive GFAP staining (in hippocampus) of *Ercc1^{fl/-}* mice. (scale bar 1 mm)

(B) Confocal immunostaining images of CA1 area in the hippocampus showing normal levels of MAP2 (left panels) and increased GFAP staining in *Ercc1^{fl/-}* mice. (scale bar 100 μ m)

(C) Silver staining showing increasing axonal degeneration in fimbria fornix of *Ercc1^{fl/-}* and not in *Ercc1^{fl/+}* mice at 6 months of age. (scale bar 200 μ m)

(D) Quantification of cortical cell density positive for ATF3, p53 or caspase 3 (y-axis on left indicates values for ATF3; y-axis on the right indicates values for p53 and caspase 3). All data are reported as mean \pm SEM. Two-way ANOVA revealed a significant effect for genotype, age and their interaction for ATF3 (all $p < 0.0001$), p53 (all $p < 0.0001$) and caspase 3 (all $p < 0.05$). See also Figure S3

similar pathologies in hippocampus and cortex as the *Ercc1^{A/-}* mice, establishing a cell intrinsic cause of the neuronal phenotype and demonstrating that increased unrepaired DNA damage in excitatory neurons is sufficient to cause increased expression of markers that are indicative for neuronal (genotoxic) stress and degeneration.

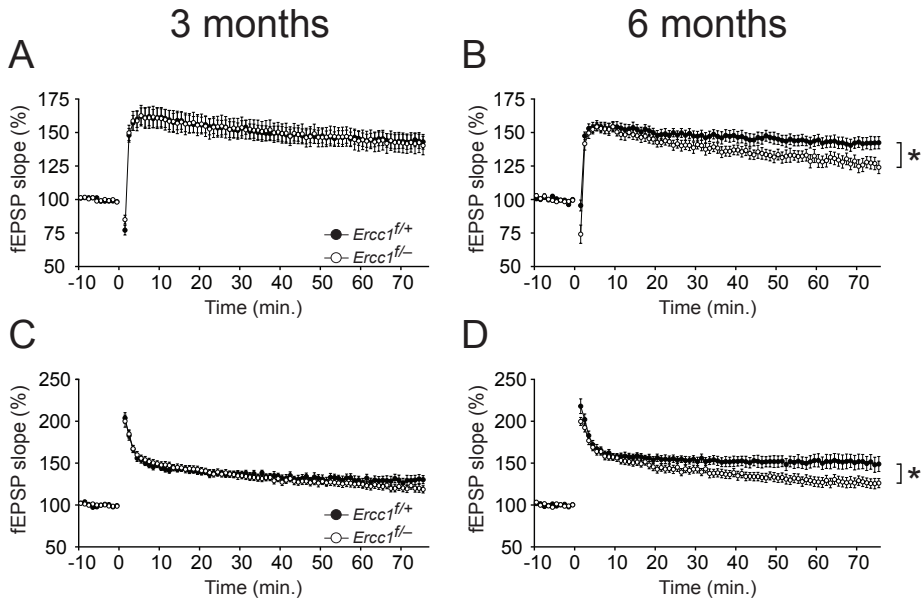


Figure 4. *Ercc1^{fl/-}* mice show reduced synaptic plasticity at 6 months of age

(A) 10 Hz LTP in 3 months old mice shows no difference between *Ercc1^{fl/-}* and *Ercc1^{fl/+}* mice.

(B) 10 Hz LTP in 6 months old mice shows reduced LTP in *Ercc1^{fl/-}* mice.

(C) 100 Hz LTP in 3 months old mice shows no difference between *Ercc1^{fl/-}* and *Ercc1^{fl/+}* mice.

(D) 100 Hz LTP in 6 months old mice shows reduced LTP in *Ercc1^{fl/-}* mice.

All data are reported as mean \pm SEM. All data are reported as mean \pm SEM. Significantly different ($P < 0.05$) from age-matched *Ercc1^{fl/+}* mice indicated by *. See also Figure S4

Unrepaired DNA damage in excitatory neurons causes a reduction of LTP

We studied the electrophysiological properties of the *Ercc1^{fl/-}* mouse hippocampus to determine whether neuronal DNA damage is sufficient to cause the aging-like phenotype at the level of synaptic plasticity. Similar to the *Ercc1^{A/-}* mice, the *Ercc1^{fl/-}* mice showed no detectable impairment in synaptic transmission. The ratio between fEPSP slope and fiber volley did not differ at both 3 and 6 months of age (Figure S4A and S4B; $F_{1,89} = 2.9$, $P = 0.09$; $F_{1,95} = 2.2$, $P = 0.14$ one-way ANOVA for 3 and 6 months old respectively). Next we investigated the ability to induce LTP at the Schaffer-collateral synapse using a 10 Hz stimulus. Although LTP was observed in all 4 groups, 6 months old *Ercc1^{fl/-}*

mice showed significantly less LTP as compared with their littermate *Ercc1^{f/+}* controls whereas no significant difference was observed for the 3 months old mice (Figure 4A and 4B; $F_{1,33} < 0.001$, $P = 1.0$; $F_{1,23} = 5.8$, $P < 0.05$, one way ANOVA for 3 and 6 months old respectively). With the strong 100 Hz stimulus we got similar results; 6 months old *Ercc1^{f/-}* mice but not 3 months old mice showed significantly reduced LTP as compared to their age-matched controls (Figure 4C and 4D; $F_{1,29} = 1.6$, $P = 0.20$; $F_{1,30} = 5.6$, $P < 0.05$, one way ANOVA for 3 and 6 months old respectively). Hence, by restricting the defect in DNA repair to the excitatory neurons of the hippocampus, the mice are overall healthy, but hippocampal plasticity is still affected in an age-dependent fashion.

Unrepaired DNA damage exclusively in neurons causes impaired hippocampal learning

Having shown that the *Ercc1^{f/-}* mice are physically in good condition, but with regard to the hippocampus still display a similar accelerated aging phenotype as the *Ercc1^{d/-}* mice, both in cellular pathology and *in vitro* synaptic plasticity, we continued to test hippocampus-dependent learning using the Morris water maze test. In this test animals are trained over several days to locate a submerged platform in a circular pool filled with opaque water using distal visual cues. All 4 groups showed a significant reduction of their latency times to find the platform across training days (Figure 5A and 5B; effect of training: $F_{4,88} = 38.8$, $P < 0.01$; $F_{4,104} = 21.2$, $P < 0.01$, repeated measures ANOVA for 3 and 6 months old respectively). There was no significant effect of genotype in both age groups (Figure 5A and 5B; effect of genotype: $F_{1,22} = 0.6$, $P = 0.44$; $F_{1,26} = 2.1$, $P = 0.15$, repeated measures ANOVA for 3 and 6 months old respectively). These data indicate that mice in all 4 groups were able to execute this task and improve their performance. To test whether the mutants had indeed learned the spatial location, a probe trial in which the platform was removed, was given after 5 days of training. This probe trial showed that all 4 groups of mice spent significantly more time in the target quadrant than in any of the other quadrants indicating that the mutants had indeed learned and remembered the platform location at both 3 and 6 months of age (Figure 5C and 5D). However, although all four groups showed preference for the target location, 6 months old mutants spent significant less time in the target quadrant as compared to 3 month old mutants ($F_{1,30} = 4.4$, $P = 0.0001$ one-way ANOVA), and the heat-plot of the search pattern of the 6 months old *Ercc1^{f/-}* mice indicates less specific searching in the aged mutants, as compared to the other groups (Figure 5E and 5F), suggesting that they have not learned the platform position as well as the age-matched controls.

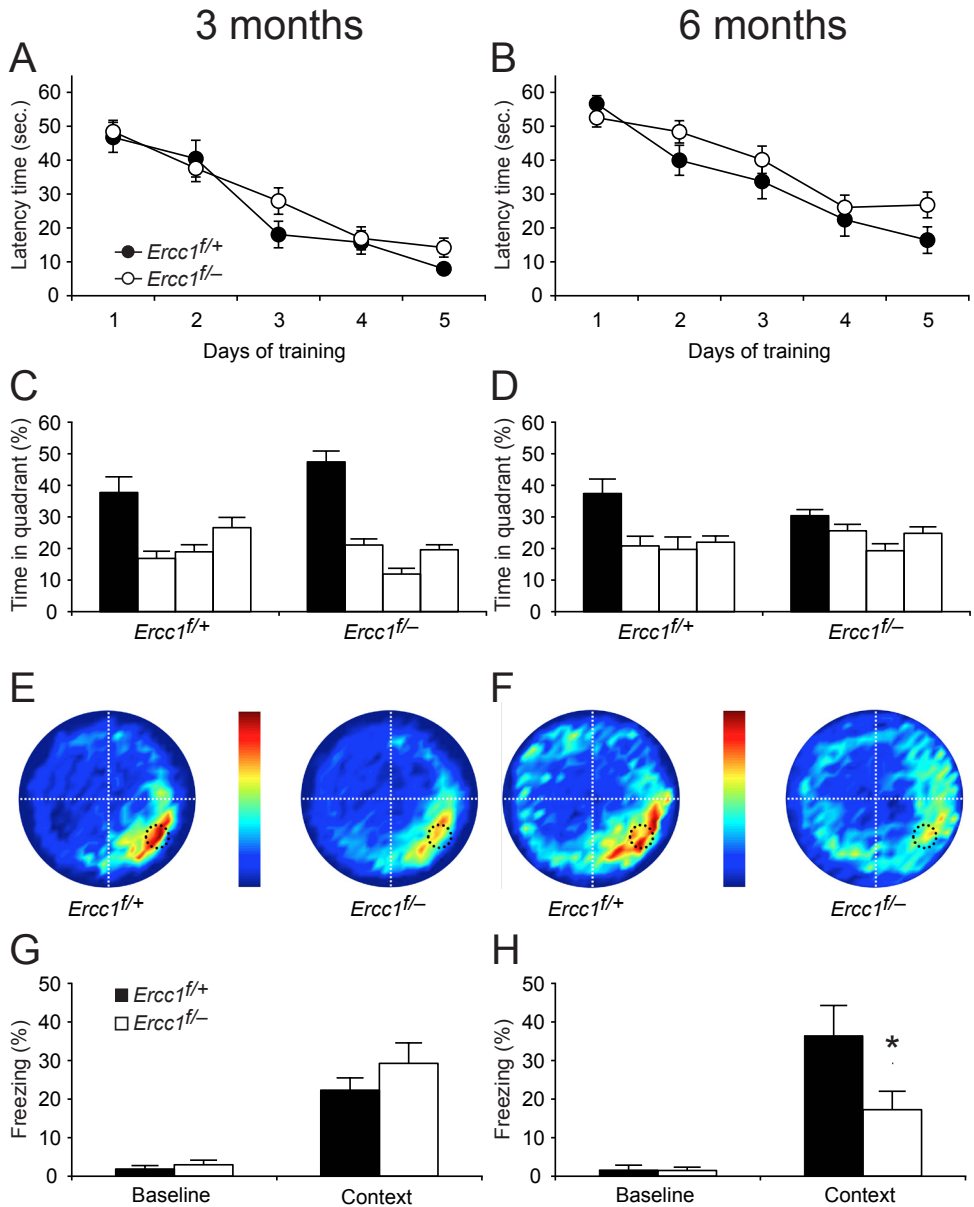


Figure 5. *Ercc1^{f/-}* mice show impaired fear conditioning and normal water maze performance at 6 months of age

(A and B) Escape latency of 3 months old (A) and 6 months old mice (B) shows no difference between *Ercc1^{f/-}* and *Ercc1^{f/+}* mice.

(C and D) Quantification of quadrant occupancy in 3 months old (C) and 6 months old mice (D), during the probe trial performed at day 5. Although all groups searched significantly more in the target quadrant, *Ercc1^{f/-}* mice spent significantly less time in the target quadrant as compared to the 3 months old *Ercc1^{f/-}* mice.

(E and F) Visual representation of all search tracks during the probe trial of the 3 months old (E) and 6 months (F) old mice. The color of the heat plots indicate the mean time spent at a certain location. The white and black dashed lines indicate quadrants and former platform location respectively.

(G and H) Contextual fear conditioning in 3 months old mice (G) and 6 months old mice (H). 6 months old *Ercc1^{-/-}* mice show normal baseline freezing before the shock but significantly reduced freezing when placed in the context 24 h after the shock. All data are reported as mean \pm SEM. Significantly different ($P < 0.05$) from age-matched *Ercc1^{+/+}* mice indicated by *.

As an additional test to assess hippocampus-dependent learning, we made use of contextual fear conditioning. In this single-trial learning task, mice are conditioned to associate a certain context with a mildly aversive foot shock. This learning paradigm has been shown to require both a functional hippocampus as well as amygdala [40]. Learning is assessed by measuring freezing behavior, *i.e.* the cessation of all movement except respiration, which is a natural expression of fear in mice. At 3 months of age the *Ercc1^{-/-}* mice showed an indistinguishable freezing response from their littermate *Ercc1^{+/+}* controls (Figure 5G; $F_{1,27}=0.7$, $P = 0.40$, one way ANOVA). However, at 6 months the *Ercc1^{-/-}* mice froze significantly less than their littermate *Ercc1^{+/+}* controls (Figure 5H; $F_{1,21}=4.2$, $P < 0.05$, one way ANOVA). Neither the 3 months old groups nor the 6 months old groups showed a difference in baseline freezing, thereby indicating that the mutation did not affect anxiety levels (Figure 5G and 5H; $F_{1,27}=0.3$, $P = 0.6$; $F_{1,13}=1.3$, $P = 0.3$, one way ANOVA for 3 and 6 months old respectively). These results show that mice in which the defect in DNA repair is limited to neurons develop an age-related impairment of context-dependent fear learning.

Discussion

Despite strong correlative data suggesting a relation between DNA damage and age-related cognitive decline there is no direct causal proof that a defect in DNA repair resulting in accumulation of unrepaired DNA damage can induce cognitive deficits. This study shows that defective DNA repair, either in the entire body or in neurons alone, causes an accelerated aging-like phenotype of the brain with respect to both cellular pathology and synaptic plasticity deficits. In addition, we show that in otherwise healthy animals, defective DNA repair restricted to excitatory neurons is sufficient to affect learning. Taken together these results indicate that DNA damage accumulation can contribute to age-related cognitive decline.

The cellular pathology observed was very similar in both the global and the

neuron-specific *Ercc1* mutant and resembles mild neurodegeneration. This indicates that DNA damage in neurons alone is sufficient to cause neurodegeneration and suggests that the phenotype in the global *Ercc1*^{Δ/Δ} mutant could mostly be due to the effect of neuronal DNA damage. Using the neuron-specific NeuN marker we have shown that the vast majority of p53- and ATF3-positive cells in the global *Ercc1*^{Δ/Δ} mutants are neurons. As the same is observed in the neuron-specific mutant this indicates that the activation of p53 and ATF3 is a direct effect of neuronal DNA damage in the *Ercc1*^{Δ/Δ} mutant and not a secondary effect of other affected cell types. Moreover, this suggests that neurons are more sensitive to DNA damage. Alternatively, glial cells respond differently to DNA damage or are p53- and ATF3-positive for a shorter period. However, in the spinal cord of the *Ercc1*^{Δ/Δ} mutant similar amounts of neurons and glial cells are p53-positive [33]. Therefore, either glial cells respond differently to DNA damage depending on the tissue within the CNS or the NeuN positive neurons in the cortex are more sensitive to DNA damage. The increased expression of GFAP, indicative of reactive astrogliosis, in our mutants is also seen in normal aging brains of rats, mice and humans [41-43]. Moreover, GFAP expression is correlated with Braak stage in AD [44]. In addition, the increased p53 expression we found is observed in normal aging rat brain [2, 45] and in AD and other neurodegenerative diseases [46-48]. Taken together this shows that (neuronal) DNA damage results in brain pathology that shares characteristics with both normal aging and AD.

We observed an age-dependent impairment in both synaptic plasticity as well as learning in the DNA repair-deficient *Ercc1* mutants. There is a clear similarity between these phenotypes and normal aging symptoms, as LTP is commonly found to be impaired in aged rodents, as well as impairments in contextual conditioning and spatial learning [49-61]. Interestingly, AD mouse models also show reduced LTP and learning [62-67]. Importantly, humans show a similar age-related deficit in performance on a virtual Morris water maze [68]. Hence, our results support the hypothesis that DNA damage can directly contribute to age-related decline of cognition and synaptic plasticity.

Possible mechanisms

Now that we have established that the progressive neurodysfunction can be attributed to a cell-autonomous process caused by DNA damage an important question is which type(s) of DNA damage may be involved. Unfortunately, current methodology to determine in a quantitatively reliable manner physiological levels of heterogeneous types of DNA damage in mammalian organs and tissues is extremely difficult and only possible for

a very limited subset of lesions [69, 70]. Nevertheless, our findings allow a number of important conclusions about the nature of the responsible DNA damage. First, since the mice used in our studies were not deliberately exposed to genotoxic agents the DNA injury must originate from one or more endogenous sources. Another conclusion is that the DNA lesions responsible for the neurodegenerative processes should be within the spectrum of DNA damage that normally would have been removed by the DNA repair pathways affected in *Ercc1*-deficient mice. These are multiple and also broad spectrum. The ERCC1/XPF complex is implicated in both subpathways of NER: global genome NER and transcription-coupled NER as well as in the removal of interstrand crosslinks and likely also in homologous recombination repair of specific types of double strand breaks [23-27]. Detailed analysis of the neurological phenotype of mouse mutants (and corresponding human syndromes) defective in any of these separate repair systems should disclose which of these pathways (or a combination) is the most important for protecting against aging-related neurological abnormalities.

DNA damage can have three different consequences for the cell: (i) a mutagenic effect in proliferating cells promoting the risk of cancer, (ii) a cytotoxic effect, eventually contributing to aging through apoptosis or necrosis of differentiated (post-mitotic as well as proliferating) cells and stem cells, or (iii) a cytostatic effect contributing to aging through cellular senescence, a mechanism which is not applicable to post-mitotic neurons [71]. In the global *Ercc1*^{Δ/Δ} mouse model it is difficult to determine the precise mechanism behind the reduced vitality and functioning of the neurons, because the mutation is not limited to a certain cell type, causing a mix of deleterious direct effects from within the neuron and indirect effects from other cell types. Although this mimics normal aging, which also affects all cell types simultaneously, the complexity does not allow the identification of the underlying mechanisms. In contrast, the cognitive deficits as observed in the forebrain-specific *Ercc1*^{fl/fl} mice, is directly attributable to the lack of DNA repair in the neurons themselves. These deficits could either arise from decreased functioning of the neuronal circuit (reduced plasticity of the affected neurons) or result from the loss of the affected excitatory neurons. However, since loss of neurons does not appear to be widespread, and since we observed normal synaptic transmission but clear synaptic plasticity deficits, it seems likely that the cognitive deficits are mostly caused by the plasticity deficits of the neuronal circuit rather than by the loss of excitatory neurons. DNA damage could cause reduced neuronal plasticity by interfering with transcription of genes necessary for synaptic plasticity. Stalled transcription may prevent or reduce the production of the necessary proteins. Alternatively, DNA damage and aging lead to the

reduction of the somatotroph axis by down regulating growth hormone (GH)/ insulin-like growth factor 1 (IGF-1) signaling [32, 72-74]. DNA damage-induced stalling of RNA polymerase II leads to suppression of IGF-1 and GH receptors and other genes of the somato-, lacto- and thyrotrophic axes in a cell autonomous fashion through an unknown mechanism, even in non-proliferating cells and cells of neuronal origin [73]. We speculate that this reduction in IGF-1 signaling could impair neuronal function because it has been shown that IGF-1 regulates synaptic plasticity in the adult central nervous system [75, 76] and age-related behavioral impairments can be alleviated by IGF-1 [77, 78] thereby strongly suggesting that IGF-1 reduction could be a factor in age-related reduction of synaptic plasticity.

Notably, the complete, homozygous, deletion of *Ercc1* in excitatory neurons of the *Ercc1^{fl/fl}* mouse, results in a later onset of neuronal pathology and plasticity impairments as compared to the genetically less severe *Ercc1^{ΔL}* mutation. This finding could indicate that the more severe *Ercc1^{ΔL}* phenotype is mostly caused by reduced functioning of cells other than excitatory neurons. This could be caused by damage to for instance glia and inhibitory neurons, but also to peripheral cells causing reduced overall health of these animals. Alternatively, the *Ercc1^{fl/fl}* mutation is milder because most of the DNA damage occurs early in life, and therefore it is less abundant in the *Ercc1^{fl/fl}* mice, due to the late onset of the CaMKII promoter that drives the Cre-mediated *Ercc1* gene deletion.

Taken together, although further experiments are required to determine to which extent DNA damage contributes to age-related cognitive decline in human, and by which mechanism DNA damage affects neuronal function, our results are the first direct demonstration that accumulated DNA damage, as caused by deficient DNA repair, is sufficient to cause neuronal pathology, neuronal plasticity deficits and cognitive decline. These results may therefore prove to be important for the development of better therapeutic strategies to battle age-related cognitive decline or to prevent the devastating effects of neurodegenerative diseases.

Acknowledgements

This work was supported by a Top Institute Pharma grant to GCMZ, JHJH and YE, and by a NWO-ZoNMW grant to YE and GTJH. Additional support is acknowledged from EU FP 7 (MarkAge 200880; Dept of Genetics and DNage) and EU FP6 (Lifespan, (EC-LSHG-CT-2007-036894); Dept of Genetics) as well as grants from NIH (1P01 AG17242-02) and NIEHS (1U01 ES011044). JHJH is CSO of DNage, however no

conflict of interest is declared.

Materials and Methods

Experiments were performed in accordance with the “Principles of laboratory animal care” (NIH publication no. 86-23) and the guidelines approved by the Erasmus University animal care committee.

Generation and breeding of mutants

The generation and characterization of nucleotide excision repair-deficient *Ercc1^{Δ/Δ}* and *Ercc1^{-/-}* mice has been previously described [29]. *Ercc1^{Δ/-}* mice were obtained by crossing *Ercc1^{+/-}* with *Ercc1^{Δ/+}* mice of C57Bl6J and FVB backgrounds, respectively and vice versa to yield *Ercc1^{Δ/-}* with an F1 C57Bl6J/FVB hybrid background. Wild-type littermates were used as controls.

We have obtained a mouse line that has *loxP* sites inserted into its *Ercc1* gene (floxed *Ercc1*, *Ercc1^{fl/fl}*) [79], kindly provided by David Melton. To achieve *Ercc1* gene inactivation, we used a transgenic line where Cre recombinase is under the control of the alphaCaMKII promoter [80]. Expression from this promoter is specific for post-mitotic excitatory neurons. *Ercc1^{fl/-}-CaMKII-Cre* mice were obtained by crossing *Ercc1^{fl/fl}* with *Ercc1^{+/-}-CaMKII-Cre* mice, of FVB and C57Bl6J backgrounds respectively, to yield *Ercc1^{fl/-}-CaMKII-Cre* with FVB/ C57Bl6J hybrid background. *Ercc1^{fl/-}-CaMKII-Cre* mice are heterozygous for *Ercc1* in their entire body, except for the excitatory post-mitotic neurons in the forebrain, which are complete knockouts and will be referred to as *Ercc1^{fl/-}* in the rest of the paper. As controls we used *Ercc1^{fl/+}-CaMKII-Cre* littermates, which are wild-type in their entire body, except for the excitatory post-mitotic neurons in the forebrain, which are heterozygous and will be referred to as *Ercc1^{fl/+}* in the rest of the paper. We used these mice as controls, because both mice will express Cre and heterozygous *Ercc1* mice do not show any phenotype (data not shown and [29]).

Animals were screened for discomfort and weighed once a week. Animals are maintained in a controlled environment (19-24°C, 12 hr light:12 hr dark cycle), received CRM(P) received standard rodent maintenance chow (Special Diets Services, Witham, UK) and water *ad libitum*, and were housed in individual ventilated cages at the Animal Resource Center (Erasmus University Medical Center). *Ercc1^{Δ/-}* mice received liquefied food when they were not able to reach the food due to movement disabilities.

Antibodies

Primary antibodies [supplier; applications: immunohistochemistry (IHC); immunofluorescence (IF); and dilutions] reported in this study are: rabbit anti-ATF3 (Santa Cruz; IHC; 1:1000); rabbit anti-GFAP (DAKO; IHC; 1:10,000; IF; 1:5000); rabbit anti-cleaved caspase 3 (Asp175, Cell Signalling; IHC; 1:1000); MAP2 (Chemicon (clone AP20; Sigma; IF; 1:200) and rabbit anti-p53 (Leica; IHC; 1:1000). NeuN (Millipore MAB377, IF, 1:1000)

For avidin–biotin–peroxidase immunocytochemistry biotinylated secondary antibodies from Vector Laboratories, USA, diluted 1:200 were used. FITC-, Cy3- and Cy5-conjugated secondary antibodies raised in donkey (Jackson Immunoresearch, USA) diluted at 1:200 were used for confocal immunofluorescence.

Immunohistochemical and histopathological procedures

For immunocytochemistry and immunofluorescence mice were anaesthetized with pentobarbital and perfused transcardially with 4% paraformaldehyde. The brain was carefully dissected out and postfixed overnight in 4% paraformaldehyde. Routinely, brain tissue was embedded in gelatin blocks [81], sectioned at 40 μ m with a freezing microtome, and sections were processed, free-floating, employing a standard avidin–biotin–immunoperoxidase complex method (ABC, Vector Laboratories, USA) with diaminobenzidine (0.05%) as the chromogen, or single-, double- and triple-labeling immunofluorescence [81-83]. In addition, a selected number of frozen sections were processed for a silver or thionine staining procedure that selectively labels dying neurons and their processes [81]. For double-labeling immunofluorescence with two rabbit or two mouse antibodies sections, Cy3-conjugated donkey anti-rabbit or donkey anti-mouse Fab fragments were used to label and sterically cover the first antibody, as described by the manufacturer (Jackson Immunoresearch). Then the sections were incubated with the second antibody that consecutively was labeled with FITC-conjugated secondaries. Single-labeling experiments were always performed in parallel to these double-labeling experiments to evaluate the specificity of the staining.

Immunoperoxidase-stained sections were analysed and photographed using a Leica DM-RB microscope and a Leica DC300 digital camera. Sections stained for immunofluorescence were analysed with a Zeiss LSM 510 confocal laser scanning microscope.

Quantitative analyses were performed with serial saggital sections that were serially immunoperoxidase-labeled for ATF3, cleaved caspase 3 and p53, respectively. All analyses were done with control and mutant mouse brains of different ages embedded in the same gelatin blocks [83].

Water Maze

To test spatial memory we used the Water Maze. Prior to the test the mice were handled extensively (2min./per day; 5 days). Our pool is 1.2 meters in diameter and has an 11 cm diameter platform submerged 1 cm below the surface. The water is painted milk-white with non-toxic paint and water temperature is kept constant at 26°C. We used dimmed lighting, and mouse tracking is performed using SMART version 2.0 (Panlab, Barcelona, Spain). Mice were given 2 trials per day, with 30 seconds inter trial interval for 5 consecutive days. At a training session, the mouse was placed on the platform for 30 seconds. Then it was placed in the water at a pseudo random start position and it was given a maximum of 60 seconds to find the platform. If the mouse did not find the platform in 60 seconds it was placed back on the platform. After 30 seconds on the platform, this training procedure was performed once more. The platform remained at the same position during all trials.

One hour after the training on day 5 a probe trial was given to test spatial learning. Mice were placed on the platform for 30 seconds, after which the platform was removed and the mice were placed in the pool at the opposite side of the former platform location. The mice were then allowed to search for the platform for 60 seconds.

Fear conditioning

Fear conditioning was performed in a conditioning chamber (Med Associates Inc., St. Albans, VT) equipped with a grid floor via which the foot shock could be administered. For context conditioning, each mouse was placed inside the conditioning chamber for 180 seconds. A foot shock (2 seconds, 0.4 mA) was delivered 148 seconds after placement in the chamber. Twenty-four hours later, context-dependent freezing was measured during 3 minutes.

Electrophysiology

After the animals had been sacrificed sagittal slices (400 μm) were made submerged in ice-cold artificial CSF (ACSF) using a vibratome and hippocampi were dissected out. These sagittal hippocampal slices were maintained at room temperature for at least 1.5 hours to recover before experiments were initiated. Then they were placed in a submerged recording chamber and perfused continuously at a rate of 2 ml/min with ACSF equilibrated with 95% O_2 , 5% CO_2 at 31°C. ACSF contained the following (in mM): 120 NaCl, 3.5 KCl, 2.5 CaCl_2 , 1.3 MgSO_4 , 1.25 NaH_2PO_4 , 26 NaHCO_3 , and 10 D-glucose.

Extracellular recording of field EPSP (fEPSPs) were made in CA1 stratum radiatum with platinum/iridium electrodes (Frederick Haer Companu, Bowdoinham, ME). A bipolar Pt/Ir was used to stimulate Schaffer-collateral/commissural afferents with a stimulus duration of 100 μ s. Stimulus response curves were obtained at the beginning of each experiment, 20 minutes after placing the electrodes, with 10, 20 40, 60, 80, and 100 μ A stimuli. For analyses the data from the strongest stimulation were used. LTP was evoked using two different tetani: (i) 10 Hz (1 train of 10 seconds at 10 Hz) and (ii) 100 Hz (1 train of 1 second 100 Hz). The 10 Hz protocols were performed at two-thirds and the 100 Hz protocol at one-third of the maximum fEPSP. fEPSP measurements were done once per minute. Potentiation was measured as the normalized increase of the mean fEPSP slope for the duration of the baseline. Only stable recordings were included and this judgment was made blind to genotype. Average LTP was defined as the mean last 10 minutes of each protocol. We used maximally 2 slices per mouse per protocol.

References

1. Hoeijmakers, J.H., *DNA damage, aging, and cancer*. N Engl J Med, 2009. **361**(15): p. 1475-85.
2. Dorszewska, J. and Z. Adamczewska-Goncerzewicz, *Oxidative damage to DNA, p53 gene expression and p53 protein level in the process of aging in rat brain*. Respir Physiol Neurobiol, 2004. **139**(3): p. 227-36.
3. Sohal, R.S., et al., *Effect of age and caloric restriction on DNA oxidative damage in different tissues of C57BL/6 mice*. Mech Ageing Dev, 1994. **76**(2-3): p. 215-24.
4. Gedik, C.M., et al., *Effects of age and dietary restriction on oxidative DNA damage, antioxidant protection and DNA repair in rats*. Eur J Nutr, 2005. **44**(5): p. 263-72.
5. Hamilton, M.L., et al., *Does oxidative damage to DNA increase with age?* Proc Natl Acad Sci U S A, 2001. **98**(18): p. 10469-74.
6. Moller, P., et al., *Aging and oxidatively damaged nuclear DNA in animal organs*. Free Radic Biol Med, 2010. **48**(10): p. 1275-1285.
7. Cai, Q., L. Tian, and H. Wei, *Age-dependent increase of indigenous DNA adducts in rat brain is associated with a lipid peroxidation product*. Exp Gerontol, 1996. **31**(3): p. 373-85.
8. Leutner, S., A. Eckert, and W.E. Muller, *ROS generation, lipid peroxidation and antioxidant enzyme activities in the aging brain*. J Neural Transm, 2001. **108**(8-

- 9): p. 955-67.
9. Serrano, F. and E. Klann, *Reactive oxygen species and synaptic plasticity in the aging hippocampus*. *Ageing Res Rev*, 2004. **3**(4): p. 431-43.
 10. Velculescu, V.E., et al., *Analysis of human transcriptomes*. *Nat Genet*, 1999. **23**(4): p. 387-8.
 11. Lovell, M.A. and W.R. Markesbery, *Oxidative DNA damage in mild cognitive impairment and late-stage Alzheimer's disease*. *Nucleic Acids Res*, 2007. **35**(22): p. 7497-504.
 12. Keller, J.N., et al., *Evidence of increased oxidative damage in subjects with mild cognitive impairment*. *Neurology*, 2005. **64**(7): p. 1152-6.
 13. Wang, J., et al., *Increased oxidative damage in nuclear and mitochondrial DNA in Alzheimer's disease*. *J Neurochem*, 2005. **93**(4): p. 953-62.
 14. Ahles, T.A. and A.J. Saykin, *Candidate mechanisms for chemotherapy-induced cognitive changes*. *Nat Rev Cancer*, 2007. **7**(3): p. 192-201.
 15. Konat, G.W., et al., *Cognitive dysfunction induced by chronic administration of common cancer chemotherapeutics in rats*. *Metab Brain Dis*, 2008. **23**(3): p. 325-33.
 16. Nance, M.A. and S.A. Berry, *Cockayne syndrome: review of 140 cases*. *Am J Med Genet*, 1992. **42**(1): p. 68-84.
 17. Lehmann, A.R., *DNA repair-deficient diseases, xeroderma pigmentosum, Cockayne syndrome and trichothiodystrophy*. *Biochimie*, 2003. **85**(11): p. 1101-11.
 18. Kraemer, K.H., et al., *Xeroderma pigmentosum, trichothiodystrophy and Cockayne syndrome: a complex genotype-phenotype relationship*. *Neuroscience*, 2007. **145**(4): p. 1388-96.
 19. Rapin, I., et al., *Cockayne syndrome and xeroderma pigmentosum*. *Neurology*, 2000. **55**(10): p. 1442-9.
 20. Niedernhofer, L.J., *Nucleotide excision repair deficient mouse models and neurological disease*. *DNA Repair (Amst)*, 2008. **7**(7): p. 1180-9.
 21. Niedernhofer, L.J., *Tissue-specific accelerated aging in nucleotide excision repair deficiency*. *Mech Ageing Dev*, 2008. **129**(7-8): p. 408-15.
 22. Hoeijmakers, J.H., *Genome maintenance mechanisms for preventing cancer*. *Nature*, 2001. **411**(6835): p. 366-74.
 23. Houtsmuller, A.B., et al., *Action of DNA repair endonuclease ERCC1/XPF in living cells*. *Science*, 1999. **284**(5416): p. 958-61.

24. Bergstralh, D.T. and J. Sekelsky, *Interstrand crosslink repair: can XPF-ERCCI be let off the hook?* Trends Genet, 2008. **24**(2): p. 70-6.
25. Bhagwat, N., et al., *XPF-ERCCI participates in the Fanconi anemia pathway of cross-link repair.* Mol Cell Biol, 2009. **29**(24): p. 6427-37.
26. Ahmad, A., et al., *ERCCI-XPF endonuclease facilitates DNA double-strand break repair.* Mol Cell Biol, 2008. **28**(16): p. 5082-92.
27. Zhu, X.D., et al., *ERCCI/XPF removes the 3' overhang from uncapped telomeres and represses formation of telomeric DNA-containing double minute chromosomes.* Mol Cell, 2003. **12**(6): p. 1489-98.
28. McWhir, J., et al., *Mice with DNA repair gene (ERCC-1) deficiency have elevated levels of p53, liver nuclear abnormalities and die before weaning.* Nat Genet, 1993. **5**(3): p. 217-24.
29. Weeda, G., et al., *Disruption of mouse ERCCI results in a novel repair syndrome with growth failure, nuclear abnormalities and senescence.* Curr Biol, 1997. **7**(6): p. 427-39.
30. Prasher, J.M., et al., *Reduced hematopoietic reserves in DNA interstrand crosslink repair-deficient Ercc1-/- mice.* EMBO J, 2005. **24**(4): p. 861-71.
31. Schumacher, B., et al., *Delayed and accelerated aging share common longevity assurance mechanisms.* PLoS Genet, 2008. **4**(8): p. e1000161.
32. Niedernhofer, L.J., et al., *A new progeroid syndrome reveals that genotoxic stress suppresses the somatotroph axis.* Nature, 2006. **444**(7122): p. 1038-43.
33. de Waard, M.C., et al., *Age-related motor neuron degeneration in DNA repair-deficient Ercc1 mice.* Acta Neuropathol, 2010. **120**(4): p. 461-475.
34. Hai, T., et al., *ATF3 and stress responses.* Gene Expr, 1999. **7**(4-6): p. 321-35.
35. Levine, A.J., W. Hu, and Z. Feng, *The P53 pathway: what questions remain to be explored?* Cell Death Differ, 2006. **13**(6): p. 1027-36.
36. Logue, S.E. and S.J. Martin, *Caspase activation cascades in apoptosis.* Biochem Soc Trans, 2008. **36**(Pt 1): p. 1-9.
37. Vlug, A.S., et al., *ATF3 expression precedes death of spinal motoneurons in amyotrophic lateral sclerosis-SOD1 transgenic mice and correlates with c-Jun phosphorylation, CHOP expression, somato-dendritic ubiquitination and Golgi fragmentation.* Eur J Neurosci, 2005. **22**(8): p. 1881-94.
38. Lawrence, N.J., et al., *A neurological phenotype in mice with DNA repair gene Ercc1 deficiency.* DNA Repair (Amst), 2008. **7**(2): p. 281-91.
39. Selfridge, J., et al., *Correction of liver dysfunction in DNA repair-deficient mice*

- with an ERCCI transgene*. Nucleic Acids Res, 2001. **29**(22): p. 4541-50.
40. Fanselow, M.S., *Factors governing one-trial contextual conditioning*. animal learning and behavior, 1990. **18**(3): p. 264-270.
41. Nichols, N.R., et al., *GFAP mRNA increases with age in rat and human brain*. Neurobiol Aging, 1993. **14**(5): p. 421-9.
42. O'Callaghan, J.P. and D.B. Miller, *The concentration of glial fibrillary acidic protein increases with age in the mouse and rat brain*. Neurobiol Aging, 1991. **12**(2): p. 171-4.
43. Takahashi, T., et al., *Correlation between glial fibrillary acidic protein-positive astrocytes and age in the human hippocampus*. Leg Med (Tokyo), 2006. **8**(3): p. 161-5.
44. Wharton, S.B., et al., *Population variation in glial fibrillary acidic protein levels in brain ageing: relationship to Alzheimer-type pathology and dementia*. Dement Geriatr Cogn Disord, 2009. **27**(5): p. 465-73.
45. Chung, Y.H., et al., *Immunocytochemical study on the distribution of p53 in the hippocampus and cerebellum of the aged rat*. Brain Res, 2000. **885**(1): p. 137-41.
46. de la Monte, S.M., et al., *P53- and CD95-associated apoptosis in neurodegenerative diseases*. Lab Invest, 1998. **78**(4): p. 401-11.
47. de la Monte, S.M., Y.K. Sohn, and J.R. Wands, *Correlates of p53- and Fas (CD95)-mediated apoptosis in Alzheimer's disease*. J Neurol Sci, 1997. **152**(1): p. 73-83.
48. Martin, L.J., *p53 is abnormally elevated and active in the CNS of patients with amyotrophic lateral sclerosis*. Neurobiol Dis, 2000. **7**(6 Pt B): p. 613-22.
49. Bach, M.E., et al., *Age-related defects in spatial memory are correlated with defects in the late phase of hippocampal long-term potentiation in vitro and are attenuated by drugs that enhance the cAMP signaling pathway*. Proc Natl Acad Sci U S A, 1999. **96**(9): p. 5280-5.
50. Barnes, C.A., *Long-term potentiation and the ageing brain*. Philos Trans R Soc Lond B Biol Sci, 2003. **358**(1432): p. 765-72.
51. Erickson, C.A. and C.A. Barnes, *The neurobiology of memory changes in normal aging*. Exp Gerontol, 2003. **38**(1-2): p. 61-9.
52. Rosenzweig, E.S. and C.A. Barnes, *Impact of aging on hippocampal function: plasticity, network dynamics, and cognition*. Prog Neurobiol, 2003. **69**(3): p. 143-79.

53. Blank, T., et al., *Small-conductance, Ca²⁺-activated K⁺ channel SK3 generates age-related memory and LTP deficits*. Nat Neurosci, 2003. **6**(9): p. 911-2.
54. Watson, J.B., et al., *Age-related deficits in long-term potentiation are insensitive to hydrogen peroxide: coincidence with enhanced autophosphorylation of Ca²⁺/calmodulin-dependent protein kinase II*. J Neurosci Res, 2002. **70**(3): p. 298-308.
55. Blalock, E.M., et al., *Gene microarrays in hippocampal aging: statistical profiling identifies novel processes correlated with cognitive impairment*. J Neurosci, 2003. **23**(9): p. 3807-19.
56. Foster, T.C., et al., *Interaction of age and chronic estradiol replacement on memory and markers of brain aging*. Neurobiol Aging, 2003. **24**(6): p. 839-52.
57. Foster, T.C., et al., *Calcineurin links Ca²⁺ dysregulation with brain aging*. J Neurosci, 2001. **21**(11): p. 4066-73.
58. Kaczorowski, C.C. and J.F. Disterhoft, *Memory deficits are associated with impaired ability to modulate neuronal excitability in middle-aged mice*. Learn Mem, 2009. **16**(6): p. 362-6.
59. Liu, J., et al., *Memory loss in old rats is associated with brain mitochondrial decay and RNA/DNA oxidation: partial reversal by feeding acetyl-L-carnitine and/or R-alpha -lipoic acid*. Proc Natl Acad Sci U S A, 2002. **99**(4): p. 2356-61.
60. Moyer, J.R., Jr. and T.H. Brown, *Impaired trace and contextual fear conditioning in aged rats*. Behav Neurosci, 2006. **120**(3): p. 612-24.
61. Verbitsky, M., et al., *Altered hippocampal transcript profile accompanies an age-related spatial memory deficit in mice*. Learn Mem, 2004. **11**(3): p. 253-60.
62. Lambert, M.P., et al., *Diffusible, nonfibrillar ligands derived from Abeta1-42 are potent central nervous system neurotoxins*. Proc Natl Acad Sci U S A, 1998. **95**(11): p. 6448-53.
63. Chapman, P.F., et al., *Impaired synaptic plasticity and learning in aged amyloid precursor protein transgenic mice*. Nat Neurosci, 1999. **2**(3): p. 271-6.
64. Walsh, D.M., et al., *Naturally secreted oligomers of amyloid beta protein potently inhibit hippocampal long-term potentiation in vivo*. Nature, 2002. **416**(6880): p. 535-9.
65. Wang, H.W., et al., *Soluble oligomers of beta amyloid (1-42) inhibit long-term potentiation but not long-term depression in rat dentate gyrus*. Brain Res, 2002. **924**(2): p. 133-40.
66. Jacobsen, J.S., et al., *Early-onset behavioral and synaptic deficits in a mouse*

- model of Alzheimer's disease*. Proc Natl Acad Sci U S A, 2006. **103**(13): p. 5161-6.
67. Lauren, J., et al., *Cellular prion protein mediates impairment of synaptic plasticity by amyloid-beta oligomers*. Nature, 2009. **457**(7233): p. 1128-32.
68. Driscoll, I., et al., *The aging hippocampus: cognitive, biochemical and structural findings*. Cereb Cortex, 2003. **13**(12): p. 1344-51.
69. Dizdaroglu, M., et al., *Free radical-induced damage to DNA: mechanisms and measurement*. Free Radic Biol Med, 2002. **32**(11): p. 1102-15.
70. Himmelstein, M.W., et al., *Creating context for the use of DNA adduct data in cancer risk assessment: II. Overview of methods of identification and quantitation of DNA damage*. Crit Rev Toxicol, 2009. **39**(8): p. 679-94.
71. Mitchell, J.R., J.H. Hoeijmakers, and L.J. Niedernhofer, *Divide and conquer: nucleotide excision repair battles cancer and ageing*. Curr Opin Cell Biol, 2003. **15**(2): p. 232-40.
72. van der Pluijm, I., et al., *Impaired genome maintenance suppresses the growth hormone--insulin-like growth factor 1 axis in mice with Cockayne syndrome*. PLoS Biol, 2007. **5**(1): p. e2.
73. Garinis, G.A., et al., *Persistent transcription-blocking DNA lesions trigger somatic growth attenuation associated with longevity*. Nat Cell Biol, 2009. **11**(5): p. 604-15.
74. van de Ven, M., et al., *Adaptive stress response in segmental progeria resembles long-lived dwarfism and calorie restriction in mice*. PLoS Genet, 2006. **2**(12): p. e192.
75. Sonntag, W.E., et al., *Age and insulin-like growth factor-1 modulate N-methyl-D-aspartate receptor subtype expression in rats*. Brain Res Bull, 2000. **51**(4): p. 331-8.
76. Torres-Aleman, I., *Insulin-like growth factors as mediators of functional plasticity in the adult brain*. Horm Metab Res, 1999. **31**(2-3): p. 114-9.
77. Shi, L., et al., *Differential effects of aging and insulin-like growth factor-1 on synapses in CA1 of rat hippocampus*. Cereb Cortex, 2005. **15**(5): p. 571-7.
78. Markowska, A.L., M. Mooney, and W.E. Sonntag, *Insulin-like growth factor-1 ameliorates age-related behavioral deficits*. Neuroscience, 1998. **87**(3): p. 559-69.
79. Doig, J., et al., *Mice with skin-specific DNA repair gene (Ercc1) inactivation are hypersensitive to ultraviolet irradiation-induced skin cancer and show more*

- rapid actinic progression*. *Oncogene*, 2006. **25**(47): p. 6229-38.
80. Madisen, L., et al., *A robust and high-throughput Cre reporting and characterization system for the whole mouse brain*. *Nat Neurosci*, 2010. **13**(1): p. 133-40.
81. Jaarsma, D., et al., *Human Cu/Zn superoxide dismutase (SOD1) overexpression in mice causes mitochondrial vacuolization, axonal degeneration, and premature motoneuron death and accelerates motoneuron disease in mice expressing a familial amyotrophic lateral sclerosis mutant SOD1*. *Neurobiol Dis*, 2000. **7**(6 Pt B): p. 623-43.
82. Jaarsma, D., et al., *CuZn superoxide dismutase (SOD1) accumulates in vacuolated mitochondria in transgenic mice expressing amyotrophic lateral sclerosis-linked SOD1 mutations*. *Acta Neuropathol*, 2001. **102**(4): p. 293-305.
83. Maatkamp, A., et al., *Decrease of Hsp25 protein expression precedes degeneration of motoneurons in ALS-SOD1 mice*. *Eur J Neurosci*, 2004. **20**(1): p. 14-28.

Supplemental Data

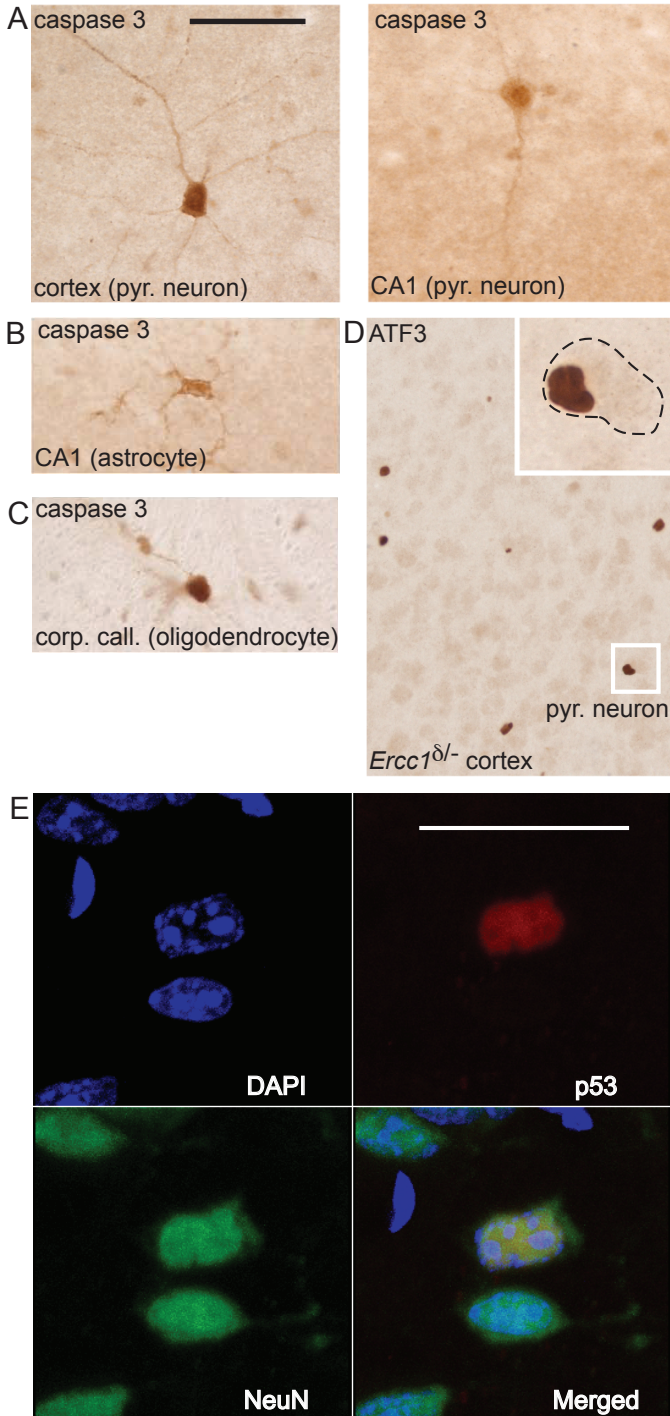


Figure S1, related to Figure 1. *Ercc1^{Δ/Δ}* mice express markers for cellular stress (p53 and ATF3) and apoptosis (caspase 3) mostly in neurons (A) Caspase 3 positive neurons in cortex (left) and CA1 area of hippocampus (right) in 4 months old *Ercc1^{Δ/Δ}* mice. (scale bar 50 μm ; valid for A-D) (B) Caspase 3 positive astrocyte in CA1 area of hippocampus in 4 months old *Ercc1^{Δ/Δ}* mouse. (C) Caspase 3 positive oligodendrocyte in corpus callosum of 4 months old *Ercc1^{Δ/Δ}* mouse. (D) ATF3 positive neurons in cortex. Enlarged neuron in inset showing eccentric nucleus. (E) Confocal image showing an example of a triple staining with a p53 (red) positive neuron (NeuN in green) and DAPI staining for DNA (blue). (scale bar 25 μm)

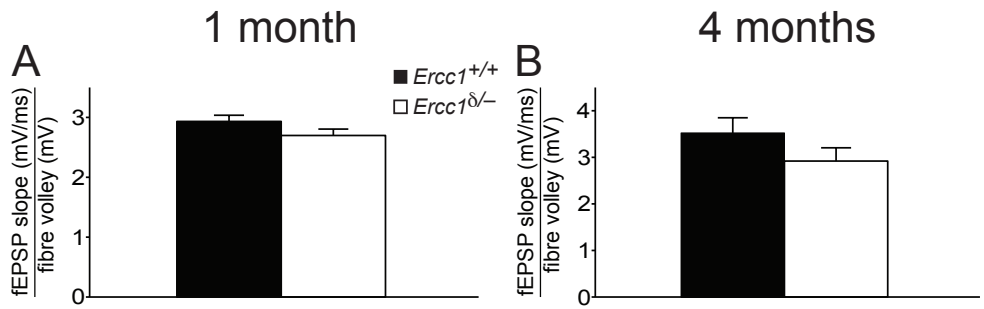


Figure S2, related to Figure 2. *Ercc1*^{Δ/Δ} mice have normal synaptic transmission at 1 month and 4 months of age

(A) Synaptic transmission (fEPSP slope plotted as function of fiber volley) of 1 months old mice showing normal transmission in *Ercc1*^{Δ/Δ} mice.

(B) Synaptic transmission (fEPSP slope plotted as function of fiber volley) of 4 months old mice showing normal transmission in *Ercc1*^{Δ/Δ} mice. All data are reported as mean \pm SEM.

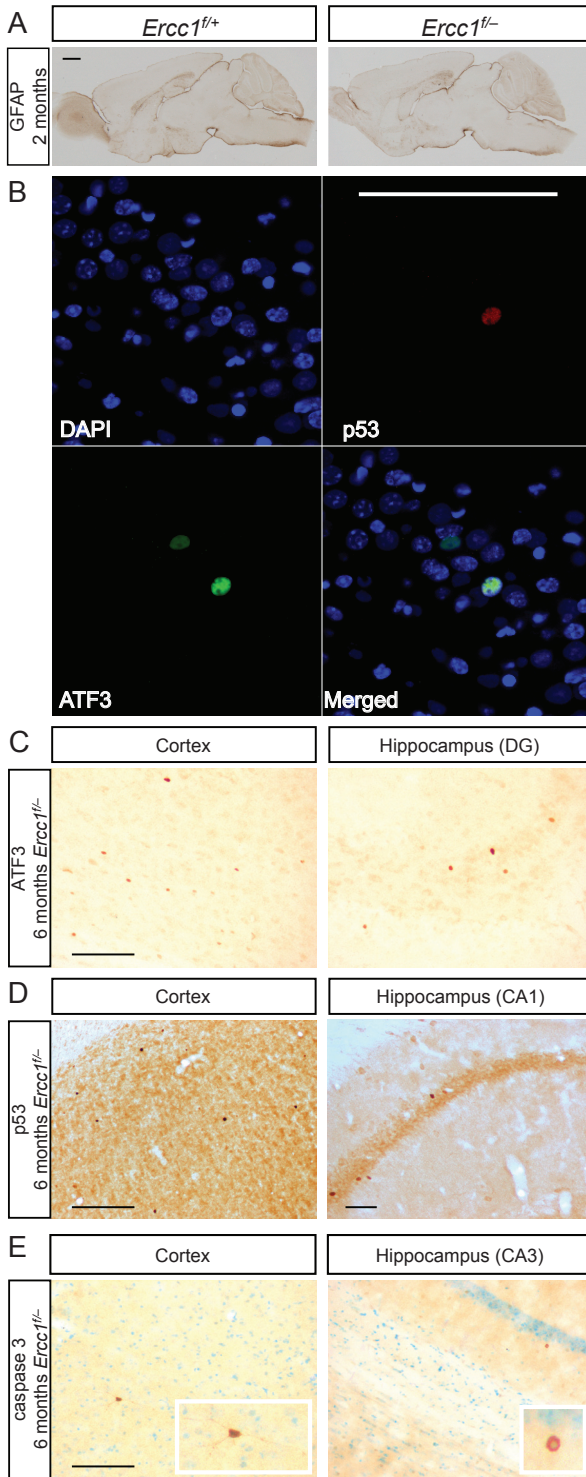


Figure S3, related to Figure 3. *Ercc1*^{-/-} mice have normal levels of GFAP at 2 months and express markers for cellular stress (p53 and ATF3) and apoptosis (caspase 3) mostly in neurons

(A) Immunostaining with GFAP showing similar GFAP staining in sagittal brain slices of *Ercc1*^{-/-} mice and not in *Ercc1*^{+/+} mice at 2 months of age. (scale bar 1mm)

(B) Confocal image showing an example of a triple staining for p53 (red), DNA (blue) and ATF3 (green) with a cell positive for both ATF3 and p53 and a cell only positive for ATF3. (scale bar 100 μm)

(C) Immunostaining with ATF3 of cortex (left) and Dentate Gyrus (DG) of the hippocampus (right) of 6 months old *Ercc1*^{-/-} mice. (scale bar 100 μm)

(D) Immunostaining with p53 of cortex (left) and CA1 area of the hippocampus (right) of 6 months old *Ercc1*^{-/-} mice. (scale bar 100 μm)

(E) Immunostaining with caspase 3 of cortex (left) CA3 area of the hippocampus (right) of 6 months old *Ercc1*^{-/-} mice (insets show positive neurons enlarged). (scale bar 100 μm)

Figure S4 related to Figure 4

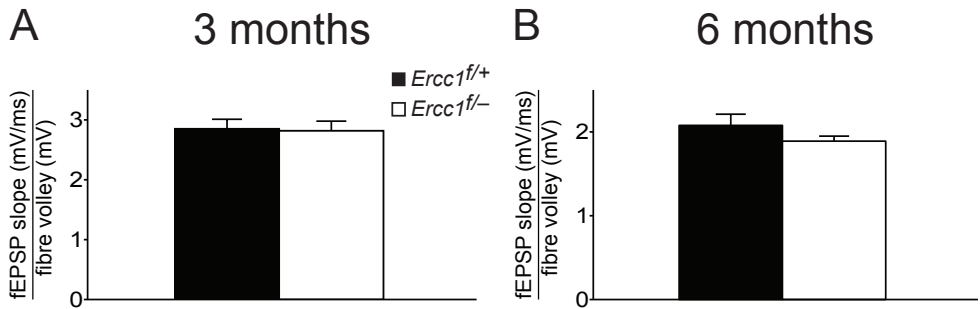


Figure S4, related to figure 4. *Ercc1^{f/-}* mice have normal synaptic transmission at 3 months and 6 months of age

(A) Synaptic transmission (fEPSP slope plotted as function of fiber volley) of 3 months old mice showing normal transmission in *Ercc1^{f/-}* mice.

(B) Synaptic transmission (fEPSP slope plotted as function of fiber volley) of 6 months old mice showing normal transmission in *Ercc1^{f/-}* mice. All data are reported as mean \pm SEM.

Chapter 3

Age-related loss of hearing and vision in the DNA-repair deficient *Ercc1*^{δ/-} mouse

Marcella Spoor*, A. Paul Nagtegaal*, **Nils Z. Borgesius**, Bart van Alphen, Yanto Ridwan, Ingrid van der Pluijm, Jan H. J. Hoeijmakers, Ype Elgersma, Maarten A. Frens and J. Gerard G. Borst

* These authors have contributed equally

Abstract

Age-related loss of hearing (presbycusis) and vision are two very common and disabling conditions, but the underlying mechanisms are still poorly understood. Damage by reactive oxygen species, which in turn might damage macromolecules such as DNA, has been implicated in both processes. To investigate directly whether DNA damage could indeed be driving presbycusis and age-related vision loss, we tested hearing and vision of *Ercc1*^{Δ/-} mice, which are deficient in several DNA repair pathways. *Ercc1*^{Δ/-} mice showed a progressive increase of hearing level thresholds over time, most likely arising from deteriorating cochlear function. *Ercc1*^{Δ/-} mutants also showed a progressive decrease in contrast sensitivity as well as thinning of the outer nuclear layer. These results indicate that DNA damage can induce the age-related decline of the auditory and visual system.

Introduction

Among the most common impairments accompanying aging are presbycusis and age-related vision loss. However, the underlying molecular mechanisms are still poorly understood. One of the main theories of aging is that it results from damage induced by free radicals such as reactive oxygen species (ROS) to proteins or DNA [1, 2]. A central role for DNA damage in aging is suggested by the observation that DNA can accumulate damage during life [3-6]. In support of this theory, certain defects in DNA repair cause human progeroid syndromes, which show hallmarks of accelerated segmental aging [7, 8]. Importantly, Cockayne syndrome and subgroups of xeroderma pigmentosum patients, both caused by impairment of the DNA repair pathway Nucleotide Excision Repair (NER), have accelerated segmental aging such as growth retardation and premature death, accompanied by many neurological features. These patients show loss of hearing and vision already at a very young age [9-13]. Taken together these findings suggest that DNA damage could indeed play a significant role in presbycusis and age-related vision loss.

Presbycusis

Presbycusis is a major social and health problem that results from a lifetime of insults to the auditory system [14-17]. Presbycusis is characterized by increased hearing thresholds, especially at higher frequencies, mainly resulting from loss of functional outer hair cells (OHC) in the cochlea [14, 18], accompanied by a progressive reduction of distortion product otoacoustic emissions (DPOAE) [19-21]. There is uncertainty about the mechanisms underlying auditory decline, but because of the high oxidative metabolism in the cochlea [22], DNA damage inflicted by free radicals may make a large contribution [23, 24]. Further support for the idea that accumulating DNA damage contributes to presbycusis comes from xeroderma pigmentosum and Cockayne syndrome patients, which show progressive hearing loss. Genes involved in NER, i.e. XPC and XPA, are highly expressed in the cochlea [25]. Importantly, noise induced damage is likely mediated by ROS [26], since mice with impaired antioxidant mechanisms have increased noise induced hearing loss (NIHL) [27] and polymorphisms in human antioxidant systems are correlated with susceptibility to NIHL [28]. Moreover, ROS-induced DNA damage is increased during aging in the cochlea of C57BL/6J mice [29]; these mice carry the recessive mutation *Cdh23*^{753A}, which causes early onset presbycusis [30]. Finally, reducing oxidative stress and DNA damage slows down presbycusis [29]. These findings strongly suggest that ROS-induced DNA damage plays a causative role

in presbycusis [16, 31].

Age-related vision loss

Visual functioning changes with age. The major optic changes during aging are insufficient accommodation ability due to hardening of the lens, decrease in pupil size and increase in density and yellowing of the lens. Within the retina, a loss of photoreceptors, bipolar cells, ganglion cells, or changes in connections among these cells could impair vision [32].

Senescent changes in vision include declines in visual acuity and spatial contrast sensitivity [32]. Visual, or Snellen, acuity defines the highest spatial frequency or smallest detail that can be resolved at high contrast levels. Contrast sensitivity measures the ability to detect small increments in shades of gray on a uniform background. This function measures the least amount of contrast needed to detect a spatial frequency and provides a more complete quantification of a person's visual capabilities. Studies on the effect of age on the spatial contrast sensitivity curve in humans have shown a fall in high frequency sensitivity in middle age [32-36] leading to intermediate and high spatial frequency attenuation above 60 years of age [33, 35]. Moreover, an age-related decline in contrast sensitivity was found across all spatial frequencies when measured under scotopic conditions [37]. Recently, an age-related decline in contrast sensitivity was also shown in mice [38].

The etiology of age-related vision loss is unknown and probably multicausal. As mentioned before, the human progeroid syndromes xeroderma pigmentosum and Cockayne syndrome are accompanied by a loss of vision, and degeneration of the retina [9-11]. Moreover, a mouse model of Cockayne syndrome showed an age-dependent thinning of the outer nuclear layer (ONL) of the retina due to spontaneous loss of photoreceptors [39]. Finally, loss of photoreceptors or thinning of the ONL is commonly seen in aging humans [40-43], rats [44-48] and mice [49, 50].

These findings suggest that (retinal) DNA damage might play an important role in age-related vision loss. This idea is further strengthened by the observation that the retina has high oxidative metabolism [51] and that the retinal pigment epithelium (RPE) has very high antioxidant capacity and high DNA repair capacity [52]. Cataract is the major contributor to age-related visual impairment and age-related macula degeneration (AMD) is the main contributor to blindness over the age of 75 [53]. Damage by ROS has been implicated in the etiology of both cataract and AMD [54-59]. Finally, DNA damage has found to be increased and DNA repair decreased in AMD patients [60, 61].

Taken together, these results suggest that in age-related vision loss DNA damage could also play a causative role [62].

Here, we investigated the role of unrepaired DNA damage on presbycusis and age-related vision loss in *Ercc1*^{δ/-} mice of different ages. The *Ercc1*^{δ/-} mouse mutant lacks one allele of the excision repair cross-complementing group 1 (*Ercc1* (*ERCC1* in human)) gene. The protein derived from the other allele shows reduced activity, due to a seven amino-acid carboxy-terminal truncation [63]. This hypomorph mutation results in severely impaired NER, interstrand crosslink repair [63] and double strand break repair [64]. Consequently, naturally occurring DNA damage remains largely unrepaired, causing accelerated segmental aging resulting in premature death. The maximum lifespan of these mice in the F1 C57BL/6J-FVB/N genetic background used here is approximately 6 months [65].

We found that unrepaired DNA damage in the *Ercc1*^{δ/-} mouse results in: (i) progressively increasing hearing thresholds, especially at higher frequencies, (ii) accompanied by reduced DPOAEs, strongly suggesting OHC loss, (iii) progressive decline in contrast sensitivity and (iv) progressive thinning of the outer nuclear layer of the retina.

Results

Progressive hearing loss in *Ercc1*^{δ/-} mice

Auditory thresholds in *Ercc1*^{δ/-} mice were determined longitudinally at 5 and 14 weeks of age by auditory-evoked brainstem response (ABR) recordings (Fig. 1A). Hearing level thresholds were measured at 4, 8, 16 and 32 kHz. Thresholds were defined as the lowest Sound Pressure Level (SPL) (5 dB resolution) at which a reproducible peak (usually peak II or IV) was still evoked by stimulation of either ear. We performed a three-way repeated measures ANOVA with genotype and age as between, and frequency as within subjects factors. All main effects and their interactions were significant (all $p < 0.001$). To clarify the origin of these significant effects we performed a two-way repeated measures ANOVA. The *Ercc1*^{δ/-} mice show a significant effect of age ($p < 0.001$) and a significant interaction of age and frequency ($p < 0.001$). In contrast there is no effect of age in the wildtype mice ($p = 0.296$). This shows that only the *Ercc1*^{δ/-} mice have an age-dependent increase in hearing threshold and importantly that the increase is not the same for all frequencies. We determined using Bonferroni *post hoc* tests that age had a significant effect for 8 kHz ($p < 0.05$), 16 kHz and 32 kHz (both $p < 0.001$) but not for 4 kHz ($p > 0.05$).

Taken together these findings show that the *Ercc1*^{δ/−} mice have an age-dependent increase in hearing thresholds especially at higher frequencies while their wildtype littermates are not affected.

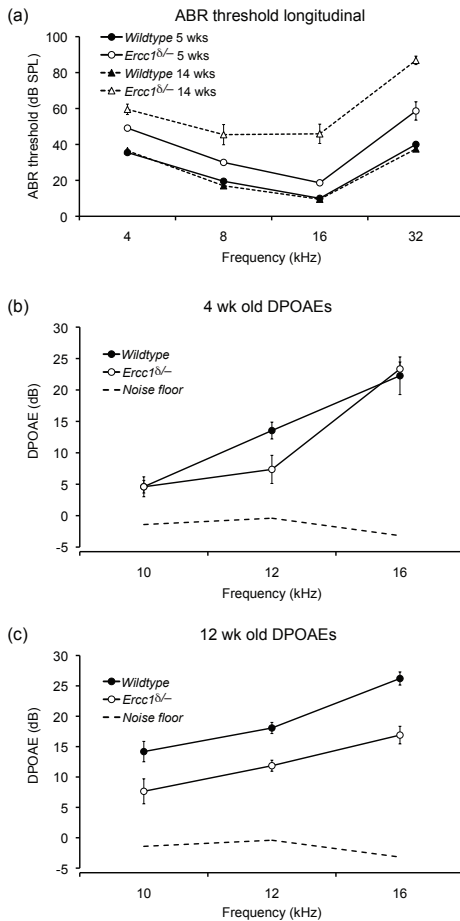


Figure 1. Increasing ABR thresholds and reducing DPOAEs output suggesting OHC loss in *Ercc1*^{δ/−} mice. (a) *Ercc1*^{δ/−} mice show hearing loss, especially at higher frequencies, from 5 to 14 weeks of age in contrast to their littermates. Filled symbols represent wildtype and open symbols *Ercc1*^{δ/−} mice. Circles 5 weeks old animals and triangles represent 14 week old animals. (b) 4 week old *Ercc1*^{δ/−} mice have similar DPOAEs as their littermates. (c) 12 week old *Ercc1*^{δ/−} mice have reduced DPOAEs at higher frequencies compared to their littermates suggesting OHC loss. All data represented as means ± SEM.

Progressive hearing loss in *Ercc1*^{δ/−} mice is caused by hair cell loss

To test if there is evidence for retrocochlear pathology, we identified peaks I to V in the ABR and compared the inter-peak latencies of the most prominent peaks, II and IV, at ages 4 and 12 weeks between wildtype and *Ercc1*^{δ/−} mice at 4 and 16 kHz. No latency differences were observed between wildtype and *Ercc1*^{δ/−} mice and no statistical significance was reached ($p > 0.05$), neither when data were corrected for difference in minimum hearing level threshold. II-IV inter-peak latencies at 4 kHz were 1.89 ± 0.06 (mean ± SEM) and 1.82 ± 0.11 ms for wildtype and 1.91 ± 0.03 and 1.71 ± 0.08 ms for *Ercc1*^{δ/−} mice at 4 and 12 weeks, respectively. At 16 kHz, II-IV intervals were 1.99 ± 0.04 and 1.83 ± 0.10 ms for wildtype and 2.03 ± 0.08 and 1.82 ± 0.09 ms for *Ercc1*^{δ/−} mice at 4 and 12 weeks, respectively. This suggests that the observed differences in threshold are not due to retrocochlear deficits in the mutants.

To assess cochlear function, we measured the presence of otoacoustic emissions. We evoked DPOAEs at 4 and 12 weeks of age in *Ercc1*^{δ/−} mice and their age-matched littermates. A three-way repeated measures ANOVA with genotype and age as

between and frequency as within subjects factors, revealed that all main effects and their interactions were significant (all $p < 0.05$). Two-way ANOVA testing indicated no effect of genotype ($p = 0.27$) at 4 weeks (Fig. 1B), while a highly significant effect size ($p < 0.0001$) was observed at 12 weeks (Fig. 1C).

Together, the lack of a significant difference in ABR inter-peak latencies and the decreased DPOAEs in 12 week old *Ercc1*^{δ/δ} mice indicate a cochlear origin of the hearing loss, probably resulting from outer hair cell damage.

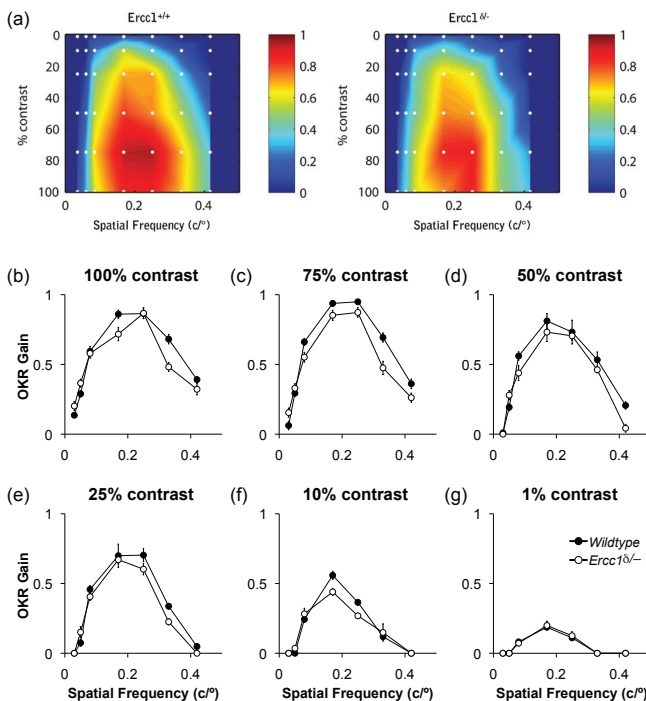


Figure 2. Normal contrast sensitivity in *Ercc1*^{δ/δ} mice and their littermates at 6 weeks of age. (a) The color reflects the OKR gains at 42 different combinations of spatial frequency and contrast. Measured points are connected through linear interpolation. (b-g) Six cross sections of A and B are plotted, one for each contrast. All data represented as means \pm SEM. Filled circles represent wildtype and open circles *Ercc1*^{δ/δ} mice.

Vision

Progressive decline of vision in *Ercc1*^{δ/δ} mice

We measured compensatory eye movements to infer the contrast sensitivity of mice. Afoveate mammals (like mice) show robust gaze-stabilizing movements, e.g. the optokinetic reflex (OKR). The OKR prevents the image of the surroundings to slip across the retina during movement of the visual scene. By calculating the gain (the ratio between stimulus velocity and eye velocity) of different combinations of contrast and spatial frequency, we were able to see both the presence and the magnitude of an animal response to a stimulus.

At 6 weeks of age, all stimuli evoked OKR gains that were similar in both genotypes (Fig. 2). The only exception was at 75% contrast, where the gain was slightly

lower in *Ercc1*^{δ/δ}. Both groups showed a similar optimum for all contrasts, which was reached at 0.17-0.25 c/°. At 10 weeks of age, OKR gains were lower in *Ercc1*^{δ/δ} mutants (Fig. 3; 75% p<0.05; 50%, 25% and 10% p<0.001; 1% p<0.01). *Ercc1*^{δ/δ} mice performed worse than their wildtype littermates at all contrast levels, except at 100% contrast. Gains were lower and the window in which responses occurred narrowed, i.e. the highest (0.42 c/°) and lowest (0.03 c/°) spatial frequencies did not elicit any response in mutant mice at contrasts below 100%. Four weeks later, at 14 weeks of age, all OKR gains were strongly reduced in *Ercc1*^{δ/δ} mutants (Fig. 4; p<0.001). The response window narrowed further, i.e. there was almost no response below 0.08 c/° or above 0.25 c/°. Below 50% contrast, hardly any response was observed. Moreover, even within the optimal stimulus window, i.e. 100% contrast and 0.17-0.25 c/°, the evoked OKR gain was lower in the *Ercc1*^{δ/δ} mice.

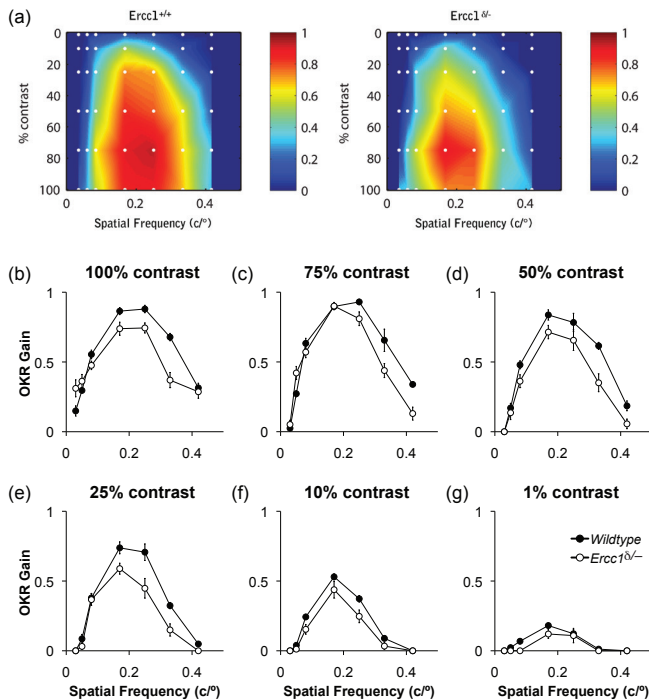


Figure 3. Reduced contrast sensitivity in *Ercc1*^{δ/δ} mice and their littermates at 10 weeks of age. (a) The color reflects the OKR gains at 42 different combinations of spatial frequency and contrast. Measured points are connected through linear interpolation. (b-g) Six cross sections of A and B are plotted, one for each contrast. All data represented as means ± SEM. Filled circles represent wildtype and open circles *Ercc1*^{δ/δ} mice.

The quality of the OKR not only depends on which stimuli the animal is able to perceive, but also on the underlying sensorimotor system. Therefore we tested if the sensorimotor system was affected. To this end, OKRs were evoked using stimuli with many spatial frequencies, which allowed a test of the OKR performance that was independent of spatial frequency. At 6 weeks of age, there was no significant difference in OKR performance between wildtype and *Ercc1*^{δ/δ} mice (Fig. 4A; repeated measures

ANOVA, $p = 0.84$). In contrast, at 10 weeks OKR gain was significantly decreased (Fig. 5B; repeated measures ANOVA, $p < 0.001$), indicating a decline in the sensorimotor system. Importantly, however, there was no significant difference in the OKR between genotypes at the low stimulus velocity ($3^\circ/\text{s}$) that we used to probe for visual function in Figures 2-4. Therefore, the OKR provides a reliable measure of contrast sensitivity and visual acuity at these low frequencies. In contrast, at 14 weeks of age (Fig. 5C), the OKR was impaired at all stimulus velocities (repeated measures ANOVA, $p < 0.001$), which means that the OKR data could not be used to infer visual function in 14 week old *Ercc1* $^{\delta/-}$ mice.

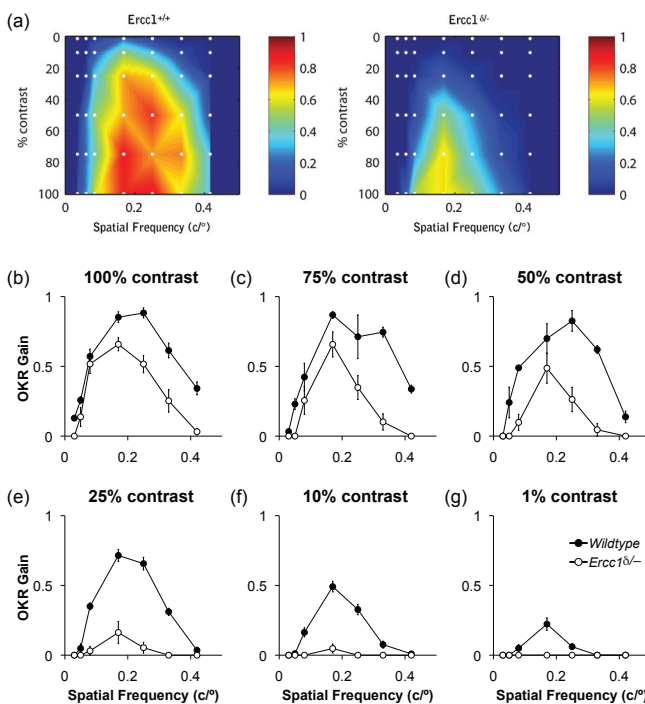


Figure 4. Severely reduce contrast sensitivity in *Ercc1* $^{\delta/-}$ mice and their littermates at 14 weeks of age. (a) The color reflects the OKR gains at 42 different combinations of spatial frequency and contrast. Measured points are connected through linear interpolation. (b-g) Six cross sections of A and B are plotted, one for each contrast. All data represented as means \pm SEM. Filled circles represent wildtypes, open circles *Ercc1* $^{\delta/-}$ mice.

Progressive reduction of outer nuclear layer in *Ercc1* $^{\delta/-}$ mice

We determined the surface area of the ONL in cross sections of the eye at 4, 9, 18 and 25 weeks of age in *Ercc1* $^{\delta/-}$ mice and their age-matched littermates (Fig. 6A). We performed a two-way ANOVA and found a significant effect for both age and genotype ($p < 0.0001$) and for their interaction ($p < 0.005$). Bonferroni *post-hoc* tests revealed that only at 25 weeks of age there was a significant genotype effect ($p < 0.001$). This shows an age-dependent reduction of the ONL in *Ercc1* $^{\delta/-}$ mice suggestive of loss of cells, most likely photoreceptors. To further investigate the cause of the reduction of the ONL we

determined the number of TUNEL positive cells, i.e. cells in apoptosis, in the ONL at 4, 9, 18 and 25 weeks of age (Fig. 6B). Two-way ANOVA analyses revealed a significant effect of age, genotype and their interaction ($p < 0.0001$). Taken together this strongly suggests that the progressive reduction of the ONL is caused by loss of cells through apoptosis.

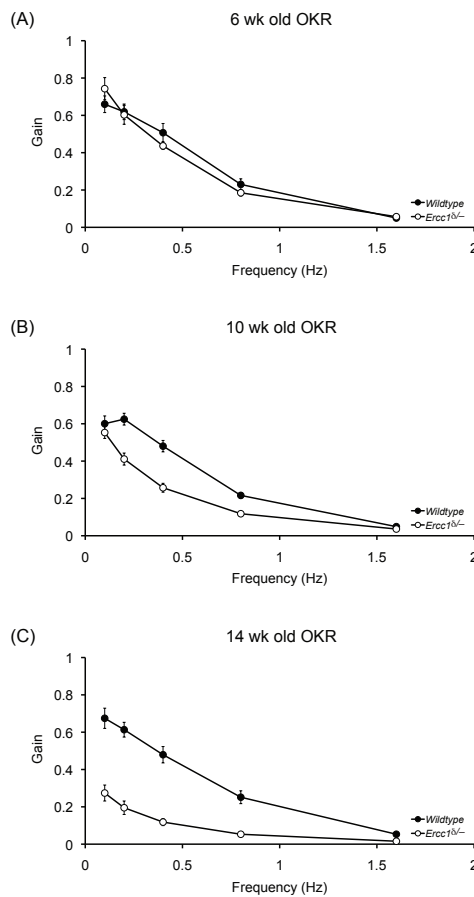


Figure 5. Progressive reduction of OKR in *Ercc1*^{δ/δ} mice. (a) Normal OKR at 6 weeks old in *Ercc1*^{δ/δ} mice. (b) Reduced OKR in 10 weeks old *Ercc1*^{δ/δ} mice, except at low stimulus velocity (1°/s, 2°/s), which we used to probe for visual function above. (c) Reduced OKR at all stimulus velocities in 14 weeks old *Ercc1*^{δ/δ} mice. All data represented as means \pm SEM. Filled circles represent wildtypes, open circles *Ercc1*^{δ/δ} mice.

Discussion

Here we show that unrepaired DNA damage in the DNA repair deficient *Ercc1*^{δ/δ} mouse, results in accelerated age-related decline of both vision and hearing compared to wildtype littermates.

Presbycusis

We used the objective electrophysiological measurement of ABRs to establish hearing thresholds. We showed that *Ercc1*^{δ/δ} mice display a progressive increase of hearing threshold in combination with reduced DPOAEs. However, their threshold is already elevated at the youngest age we tested. We presume this is caused by very rapid deterioration, although we cannot exclude developmental effects. Previous studies have shown a strong correlation between a reduction in DPOAEs and a loss of OHCs [68-76]. Hence we propose that the increasing hearing thresholds are due to a loss of functional OHCs. Moreover, the unchanged inter-peak latencies show that the transmission speed in the retrocochlear part of the nervous system is unaffected in *Ercc1*^{δ/δ} mice, although more subtle differences in the central auditory processing cannot be excluded [77]. This

suggests that the hearing loss in the *Ercc1*^{δ/δ} mice is not caused by defects in the central

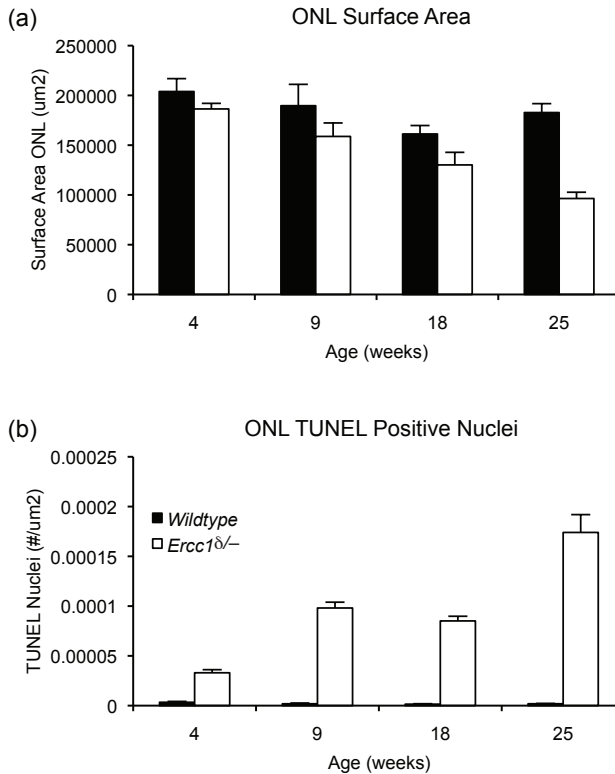


Figure 6. Age-dependent loss of cells through apoptosis in the ONL in *Ercc1*^{δ/δ} mice.

(a) Age-dependent reduction of ONL surface in cross sections of *Ercc1*^{δ/δ} eyes compared to those of their littermates. (b) Age-dependent increase of TUNEL positive cells normalized to ONL surface in *Ercc1*^{δ/δ} mice. Black columns represent wildtypes, open columns *Ercc1*^{δ/δ} mice. All data represented as means ± SEM. For wildtypes of 4, 9, 18 and 25 weeks n=4, 4, 4 and 13 respectively. For *Ercc1*^{δ/δ} mice of 4, 9, 18 and 25 weeks n=7, 9, 6 and 12 respectively.

nervous system. The phenotype of the *Ercc1*^{δ/δ} mice, i.e. increased hearing threshold, reduced DPOAE and normal ABR inter peak latencies, is very similar to what is seen in human presbycusis [14, 16-21, 78].

Considerable evidence for a causative role of mtDNA damage in presbycusis has been presented [29, 79-82]. However, to our knowledge the *Ercc1*^{δ/δ} mutation does not affect mtDNA repair [83]. Hence, our results suggest that, in addition to mtDNA damage, nDNA damage plays a causative role in presbycusis.

Age-related vision loss

We measured OKR gains to infer the contrast sensitivity and visual acuity of mice. To this end we presented visual stimuli with specific spatial frequencies and contrasts. Furthermore, we assessed OKR performance by presenting different sets of visual stimuli that contain many spatial frequencies and therefore more readily evoke OKRs. OKR performance should be intact when using it as a probe for visual function.

When testing OKR performance at the age of 6 weeks there was no difference in the OKR gains between the wildtypes and mutants. Gaze stabilization reflexes in

both groups were similar. OKR gains showed low pass filter characteristics, with high gains at low stimulus velocities and low gains at high stimulus velocities comparable to what has been observed in C57Bl6 mice [84, 85]. At the age of 10 weeks, the first signs of oculomotor deterioration in the *Ercc1*^{δ/-} mice were observed, as gains of the OKR decreased at higher stimulus frequencies. Because OKR gains were not significantly different at the stimulus velocity used to measure contrast sensitivity, they could be used reliably to infer contrast sensitivity for animals of 6 or 10 weeks old. In contrast, at 14 weeks of age the OKR gains of the *Ercc1*^{δ/-} mutant were approximately halved while wildtypes were unaffected. Thus, OKR gains are not a reliable measure of contrast sensitivity for this age group and should be interpreted cautiously.

During contrast sensitivity experiments the OKR was used as a probe. Surprisingly, the measured gains were generally higher than those measured during OKR performance recordings. This was probably caused by the use of different stimulus paradigms. OKR performance was recorded using sinusoidal stimuli and gains were calculated by dividing peak eye velocity by peak stimulus velocity. Due to the sinusoidal character of the stimulus, the eye has only a moment to reach a similar velocity. Contrast sensitivity measurements used constant velocity stimuli, which allowed the eye more time to reach stimulus velocity.

In 6 week old mice, there were no differences in contrast sensitivity between wildtypes and mutants, as similar OKR gains were recorded for all stimuli. The contrast sensitivity function showed a profile that is very similar to that of the C57Bl6 mice [38]. Gains were highest at 75-100% contrast and a spatial frequency of 0.17–0.25 c/° and decreased as contrast decreased or the spatial frequency fell outside this optimal window. At 10 weeks of age contrast sensitivity begun to decrease at contrasts below 100%. Also, sensitivity to the highest and lowest spatial frequencies disappeared as responses to those stimuli decreased to zero for contrasts below 50%. This decrease in contrast sensitivity followed a similar pattern as was reported for aging C57Bl6 mice [38], where the ability to perceive low contrasts and high spatial frequencies disappeared first. At 14 weeks of age inferring visual function from OKR gains is problematic as OKR performance in the *Ercc1*^{δ/-} mice were much lower when tested in the control experiment (Fig. 5). However, the reduction in OKR gains when probing for contrast sensitivity could not be fully explained by deterioration of the oculomotor system of *Ercc1*^{δ/-} mice, as they were still able to reach gains up to 0.65 (Fig. 4 C) provided that the contrast was high enough, i.e. 100%. Therefore we cautiously conclude that in 14 week old *Ercc1*^{δ/-} mice contrast sensitivity had decreased to the point where the mouse was only able to observe a small

set of contrast-spatial frequency combinations, in the same window that was optimal for 6 week old mice (0.17-0.25 c/°, 74-100% contrast).

In humans OKR gains decline with age, at high frequencies as well as at high velocities due to an impaired sensori-motor system [86, 87]. In contrast, this effect was not found in mice [88, 89]. However, it could be that the mice were too young (\pm 15 months) to reveal an age-dependent effect. Studies in human on the effect of age on the spatial contrast sensitivity function curve have shown a decline in high frequency sensitivity in middle age, leading to intermediate and high spatial frequency attenuation with increasing age due to optical and neural degeneration [33, 35, 36, 90-94]. Also in mice, the contrast sensitivity function is known to decrease as a function of age [38].

Our histology data suggests age-related loss of photoreceptors. However, it is unlikely that this fully explains the level of vision loss, as the effects of age on vision are already apparent at 10 weeks while the reduction of the ONL is only significant at 25 weeks. Therefore, reduced function before cell loss or pathology at other levels, i.e. optical or CNS should also play a role. Although photoreceptor loss or thinning of the ONL is commonly seen in aging in humans [40-43], rats [44-48], mice [49, 50] and mouse models of accelerated aging [39, 95, 96] it is not clear how relevant this phenomenon is to ARVL. However, as optic changes cannot fully explain ARVL it is likely that photoreceptor loss or reduced function contributes to ARVL [31].

In conclusion, the *Ercc1* ^{δ -} mutant shows accelerated age-related loss of hearing and vision with characteristics very similar to human presbycusis and ARVL. This suggests a causative role of DNA damage in the etiology of presbycusis and ARVL. Additional research using conditional knockouts will help resolve the relative contribution of different cell types to these processes.

Acknowledgements

Efstathios B. Papachristos for help with the statistical analyses. HFSP for financial support of M. Spoor, NWO-ALW for financial support of B. van Alphen.

Materials and Methods

In this study 60 *Ercc1* ^{δ -} mutants and 53 wildtype littermates in an F1 hybrid Fvb/N-C57Bl/6J background strain were used. All mice were housed on a 12 h light / 12 h dark cycle with unrestricted access to food and water. Experiments were done during the light phase. All experiments were done with approval of the local ethics committee and

were in accordance with the European Communities Council Directive (86/609/EEC). For the contrast sensitivity experiments 14 *Ercc1*^{δ/-} mutants and 14 wildtype littermates were used, which were measured longitudinally. For Auditory-evoked Brainstem Response (ABR) recordings 11 *Ercc1*^{δ/-} mutants and 10 wildtype littermates were measured longitudinally. For DPOAE measurements, 2 groups of 6 *Ercc1*^{δ/-} mutants and 6 littermates, were measured, one group at 4 and one group at 12 weeks of age. For histology 34 *Ercc1*^{δ/-} mutants and 27 littermates were used.

ABR recordings

ABR recordings were performed largely as described previously [66]. The mice were anesthetized with a mixture of ketamine/xylazine (60/10 mg/kg) i.p. and placed in a sound-attenuated box with the ears at a distance of 4 cm from a frontally placed tweeter loudspeaker (Radio Shack Super Tweeter 40-1310B). Active needle electrodes were positioned subdermally at the base of both pinnae. The reference electrode was placed at the vertex. In addition, a ground electrode was placed near the sacrum. Presentation of stimuli and averaging of responses was controlled by custom-made software (EUPHRA = Erasmus University Physiological Response Averager). Tone pip stimuli (1 ms duration, 0.5 ms cosine-squared ramps, alternating polarity, repetition rate 80 per second) were generated by a Hewlett Packard 33120A waveform generator. Responses were acquired and averaged by a 32 MHZ DSP Motorola 56002 board. The sound pressure level (SPL; re 20 μPa) of the stimuli ranged between -10 and 110 dB. For determining ABR thresholds, 500 responses with artifacts <30 μV were averaged. Stimuli were calibrated by comparing peak-to-peak values of the tone pip stimuli (measured with a 1/2" Bruel and Kjaer microphone, type 4192) with a calibrated tone (Bruel and Kjaer sound calibrator, type 4231, 94 dB) on an oscilloscope (Tektronix TDS 1002). Hearing level thresholds were measured at 4, 8, 16 and 32 kHz. Thresholds were defined as the lowest SPL (5 dB resolution) at which a reproducible peak (usually peak II or IV) was still present in either ear. After finishing recordings the mice were injected with atipamezole (25 μg s.c.) to facilitate recovery from anesthesia.

DPOAE

We used the DP 2000, Starkey system to measure *2f1-f2* DPOAEs, with $f2/f1 = 1.2$. The intensity of *f1* and *f2* was set at 65 and 55 dB SPL, respectively. Recordings were done at *f2* = 4, 6, 8, 10, 12 and 16 kHz. First the speaker was calibrated, followed by three measurements in both ears. The maximum DPOAE amplitude per frequency in each

mouse was included in the analysis. Noise floor values were obtained from recordings in a dead animal. DPOAEs of wildtype animals were not above baseline between 4 and 8 kHz and consequently only results obtained at 10, 12 and 16 kHz are presented.

Vision

Mouse contrast sensitivity function was determined as described previously [38]. This method infers contrast sensitivity by measuring how the magnitude (gain) of compensatory eye movements varies with different combinations of contrast and spatial frequency.

Surgery

Animals were prepared for head fixation by attaching two metal nuts to the skull using a construct made of a micro glass composite [38].

Stimulus setup

Optokinetic stimuli were created using a modified Electrohome Marquee 9000 CRT projector (Christie Digital Systems, Cypress CA, USA), which projected stimuli via mirrors onto three transparent anthracite-colored screens (156*125 cm) that were placed in a triangular formation around the recording setup (see [38] for more details). This created a green monochrome panoramic stimulus fully surrounding the animal. The stimuli were programmed in C++ and rendered in OpenGL and consisted of a virtual, vertically oriented cylinder with a dotted pattern or vertically oriented sine grating on its wall. Each pixel subtended 4.5 x 4.5 arcminutes. Contrast (C) in the projected sine gratings was calculated using the Michelson formula: $C = (L_{max} - L_{min}) / (L_{max} + L_{min})$, where L_{max} and L_{min} are the maximum and minimum luminance in a grating, respectively. The average luminance was kept constant at 17.5 cd/m² in all stimulus conditions. At maximum contrast, the minimum and maximum luminance of the stimulus were 0.05 cd/m² and 35.0 cd/m², respectively.

Eye movement recordings

Mice were immobilized by placing them in a plastic tube, with the head pedestal bolted to a restrainer that allowed placing the eye of the mouse in the centre of the visual stimulus, in front of the eye position recording apparatus.

Eye movements were recorded with an infrared video system (Iscan ETL-200). Images of the eye were captured at 120 Hz with an infrared sensitive CCD camera (see [38] for

more details). To keep the field of view as free from obstacles as possible, the camera and lens were mounted under the table surface, and recordings were made with a hot mirror that was transparent to visible light and reflective to infrared light. The eye was illuminated with two infrared LEDs at the base of the hot mirror. The camera, mirror and LEDs were all mounted on an arm that could rotate about the vertical axis over a range of 26.12° (peak to peak). Eye movement recordings and calibration procedures were similar to those described by [67]. Trials were randomized, mice were assigned a number and the data analysis scripts were automated. All data was analyzed after the experiment.

Contrast sensitivity function

Contrast sensitivity was tested by presenting moving visual stimuli to the mice and recording eye movements evoked by those stimuli [38]. Each stimulus was a vertical sine wave grating made up of a combination of one of seven spatial frequencies (0.03, 0.05, 0.08, 0.17, 0.25, 0.33, or $0.42\text{ c}/^\circ$) and one of six contrast values (100%, 75%, 50%, 25%, 10%, 1%). The 42 stimulus combinations were presented in random order. A stimulus was first projected and kept stationary for one minute, allowing the animal to adjust to changes in the stimulus. Subsequently, the stimulus started to move with a constant velocity of $1.5\text{ }^\circ/\text{s}$. After moving to one direction for two seconds, it changed direction and moved in the opposite direction for two seconds. This was repeated six times, yielding 10 changes in direction. As the stimulus was moving, motion of the left eye was recorded.

Recorded eye positions were transformed offline into a velocity signal. Fast phases were removed from the contrast sensitivity function recordings using a velocity threshold of twice the stimulus velocity (i.e., $3\text{ }^\circ/\text{s}$??). The first 200 ms after stimulus onset and before and after each change in direction were removed as well. Because the stimulus velocity was constant and eye data in the first 200 ms after the stimulus direction changes were ignored, average absolute eye velocity could be divided directly by the stimulus velocity to calculate a gain value for each combination of spatial frequency and contrast. An eye movement that perfectly follows the visual stimulus has a gain of 1 (Collewijn, 1969).

Optokinetic reflex performance

The visual system has various channels, each tuned to a specific spatial frequency [68, 69]. In control experiments, we used stimuli with many spatial frequencies (patches). By ensuring that the optokinetic response was independent of spatial frequency, these

experiments thus allowed a test of the suitability of the optokinetic reflex (OKR) for measuring contrast sensitivity in the different mouse lines. In these experiments, the OKR was induced using a visual stimulus consisting of 1592 sharp edged dots that were equally spaced on a virtual sphere that had its center at eye height above the center of the table. The stimulus oscillated sinusoidally about the earth vertical axis with constant amplitude of 5° and 100% contrast. By using different oscillation frequencies (0.1, 0.2, 0.4, 0.8, 1.6 Hz) the peak velocity of the stimulus was varied. During the optokinetic stimulation the eye position was recorded and stored to be analyzed offline. Fast phases and blinks were removed and the signal was differentiated to get eye velocity. A sine wave was fitted through the velocity trace. OKR gain was calculated by dividing the peak of the fitted eye velocity by the peak velocity of the stimulus [38].

Immunohistochemistry

For isolation of the eyes animals were euthanized by CO₂ inhalation. Eyes were marked on the nasal side with Alcian blue (5% Alcian blue in 96% ethanol), dissected and subsequently fixed in 4% paraformaldehyde in 0.1 M phosphate buffer and embedded in paraffin. Five µm thick, transverse paraffin sections were cut. For determination of retinal surface area digital images of the whole retina were taken by using a microscope equipped with a high-resolution camera (BX40 microscope, ColorViewIllu camera and the Cella program). The Cella program was used to make digital images of the same sections used for quantification of the apoptotic cells in the outer nuclear layer (ONL). The program Sigmascan Pro5 was used to measure the surface area of the ONL. Apoptotic cells were visualized using the TdT-mediated dUTP Nick-End Labeling (TUNEL) method, according to the specifications of the manufacturer of the kit (Apoptag Plus Peroxidase *In Situ* Apoptosis Detection Kit, Chemicon). For quantification, the number of TUNEL-positive cells in the ONL was counted using a BX40 microscope with a minimum of 5 transverse cut sections per mouse. To standardize the chosen area of the retina, the sections closest to the eye nerve were selected for immunohistochemistry and quantification. The number of apoptotic cells and retinal surface area in 5 sections per animal were averaged and animals (numbers in Figure 6) were averaged per group accordingly.

Statistics

The effect of the *Erccl*^{δ/-} mutation on contrast sensitivity, hearing thresholds and DPOAEs was analyzed using a repeated measures ANOVA with three factors. For

contrast sensitivity we used genotype as between subjects factor and contrast and spatial frequency as within subject factor. *Post hoc*, groups were compared at each contrast by averaging OKR gains over spatial frequencies. Differences between groups were analyzed for significance with a Student's t-test. For the effect of the *Ercc1*^{δ/-} mutation on hearing thresholds and DPOAEs we used genotype and age as between and frequency as within subjects factors. *Post hoc*, groups were compared with two-way ANOVAs and Bonferroni tests

References

1. Harman, D., *Aging: a theory based on free radical and radiation chemistry*. J Gerontol, 1956. **11**(3): p. 298-300.
2. Sohal, R.S., R.J. Mockett, and W.C. Orr, *Mechanisms of aging: an appraisal of the oxidative stress hypothesis*. Free Radic Biol Med, 2002. **33**(5): p. 575-86.
3. Sohal, R.S., et al., *Effect of age and caloric restriction on DNA oxidative damage in different tissues of C57BL/6 mice*. Mech Ageing Dev, 1994. **76**(2-3): p. 215-24.
4. Dorszewska, J. and Z. Adamczewska-Goncerzewicz, *Oxidative damage to DNA, p53 gene expression and p53 protein level in the process of aging in rat brain*. Respir Physiol Neurobiol, 2004. **139**(3): p. 227-36.
5. Hamilton, M.L., et al., *Does oxidative damage to DNA increase with age?* Proc Natl Acad Sci U S A, 2001. **98**(18): p. 10469-74.
6. Gedik, C.M., et al., *Effects of age and dietary restriction on oxidative DNA damage, antioxidant protection and DNA repair in rats*. Eur J Nutr, 2005. **44**(5): p. 263-72.
7. Andressoo, J.O. and J.H. Hoeijmakers, *Transcription-coupled repair and premature ageing*. Mutat Res, 2005.
8. de Boer, J., et al., *Premature aging in mice deficient in DNA repair and transcription*. Science, 2002. **296**(5571): p. 1276-9.
9. Lindenbaum, Y., et al., *Xeroderma pigmentosum/cockayne syndrome complex: first neuropathological study and review of eight other cases*. Eur J Paediatr Neurol, 2001. **5**(6): p. 225-42.
10. Weidenheim, K.M., D.W. Dickson, and I. Rapin, *Neuropathology of Cockayne syndrome: Evidence for impaired development, premature aging, and neurodegeneration*. Mech Ageing Dev, 2009. **130**(9): p. 619-36.
11. Robbins, J.H., et al., *Neurological disease in xeroderma pigmentosum*.

- Documentation of a late onset type of the juvenile onset form.* Brain, 1991. **114** (Pt 3): p. 1335-61.
12. Niedernhofer, L.J., *Nucleotide excision repair deficient mouse models and neurological disease.* DNA Repair (Amst), 2008. **7**(7): p. 1180-9.
 13. Rapin, I., et al., *Cockayne syndrome and xeroderma pigmentosum.* Neurology, 2000. **55**(10): p. 1442-9.
 14. Gates, G.A. and J.H. Mills, *Presbycusis.* Lancet, 2005. **366**(9491): p. 1111-20.
 15. Willott, J.F., T. Hnath Chisolm, and J.J. Lister, *Modulation of presbycusis: current status and future directions.* Audiol Neurootol, 2001. **6**(5): p. 231-49.
 16. Liu, X.Z. and D. Yan, *Ageing and hearing loss.* J Pathol, 2007. **211**(2): p. 188-97.
 17. Howarth, A. and G.R. Shone, *Ageing and the auditory system.* Postgrad Med J, 2006. **82**(965): p. 166-71.
 18. Ohlemiller, K.K., *Contributions of mouse models to understanding of age- and noise-related hearing loss.* Brain Res, 2006. **1091**(1): p. 89-102.
 19. Dorn, P.A., et al., *On the existence of an age/threshold/frequency interaction in distortion product otoacoustic emissions.* J Acoust Soc Am, 1998. **104**(2 Pt 1): p. 964-71.
 20. Uchida, Y., et al., *The effects of aging on distortion-product otoacoustic emissions in adults with normal hearing.* Ear Hear, 2008. **29**(2): p. 176-84.
 21. Oeken, J., A. Lenk, and F. Bootz, *Influence of age and presbycusis on DPOAE.* Acta Otolaryngol, 2000. **120**(3): p. 396-403.
 22. Kopke, R., et al., *A radical demise. Toxins and trauma share common pathways in hair cell death.* Ann N Y Acad Sci, 1999. **884**: p. 171-91.
 23. Seidman, M.D., N. Ahmad, and U. Bai, *Molecular mechanisms of age-related hearing loss.* Ageing Res Rev, 2002. **1**(3): p. 331-43.
 24. Pickles, J.O., *Mutation in mitochondrial DNA as a cause of presbycusis.* Audiol Neurootol, 2004. **9**(1): p. 23-33.
 25. Guthrie, O.W. and F.A. Carrero-Martinez, *Real-Time Quantification of Xeroderma pigmentosum mRNA From the Mammalian Cochlea.* Ear Hear, 2010.
 26. Henderson, D., et al., *The role of antioxidants in protection from impulse noise.* Ann N Y Acad Sci, 1999. **884**: p. 368-80.
 27. Ohlemiller, K.K., et al., *Targeted mutation of the gene for cellular glutathione peroxidase (Gpx1) increases noise-induced hearing loss in mice.* J Assoc Res

- Otolaryngol, 2000. **1**(3): p. 243-54.
28. Fortunato, G., et al., *Paraoxonase and superoxide dismutase gene polymorphisms and noise-induced hearing loss*. Clin Chem, 2004. **50**(11): p. 2012-8.
 29. Someya, S., et al., *Age-related hearing loss in C57BL/6J mice is mediated by Bak-dependent mitochondrial apoptosis*. Proc Natl Acad Sci U S A, 2009. **106**(46): p. 19432-7.
 30. Noben-Trauth, K., Q.Y. Zheng, and K.R. Johnson, *Association of cadherin 23 with polygenic inheritance and genetic modification of sensorineural hearing loss*. Nat Genet, 2003. **35**(1): p. 21-3.
 31. Darrat, I., et al., *Auditory research involving antioxidants*. Curr Opin Otolaryngol Head Neck Surg, 2007. **15**(5): p. 358-63.
 32. Spear, P.D., *Neural bases of visual deficits during aging*. Vision Res, 1993. **33**(18): p. 2589-609.
 33. Derfeldt, G., G. Lennerstrand, and B. Lundh, *Age variations in normal human contrast sensitivity*. Acta Ophthalmol (Copenh), 1979. **57**(4): p. 679-90.
 34. Wright, C.E. and N. Drasdo, *The influence of age on the spatial and temporal contrast sensitivity function*. Doc Ophthalmol, 1985. **59**(4): p. 385-95.
 35. Owsley, C., R. Sekuler, and D. Siemsen, *Contrast sensitivity throughout adulthood*. Vision Res, 1983. **23**(7): p. 689-99.
 36. Arundale, K., *An investigation into the variation of human contrast sensitivity with age and ocular pathology*. Br J Ophthalmol, 1978. **62**(4): p. 213-5.
 37. Scheffrin, B.E., et al., *Senescent changes in scotopic contrast sensitivity*. Vision Res, 1999. **39**(22): p. 3728-36.
 38. van Alphen, B., B.H. Winkelman, and M.A. Frens, *Age- and sex-related differences in contrast sensitivity in C57BL/6 mice*. Invest Ophthalmol Vis Sci, 2009. **50**(5): p. 2451-8.
 39. Gorgels, T.G., et al., *Retinal degeneration and ionizing radiation hypersensitivity in a mouse model for Cockayne syndrome*. Mol Cell Biol, 2007. **27**(4): p. 1433-41.
 40. Gao, H. and J.G. Hollyfield, *Aging of the human retina. Differential loss of neurons and retinal pigment epithelial cells*. Invest Ophthalmol Vis Sci, 1992. **33**(1): p. 1-17.
 41. Curcio, C.A., et al., *Aging of the human photoreceptor mosaic: evidence for selective vulnerability of rods in central retina*. Invest Ophthalmol Vis Sci,

1993. **34**(12): p. 3278-96.
42. Aggarwal, P., T.C. Nag, and S. Wadhwa, *Age-related decrease in rod bipolar cell density of the human retina: an immunohistochemical study*. J Biosci, 2007. **32**(2): p. 293-8.
 43. Panda-Jonas, S., J.B. Jonas, and M. Jakobczyk-Zmija, *Retinal photoreceptor density decreases with age*. Ophthalmology, 1995. **102**(12): p. 1853-9.
 44. Weisse, I., H. Loosen, and H. Peil, *Age-related retinal changes--comparison between albino and pigmented rats*. Lens Eye Toxic Res, 1990. **7**(3-4): p. 717-39.
 45. Imai, R. and Z. Tanakamaru, *Visual dysfunction in aged Fischer 344 rats*. J Vet Med Sci, 1993. **55**(3): p. 367-70.
 46. O'Steen, W.K., et al., *Analysis of severe photoreceptor loss and Morris water-maze performance in aged rats*. Behav Brain Res, 1995. **68**(2): p. 151-8.
 47. Spencer, R.L., W.K. O'Steen, and B.S. McEwen, *Water maze performance of aged Sprague-Dawley rats in relation to retinal morphologic measures*. Behav Brain Res, 1995. **68**(2): p. 139-50.
 48. Feng, L., et al., *No age-related cell loss in three retinal nuclear layers of the Long-Evans rat*. Vis Neurosci, 2007. **24**(6): p. 799-803.
 49. Bravo-Nuevo, A., N. Walsh, and J. Stone, *Photoreceptor degeneration and loss of retinal function in the C57BL/6-C2J mouse*. Invest Ophthalmol Vis Sci, 2004. **45**(6): p. 2005-12.
 50. Sanyal, S. and R.K. Hawkins, *Development and degeneration of retina in rds mutant mice: effects of light on the rate of degeneration in albino and pigmented homozygous and heterozygous mutant and normal mice*. Vision Res, 1986. **26**(8): p. 1177-85.
 51. Sickel, W., *Electrical and metabolic manifestations of receptor and higher-order neuron activity in vertebrate retina*. Adv Exp Med Biol, 1972. **24**(0): p. 101-18.
 52. Jarrett, S.G., J. Albon, and M. Boulton, *The contribution of DNA repair and antioxidants in determining cell type-specific resistance to oxidative stress*. Free Radic Res, 2006. **40**(11): p. 1155-65.
 53. Klaver, C.C., et al., *Age-specific prevalence and causes of blindness and visual impairment in an older population: the Rotterdam Study*. Arch Ophthalmol, 1998. **116**(5): p. 653-8.
 54. Vrensen, G.F., *Early cortical lens opacities: a short overview*. Acta

- Ophthalmol, 2009. **87**(6): p. 602-10.
55. Ting, A.Y., T.K. Lee, and I.M. MacDonald, *Genetics of age-related macular degeneration*. *Curr Opin Ophthalmol*, 2009. **20**(5): p. 369-76.
56. Chiu, C.J. and A. Taylor, *Nutritional antioxidants and age-related cataract and maculopathy*. *Exp Eye Res*, 2007. **84**(2): p. 229-45.
57. Sackett, C.S. and S. Schenning, *The age-related eye disease study: the results of the clinical trial*. *Insight*, 2002. **27**(1): p. 5-7.
58. Delcourt, C., et al., *Age-related macular degeneration and antioxidant status in the POLA study*. *POLA Study Group. Pathologies Oculaires Liees a l'Age*. *Arch Ophthalmol*, 1999. **117**(10): p. 1384-90.
59. Delcourt, C., et al., *Associations of antioxidant enzymes with cataract and age-related macular degeneration*. *The POLA Study. Pathologies Oculaires Liees a l'Age*. *Ophthalmology*, 1999. **106**(2): p. 215-22.
60. Wozniak, K., et al., *DNA damage/repair and polymorphism of the hOGG1 gene in lymphocytes of AMD patients*. *J Biomed Biotechnol*, 2009. **2009**: p. 827562.
61. Szaflik, J.P., et al., *DNA damage and repair in age-related macular degeneration*. *Mutat Res*, 2009. **669**(1-2): p. 169-76.
62. Ding, X., M. Patel, and C.C. Chan, *Molecular pathology of age-related macular degeneration*. *Prog Retin Eye Res*, 2009. **28**(1): p. 1-18.
63. Weeda, G., et al., *Disruption of mouse ERCC1 results in a novel repair syndrome with growth failure, nuclear abnormalities and senescence*. *Curr Biol*, 1997. **7**(6): p. 427-39.
64. Ahmad, A., et al., *ERCC1-XPF endonuclease facilitates DNA double-strand break repair*. *Mol Cell Biol*, 2008. **28**(16): p. 5082-92.
65. de Waard, M.C., et al., *Age-related motor neuron degeneration in DNA repair-deficient Ercc1 mice*. *Acta Neuropathol*, 2010. **120**(4): p. 461-475.
66. van Looij, M.A., et al., *Impact of conventional anesthesia on auditory brainstem responses in mice*. *Hear Res*, 2004. **193**(1-2): p. 75-82.
67. Stahl, J.S., A.M. van Alphen, and C.I. De Zeeuw, *A comparison of video and magnetic search coil recordings of mouse eye movements*. *J Neurosci Methods*, 2000. **99**(1-2): p. 101-10.
68. Maffei, L. and A. Fiorentini, *The visual cortex as a spatial frequency analyser*. *Vision Res*, 1973. **13**(7): p. 1255-67.
69. Watson, A.B. and J.G. Robson, *Discrimination at threshold: labelled detectors*

- in human vision*. Vision Res, 1981. **21**(7): p. 1115-22.
70. Collewijn, H., *Optokinetic eye movements in the rabbit: input-output relations*. Vision Res, 1969. **9**(1): p. 117-32.
 71. Chen, G.D., et al., *Aging outer hair cells (OHCs) in the Fischer 344 rat cochlea: function and morphology*. Hear Res, 2009. **248**(1-2): p. 39-47.
 72. Dallos, P., *The active cochlea*. J Neurosci, 1992. **12**(12): p. 4575-85.
 73. Brownell, W.E., *Outer hair cell electromotility and otoacoustic emissions*. Ear Hear, 1990. **11**(2): p. 82-92.
 74. Horner, K.C., M. Lenoir, and G.R. Bock, *Distortion product otoacoustic emissions in hearing-impaired mutant mice*. J Acoust Soc Am, 1985. **78**(5): p. 1603-11.
 75. Salvi, R.J., et al., *A review of the effects of selective inner hair cell lesions on distortion product otoacoustic emissions, cochlear function and auditory evoked potentials*. Noise Health, 2000. **2**(6): p. 9-26.
 76. Brown, A.M., B. McDowell, and A. Forge, *Acoustic distortion products can be used to monitor the effects of chronic gentamicin treatment*. Hear Res, 1989. **42**(2-3): p. 143-56.
 77. Norton, S.J., J.Y. Bargones, and E.W. Rubel, *Development of otoacoustic emissions in gerbil: evidence for micromechanical changes underlying development of the place code*. Hear Res, 1991. **51**(1): p. 73-91.
 78. Whitehead, M.L., B.L. Lonsbury-Martin, and G.K. Martin, *Evidence for two discrete sources of 2f1-f2 distortion-product otoacoustic emission in rabbit: I. Differential dependence on stimulus parameters*. J Acoust Soc Am, 1992. **91**(3): p. 1587-607.
 79. Trautwein, P., et al., *Selective inner hair cell loss does not alter distortion product otoacoustic emissions*. Hear Res, 1996. **96**(1-2): p. 71-82.
 80. Walton, J.P., *Timing is everything: temporal processing deficits in the aged auditory brainstem*. Hear Res, 2010. **264**(1-2): p. 63-9.
 81. Huang, Q. and J. Tang, *Age-related hearing loss or presbycusis*. Eur Arch Otorhinolaryngol, 2010. **267**(8): p. 1179-91.
 82. Someya, S. and T.A. Prolla, *Mitochondrial oxidative damage and apoptosis in age-related hearing loss*. Mech Ageing Dev, 2010. **131**(7-8): p. 480-6.
 83. Kujoth, G.C., et al., *Mitochondrial DNA mutations, oxidative stress, and apoptosis in mammalian aging*. Science, 2005. **309**(5733): p. 481-4.
 84. Someya, S., et al., *The role of mtDNA mutations in the pathogenesis of age-*

- related hearing loss in mice carrying a mutator DNA polymerase gamma.* Neurobiol Aging, 2008. **29**(7): p. 1080-92.
85. Niu, X., et al., *Somatic mtDNA mutations cause progressive hearing loss in the mouse.* Exp Cell Res, 2007. **313**(18): p. 3924-34.
86. Liu, P. and B. Dimple, *DNA repair in mammalian mitochondria: Much more than we thought?* Environ Mol Mutagen, 2010. **51**(5): p. 417-26.
87. Faulstich, M., et al., *Oculomotor plasticity during vestibular compensation does not depend on cerebellar LTD.* J Neurophysiol, 2006. **96**(3): p. 1187-95.
88. van Alphen, A.M., J.S. Stahl, and C.I. De Zeeuw, *The dynamic characteristics of the mouse horizontal vestibulo-ocular and optokinetic response.* Brain Res, 2001. **890**(2): p. 296-305.
89. Paige, G.D., *Senescence of human visual-vestibular interactions: smooth pursuit, optokinetic, and vestibular control of eye movements with aging.* Exp Brain Res, 1994. **98**(2): p. 355-72.
90. Leigh, R.J., Zee, D. S., *The Neurology of Eye Movements.* 2006: Oxford University Press.
91. Stahl, J.S., *Eye movements of the murine P/Q calcium channel mutant rocker, and the impact of aging.* J Neurophysiol, 2004. **91**(5): p. 2066-78.
92. Stahl, J.S., et al., *Eye movements of the murine P/Q calcium channel mutant tottering, and the impact of aging.* J Neurophysiol, 2006. **95**(3): p. 1588-607.
93. Wang, Y.Z., *Effects of aging on shape discrimination.* Optom Vis Sci, 2001. **78**(6): p. 447-54.
94. McGrath, C. and J.D. Morrison, *The effects of age on spatial frequency perception in human subjects.* Q J Exp Physiol, 1981. **66**(3): p. 253-61.
95. Owsley, C., R. Sekuler, and C. Boldt, *Aging and low-contrast vision: face perception.* Invest Ophthalmol Vis Sci, 1981. **21**(2): p. 362-5.
96. Nameda, N., T. Kawara, and H. Ohzu, *Human visual spatio-temporal frequency performance as a function of age.* Optom Vis Sci, 1989. **66**(11): p. 760-5.
97. Nomura, H., et al., *Age-related change in contrast sensitivity among Japanese adults.* Jpn J Ophthalmol, 2003. **47**(3): p. 299-303.

Chapter 4

Age-related motor neuron degeneration in DNA-repair deficient Ercc1 mice

Nils Z. Borgesius*, Monique C. de Waard*, Ingrid van der Pluijm*, Laura H. Comley, Elize D. Haasdijk, Yvonne Rijksen, Yanto Ridwan, Gerben C. M. Zondag, Gijsbertus T. J. van der Horst, Jan H. J. Hoeijmakers, Ype Elgersma, Thomas H. Gillingwater, Dick Jaarsma

* these authors have contributed equally
adapted from Acta Neuropathol, 2010. 120(4): p. 461-475.

Abstract

Degeneration of motor neurons contributes to senescence-associated loss of muscle function and underlies human neurodegenerative conditions such as amyotrophic lateral sclerosis and spinal muscular atrophy. The identification of genetic factors contributing to motor neuron vulnerability and degenerative phenotypes in vivo are therefore important for our understanding of the neuromuscular system in health and disease. Here, we analyzed neurodegenerative abnormalities in the spinal cord of progeroid *Ercc1^{Δ/-}* mice that are impaired in several DNA repair systems, i.e. nucleotide excision repair, interstrand crosslink repair, and double strand break repair. *Ercc1^{Δ/-}* mice develop age-dependent motor abnormalities, and have a shortened life span of 6–7 months. Pathologically, *Ercc1^{Δ/-}* mice develop widespread astrocytosis and microgliosis, and motor neuron loss and denervation of skeletal muscle fibers. Degenerating motor neurons in many occasions expressed genotoxic-responsive transcription factors p53 or ATF3, and in addition, displayed a range of Golgi apparatus abnormalities. Furthermore, *Ercc1^{Δ/-}* motor neurons developed perikaryal and axonal intermediate filament abnormalities reminiscent of cytoskeletal pathology observed in aging spinal cord. Our findings support the notion that accumulation of DNA damage and genotoxic stress may contribute to neuronal aging and motor neuron vulnerability in human neuromuscular disorders.

Introduction

Functional decline and loss of motor neurons are key pathological hallmarks of many human neuromuscular diseases, including motor neuron diseases such as amyotrophic lateral sclerosis (ALS) and spinal muscular atrophy [1-3]. Degeneration of motor neurons also contributes to age-associated loss of muscle function causing slowing of movement, decline in strength and, eventually, disability [4-6]. Genotoxic stress resulting from cumulative damage to DNA is regarded as a dominant mechanism underlying aging, and several lines of evidence indicate that it contributes to aging processes in neurons [7-9]. DNA is subject to spontaneous hydrolytic decay as well as continuous modification from both endogenous reactive chemicals, such as reactive oxygen species and malondialdehyde, and exogenous environmental factors [10, 11]. Several forms of DNA damage, such as strand breaks, base modifications, and cross-links (particularly protein–DNA) have been reported to accumulate with age in a variety of tissues [8, 10, 12-14]. Being post-mitotic, irreplaceable cells, neurons may accumulate DNA lesions throughout life eventually causing functional deterioration and cell death by interfering with transcription [15-19]. The vulnerability of neurons to DNA lesions and the importance of DNA repair pathways for neuronal maintenance and survival are highlighted by a number of DNA repair deficiency disorders that are characterized by neurological deficits and neurodegenerative changes, in some instances resembling accelerated aging of the nervous system [9, 14, 15, 20]. DNA repair disorders with neurodegenerative changes include a variety of syndromes associated with single strand break (SSB) and double strand break (DSB) repair deficiency [9, 14], as well as disorders resulting from defects in the nucleotide excision repair (NER) pathway that removes helix-distorting and transcription blocking lesions [21, 22]. Neuropathological data have indicated that different brain regions and neuronal types display differential susceptibility towards specific DNA repair defects, and that the cerebellum is particularly affected in many DNA repair deficiency syndromes [9, 14, 15, 21, 22]. However, for most DNA repair disorders the spatiotemporal distribution of degenerative changes throughout the brain and spinal cord remains to be systematically examined, and the role of DNA damage and repair in maintenance and aging of motor neurons has yet to be investigated.

Here, we have investigated the consequences of a failure to repair DNA damage in motor neurons from DNA repair deficient *Ercc1*^{4/-} mice. These mice lack one allele of the excision repair cross-complementing group 1 (*Ercc1*) gene, whereas the protein derived from the other allele shows reduced activity, due to a seven amino-acid carboxyterminal truncation [23]. ERCC1 in complex with XPF acts as a nuclease

in the NER pathway [24], but in addition, it is involved in interstrand crosslink and DSB repair [25-29]. Previous studies with ERCC1- and XPF-deficient patients [28, 30-32] as well as *Ercc1*^{-/-} and *XPF*^{-/-} mice [23, 28, 33-35] have indicated that loss of ERCC1/XPF nuclease function causes a progeroid degenerative phenotype in several organ systems and juvenile death. *Ercc1*^{Δ/-} and *Ercc1*^{Δ/Δ} mice show prolonged life span and an attenuated degenerative phenotype compared to *Ercc1*^{-/-} mice, which can be explained by the low level of residual ERCC1/XPF activity [23, 36]. Our data show that *Ercc1*^{Δ/-} mice develop age-dependent motor abnormalities, disruption of neuromuscular connectivity at the neuromuscular junction, and degeneration of motor neurons. The data support the hypothesis that accumulation of DNA damage and genotoxic stress significantly influences neuronal aging processes and may contribute to motor neuron vulnerability in human neuromuscular disorders.

Results

***Ercc1*^{Δ/-} mice show reduced life span and develop progressive motor abnormalities**

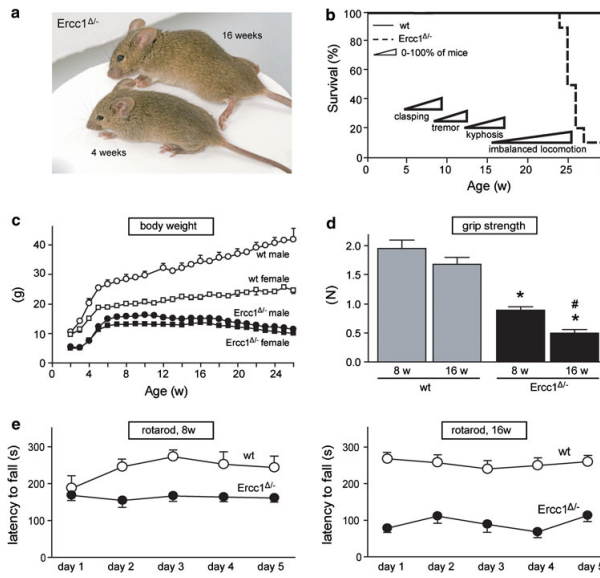


Figure. 1 Progressive motor abnormalities and reduced life span in *Ercc1*^{Δ/-} mice.

a Photograph of 4- and 16-week-old *Ercc1*^{Δ/-} mice, illustrating kyphosis and abnormal limb position in the 16-week-old mouse.

b Survival plot of *Ercc1*^{Δ/-} mice (n = 10) and wild-type (wt) littermates (n = 10) showing reduced life span of *Ercc1*^{Δ/-} mice.

c X-Y plot of body weight (mean ± SE, n = 5 per group) of *Ercc1*^{Δ/-} and wt mice used for survival analysis.

d Bar graph (mean ± SE, n = 8 per group) of grip strength of *Ercc1*^{Δ/-} and wt mice determined by placing mice with four limbs on a grid attached to a force gauge and steadily pulling the mice by their tails. Grip strength is defined as the maximum strength produced by the mouse before releasing the grid. *P<0.01 compared to wild-types; #P<0.01 compared to 8-week-old *Ercc1*^{Δ/-} mice (two-tailed Student's t test).

e Average time spent on an accelerating rotarod of 8- and 16-week-old *Ercc1*^{Δ/-} mice and wt littermates. Mice were given two trials of maximally 5 min per day with a 45–60-min inter-trial interval for five consecutive days. Values represent mean ± SE (n = 8 per group)

Ercc1^{-/-} and *Ercc1*^{Δ/Δ} mice in pure C57Bl/6 or FVB backgrounds are born at a frequency below Mendelian expectation [23]. Therefore, in this study we have used *Ercc1*^{Δ/-} mice in a C57Bl6J/FVB hybrid background, generated by *Ercc1*^{-/+} with *Ercc1*^{Δ/+} mice of pure C57Bl6J and FVB backgrounds, respectively, which were born at a predicted Mendelian frequency. *Ercc1*^{-/+} with *Ercc1*^{Δ/+} do not differ from wild-type mice and show normal aging [23, 36], instead *Ercc1*^{Δ/-} mice were noticeably smaller and showed reduced body weight compared to wild-type littermates (Fig. 1a, c).

The mice reached a maximal weight of 10–15 g at 6–8 weeks of age, before gradually losing weight during subsequent aging (Fig. 1c). From 3 to 8 weeks of age *Ercc1*^{Δ/-} mice started to show clasping of the hind limbs when lifted by their tails. Subsequently, *Ercc1*^{Δ/-} mice developed fine tremors and kyphosis, and from 16 to 24 weeks they showed severe locomotor deficits and reduced ability to maintain balance (Fig. 1a, b). Grip strength and accelerating rotarod analyses showed reduced motor performance in 16 weeks compared to 8-week-old *Ercc1*^{Δ/-} mice (Fig. 1d, e). From 20 to 24 weeks *Ercc1*^{Δ/-} mice had problems with feeding themselves and became moribund. From this stage life span could be extended by 2–6 weeks by giving liquefied food, yielding a maximum life span of 24–30 weeks (Fig. 1b).

***Ercc1*^{Δ/-} mice show age-related increase in astrocytosis and microgliosis**

Pathologically, *Ercc1*^{Δ/-} mice develop mild histological abnormalities in several tissues, in particular liver and kidney, consistent with previous reported findings in *Ercc1*^{Δ/Δ} and *Ercc1*^{-/-} mice [23, 28, 32, 34]. From a neuronal perspective, the brains and spinal cords of *Ercc1*^{Δ/-} mice were smaller than those from wild-type mice proportional to their reduced size (Supplementary Fig. 1a, b). The gross histological organization analyzed using thionine-stained sections appeared normal (data not shown). Similarly, the distributions of markers that identify anatomically distinct subpopulations of neurons such as calbindin (Supplementary Fig. 1c, d) or non-phosphorylated neurofilament (Smi32-epitope, data not shown) were indistinguishable in *Ercc1*^{Δ/-} and wild-type mice. To determine whether *Ercc1*^{Δ/-} mice develop neurodegenerative changes, we first examined glial markers that are known to be up-regulated in response to neuronal injury and degeneration. In 4-week-old *Ercc1*^{Δ/-} mice, glial acidic filament protein (GFAP)-immunohistochemistry revealed small areas of increased GFAP staining throughout the brain (Supplementary Fig. 1f) and spinal cord as shown in Fig. 2b. The amount of GFAP staining increased with subsequent aging resulting in high levels of GFAP staining throughout the brain and spinal cord of *Ercc1*^{Δ/-} mice of 16 weeks and older (Supplementary Fig. 1h and Fig. 2d).

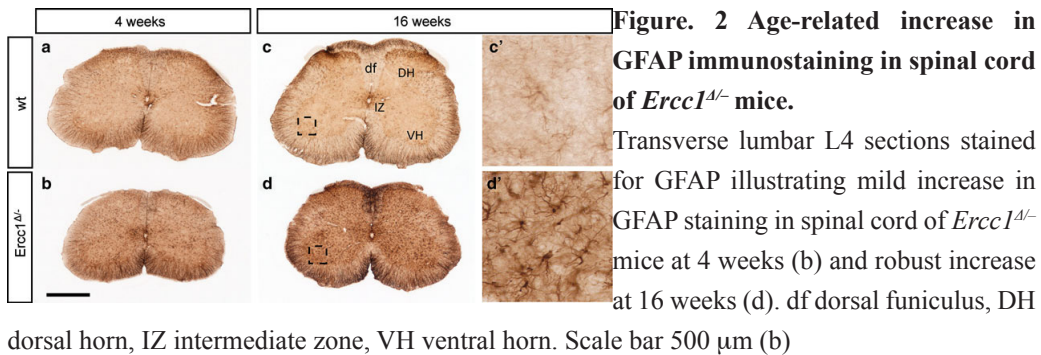


Figure. 2 Age-related increase in GFAP immunostaining in spinal cord of *Ercc1 Δ/Δ* mice.

Transverse lumbar L4 sections stained for GFAP illustrating mild increase in GFAP staining in spinal cord of *Ercc1 Δ/Δ* mice at 4 weeks (b) and robust increase at 16 weeks (d). df dorsal funiculus, DH dorsal horn, IZ intermediate zone, VH ventral horn. Scale bar 500 μm (b)

This age-related increase of GFAP staining was particularly evident in the molecular layer of cerebellar cortex where the size and number of areas with intensely GFAP-immunoreactive astrocytes correlated with increased age, and loss of calbindin immunoreactivity, which in cerebellum represents a selective marker for Purkinje cells (Supplementary Fig. 2). To examine parallel changes in microglia, we stained for the complement 3 receptor (CR3) present on all microglia cells [43] and Mac2 (also known as galectin-3), a protein that is expressed by activated phagocytosing microglia [44]. Control brain and spinal cord show no or very low levels of Mac2-positive microglial cells (Fig. 3a, c–e), while CR3-positive microglia cells showed a quiescent morphology (Supplementary Fig. 3a). In *Ercc1 Δ/Δ* mice, a low level of Mac2-positive microglia cells occurred throughout the brain (not shown) and spinal cord (Fig. 3c, f) at 4 weeks. At older age, *Ercc1 Δ/Δ* mice showed an increasing amount of clusters of Mac2-positive microglia cells throughout the nervous system, but in particular in the caudal brain stem and spinal cord (Fig. 3b, g). Within the spinal cord, activated microglia were present both in the gray and white matter, with relatively high levels in the ventral horn, often in close proximity of motor neurons (Supplementary Fig. 3). Taken together, these data indicate that *Ercc1 Δ/Δ* mice show age-dependent astrogliosis and microglia cell activation, pointing to an increased occurrence of neuronal degeneration throughout the brain and spinal cord.

Death of neurons and non-neuronal cells in the spinal cord of *Ercc1 Δ/Δ* mice

To obtain direct evidence for neuronal degeneration in the spinal cord, we used a silver staining method that selectively labels degenerating neurons and their processes (Fig. 4). *Ercc1 Δ/Δ* mice showed an age-related increase in staining of argyrophilic processes and neuronal cell bodies throughout the spinal cord, not observed in wild-type controls (Fig. 4). Argyrophilic processes, mostly representing degenerating axons, were more frequent

in the white matter as compared to the gray matter, in particular in the dorsal columns (Fig. 4c–e).

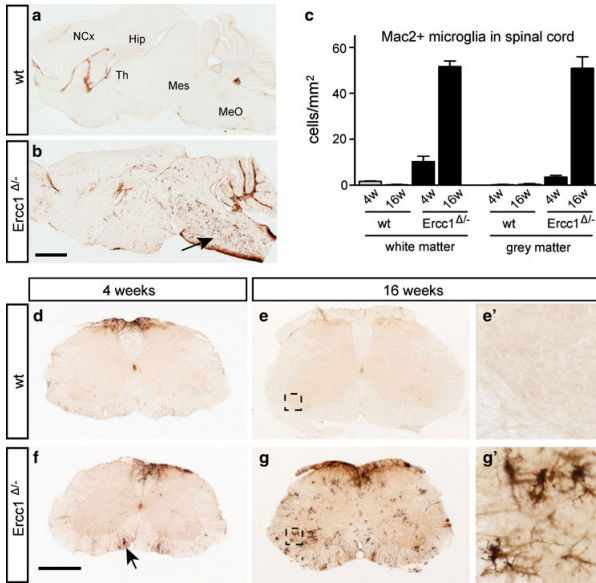


Figure 3 Mac2-positive microgliosis in *Ercc1*^{Δ/Δ} brain and spinal cord.

Parasagittal brain (a, b) and transverse lumbar L4 sections (d–g) of *Ercc1*^{Δ/Δ} and wt mice stained for the phagocytosing microglia marker Mac2 showing Mac2-positive microglia throughout *Ercc1*^{Δ/Δ} brain and spinal cord at 16 weeks (b, g).

In the brain, the highest levels of Mac2-positive microglia occur in caudal brain stem (arrow, b) and white matter of cerebellar cortex. In spinal cord, highest levels of Mac2-positive microglia occur in white matter and motor columns in the ventral horn (g). Mac2-positive

microglia cells are also present in 4-week-old *Ercc1*^{Δ/Δ} spinal cord (arrow, f), but at much lower levels than at 16 weeks. (c) Values in bar graph are mean ± SE of four mice based on countings of three L4 sections per mouse. Hip hippocampus, MeO medulla oblongata, Mes mesencephalon, NCx neocortex, Th thalamus. Scale bars 2 mm (a) and 500 μm (d)

In addition, infrequent argyrophilic neuronal cell bodies were observed in the motor columns of spinal cord from 8- and 16-week-old *Ercc1*^{Δ/Δ} mice (Fig. 4b). Analysis of 25 L4 sections of 16-week-old *Ercc1*^{Δ/Δ} mice (n = 4), containing approximately 1,000 motor neurons, identified two argyrophilic motor neurons, suggesting that approximately one in 500 motor neurons was in a moribund stage. The same frequency of dying motor neurons was observed in spinal cord sections stained for active caspase 3, a major proteolytic protein in multiple cell death pathways (Supplementary Fig. 4b). Active caspase 3 staining was also associated with cells with a shrunken apoptotic morphology or with irregular structures, putatively reflecting remnants of dead cells (Supplementary Fig. 4). Apoptotic cells were also identified in the white matter (Supplementary Fig. 4c, d), indicating that glial cell death was likely to be occurring in *Ercc1*^{Δ/Δ} mice. Data from active caspase 3 staining were confirmed by TUNEL staining for detecting DNA fragmentation [45], showing increased levels of TUNEL positive cells in spinal cord of *Ercc1*^{Δ/Δ} mice (Supplementary Fig. 4e–g). Taken together, these cell death markers provide evidence for a low level of ongoing cell death in *Ercc1*^{Δ/Δ} spinal cord.

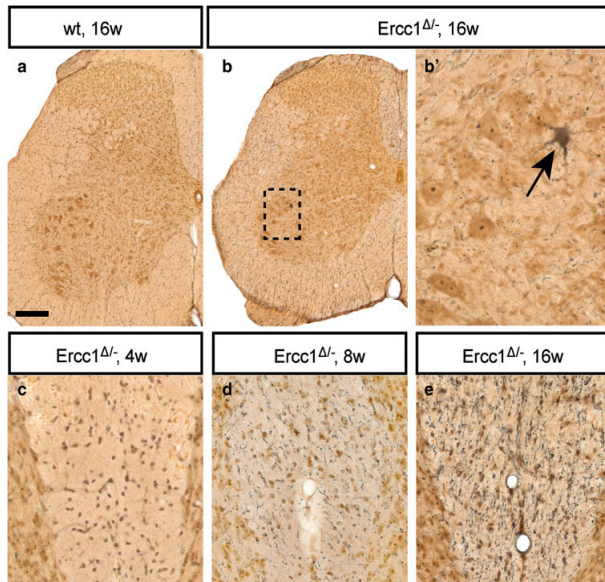


Figure. 4 Neuronal degeneration in *Ercc1^{Δ/Δ}* spinal cord.

Silver degeneration staining visualizing the distribution of neuronal degeneration in *Ercc1^{Δ/Δ}* spinal cord. Note an argyrophilic motor neuron (b, arrow) and an age-related increase in the amount of argyrophilic fibers in the dorsal funiculus (c–e). Scale bars 250 μm (a), 50 μm (c)

Loss of motor neurons, axonal pathology, and neuromuscular denervation in *Ercc1^{Δ/Δ}* mice

To directly examine the extent of motor neuron loss, we counted motor neurons in serial sections immunostained for choline acetyltransferase (ChAT), or CGRP, a peptide expressed by a subpopulation of large motor neurons [40]. The numbers of both ChAT-labeled and CGRP-labeled motor neurons were significantly reduced in 8- and 16-week-old *Ercc1^{Δ/Δ}* mice compared to 4-week-old *Ercc1^{Δ/Δ}* mice and age-matched wild-type controls (Fig. 5a–e). As motor nerve terminals at the neuromuscular junction are known to be early pathological targets in degenerating lower motor neurons [1, 2], we analyzed neuromuscular junction integrity in deep lumbrical muscles (Fig. 6). There was widespread evidence of denervated muscle fibers where pre-synaptic motor nerve terminals had degenerated, entirely or partially vacating the post-synaptic motor endplate from *Ercc1^{Δ/Δ}* mice at 8 and 16 weeks (Fig. 6). A subset of motor endplates was innervated by more than one incoming axon collateral (Fig. 6b). Quantification of neuromuscular morphology revealed a significant decrease in normal neuromuscular junctions and corresponding increases in the numbers of partially occupied, vacant and poly-innervated neuromuscular junctions in *Ercc1^{Δ/Δ}* mice at 8 and 16 weeks (Fig. 6d–g). Analysis of motor nerve terminals revealed signs of neurofilament accumulation (Fig. 6a) as well as axon blebbing in distal motor axons (Fig. 6c). Neurofilament abnormalities also occurred in the proximal motor axons and the cell body (not shown). The same changes were observed with an antibody against peripherin (Fig. 5f–h), a type III intermediate filament protein predominantly expressed in axons of dorsal root ganglion cells and motor neurons that is associated with cytoskeletal pathology in ALS and aging motor neurons [46]. Hence, a subset of motor neurons

showed substantial increased peripherin immunoreactivity in the cell body and the proximal axon coursing through the ventral gray and white matter. Axons with increased neurofilament and peripherin immunoreactivity showed an expanded morphology (Fig. 5g, h) reminiscent of axonal swellings such as those observed in ALS and aging spinal cord [46]. The neurofilament and peripherin abnormalities were already present at 4 weeks of age (not shown), and were more frequent at 8 (Fig. 5g, h) and 16 weeks.

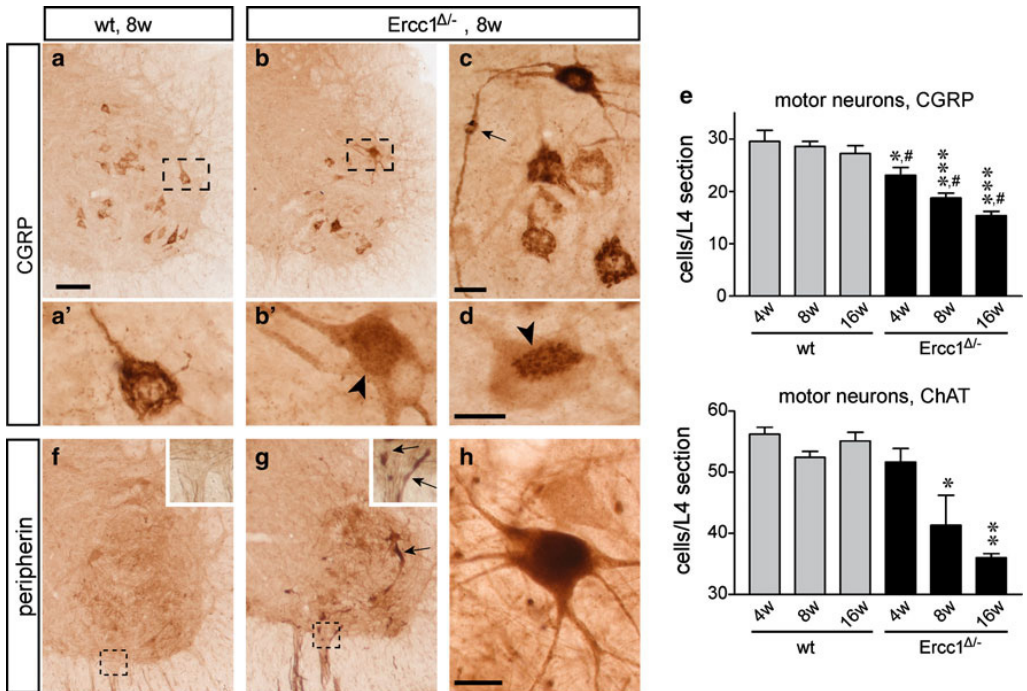


Figure. 5 Motor neuron loss in *Ercc1*^{Δ/-} spinal cord.

a–d Low- (a, b) and high-magnification (a', b', c, d) photomicrographs of CGRP staining in the ventral horn of wt (a) and *Ercc1*^{Δ/-} (b–d) spinal cord. In control motor neurons, CGRP is predominantly localized to a network of linear profiles representing the Golgi apparatus. Note a variety of abnormalities of CGRP distribution in a subset of *Ercc1*^{Δ/-} motor neurons, including diffuse punctate staining in the cell body (b'), axonal accumulation of CGRP (arrow, c), and redistribution of the labeling to part of the cell body (d). e Bar graphs showing the number of CGRP and choline acetyltransferase (ChAT)-labeled motor neurons in L4 spinal cord sections of wt and *Ercc1*^{Δ/-} mice. Values are mean ± SE of four mice, while value per mouse is the mean of six L4 sections. Note age-related decrease of the number of motor neurons in *Ercc1*^{Δ/-} mice. *, **, ***P<0.05, 0.01, and 0.001 compared to wt mice of the same age (one-way ANOVA with Tukey's multiple comparison test); #P = 0.002 (post-test for linear trend). f–h Photomicrographs of peripherin immunostaining in the ventral horn of wt (f) and *Ercc1*^{Δ/-} (g, h) spinal cord, showing

increased peripherin immunostaining in a subset of motor neurons and motor axons (arrows, g). Scale bars 100 μm (a) and 25 μm (c, d, h)

p53 and ATF3 activation in partially overlapping populations of *Ercc1*^{Δ/Δ} motor neurons

To further examine the link between motor neuron degeneration and DNA damage, we studied the expression of the transcription factor p53, which is known to be activated by multiple types of DNA damage and to mediate neuronal degeneration [47]. P53-immunohistochemistry revealed cells with intense nuclear p53-staining throughout *Ercc1*^{Δ/Δ} spinal cord, while no labeled cells occurred in wild-type or *Ercc1*^{-/+} spinal cords (Fig. 7a–c). Labeled cells were present in the white and the gray matter, and occasionally could be identified as motor neurons on the basis of localization in the ventral horn and somatodendritic morphology and size. Double labeling with the astrocytic marker GFAP, the neuronal marker NeuN or the motor neuron marker ChAT, respectively, confirmed that p53 labeling was present in neurons and astrocytes (Fig. 7g–i), with the latter accounting for most p53-positive cells in white matter. P53-positive astrocytes and neurons were present in spinal cord of 4-week-old *Ercc1*^{Δ/Δ} mice, but were more frequent at 8 and 16 weeks (Fig. 7c). To further explore the DNA damage response in neurons in *Ercc1*^{Δ/Δ} spinal cord, we studied the expression of the stress-inducible transcription factor ATF3, which is induced following genotoxic stress via p53-dependent and -independent pathways [48-50]. ATF3, while minimally expressed in control spinal cord, was clearly present in an increasing amount of *Ercc1*^{Δ/Δ} motor neurons as well as other spinal cord neurons localized in the intermediate zone and dorsal horn (Fig. 7d–f). Quantitative analysis of L4 lumbar sections indicated that ATF3-positive motor neurons were more frequent than p53-positive motor neurons. Accordingly, double-labeling for p53 and ATF3 indicated that the majority of ATF3-positive motor neurons (33 of 38) were p53-negative, while approximately equal amounts of p53-positive motor neurons were ATF3-negative (6 of 11) or ATF3-positive (5 of 11; Fig. 7j–l).

A variety of Golgi apparatus abnormalities in *Ercc1*^{Δ/Δ} motor neurons

Sections stained for CGRP, which in wild-type motor neurons is predominantly localized in the Golgi apparatus (Fig. 5a), revealed subcellular abnormalities suggestive of an abnormal Golgi apparatus in a subset of *Ercc1*^{Δ/Δ} motor neurons (Fig. 5d). To systematically characterize Golgi abnormalities, we performed double labeling of p53 or ATF3 with an antibody against the cis-Golgi protein GM130 [51]. This analysis

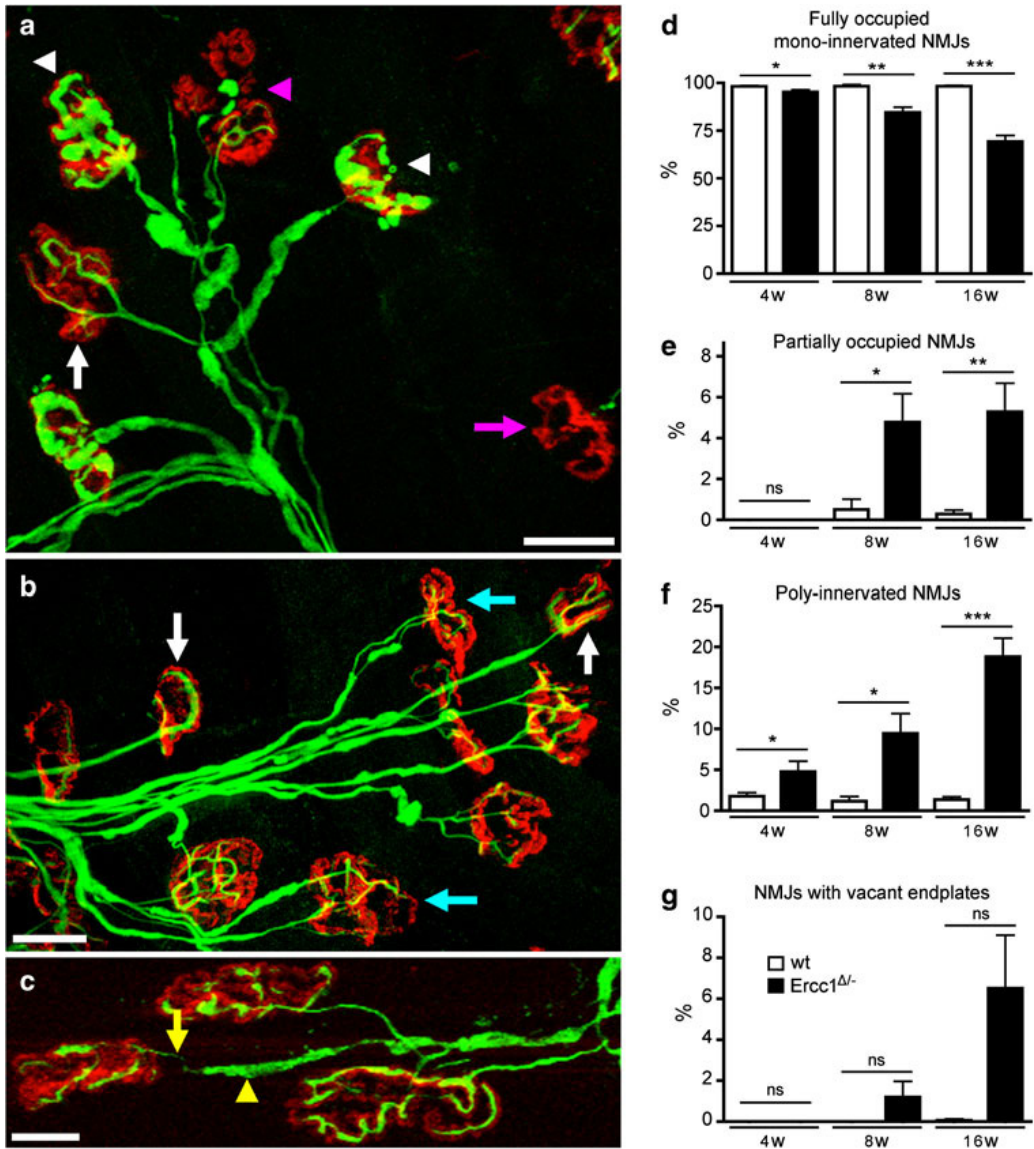


Figure. 6 Synaptic pathology at the neuromuscular junction in *Ercc1*^{Δ/Δ} mice.

a–c Confocal micrographs of neuromuscular junctions from lumbrical muscles of 16-week-old *Ercc1*^{Δ/Δ} mice labeled with rhodamine a-bungarotoxin to reveal post-synaptic motor endplates (red) and antibodies against 150 kDa neurofilaments to reveal presynaptic axons and motor nerve terminals (green). Examples of ‘normal’ (white arrows), denervated (pink arrow, a), partially denervated (pink arrowhead, a), poly-innervated (cyan arrows, b), and neuromuscular junctions are shown. Examples of motor nerve terminals with conspicuous neurofilament accumulation are indicated by the white arrowheads in a. Also note the presence of axon blebbing in c where the incoming axon is very thin (yellow arrow), but is interspersed by regions of neurofilament accumulations (yellow arrowhead). d–g Quantification of synaptic pathology in 4–16-weekold

Ercc1D^{-/-} mice compared to wild-type controls. *, **, *** $P < 0.05$, 0.01, and 0.001, respectively, compared to wt mice of the same age (Kruskal–Wallis test with Dunn’s post-hoc test). Scale bars 40 μm (a, b) and 20 μm (c)

showed that ATF3- and p53-labeled motor neurons display a variability of abnormal morphologies of the Golgi apparatus, consisting of fragmentation of Golgi stacks (Fig. 8c, d, f–h, l, m), or the redistribution of unfragmented or fragmented Golgi stacks to part of the cell body (Fig. 8b, i, k, l). In some motor neurons, GM130 labeling was restricted to a very small portion of the cell body, occasionally giving the impression that GM130 labeling had entirely disappeared from the cell (Fig. 8b, i, k). Double labeling of GM130 and CGRP showed that in motor neurons with fragmented Golgi, GM130 and CGRP maintain their adjoining, slightly overlapping localization (Fig. 8e, f), which points to fragmentation into ministacks. Motor neurons with redistribution of GM130 staining to a restricted area of the cell body showed a similar redistribution of CGRP (Fig. 5d), but in some occasions also showed a dramatic accumulation of CGRP in the rest of the cell body (Fig. 5c), putatively representing the accumulation of post-Golgi CGRP vesicles [40]. The same was observed with an antibody against SCG10 (Fig. 8i), a tubulin-binding protein that is associated with the trans-Golgi and post-Golgi vesicles [52]. In contrast, no major changes were observed in the intracellular distribution of endoplasmic reticulum proteins calreticulin and VAPB [39], even in *Ercc1^{D/-}* motor neurons with considerably altered GM130 distribution (Fig. 8j, k). Systematic analysis of 250 lumbar L4 motor neurons in ATF3/GM130-stained sections from 16-week-old *Ercc1^{D/-}* mice ($n = 3$) indicated that at this age as many as 25% (63 of 250) of motor neurons had an abnormal Golgi morphology, 22% (14 of 63) of which showed Golgi fragmentation. This analysis also showed that all ATF3-positive *Ercc1^{D/-}* motor neurons had an abnormal Golgi with various morphologies (Fig. 8b, c). Inversely, only a minority (21 of 63) of motor neurons with an abnormal Golgi was positive for ATF3 (Fig. 8d). Similarly, analysis of p53/GM130-stained sections showed that the majority (36 of 42) of motor neurons with Golgi abnormalities were p53-negative. Inversely, all p53-positive motor neurons (6 of 6) in this analysis had an abnormal Golgi apparatus (Fig. 8g, h). These data indicate that Golgi abnormalities represent a sensitive marker for cellular deficits in motor neurons.

To determine the extent to which p53- and ATF3-positive *Ercc1^{D/-}* motor neurons and motor neurons with abnormal GM130 labeling were towards the final stages of cell death, we double-labeled for Mac2 outlining phagocytosing microglia (see above). This

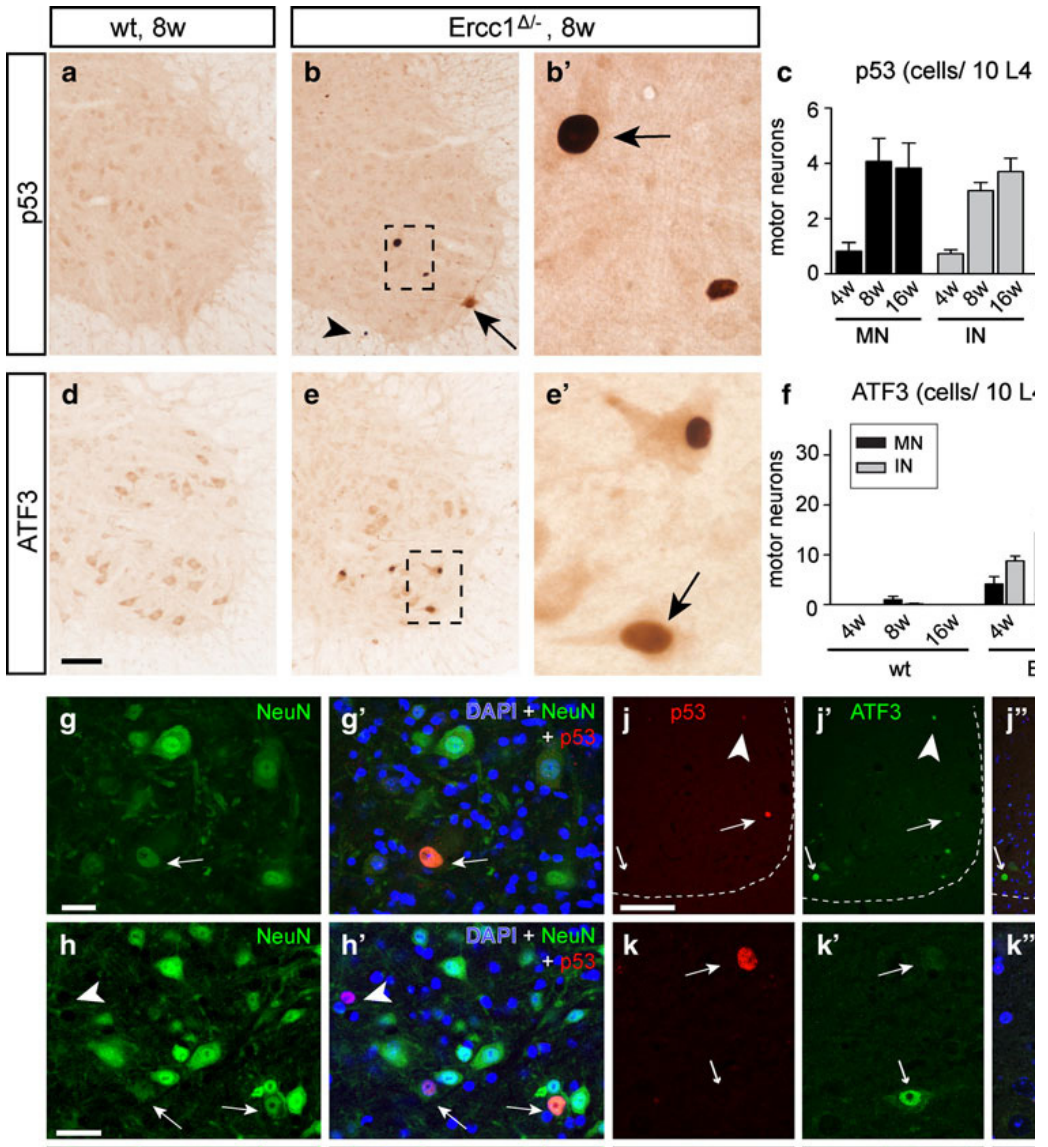


Figure. 7 Genotoxic stress-responsive transcription factor p53 and ATF3 expression in *Ercc1*^{Δ/Δ} spinal cord.

a–f Photomicrographs (a, b, d, e) and bar graphs (c, f) of p53 (a–c) and ATF3 (d–f) immunostaining, illustrating induction of p53 (arrows; b, b') and ATF3 (arrow, e') expression in *Ercc1*^{Δ/Δ} motor neurons. Prominent p53 labeling also occurred in astrocytes (arrowhead, b), while both p53 and ATF3 were expressed by interneurons in the spinal cord intermediate zone and dorsal horn (c, f). Values in c and f are mean ± SE of four mice, while value per mouse is from ten L4 sections. g–i Double-labeling confocal images showing p53–NeuN (g, h) and p53–GFAP (i) double-labeled cells in *Ercc1*^{Δ/Δ} spinal cord. j–l Double-labeling confocal immunofluorescence of p53 and ATF3 showing that p53 and ATF3 in most instances are expressed in distinct cells in *Ercc1*^{Δ/Δ} spinal cord

sections. ATF3 single-labeled motor neurons (small arrows; j, k) occurred more frequently than p53 single-labeled motor neurons (large arrows; j, k) and double-labeled cells (arrowhead; j, l). Scale bars 100 μm (d, j), 25 μm (g, h) and 10 μm (i, l)

analysis revealed a small subset (<10%) of afflicted *Ercc1*^{Δ/Δ} motor neurons surrounded by phagocytosing microglia (Supplementary Fig. 5). Taken together, our pathological analyses indicate that *Ercc1*^{Δ/Δ} motor neurons may experience a variability of cellular deficits that ultimately lead to cell death.

Motor neurons of *Ercc1*^{Δ/Δ} mice do not show TDP-43 or FUS abnormalities

Finally, we examined the extent to which the neurodegenerative phenotype observed in *Ercc1*^{Δ/Δ} motor neurons has features in common with ALS by staining for nuclear TAR-DNA-binding protein-43 (TDP-43), a DNA/RNA-binding protein whose accumulation in the cytoplasm and subsequent aggregation into inclusions represents a key pathological feature in the majority of ALS cases [53], and FUS protein, another DNA/RNA-binding protein that mislocalizes to the cytoplasm and aggregates in a familial form of ALS [54]. Screening of more than 50 spinal cord sections from six 16–20-week-old *Ercc1*^{Δ/Δ} mice indicated that all cells, including motor neurons with abnormal Golgi apparatus and nuclear morphology, showed normal nuclear TDP-43 and FUS staining (Fig. 8l, m). Accordingly, immunostaining with an anti-ubiquitin antibody did not reveal any cells with ubiquitinated pathological protein inclusions, a feature associated with TDP43 pathology in ALS [53].

Discussion

In this study, we provide direct evidence that modifications in DNA repair pathways are a robust modulator of motor neuron vulnerability in vivo. We show that *Ercc1*^{Δ/Δ} mice develop an age-dependent degeneration of motor neurons and progressive loss of neuromuscular connectivity. Motor neuron degeneration occurred in parallel with signs of astrocyte and microglia activation, and was associated with several morphological and molecular changes, including neurofilament and peripherin abnormalities in the cell body and the axon, misplaced and flattened nuclei, morphological changes of the Golgi apparatus, and expression of the transcription factors p53 and ATF3. Neurofilament accumulations in distal axons and motor nerve terminals are a well-documented feature of motor neuron pathology in many different animal models of motor neuron degeneration, thought to occur due to disrupted cytoskeletal organization and impaired axonal transport

[1, 55]. P53 and ATF3, which are both known to be activated in response to genotoxic stress [47, 48, 56], were expressed in largely non-overlapping populations of motor

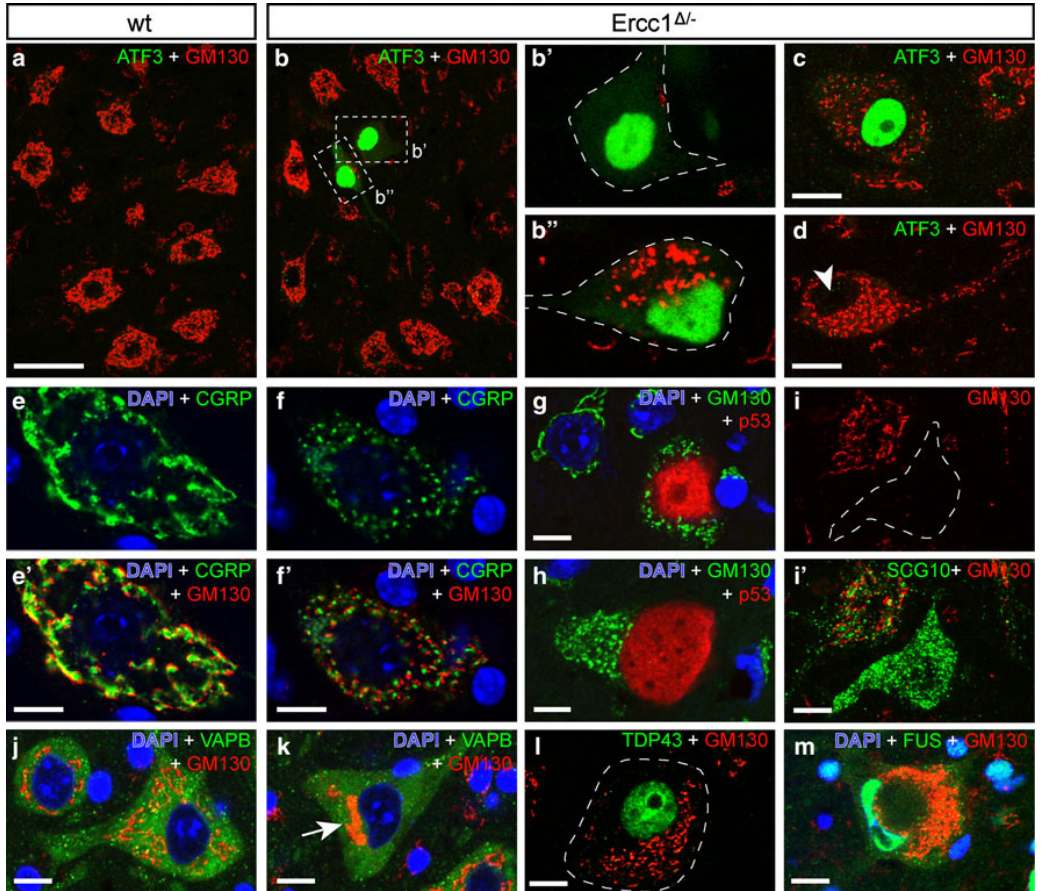


Figure. 8 Golgi apparatus abnormalities in *Ercc1 Δ -* motor neurons.

Double-labeling confocal immunofluorescence of the cis-Golgi protein GM130 with ATF3 (a–d), CGRP (e, f), p53 (g, h), SCG10 (i), VAPB (j, k), TDP43 (l), or FUS (m) in motor neurons of wt (a, e, j) and *Ercc1 Δ -* spinal cord (b–d, f–i, k–m). A variety of Golgi abnormalities occur in *Ercc1 Δ -* spinal cord, including a redistribution of GM130 staining to a small part of the cell (b, i, k, l) and fragmentation (c, d, f–h, l, m). Golgi abnormalities may (b, c) or may not (arrowhead, d) be associated with ATF3 expression. Motor neurons that are positive for p53 generally display Golgi fragmentation (g, h). In motor neurons with fragmented Golgi, GM130 and CGRP, which are localized in the cis- and trans-Golgi, respectively, maintain their adjoining slightly overlapping localization (e, f). Motor neurons with redistributed Golgi apparatus show normal distribution of endoplasmic reticulum-associated protein VAPB (k). Motor neurons with severely abnormal Golgi apparatus morphologies show a normal nuclear distribution of TDP43 and FUS (l, m). Scale bars 50 μ m (a), 20 μ m (c, d, i) and 10 μ m (e–m)

neurons. This differential expression of stress genes in different motor neurons may be explained by heterogeneity of cellular damage responses triggered by different cellular deficits. A heterogeneity of cellular deficits was also suggested by the Golgi apparatus abnormalities, occurring in a large proportion of motor neurons on many occasions in the absence of ATF3 or p53 expression, and being variable as compared to the relatively stereotyped Golgi abnormalities known to occur in other neurodegenerative conditions targeting motor neurons, such as ALS [40, 57]. The Golgi apparatus is a highly dynamic organelle whose morphology depends on a large variety of protein components and cellular processes, and alters under a wide variety of conditions, including impaired endoplasmic reticulum function, disruption of the trafficking and sorting machinery, altered lipid metabolism, and activation of cell death pathways [57-61]. Thus, the large number of factors influencing the morphology and function of the Golgi apparatus may render it relatively vulnerable to stochastic DNA damage afflicting the transcription of randomly distributed genes, and might explain the high frequency and heterogeneity of Golgi abnormalities in *Ercc1^{Δ/Δ}* motor neurons. Taken together our pathological data are compatible with a model where motor neurons in *Ercc1^{Δ/Δ}* mice are afflicted by stochastic DNA lesions that block or deregulate gene expression, and indicate that motor neurons require efficient ERCC1-dependent DNA repair pathways for long-term survival. Our data complement previous observations in ERCC1 and XPF-deficient patients [28, 31] and in *Ercc1^{-/-}* and *Xpf^{-/-}* mice [23, 28, 33-35] indicating that loss of ERCC1/XPF nuclease function causes a progeroid degenerative phenotype in several organ systems and juvenile death. *Ercc1^{-/-}* mice have also been reported to develop motor problems [23, 28, 34], which were assigned to developmental and degenerative abnormalities of the cerebellar cortex [31]. The short life span of *Ercc1^{-/-}* mice used in these studies precluded the systematic investigation of age-dependent neurodegenerative changes. We did not observe obvious structural abnormalities in the nervous systems of our *Ercc1^{Δ/Δ}* mice at 4 weeks of age, apart from reduced size and some initial signs of neuronal degeneration. Although at this point subtle neurodevelopmental changes cannot be ruled out, the lack of a neurodevelopmental phenotype such as observed in *Ercc1^{-/-}* mice can be explained by the low level of residual ERCC1/XPF activity in *Ercc1^{Δ/Δ}* mice [22, 23]. Importantly, our data show that the progression of motor abnormalities in *Ercc1^{Δ/Δ}* mice correlated with the time course of neurodegenerative changes, indicating that the motor deficits observed may occur as a result of degenerative changes in the neuromuscular system. As *Ercc1^{Δ/Δ}* mice also develop age-related degenerative changes throughout the rest of the brain, also deficits in other motor areas, including the sensorimotor cortex and

the cerebellum may contribute to the progressive motor deficits. The identity of the DNA lesions triggering neurodegenerative changes in *Ercc1^{Δ/-}* mice remains to be determined. Oxidative base damage such as 7,8-dihydro-8-oxoguanine (8-oxoG) is repaired by the base excision repair (BER) pathway and may not accumulate in *Ercc1^{Δ/-}* mice. However, other oxidative lesions such as malondialdehyde adducts and 8,50-cyclopurine-20-deoxynucleotides are both NER substrates and potential threats to transcription [12, 18, 62]. The involvement of ERCC1/XPF as a nuclease in multiple repair pathways in addition to NER (interstrand crosslink repair and DSB repair) raises the question whether the neurodegenerative changes observed were caused by deficiency in one of these pathways, or by synergistic deleterious actions resulting from defects in multiple pathways [7, 23]. Patients with XPA-mutations that are selectively deficient in NER develop juvenile or adult onset of neuronal degeneration which indicates that NER deficiency alone can cause neuronal degeneration [20, 21]. However, *Xpa^{-/-}* mice that are entirely NER deficient have not been reported to develop noticeable neurological or neurodegenerative abnormalities up to 2 years of age [63, 64], and accordingly, extensive analyses of *Xpa^{-/-}* spinal cords revealed very infrequent p53-positive cells (<1 per mm²; Jaarsma, unpublished observation). Instead, the *Xpa^{-/-}* genotype causes a severe progeroid phenotype when crossed into mice that are deficient in transcription coupled repair [65, 66], indicating that NER deficiency may exacerbate the deleterious effects of deficiencies in other repair pathways [7]. Accordingly, the degenerative changes in motor neurons that we observed here may result from combined deficiencies in NER and other repair pathways depending on ERCC1/XPF.

Cumulative DNA damage and abnormalities in DNA repair pathways have been implicated in ALS and other motor neuron diseases, but genetic evidence pointing to DNA-repair genes as a risk or causative factor is inconclusive or lacking [8, 67]. A potential exception is provided by mutations in SETX that are linked to a rare dominant slowly progressing early onset motor neuron disease (ALS4) [68]. SETX is a DNA/RNA helicase that has been implicated in the defense against oxidative DNA damage [69]. The ALS4 mutation of SETX may lead to the dysfunction of its helicase activity [68], but how this is connected to motor neuron degeneration and whether it involves DNA damage is not understood. Other evidence involving DNA damage in motor neuron disease comes from pathological studies, suggesting increased levels of DNA lesions and p53 activation in post-mortem ALS motor neurons, but these changes are thought to represent late events rather than causative factors in the degenerative cascade [8]. In the present study, we show that *Ercc1^{Δ/-}* motor neurons do not develop TDP43

pathology which is a key pathological feature in the majority of ALS patients [53], a minority of which have mutations in the TDP43 gene, while the majority being caused by mechanisms that remain to be defined [54, 70]. This indicates that DNA damage resulting from ERCC1 deficiency is not sufficient to trigger the events yielding ALS pathology. Rather we propose that cumulative DNA damage may act as one of the age-related risk factors contributing to degenerative disorders such as ALS.

In summary, we propose that DNA repair pathways may have a hitherto unappreciated role in neuromuscular form and function in human neurodegenerative disease, and that the *Ercc1^{Δ/-}* mouse provides an excellent model to study the effects of accelerated aging on the neuromuscular system in vivo. In addition, the *Ercc1^{Δ/-}* mice may represent a unique mouse model for testing interventional approaches aimed at reducing genotoxic stress in neurons.

Acknowledgments

We thank Sofie van Tuijl for her assistance. This work was supported by the Prinses Beatrix Fonds (DJ), the Netherlands Organization for Scientific Research (ZonMW-TOP; YE), BBSRC (THG/LHC), BDFNewlife (THG) and the Wellcome Trust (THG).

Materials and Methods

Mice

Experiments were performed in accordance with the “Principles of laboratory animal care” (NIH publication no. 86-23) and the guidelines approved by the Erasmus University animal care committee. The generation of *Ercc1^{-/-}* and *Ercc1^Δ* alleles has been previously described [23]. *Ercc1^{Δ/-}* mice were obtained by crossing *Ercc1^{-/+}* with *Ercc1^{Δ/+}* mice of C57Bl6J and FVB backgrounds to yield *Ercc1^{Δ/-}* with C57Bl6J/FVB hybrid background [36]. Wild-type, *Ercc1^{Δ/+}* *Ercc1^{-/+}* littermates were used as controls. Mice were housed in individual ventilated cages with *ad libitum* access to standard mouse food (CRM pellets, SDS BP Nutrition Ltd; gross energy content 18.36 kJ/g dry mass, digestible energy 13.4 kJ/g) and water. *Ercc1^{Δ/-}* mice received liquefied food when they were not able to reach the food due to movement disabilities. The mice were weighed and visually inspected weekly, and were scored for gross morphological and motor abnormalities including the onset of kyphosis, abnormalities in hind limb extension when lifted by the tail, and balance and locomotion deficits. Motor performance was further determined using a grip strength test and accelerating Rotarod as described [37, 38].

Antibodies

Primary antibodies (supplier; dilutions) used in this study were as follows: rabbit anti-ATF3 (Santa Cruz; 1:1,000); rabbit anti-calbindin (Swant; 1:10,000); rabbit anti-cleaved caspase 3 (Asp175; Cell Signaling Technology; 1:500); rabbit anti-calreticulin (Affinity BioReagents; 1:5,000); rabbit anti-CGRP (Calbiochem; 1:10,000); goat anti-ChAT (Millipore; 1:500); rat anti-CR3 receptor (clone 5C6; Serotec; 1:500); rabbit anti-FUS (A300-302A RP, Bethyl Laboratories; 1:2,000); rabbit anti-GFAP (DAKO; 1:10,000); mouse anti-GFAP (Sigma; 1:10,000); mouse anti-GM130 (Transduction Laboratories; 1:100); rat anti-Mac2 (Cedarlane; 1:2,000); mouse anti-NeuN (Millipore; 1:1,000); chicken anti-neurofilament-M (Millipore; 1:2,000); rabbit anti-neurofilament160 (Millipore; 1:250); mouse antihyperphosphorylated neurofilament (SMI31, Sternberger 462 Acta Neuropathol (2010) 120:461–475 123 Monoclonals; 1:20,000); mouse anti-non-phosphorylated neurofilament (SMI32, Sternberger Monoclonals; 1:4,000); rabbit anti-p53 (Leica; 1:1,000); rabbit anti-peripherin (Millipore; 1:1,000); rabbit anti-SCG10 (gift from Dr. A. Sobel; 1:4,000); rabbit anti-TDP43 (Proteintech; 1:1,000); rabbit anti-ubiquitin (Dako; 1:2,000); rabbit anti-VAPB (#1006-00 [39]; 1:1,000).

For avidin–biotin–peroxidase immunocytochemistry, biotinylated secondary antibodies from Vector Laboratories diluted 1:200 were used. FITC-, Cy3-, and Cy5-conjugated secondary antibodies raised in donkey (Jackson Immunoresearch, USA) diluted at 1:200 were used for immunofluorescence. Cy3-conjugated donkey anti-rabbit Fab fragment (Jackson Immunoresearch) was used in double-labeling experiments with two rabbit primary antibodies.

Histological procedures

Mice were anaesthetized with pentobarbital and perfused transcardially with 4% paraformaldehyde; lumbar and cervical spinal cord were dissected out, post-fixed for 2h in ice-cold 4% paraformaldehyde, cryoprotected, embedded in 10% gelatine blocks, rapidly frozen, and sectioned at 40 µm using a freezing microtome or stored at -80°C until use [40]. Frozen sections were processed free floating for immunofluorescence or avidin–biotin–immunoperoxidase complex method (ABC, Vector Laboratories, USA) with diaminobenzidine (0.05%) as the chromogen as described previously [40]. In addition, a selected number of frozen gelatin sections was collected in 4% paraformaldehyde, and processed with a modified Gallyas silver impregnation procedure of Nadler and Evenson [41] that selectively labels degenerating neurons and their processes. For double-labeling immunofluorescence with two rabbit antibodies Cy3-conjugated donkey anti-rabbit Fab

fragments was used to label and sterically cover the first antibody, as described by the manufacturer (Jackson Immunoresearch). Sections were then incubated with the second antibody that was labeled consecutively with FITC-conjugated donkey anti-rabbit. Alternatively, brain and spinal cord specimens were paraffin-embedded, sectioned at 4 μm , and mounted on Superfrost slides. For immunohistochemistry, paraffin sections were deparaffinized, rehydrated in decreasing concentrations of ethanol, treated with 10 mM sodium citrate buffer, pH 6, in the microwave for antigen retrieval, and further processed using the ABC method. A series of paraffin sections were employed for TdT-mediated dUTP Nick-End Labeling (TUNEL) assay using a commercial kit (Apoptag Plus Peroxidase in situ apoptosis detection kit, Millipore). Sections were deparaffinized and incubated as described by the manufacturer. Immunoperoxidase-stained sections were analyzed and photographed using a Leica DM-RB microscope and a Leica DC300 digital camera. Sections stained for immunofluorescence were analyzed with a Zeiss LSM 510 confocal laser scanning microscope. Quantitative analyses of motor neurons were performed on serial lumbar 4 (L4) sections immunoperoxidase stained for ChAT or CGRP as described previously [37]. Parallel series were used for counting ATF3- and p53-labeled cells.

Neuromuscular junction analysis

Neuromuscular junctions were analyzed in deep lumbrical muscles stained for neurofilament 160 and α -bungarotoxin (5 $\mu\text{g}/\text{ml}$ for 30 min, Molecular Probes), as described previously [42]. Muscles were whole-mounted in Mowiol® (Calbiochem) on glass slides and cover-slipped for subsequent imaging using a Nikon IX71 epifluorescence microscope equipped with a 40 \times oil immersion objective (NA 0.8) or a BioRad Radiance 2000 Laser Scanning confocal microscope. All analyses were undertaken by an observer blind to the genotype of the specimen. Randomly selected endplates (minimum of 100 per muscle) were categorized as either fully innervated (e.g. ‘normal’: neurofilament staining from a single axon entirely overlies endplate), partially innervated, denervated (no neurofilament overlies endplate), or poly-innervated (more than 1 axon converging on individual endplates).

Statistical analyses

Statistical analyses were performed using GraphPad Prism Software (San Diego, CA, USA). Means from different ages and mouse groups were compared using Student’s t test, Kruskal–Wallis test with Dunn’s post-hoc test or oneway ANOVA with Tukey’s

post-hoc test.

References

1. Murray, L.M., et al., *Selective vulnerability of motor neurons and dissociation of pre- and post-synaptic pathology at the neuromuscular junction in mouse models of spinal muscular atrophy*. Hum Mol Genet, 2008. **17**(7): p. 949-62.
2. Murray, L.M., K. Talbot, and T.H. Gillingwater, *Review: neuromuscular synaptic vulnerability in motor neurone disease: amyotrophic lateral sclerosis and spinal muscular atrophy*. Neuropathol Appl Neurobiol, 2010. **36**(2): p. 133-56.
3. Valdmánis, P.N., et al., *Recent advances in the genetics of amyotrophic lateral sclerosis*. Curr Neurol Neurosci Rep, 2009. **9**(3): p. 198-205.
4. Edstrom, E., et al., *Factors contributing to neuromuscular impairment and sarcopenia during aging*. Physiol Behav, 2007. **92**(1-2): p. 129-35.
5. Faulkner, J.A., et al., *Age-related changes in the structure and function of skeletal muscles*. Clin Exp Pharmacol Physiol, 2007. **34**(11): p. 1091-6.
6. Larsson, L. and T. Ansved, *Effects of ageing on the motor unit*. Prog Neurobiol, 1995. **45**(5): p. 397-458.
7. Hoeijmakers, J.H., *DNA damage, aging, and cancer*. N Engl J Med, 2009. **361**(15): p. 1475-85.
8. Martin, L.J., *DNA damage and repair: relevance to mechanisms of neurodegeneration*. J Neuropathol Exp Neurol, 2008. **67**(5): p. 377-87.
9. Rass, U., I. Ahel, and S.C. West, *Defective DNA repair and neurodegenerative disease*. Cell, 2007. **130**(6): p. 991-1004.
10. Akbari, M. and H.E. Krokan, *Cytotoxicity and mutagenicity of endogenous DNA base lesions as potential cause of human aging*. Mech Ageing Dev, 2008. **129**(7-8): p. 353-65.
11. Wilson, D.M., 3rd and V.A. Bohr, *The mechanics of base excision repair, and its relationship to aging and disease*. DNA Repair (Amst), 2007. **6**(4): p. 544-59.
12. Brooks, P.J., *The 8,5'-cyclopurine-2'-deoxynucleosides: candidate neurodegenerative DNA lesions in xeroderma pigmentosum, and unique probes of transcription and nucleotide excision repair*. DNA Repair (Amst), 2008. **7**(7): p. 1168-79.
13. Evans, M.D., M. Dizdaroglu, and M.S. Cooke, *Oxidative DNA damage and disease: induction, repair and significance*. Mutat Res, 2004. **567**(1): p. 1-61.

14. McKinnon, P.J., *DNA repair deficiency and neurological disease*. Nat Rev Neurosci, 2009. **10**(2): p. 100-12.
15. Barzilai, A., S. Biton, and Y. Shiloh, *The role of the DNA damage response in neuronal development, organization and maintenance*. DNA Repair (Amst), 2008. **7**(7): p. 1010-27.
16. Brooks, P.J., T.F. Cheng, and L. Cooper, *Do all of the neurologic diseases in patients with DNA repair gene mutations result from the accumulation of DNA damage?* DNA Repair (Amst), 2008. **7**(6): p. 834-48.
17. Ljungman, M. and D.P. Lane, *Transcription - guarding the genome by sensing DNA damage*. Nat Rev Cancer, 2004. **4**(9): p. 727-37.
18. Nospikel, T., *DNA repair in differentiated cells: some new answers to old questions*. Neuroscience, 2007. **145**(4): p. 1213-21.
19. Saxowsky, T.T. and P.W. Doetsch, *RNA polymerase encounters with DNA damage: transcription-coupled repair or transcriptional mutagenesis?* Chem Rev, 2006. **106**(2): p. 474-88.
20. Anttinen, A., et al., *Neurological symptoms and natural course of xeroderma pigmentosum*. Brain, 2008. **131**(Pt 8): p. 1979-89.
21. Kraemer, K.H., et al., *Xeroderma pigmentosum, trichothiodystrophy and Cockayne syndrome: a complex genotype-phenotype relationship*. Neuroscience, 2007. **145**(4): p. 1388-96.
22. Niedernhofer, L.J., *Nucleotide excision repair deficient mouse models and neurological disease*. DNA Repair (Amst), 2008. **7**(7): p. 1180-9.
23. Weeda, G., et al., *Disruption of mouse ERCCI results in a novel repair syndrome with growth failure, nuclear abnormalities and senescence*. Curr Biol, 1997. **7**(6): p. 427-39.
24. Houtsmuller, A.B., et al., *Action of DNA repair endonuclease ERCCI/XPF in living cells*. Science, 1999. **284**(5416): p. 958-61.
25. Ahmad, A., et al., *ERCCI-XPF endonuclease facilitates DNA double-strand break repair*. Mol Cell Biol, 2008. **28**(16): p. 5082-92.
26. Bergstralh, D.T. and J. Sekelsky, *Interstrand crosslink repair: can XPF-ERCCI be let off the hook?* Trends Genet, 2008. **24**(2): p. 70-6.
27. Bhagwat, N., et al., *XPF-ERCCI participates in the Fanconi anemia pathway of cross-link repair*. Mol Cell Biol, 2009. **29**(24): p. 6427-37.
28. Niedernhofer, L.J., et al., *A new progeroid syndrome reveals that genotoxic stress suppresses the somatotroph axis*. Nature, 2006. **444**(7122): p. 1038-43.

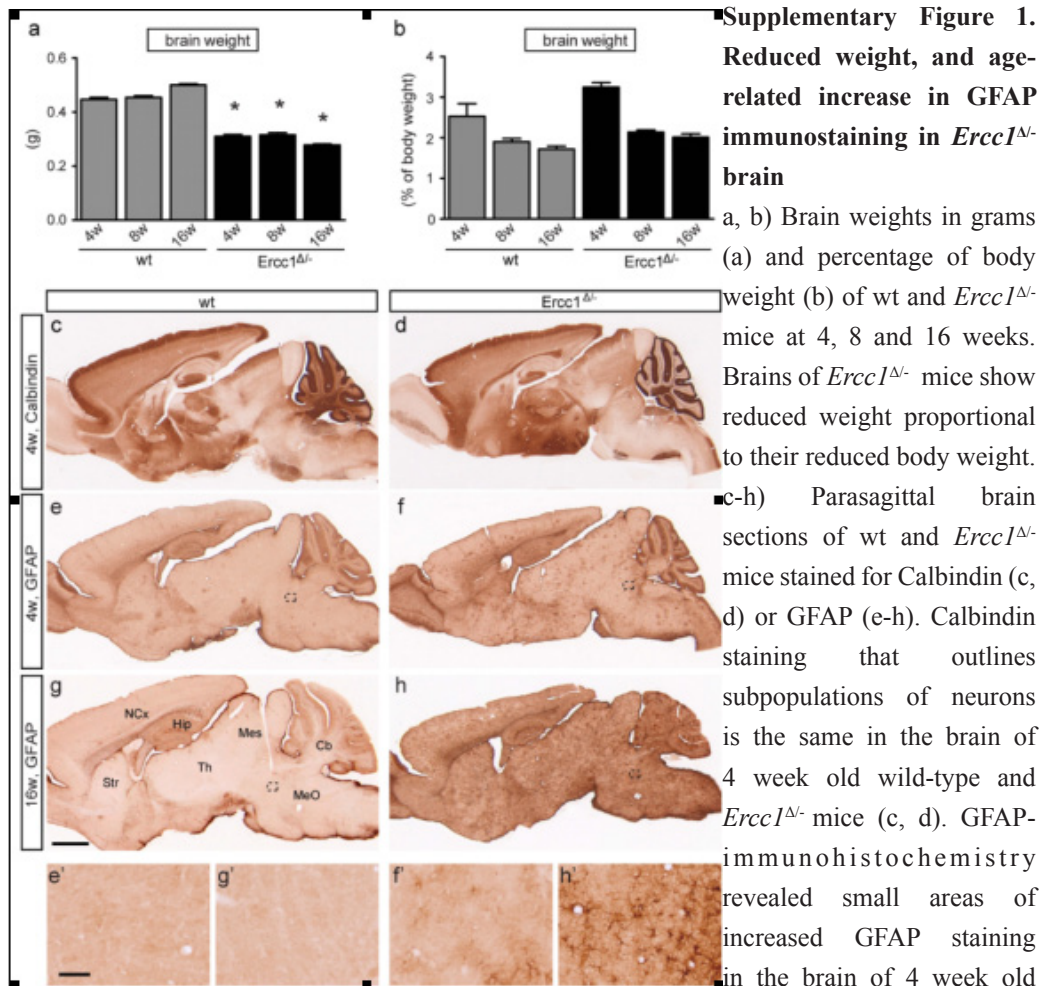
29. Zhu, X.D., et al., *ERCC1/XPF removes the 3' overhang from uncapped telomeres and represses formation of telomeric DNA-containing double minute chromosomes*. Mol Cell, 2003. **12**(6): p. 1489-98.
30. Ahmad, A., et al., *Mislocalization of XPF-ERCC1 nuclease contributes to reduced DNA repair in XP-F patients*. PLoS Genet, 2010. **6**(3): p. e1000871.
31. Jaspers, N.G., et al., *First reported patient with human ERCC1 deficiency has cerebro-oculo-facio-skeletal syndrome with a mild defect in nucleotide excision repair and severe developmental failure*. Am J Hum Genet, 2007. **80**(3): p. 457-66.
32. Selfridge, J., et al., *Correction of liver dysfunction in DNA repair-deficient mice with an ERCC1 transgene*. Nucleic Acids Res, 2001. **29**(22): p. 4541-50.
33. Lawrence, N.J., et al., *A neurological phenotype in mice with DNA repair gene Ercc1 deficiency*. DNA Repair (Amst), 2008. **7**(2): p. 281-91.
34. McWhir, J., et al., *Mice with DNA repair gene (ERCC-1) deficiency have elevated levels of p53, liver nuclear abnormalities and die before weaning*. Nat Genet, 1993. **5**(3): p. 217-24.
35. Tian, M., et al., *Growth retardation, early death, and DNA repair defects in mice deficient for the nucleotide excision repair enzyme XPF*. Mol Cell Biol, 2004. **24**(3): p. 1200-5.
36. Dolle, M.E., et al., *Increased genomic instability is not a prerequisite for shortened lifespan in DNA repair deficient mice*. Mutat Res, 2006. **596**(1-2): p. 22-35.
37. Jaarsma, D., et al., *Neuron-specific expression of mutant superoxide dismutase is sufficient to induce amyotrophic lateral sclerosis in transgenic mice*. J Neurosci, 2008. **28**(9): p. 2075-88.
38. van Woerden, G.M., et al., *Rescue of neurological deficits in a mouse model for Angelman syndrome by reduction of alphaCaMKII inhibitory phosphorylation*. Nat Neurosci, 2007. **10**(3): p. 280-2.
39. Teuling, E., et al., *Motor neuron disease-associated mutant vesicle-associated membrane protein-associated protein (VAP) B recruits wild-type VAPs into endoplasmic reticulum-derived tubular aggregates*. J Neurosci, 2007. **27**(36): p. 9801-15.
40. Vlug, A.S., et al., *ATF3 expression precedes death of spinal motoneurons in amyotrophic lateral sclerosis-SOD1 transgenic mice and correlates with c-Jun phosphorylation, CHOP expression, somato-dendritic ubiquitination and Golgi*

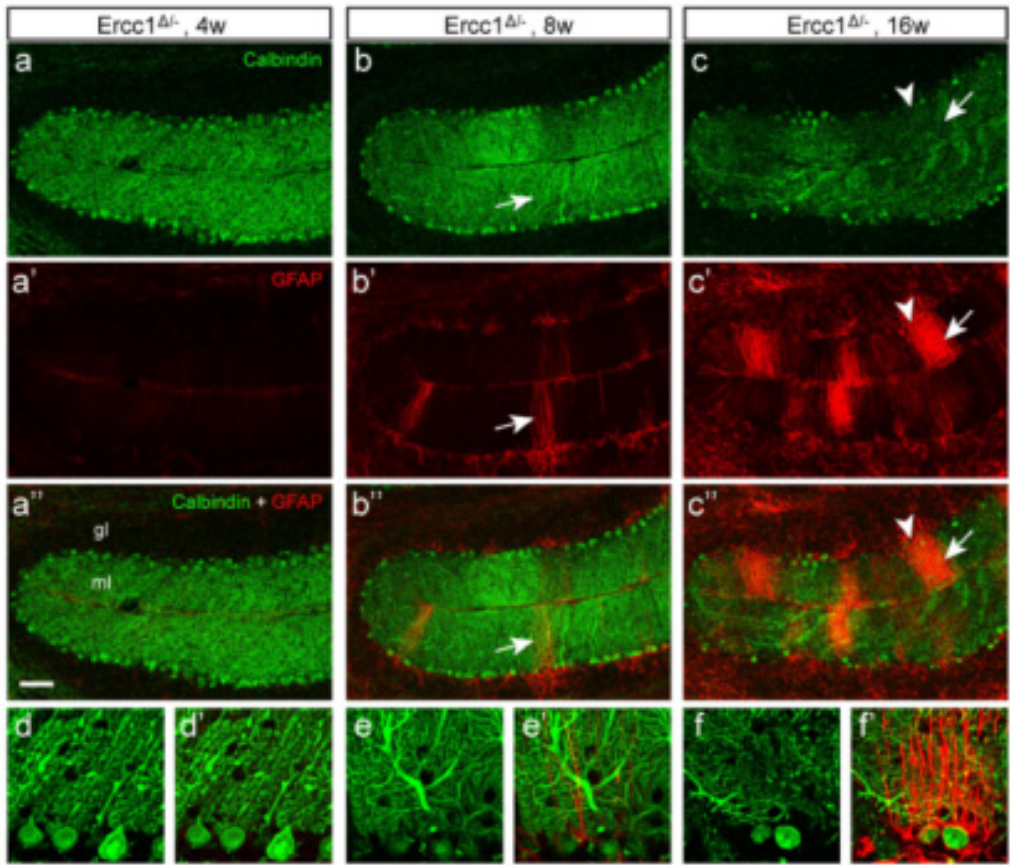
- fragmentation*. Eur J Neurosci, 2005. **22**(8): p. 1881-94.
41. Nadler, J.V. and D.A. Evenson, *Use of excitatory amino acids to make axon-sparing lesions of hypothalamus*. Methods Enzymol, 1983. **103**: p. 393-400.
42. Murray, L.M., et al., *Pre-symptomatic development of lower motor neuron connectivity in a mouse model of severe spinal muscular atrophy*. Hum Mol Genet, 2010. **19**(3): p. 420-33.
43. Andersson, P.B., V.H. Perry, and S. Gordon, *The kinetics and morphological characteristics of the macrophage-microglial response to kainic acid-induced neuronal degeneration*. Neuroscience, 1991. **42**(1): p. 201-14.
44. Rotshenker, S., et al., *Galectin-3/MAC-2, Ras and PI3K activate complement receptor-3 and scavenger receptor-AI/II mediated myelin phagocytosis in microglia*. Glia, 2008. **56**(15): p. 1607-13.
45. Gavrieli, Y., Y. Sherman, and S.A. Ben-Sasson, *Identification of programmed cell death in situ via specific labeling of nuclear DNA fragmentation*. J Cell Biol, 1992. **119**(3): p. 493-501.
46. Xiao, S., J. McLean, and J. Robertson, *Neuronal intermediate filaments and ALS: a new look at an old question*. Biochim Biophys Acta, 2006. **1762**(11-12): p. 1001-12.
47. Levine, A.J., W. Hu, and Z. Feng, *The P53 pathway: what questions remain to be explored?* Cell Death Differ, 2006. **13**(6): p. 1027-36.
48. Fan, F., et al., *ATF3 induction following DNA damage is regulated by distinct signaling pathways and over-expression of ATF3 protein suppresses cells growth*. Oncogene, 2002. **21**(49): p. 7488-96.
49. Hai, T. and M.G. Hartman, *The molecular biology and nomenclature of the activating transcription factor/cAMP responsive element binding family of transcription factors: activating transcription factor proteins and homeostasis*. Gene, 2001. **273**(1): p. 1-11.
50. Turchi, L., et al., *ATF3 and p15PAF are novel gatekeepers of genomic integrity upon UV stress*. Cell Death Differ, 2009. **16**(5): p. 728-37.
51. Nakamura, N., et al., *Characterization of a cis-Golgi matrix protein, GM130*. J Cell Biol, 1995. **131**(6 Pt 2): p. 1715-26.
52. Charbaut, E., et al., *Two separate motifs cooperate to target stathmin-related proteins to the Golgi complex*. J Cell Sci, 2005. **118**(Pt 10): p. 2313-23.
53. Neumann, M., et al., *Ubiquitinated TDP-43 in frontotemporal lobar degeneration and amyotrophic lateral sclerosis*. Science, 2006. **314**(5796): p. 130-3.

54. Lagier-Tourenne, C. and D.W. Cleveland, *Rethinking ALS: the FUS about TDP-43*. Cell, 2009. **136**(6): p. 1001-4.
55. Zhang, B., et al., *Neurofilaments and orthograde transport are reduced in ventral root axons of transgenic mice that express human SOD1 with a G93A mutation*. J Cell Biol, 1997. **139**(5): p. 1307-15.
56. Yan, C., et al., *Activating transcription factor 3, a stress sensor, activates p53 by blocking its ubiquitination*. EMBO J, 2005. **24**(13): p. 2425-35.
57. Gonatas, N.K., A. Stieber, and J.O. Gonatas, *Fragmentation of the Golgi apparatus in neurodegenerative diseases and cell death*. J Neurol Sci, 2006. **246**(1-2): p. 21-30.
58. Altan-Bonnet, N., R. Sougrat, and J. Lippincott-Schwartz, *Molecular basis for Golgi maintenance and biogenesis*. Curr Opin Cell Biol, 2004. **16**(4): p. 364-72.
59. De Matteis, M.A. and G. D'Angelo, *The role of the phosphoinositides at the Golgi complex*. Biochem Soc Symp, 2007(74): p. 107-16.
60. Ngo, M. and N.D. Ridgway, *Oxysterol binding protein-related Protein 9 (ORP9) is a cholesterol transfer protein that regulates Golgi structure and function*. Mol Biol Cell, 2009. **20**(5): p. 1388-99.
61. Teuling, E., et al., *A novel mouse model with impaired dynein/dynactin function develops amyotrophic lateral sclerosis (ALS)-like features in motor neurons and improves lifespan in SOD1-ALS mice*. Hum Mol Genet, 2008. **17**(18): p. 2849-62.
62. Fishel, M.L., M.R. Vasko, and M.R. Kelley, *DNA repair in neurons: so if they don't divide what's to repair?* Mutat Res, 2007. **614**(1-2): p. 24-36.
63. Melis, J.P., et al., *Mouse models for xeroderma pigmentosum group A and group C show divergent cancer phenotypes*. Cancer Res, 2008. **68**(5): p. 1347-53.
64. Nakane, H., et al., *Impaired spermatogenesis and elevated spontaneous tumorigenesis in xeroderma pigmentosum group A gene (Xpa)-deficient mice*. DNA Repair (Amst), 2008. **7**(12): p. 1938-50.
65. Andressoo, J.O., et al., *An Xpb mouse model for combined xeroderma pigmentosum and cockayne syndrome reveals progeroid features upon further attenuation of DNA repair*. Mol Cell Biol, 2009. **29**(5): p. 1276-90.
66. van der Pluijm, I., et al., *Impaired genome maintenance suppresses the growth hormone--insulin-like growth factor 1 axis in mice with Cockayne syndrome*. PLoS Biol, 2007. **5**(1): p. e2.
67. Coppede, F., et al., *Association study between XRCC1 gene polymorphisms and*

- sporadic amyotrophic lateral sclerosis*. *Amyotroph Lateral Scler*, 2010. **11**(1-2): p. 122-4.
68. Chen, Y.Z., et al., *DNA/RNA helicase gene mutations in a form of juvenile amyotrophic lateral sclerosis (ALS4)*. *Am J Hum Genet*, 2004. **74**(6): p. 1128-35.
69. Suraweera, A., et al., *Senataxin, defective in ataxia oculomotor apraxia type 2, is involved in the defense against oxidative DNA damage*. *J Cell Biol*, 2007. **177**(6): p. 969-79.
70. Neumann, M., *Molecular neuropathology of TDP-43 proteinopathies*. *Int J Mol Sci*, 2009. **10**(1): p. 232-46.

Supplemental data

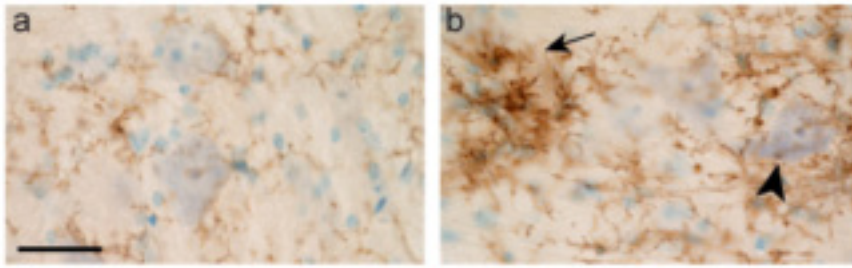




Supplementary Figure 2. Age related increase in GFAP-labeling and neuronal degeneration in *Ercc1*^{Δ/Δ} cerebellar cortex

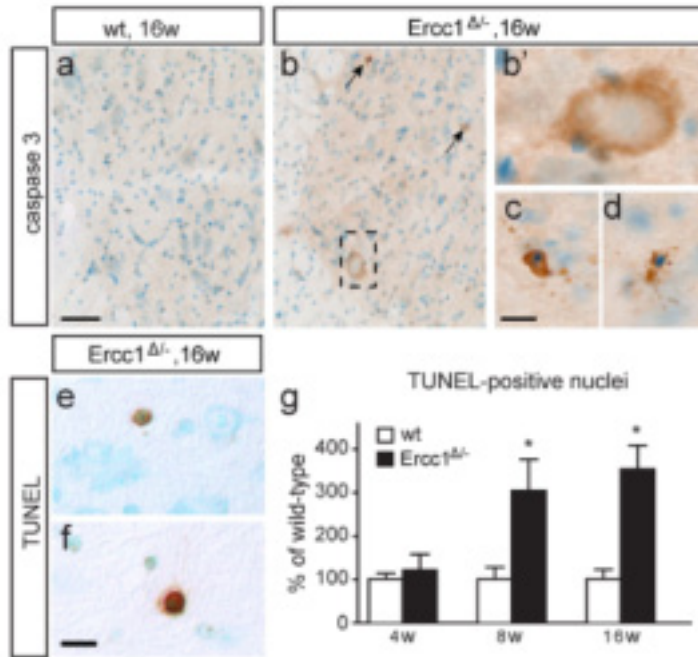
a-f) Low- (a-c) and high-magnification (d-f) double labeling confocal immunofluorescence images of calbindin and GFAP in cerebellar cortex of 4, 8 and 16 week old *Ercc1*^{Δ/Δ} mice showing areas of reduced calbindin staining, indicative of Purkinje cell loss in the molecular (ml) and Purkinje cell layer of 16 week old *Ercc1*^{Δ/Δ} mice (arrow head in c, f). In parallel clusters of intense GFAP immunostaining appear in the molecular layer (arrows in b and c) in the molecular layer. Increased GFAP-immunoreactivity also occurs in the granule cell layer (gl) of 16 week old *Ercc1*^{Δ/Δ} mice cerebellar cortex. GFAP and calbindin staining in 4 weeks *Ercc1*^{Δ/Δ} mice is the same as in wild-type. Asterisks in d indicate the cell bodies of Purkinje cells.

Scale bar: 100 μm



Supplementary Figure 3. Activated microglia cells surrounding motor neurons in *Ercc1*^{Δ/-} spinal cord

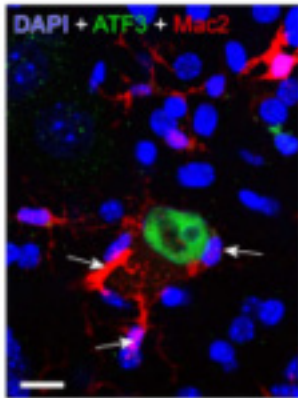
Photomicrographs of microglia cells stained for the complement 3 receptor (CR3) in motor columns in transverse lumbar L4 sections of 16 weeks old wt (a) and *Ercc1*^{Δ/-} (b) mice. Sections are counterstained for thionin to outline motor neuron cell bodies (arrow head in b). Arrow in b points to a cluster of activated microglia cells. Scale bars: 50 μm.



Supplementary Figure 4. Neuronal and non-neuronal cell death in *Ercc1*^{Δ/-} spinal cord

a-d) Low- (a and b) and high-magnification (b', c, d) photomicrographs of active caspase 3 staining in transverse *Ercc1*^{Δ/-} spinal cord sections showing a labeled motor neuron (b, b') and labeled apoptotic cells in the grey (c) and white (d) matter. Arrows in b point to irregular labeled structures, putatively reflecting remnants of dead cells.

e-g) High-magnification photomicrographs of TUNEL-positive cells in the grey (e) and white (f) matter of *Ercc1*^{Δ/-} spinal cord. Values in bar graph in g represent means ± SE (n=5 mice/bar) of TUNEL-positive cells in 4 consecutive paraffin sections expressed as % of labeled cells in wild-type littermates of the same age. The mean absolute number of TUNEL-positive cells were 2.9, 1.2 and 1.3 cells/mm² for 4, 8 and 16 week old wild-type mice, respectively. *, P < 0.05 compared to age -matched wild-type (Students *t*-test). Scale bars: 50 μm (a), 10 μm (c, f)



Supplementary Figure 5. A small subset of ATF3 positive motor neurons in *Erec1^{Δ/-}* spinal cord is surrounded by phagocytosing microglia

Double-labeling confocal immunofluorescence showing an ATF3-positive motor neuron surrounded by Mac2-positive microglia cells (arrows). Scale bar: 20 μ m

Chapter 5

β CaMKII plays a non-enzymatic role in hippocampal synaptic plasticity and learning by targeting α CaMKII to synapses

Nils Z. Borgesius, Geeske M. van Woerden, Gabrielle H. S. Buitendijk, Nanda Keijzer, Casper C. Hoogenraad, and Ype Elgersma

[βCaMKII plays a nonenzymatic role in hippocampal synaptic plasticity and learning by targeting αCaMKII to synapses.](#)

Borgesius NZ, van Woerden GM, Buitendijk GH, Keijzer N, Jaarsma D, Hoogenraad CC, Elgersma Y.

J Neurosci. 2011 Jul 13;31(28):10141-8.

PMID:

21752990

[PubMed - indexed for MEDLINE]

[Free Article](#)

Abstract

The calcium-calmodulin dependent kinase type II (CaMKII) holoenzyme of the forebrain predominantly consists of heteromeric complexes of the α CaMKII and β CaMKII isoform. Yet, in contrast to α CaMKII, the role of β CaMKII in hippocampal synaptic plasticity and learning has not been investigated. Here, we compare two targeted *Camk2b* mouse mutants to study the role of β CaMKII in hippocampal function. Using a *Camk2b*^{-/-} mutant, in which β CaMKII is absent, we show that both hippocampal-dependent learning and Schaffer collateral-CA1 long-term potentiation (LTP) are highly dependent upon the presence of β CaMKII. We further show that β CaMKII is required for proper targeting of α CaMKII to the synapse, indicating that β CaMKII regulates the distribution of α CaMKII between the synaptic pool and the adjacent dendritic shaft. In contrast, localization of α CaMKII, hippocampal synaptic plasticity and learning were unaffected in the *Camk2b*^{A303R} mutant, in which the calcium-calmodulin dependent activation of β CaMKII is prevented, while the F-actin binding and bundling property is preserved. This indicates that the calcium-calmodulin dependent kinase activity of β CaMKII is fully dispensable for hippocampal learning, LTP and targeting of α CaMKII, but implies a critical role for the F-actin binding and bundling properties of β CaMKII in synaptic function. Taken together, our data provide compelling support for a model of CaMKII function in which α CaMKII and β CaMKII act in concert, but with distinct functions, to regulate hippocampal synaptic plasticity and learning.

Introduction

Calcium/calmodulin-dependent kinase type II (CaMKII) is one of the most abundant proteins of the hippocampus, and its role in hippocampal plasticity and learning has been thoroughly investigated by pharmacological and genetic approaches. However, in the hippocampus there are two major isoforms of CaMKII, alpha (α) and beta (β), which cannot be distinguished using pharmacological approaches. In addition, almost all genetic approaches have focused on the α isoform [1-6]. Collectively, these studies have demonstrated that activation of α CaMKII is both necessary and sufficient to induce LTP.

In the hippocampus, α CaMKII and β CaMKII form a holoenzyme consisting of approximately 12 subunits in a 2:1 ratio [7]. α CaMKII and β CaMKII are highly homologous but they are encoded by two distinct genes (*Camk2b* and *Camk2a*, respectively) [8]. The most noticeable difference between these isoforms is that β CaMKII is able to bind to F-actin in an activity-controlled manner, through its extra domain in the variable region [9, 10]. Two β CaMKII subunits per holoenzyme are already sufficient to change the localization of the entire holoenzyme [9]. Mainly due to these different actin-binding properties, α CaMKII and β CaMKII were shown to have opposing effects on synaptic strength in cultured neurons [11]. Interestingly, β CaMKII does not only bind to actin, but that it is also capable of bundling actin, in a kinase-independent manner [12-14]. This non-enzymatic bundling feature is likely achieved by single CaMKII oligomers binding to multiple actin filaments.

Studies addressing the role of β CaMKII in synaptic plasticity and learning have only recently been initiated. Inducible over-expression of β CaMKII in the dentate gyrus did not affect acquisition of hippocampal learning, but did affect the long-term consolidation of memories [15]. Additionally, it was shown that the absence of β CaMKII reverses the polarity of plasticity at cerebellar parallel fiber-Purkinje cell synapses, and causes significant cerebellar learning deficits [16]. The reversal of plasticity is caused in part by a non-enzymatic property of β CaMKII, which prevents precocious activation of α CaMKII under low-calcium conditions.

Here we examined the role of β CaMKII in hippocampal synaptic plasticity and learning using two different β CaMKII mutants, (i) the *Camk2b*^{-/-} mouse which does not express β CaMKII and (ii) the *Camk2b*^{A303R} mouse where a point mutation blocks calcium/calmodulin binding, selectively preventing its enzymatic activation, while preserving its ability to bind to actin [10, 17, 18]. We found that the absence of β CaMKII causes mislocalization of α CaMKII, impaired hippocampal synaptic plasticity and impaired hippocampus-dependent learning. In contrast, these phenotypes were not present in the

Camk2b^{A303R} mutants, arguing that the actin binding and bundling function of β CaMKII governs a major aspect of its synaptic function. These results strongly suggest an essential, but non-enzymatic role for β CaMKII in hippocampal plasticity.

Results

Camk2b^{-/-} mice show normal hippocampal morphology and no change in α CaMKII protein levels and autophosphorylation

Generation of the *Camk2b*^{-/-} mouse has been described previously [16]. Using immunohistochemistry and Western blot, we confirmed the absence of β CaMKII in the hippocampus of the *Camk2b*^{-/-} mouse (Fig. 1a and b). Since *in vitro* experiments showed that up-regulation of β CaMKII causes down-regulation of α CaMKII [11], we tested whether the absence of β CaMKII caused up-regulation of α CaMKII *in vivo*. However we did not observe a change in α CaMKII protein levels (100 ± 5.4 n=6; 91.5 ± 6.3 n=7 for wild-type and *Camk2b*^{-/-} respectively; Mann-Whitney U test, $U = 13.00$, $P = 0.29$; Fig. 1c) nor was there a significant change in basal levels of α CaMKII Thr²⁸⁶ phosphorylation (100 ± 17.1 n=6; 92.7 ± 13.9 n=7 for wild-type and *Camk2b*^{-/-} respectively; Mann-Whitney U test, $U = 20.00$, $P = 0.95$; Fig. 1d). These data show that in *Camk2b*^{-/-} mice β CaMKII is absent and that protein expression and basal levels of autophosphorylation of α CaMKII are unaltered.

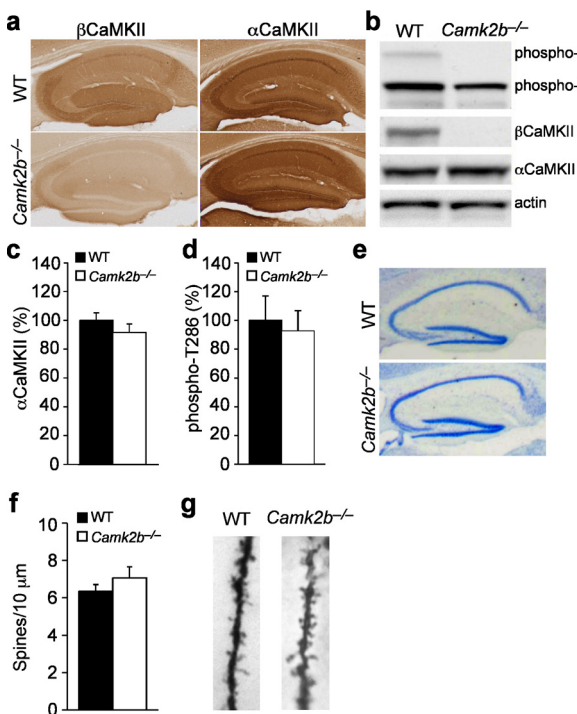


Figure 1. Morphological and molecular analysis of the *Camk2b*^{-/-} mice.

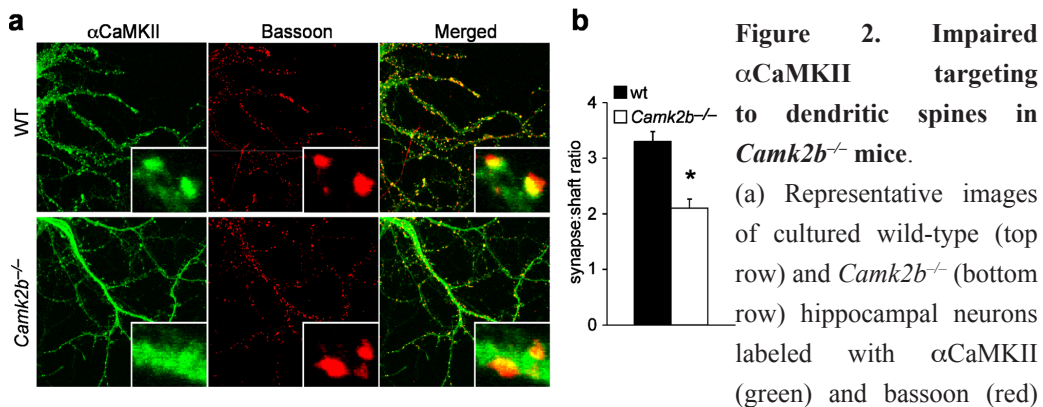
(a) Immunocytochemistry analysis using α CaMKII and β CaMKII specific antibodies shows complete absence of β CaMKII in the hippocampus, with no apparent change in α CaMKII expression. (b) Western blot analysis using α CaMKII and β CaMKII specific antibodies reveals no change in the levels of α CaMKII protein nor in the levels of α CaMKII-T286 phosphorylation. In contrast, β CaMKII protein and β CaMKII T287 phosphorylation are completely absent. (c) Quantification of the level of α CaMKII. (d) Quantification of the level of Thr286 phosphorylation.

(e) Thionin staining shows no apparent morphological change in the hippocampus of *Camk2b*^{-/-} mice compared to wild-types. (f and g) Quantification of Golgi analysis of the hippocampal pyramidal cells does not reveal any difference in spine density (wild-type, n=15 cells from 3 mice; *Camk2b*^{-/-}, n=15 cells from 3 mice).

Previous studies showed that up- or down-regulation of β CaMKII *in vitro* caused respectively an increased or decreased dendritic arborization, suggesting that β CaMKII might be critical for normal dendritic development *in vivo* [17]. Therefore, we performed a detailed examination of the hippocampus using thionin staining. However, we found no evidence of significant changes in hippocampal structure at the light microscopy level (Fig. 1e). Furthermore we investigated the morphology of the CA1 pyramidal cells using Golgi-Cox staining. We found no significant change in the density of spines (6.35 ± 0.36 n=15 cells from 3 mice; 7.07 ± 0.61 n=15 from 3 mice for wild-type and *Camk2b*^{-/-} mice respectively; unpaired two-tailed t-test, $t(28) = 1.8$, $P = 0.09$; Fig. 1f and g), which is consistent with our previous findings for the cerebellum [16]. Together these data show that gross neuronal development is preserved in *Camk2b*^{-/-} mice.

α CaMKII is mislocalized in *Camk2b*^{-/-} neurons

Since β CaMKII is able to bind F-actin in an activity-controlled manner [9, 10] and pharmacologically induced changes in actin bundling have a large effect on CaMKII delivery in spines [19, 20], it is possible that β CaMKII can change actin dynamics and the localization of the CaMKII holoenzyme. Therefore we hypothesized that absence of β CaMKII might result in abnormalities in synaptic localization of α CaMKII. To test this, we studied the subcellular localization of α CaMKII, using cultured E18 hippocampal neurons from *Camk2b*^{-/-} and wild-type mice. Neurons were fixed at DIV14 and stained with an antibody against bassoon, a marker for the presynaptic active zone, and an antibody against α CaMKII (Fig. 2a). We measured the ratio of α CaMKII in the synapse (colocalizing with bassoon) over α CaMKII in the dendritic shaft, and found that this ratio is significantly decreased in the *Camk2b*^{-/-} neurons (α CaMKII_{synapse}: α CaMKII_{shaft} = 3.3 ± 0.2 n=15 and 2.1 ± 0.2 n=14 for wild-type and *Camk2b*^{-/-} neurons respectively; Mann-Whitney U test, $U = 17.00$, $P = 0.0002$; Fig. 2b), highlighting that β CaMKII regulates the movement of α CaMKII between the synaptic pool and the adjacent dendritic shaft. Importantly, the total amount of α CaMKII was unchanged in *Camk2b*^{-/-} neurons. Together, these data confirm that β CaMKII regulates the localization of endogenous α CaMKII into the synapse.



and their colocalization (merged), showing reduced targeting of α CaMKII to spines in $Camk2b^{-/-}$ hippocampal neurons. Inserts show an enlargement of a dendritic segment with two spines. (b) Quantification of the ratio of α CaMKII in the synapse (colocalizing with bassoon) over α CaMKII in the dendritic shaft showing reduced targeting of α CaMKII to spines (wild-type, $n=15$; $Camk2b^{-/-}$, $n=14$).

$Camk2b^{-/-}$ mice show impaired LTP

Given that overall neuronal morphology was unaffected in $Camk2b^{-/-}$ mutants with an impaired localization of α CaMKII into dendritic spines, we examined the functional implications of the absence of β CaMKII by investigating synaptic plasticity at the hippocampal CA1 synapse. Using extracellular recordings in acute hippocampal slices, we focused on the Schaffer-collateral pathway given the large literature implicating this synapse in many forms of hippocampus-dependent learning and memory. No significant impairment in basal synaptic transmission was observed in the $Camk2b^{-/-}$ mice (Fig. 3a), with neither significant changes in fiber volley (repeated measures ANOVA $F_{1,135}=0.22$; $P=0.64$) nor in fEPSP slope (repeated measures ANOVA $F_{1,135}=1.4$; $P=0.23$). However, we found a significant deficit in long-term potentiation (LTP) in $Camk2b^{-/-}$ mutants compared to wild-type littermates (152.6 ± 7.7 $n=27$; 119.3 ± 4.4 $n=21$ for wild-type and $Camk2b^{-/-}$ mice respectively; Mann-Whitney U test, $U = 130.00$, $P = 0.0015$; Fig. 3b), indicating that β CaMKII plays an essential role in synaptic plasticity at the hippocampal Schaffer-collateral pathway. Notably, the LTP deficit in the $Camk2b^{-/-}$ mice induced by a 100Hz/1s tetanus, is as severe as after the loss of the far more abundant α CaMKII [1]. Moreover, it should be noted that hippocampal LTP is unaffected in the heterozygous $Camk2a$ mutant [1, 21], which shows a larger decrease in total CaMKII level compared to the homozygous $Camk2b$ mutant. This indicates that the LTP deficit of the $Camk2b^{-/-}$ mice cannot only be explained in terms of loss of CaMKII activity.

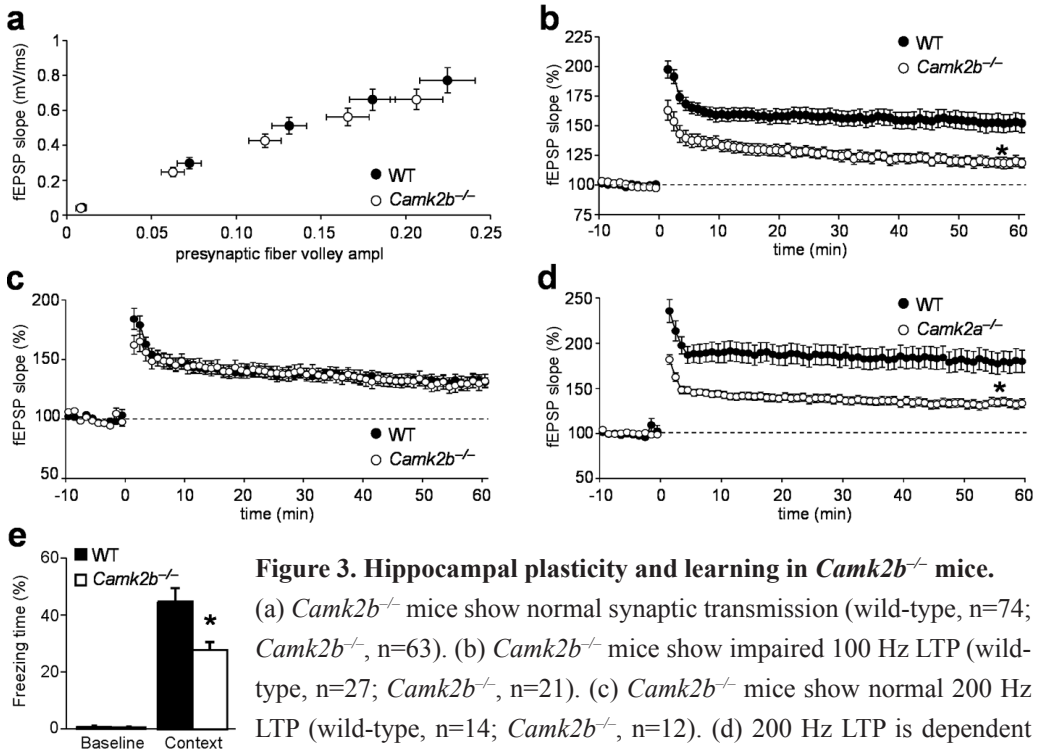


Figure 3. Hippocampal plasticity and learning in *Camk2b*^{-/-} mice.

(a) *Camk2b*^{-/-} mice show normal synaptic transmission (wild-type, n=74; *Camk2b*^{-/-}, n=63). (b) *Camk2b*^{-/-} mice show impaired 100 Hz LTP (wild-type, n=27; *Camk2b*^{-/-}, n=21). (c) *Camk2b*^{-/-} mice show normal 200 Hz LTP (wild-type, n=14; *Camk2b*^{-/-}, n=12). (d) 200 Hz LTP is dependent on α CaMKII, as *Camk2a*^{-/-} mice show impaired 200 Hz LTP (wild-type, n=12; *Camk2a*^{-/-}, n=18). (e) Impaired contextual fear conditioning in *Camk2b*^{-/-} mice. Percentage of time spent freezing during training before the foot shock (Pre) and 24 hours after conditioning (Post), indicates reduced post-shock freezing while pre-shock freezing is normal (wild-type, n=10; *Camk2b*^{-/-}, n=10).

It has previously been shown that changes in the F-actin/G-actin equilibrium affect α CaMKII localization [19, 20] and that stimulation of NMDA receptors affects CaMKII localization as well as the F-actin/G-actin equilibrium [10, 19]. Together, these findings support a model in which CA1 LTP is highly dependent on proper targeting of α CaMKII into spines, for which β CaMKII is required. To test this further, we took advantage of a stimulation protocol that activates both NMDA receptors and voltage gated calcium channels (VGCCs) [22]. Importantly, VGCCs activate a different pool of α CaMKII than NMDA receptors, with a stronger activation of α CaMKII in dendritic shafts than in spines [23]. Indeed, using this VGCC-dependent stimulation protocol, LTP is normal in *Camk2b*^{-/-}, confirming the functional implications of the altered CaMKII localization (131.6 ± 4.4 n=14; 129.7 ± 5.7 n=12 for wild-type and *Camk2b*^{-/-} respectively; unpaired two-tailed t-test, $t(24) = 0.36$, $P = 0.72$; Fig. 3c). To confirm that

VGCC LTP requires α CaMKII, we also performed this experiment in *Camk2a*^{-/-} mice. Indeed, *Camk2a*^{-/-} mice show a significant impairment in VGCC LTP (179.6 ± 13.3 n=12; 133.3 ± 4.8 n=18 for wild-type and *Camk2a*^{-/-} respectively; Mann-Whitney U test, $U = 36.00$, $P = 0.0025$; Fig. 3d), indicating that the VGCC LTP protocol is dependent on CaMKII activity. Taken together, these results show that the LTP deficit in the *Camk2b*^{-/-} mice can be overcome by an LTP induction protocol which preferentially activates CaMKII in dendritic shafts as compared to CaMKII in spines. This is in support of our hypothesis and strongly suggests that in hippocampal synaptic plasticity the function of β CaMKII is to target the CaMKII holoenzyme into dendritic spines.

***Camk2b*^{-/-} mice show impaired hippocampus-dependent learning**

To test if the mislocalization of CaMKII in the *Camk2b*^{-/-} mouse also affected hippocampal learning, we made use of contextual fear conditioning. In this task mice are conditioned to associate a certain context with a mild, aversive foot shock. Learning is assessed by measuring freezing behavior, i.e. the cessation of all movement except respiration, which is a natural expression of fear in mice. *Camk2b*^{-/-} mutants did not differ from their wild-type littermates in pre-shock baseline freezing behavior ($0.9 \pm 0.2\%$ n=11; $0.7 \pm 0.2\%$ n=9 for wild-type and *Camk2b*^{-/-} mice respectively; two-tailed t-test, $t(18) = (0.72)$, $P = 0.48$; Fig. 3e), but showed significantly less freezing in the 24 hour long-term memory test, demonstrating an impairment of hippocampus-dependent memory ($44.8 \pm 4.6\%$ n=11; $27.8 \pm 2.7\%$ n=9 for wild-type and *Camk2b*^{-/-} mice respectively; two-tailed t-test, $t(18) = (3.0)$, $P = 0.0079$; Fig. 3e).

Generation and characterization of the *Camk2b*^{A303R} mouse

The results above suggest that β CaMKII strongly influences hippocampal plasticity by regulating α CaMKII targeting into dendritic spines. However, the affinity of β CaMKII for calcium/calmodulin is nearly 10-fold higher than of α CaMKII, and the sensitivity range of the heteromeric holoenzyme is dependent on the ratio of α to β subunits [7, 24]. Hence, we cannot rule out that the deficits in CA1 LTP and hippocampus-dependent learning are caused by the loss of the enzymatic activity of β CaMKII, rather than the abnormal localization of α CaMKII. Therefore, we sought to distinguish between these possibilities using a well-described mutation of β CaMKII (A303R), which prevents

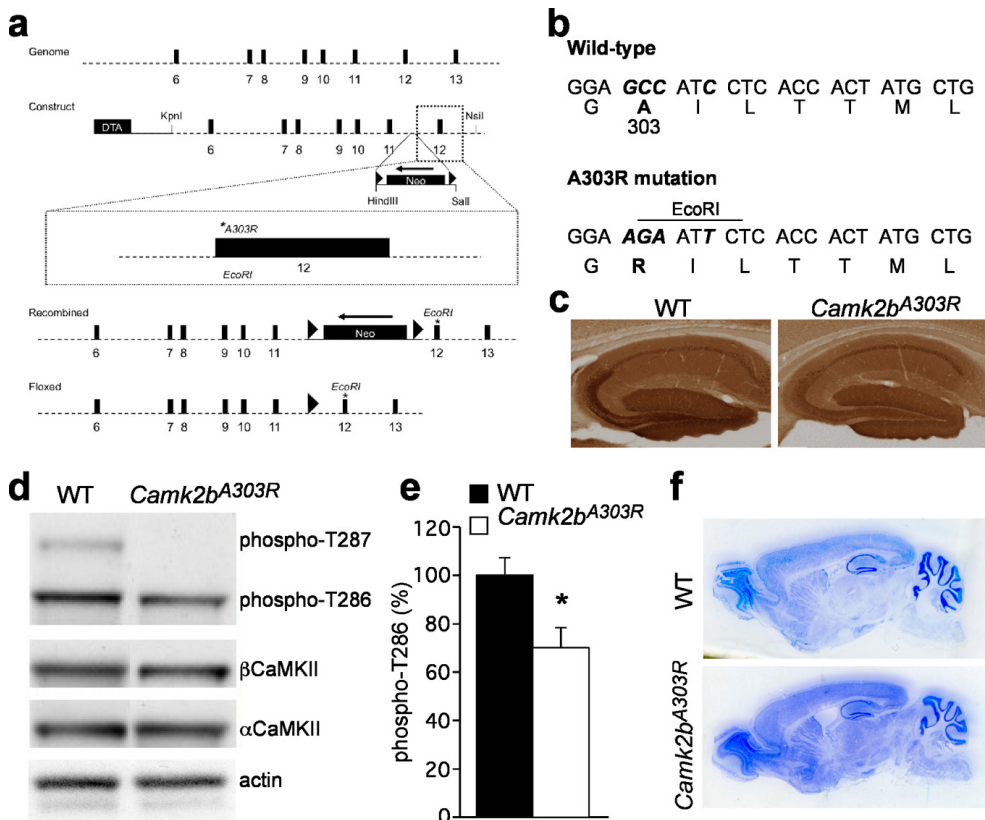


Figure 4. Generation of *Camk2b*^{A303R} mice.

(a) Schematic diagram for the generation of the *Camk2b*^{A303R} mutants. (Genome) wild-type *Camk2b* locus with the exons around Ala303 depicted as black boxes. (Construct) Targeting construct used for introducing the mutation in Ala303. The asterisk in exon 12 indicates the mutation in Ala303. The LoxP sites flanking the neomycin gene are depicted as triangles. The Diphtheria Toxin cassette (DTA) was cloned in the construct for positive selection. (Recombined) Mutant *Camk2b*^{A303R} locus after homologous recombination in ES cells. (Floxed) Mutant *Camk2b*^{A303R} locus after Cre recombination. (b) Sequence of Ala303 in exon 12 showing the specific mutation made to induce Ala303Arg. (c) Immunocytochemistry staining using an antibody specific for βCaMKII shows no difference in βCaMKII staining in the hippocampus of *Camk2b*^{A303R} mice (bottom) compared to wild-types (top). (d) Western blot analysis using antibodies specific for αCaMKII and βCaMKII shows no difference in the levels of αCaMKII and βCaMKII in the hippocampus of the *Camk2b*^{A303R} mice. Western blot analysis using an antibody specific for detecting the phosphorylation levels of αCaMKII-T286 and βCaMKII-T287 reveals a slight reduction of Thr286 phosphorylation whereas the Thr287 phosphorylation is completely absent in the hippocampus of the *Camk2b*^{A303R} mice. (e) Quantification of Thr286 phosphorylation. (f) Thionin staining showed no gross morphological difference in the brain of *Camk2b*^{A303R} mice.

kinase activation (by interfering with calcium/calmodulin binding) while preserving F-actin binding and bundling [10, 12, 17]. In addition, the β CaMKII-A303R protein does not show a dominant negative effect on dendritic arborization *in vitro*, in contrast to cells expressing the catalytically dead β CaMKII-K42R protein, which cannot bind ATP [17]. Accordingly, this mutation elegantly permits us to dissect the requirement of β CaMKII kinase activity and F-actin bundling on LTP and learning.

We created a knock-in mutant of the *Camk2b* gene, substituting Alanine³⁰³ for Arginine (A303R) (Fig. 4a and b). Immunostaining and Western blot analysis of brains of homozygous point-mutants (designated as *Camk2b*^{A303R} mice) revealed no change in expression of β CaMKII and α CaMKII in the *Camk2b*^{A303R} mouse (Fig. 4c and d). Since binding of calcium/calmodulin is a prerequisite for auto-phosphorylation of CaMKII at Thr286/287 as reviewed by [25-27] we used the Phospho-Thr286/287 antibody to confirm that this mutation renders the β CaMKII-A303R protein insensitive to calcium/calmodulin activation. Indeed Western-blot analysis showed that β CaMKII Thr²⁸⁷ phosphorylation was entirely absent in the *Camk2b*^{A303R} mouse (Fig. 4d), confirming *in vitro* studies that the A303R mutation blocks activation of β CaMKII. We also observed a significant reduction of α CaMKII Thr²⁸⁶ autophosphorylation (100 ± 7.2 n=7; 69.9 ± 8.3 n=5 for wild-types and *Camk2b*^{A303R} respectively; Mann-Whitney U test, $U = 4.0$, $P = 0.03$; Fig. 4e), which is not unexpected given that most of the α CaMKII subunits are associated with β CaMKII subunits, and that it takes two adjacent activated CaMKII subunits to get inter-subunit auto-phosphorylation at Thr286/Thr287 [25-27]. Thionin staining did not reveal any gross morphological changes in the brain (Fig. 4f), indicating that development of the brain is normal despite the presence of an inactive form of β CaMKII.

α CaMKII shows normal subcellular distribution in *Camk2b*^{A303R} neurons

To directly examine the influence of β CaMKII on the localization of α CaMKII, we tested whether synaptic targeting of α CaMKII was altered in neurons of the *Camk2b*^{A303R} mice. Remarkably, and in strong contrast to the findings in *Camk2b*^{-/-} neurons, *Camk2b*^{A303R} neurons showed normal α CaMKII synaptic localization ($aCaMKII_{\text{synapse}} : aCaMKII_{\text{shaft}} = 4.2 \pm 0.7$ n=6 and 3.9 ± 0.6 n=7 for wild-type and *Camk2b*^{A303R} neurons respectively; Mann-Whitney U test, $U = 14.00$, $P = 0.37$; Fig. 5a and b). These results demonstrate that the β CaMKII protein itself, but not its calcium/calmodulin dependent activation is required for targeting α CaMKII to synapses.

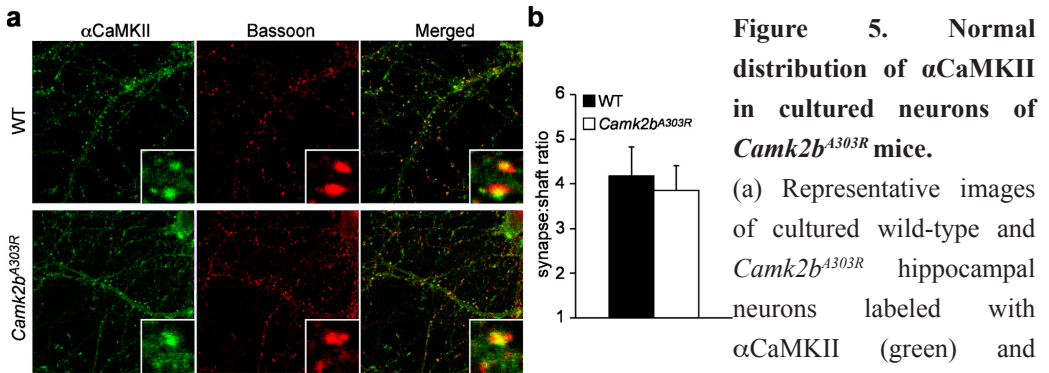


Figure 5. Normal distribution of α CaMKII in cultured neurons of *Camk2b^{A303R}* mice.

(a) Representative images of cultured wild-type and *Camk2b^{A303R}* hippocampal neurons labeled with α CaMKII (green) and bassoon (red) and their

colocalization (merged) showing normal distribution of α CaMKII in *Camk2b^{A303R}* hippocampal neurons. Inserts show an enlargement of a dendritic segment with two spines. (b) Quantification of the ratio of α CaMKII in the synapse (colocalizing with bassoon) over α CaMKII in the dendritic shaft showing normal distribution in *Camk2b^{A303R}* hippocampal neurons (wild-type, $n=6$; *Camk2b^{A303R}*, $n=7$).

The *Camk2b^{A303R}* mice show normal LTP

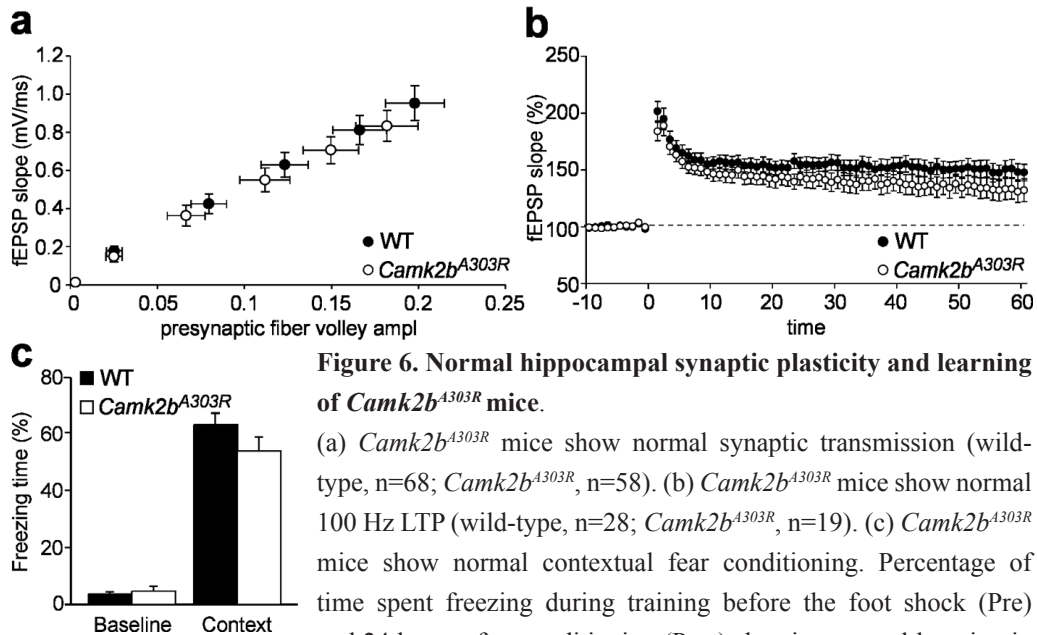
Camk2b^{A303R} mice retain normal synaptic localization of α CaMKII, despite a complete abrogation of calcium/calmodulin dependent kinase activity of β CaMKII. This provides a unique opportunity to dissect the mechanism by which β CaMKII influences synaptic plasticity and learning.

Using extracellular recordings in acute hippocampal slices, basal synaptic transmission was unchanged in *Camk2b^{A303R}* mice (basal synaptic transmission: repeated measures ANOVA fiber volley $F_{1,46}=0.44$; $P=0.51$; and fEPSP $F_{1,46}=0.93$; $P=0.34$; $n=25$ and $n=23$ for wild-type and *Camk2b^{A303R}* mice respectively; Fig. 6a). However, in contrast to the *Camk2b^{-/-}* mice which have a severe deficit in 100 Hz LTP, *Camk2b^{A303R}* mice showed normal 100 Hz LTP (149.7 ± 7.4 $n=15$; 133.4 ± 9.1 $n=10$ for wild-type and *Camk2b^{A303R}* mice respectively; two-tailed t-test, $t(23)=1.40$, $P=0.17$; Fig. 6b), although there is a subtle decrease in the magnitude of LTP. These results indicate that the kinase activity of β CaMKII is dispensable for hippocampal synaptic plasticity, and suggests that β CaMKII functions principally to regulate the targeting of α CaMKII into dendritic spines.

Contextual fear learning of the *Camk2b^{A303R}* mice

Given that *Camk2b^{-/-}* mice showed a significant deficit in contextual fear conditioning (Fig. 3e), the results from *Camk2b^{A303R}* mice provide an opportunity to determine the

mechanism of β CaMKII function in hippocampus-dependent learning. *Camk2b^{A303R}* mice showed indistinguishable freezing behavior from their wild-type littermates (62.6 ± 4.1 n=13; 53.5 ± 5.0 n=11 for wild-types and *Camk2b^{A303R}* respectively; two-tailed t-test, $t(22) = 1.42$, $P = 0.17$; Fig. 6c) without any change in baseline freezing behavior (3.5 ± 0.8 n=13; 4.6 ± 1.6 n=11 for wild-types and *Camk2b^{A303R}* respectively; Mann-Whitney U test, $U = 65.00$, $P = 0.73$; Fig. 6c). Hence, taken together with the results obtained using *Camk2b^{-/-}* mice, these results suggest that β CaMKII-dependent localization of α CaMKII is required for normal hippocampus-dependent learning.



Discussion

Through a genetic dissection in mice, we have identified that β CaMKII functions at the Schaffer collateral – CA1 synapse principally to target α CaMKII into dendritic spines. We found that the complete loss of β CaMKII protein leads to mislocalization α CaMKII and severely impairs hippocampal learning and synaptic plasticity. In contrast, the β CaMKII-A303R mutant provided an elegant dissection of β CaMKII function, since it fully retains F-actin binding despite a loss of calcium/calmodulin-dependent kinase activity. Indeed, *Camk2b^{A303R}* mice showed proper α CaMKII localization, robust LTP, and normal learning. Since we found that the subcellular localization of α CaMKII is changed only in the absence of β CaMKII, and that the LTP deficit in the absence of

β CaMKII can be overcome by using an LTP protocol, which primarily activates a non-synaptic pool of α CaMKII, our data supports a role of β CaMKII in which it regulates the targeting of α CaMKII into spines. Given the extensive literature showing that β CaMKII has F-actin binding and bundling properties, which are fully conserved in the β CaMKII-A303R mutant, we conclude that the synaptic plasticity and learning deficits observed in the *Camk2b*^{-/-} mutants result from the impaired β CaMKII-dependent targeting of α CaMKII into spines.

β CaMKII in neuronal development

We found that neither the absence nor the inactivation of β CaMKII affects brain development at the light microscopic level. Considering the developmentally earlier expression of β CaMKII compared to α CaMKII [28, 29] and the effects of β CaMKII over-expression in neuronal cultures [17, 30], an influence on gross neurodevelopment might be expected. It is plausible that germline mutations in β CaMKII might result in homeostatic compensation to prevent the neurodevelopmental changes as were seen in neuronal cultures shortly after the expression of β CaMKII was changed.

β CaMKII-dependent hippocampal synaptic plasticity

We showed that β CaMKII is required for normal hippocampal NMDA receptor dependent plasticity as well as learning. Notably, despite that β CaMKII has a 10-fold higher affinity for calcium/calmodulin compared to α CaMKII, the impairment in NMDA receptor-dependent LTP in *Camk2b*^{-/-} mice cannot be explained by a reduction in calcium/calmodulin sensitivity, since LTP deficits were not observed in the *Camk2b*^{A303R} mice, in which β CaMKII has a negligible affinity for calcium/calmodulin. Rather, the deficit in NMDA-dependent LTP is most likely caused by the reduced synaptic localization of α CaMKII. Our data shows that the subcellular localization of α CaMKII is strongly influenced by β CaMKII. Specifically, synaptic localization of α CaMKII is reduced in *Camk2b*^{-/-} neurons, whereas the localization of α CaMKII in *Camk2b*^{A303R} neurons is indistinguishable from wild-type mice. Therefore, β CaMKII functions independently of its calcium-dependent kinase activity to regulate the synaptic localization of α CaMKII. The observation that a VGCC-dependent LTP protocol which activates a distinctively different pool of α CaMKII as compared to NMDA receptors (Lee et al., 2009), was normal despite the loss of β CaMKII, further supports the hypothesis that the LTP deficits are caused by mislocalized α CaMKII. However, although the observed reduction of synaptic α CaMKII is likely to cause an NMDA-receptor dependent LTP deficit, we

cannot rule out that the loss of β CaMKII also affects other synaptic processes associated with the β CaMKII-dependent actin binding and bundling properties.

Taken together our data shows that β CaMKII is essential for hippocampus-dependent learning and for normal plasticity at the Schaffer collateral – CA1 synapse. Despite the fact that β CaMKII has a higher affinity for calcium/calmodulin as compared to α CaMKII, we found that the calcium/calmodulin-dependent activation of β CaMKII was fully dispensable for hippocampal LTP and learning. Rather, our data shows that β CaMKII in hippocampal pyramidal neurons plays a structural role, which serves to target α CaMKII to synapses.

Acknowledgements

We thank members of the Elgersma lab, Steven Kushner and Dick Jaarsma for stimulating discussions and critically reading the manuscript. We thank Mehrnoush Agha Davoud Jolfaei, John Kongasan, Minetta Elgersma, and Hans van der Burg for technical support. This work was supported by grants from NWO-ZonMW and Neuro-BSIK to YE.

Materials and Methods

Generation of the Camk2b^{A303R} mutants

The *Camk2b^{A303R}* targeting construct was generated as follows. The *Camk2b* genomic sequence (ENSMUSG00000057897) was obtained from a public database (Ensembl) and used to design the primers for the targeting constructs. PCR fragments encompassing exon 6-11 using

5' primer: 5'-GGTACCTGAGGAAGGTGCCAGCTCTGTCCC-3' and

3' primer: 5'-GTCGACCAGGGTAGTCACGGTTGTCC-3' (5.3 Kb; exon denotation according to ENSMUST00000019133) and exon 11-12 using

5' primer: 5'-GCGGCCCGCTGTAAAGGAATGGTTCTC-3' and

3' primer: 5'-ATGCATCTAAAAGGCAGGCAGGATGATCTGC-3' (6 Kb)

were amplified using High Fidelity Taq Polymerase (Roche) on ES cell genomic DNA and cloned on either site of a PGK-Neomycin selection cassette. All exons were sequenced to verify that no mutations were introduced accidentally. Site directed mutagenesis was used to introduce the pointmutation Ala303Arg. For counter selection, a gene encoding Diphtheria toxin chain A (DTA) was inserted at the 5' of the targeting construct. The targeting construct was linearized and electroporated into E14 ES cells (derived from 129P2 mice). Cells were cultured in BRL cell conditioned medium in the presence of Leukemia inhibitory factor (LIF). After selection with G418 (200 μ g/ml), targeted

clones were identified by PCR (long-range PCR from Neomycin resistance gene to the region flanking the targeted sequence). A clone with normal karyotype was injected into blastocysts of C57Bl/6 mice. Male chimeras were crossed with female C57Bl/6 mice (Harlan). The resulting F1 heterozygous mice (in the 129P2-C57Bl/6 background) were used to generate F2 homozygous mutants and wild-type littermate controls. These mice were used for all the behavioral and electrophysiological experiments. The experimenter was blind for the genotype, but homozygous mice were easily recognizable by the ataxic gait. Therefore, a second person blind to the genotype also analyzed data. Mice were housed on a 12 hours light/dark cycle with food and water available *ad libitum* and used between 2 and 6 months of age for all experiments described (including electrophysiology). All animal procedures were approved by a Dutch Ethical Committee (DEC) for animal experiments.

Western blot

Lysates were prepared by quick dissection of the brain and by homogenization of the brain tissue in lysis buffer (10mM TRIS-HCl 6.8, 2.5% SDS, 2mM EDTA and protease and phosphatase inhibitor cocktails (Sigma). The concentration of the lysates was adjusted to 1 mg/ml. 10 μ g was used for Western blot analysis. Western blots were probed with antibodies directed against α CaMKII (MAB3119, 1:10,000; Chemicon), β CaMKII (CB- β 1, 1:10,000; Zymed), Ph-T286/T87 CaMKII antibody (1:5000; #06-881, Upstate Cell Signaling Solutions) and Actin (MAB1501R, 1:2000; Chemicon). Blots were stained using Enhanced ChemoLuminescence (#32106, Pierce) Western blot quantification was performed using NIH-Image.

Immunocytochemistry

Immunocytochemistry was performed on free-floating 40 μ m thick frozen sections employing a standard avidin-biotin-immunoperoxidase complex method (ABC, Vector Laboratories, USA) with, β CaMKII (CB-b1, 1:2000; Zymed) as the primary antibody and diaminobenzidine (0.05%) as the chromogen (Hansel, 2006). For gross brain morphology sections were stained with thionin.

Dendritic arborization

Golgi-Cox staining on unfixed hippocampi of 3 *Camk2b*^{-/-} mutants and 3 wild-type mice was performed using the FD Rapid GolgiStain Kit (FD NeuroTechnologies Inc., USA), according to the manufacturers' instructions. Saggital sections, 100 μ m thick, were cut

on a microtome with cryostat adaptations. Pyramidal cell counting and selection for further detailed analysis was done by two independent observers who were both blind for genotype. A calibration grid was used to count the number of spines per 10 μ m, using a 40x objective.

Primary hippocampal cultures and immunohistochemistry

β CaMKII or β CaMKII-A303R heterozygous mice were crossed and wild type, heterozygous and knock-out hippocampal neuron cultures were prepared from brains of single embryonic day 18 (E18) embryos out of mixed genotype litters. Mouse hippocampal neurons were isolated and prepared as described [31]. In short, the two hippocampi were removed from the embryonic brain, collected in 1 ml of DMEM on ice, washed two times with 1 ml DMEM and incubated in trypsin/EDTA solution (Gibco) at 37°C for 15 minutes. After washing with 1 ml of DMEM, the cells were resuspended in Neurobasal medium (NB) supplemented with 2% B27, 1% penicillin/streptomycin and 1% glutamax (Gibco) and dissociated using a gently flamed Pasteur pipette. Neurons were plated in a small drop on poly-L-lysine (100 μ g/ml, Sigma) and laminin (50 μ g/ml, Sigma) coated 15 mm glass coverslips at a density of 75,000/coverslip in 12-well plates. After 2 hours, 1 ml of NB supplemented with 2% B27, 1% penicillin/streptomycin and 1% glutamax was added to the coverslips.

For immunohistochemistry, 14 days in vitro (DIV14) neurons were fixed for 10 minutes with 4% formaldehyde/4% sucrose in phosphate-buffered saline (PBS) at room temperature [32]. After fixation, the cells were washed two times in PBS for 30 min at room temperature, and incubated with primary antibodies in GDB buffer (0.2% BSA, 0.8 M NaCl, 0.5% Triton X-100, 30 mM phosphate buffer, pH 7.4) overnight at 4°C. The following primary antibodies were used: rabbit anti-Bassoon (Synaptic Systems) and mouse anti- α CaMKII (Sigma). Neurons were then washed three times in PBS for 30 min at room temperature and incubated with Alexa488- and Alexa568-conjugated secondary antibodies (Molecular Probes) in GDB for 2 hr at room temperature and washed three times in PBS for 30 min. Slides were mounted using Vectashield mounting medium (Vector laboratories). Confocal images were acquired using a LSM510 confocal microscope (Zeiss) with a 40x or 63x oil objective.

Image analysis and Quantification

Confocal images of neurons were obtained with sequential acquisition settings at the maximal resolution of the microscope (1024 x 1024 pixels). Each image was a z-series

of 6-8 images each averaged 2 times was chosen to cover the entire region of interested from top to bottom. The resulting z-stack was 'flattened' into a single image using maximum projection. Images were not further processed and were of similar high quality to the original single planes. The confocal settings were kept the same for all scans when fluorescence intensity was compared. Morphometric analysis, quantification and colocalization were performed using MetaMorph software (Universal Imaging Corporation). The ratio of aCaMKII in the synapse over aCaMKII in the shaft was calculated by measuring the average intensity of the fluorescent aCaMKII signal in the synapses and the shaft.

Fear conditioning

Fear conditioning was performed in a conditioning chamber (Med. Associates) equipped with a grid floor via which the foot shock could be administered. Each mouse was placed inside the conditioning chamber for 180 seconds. A foot shock (2 s, 0.4 mA) was delivered 148 s after placement in the chamber. Twenty-four hours later, context-dependent freezing was measured during 3 minutes.

Electrophysiology

After the animals had been sacrificed, sagittal slices (400 μ m) were made submerged in ice-cold artificial CSF (ACSF) using a vibratome and hippocampi were dissected out. These sagittal hippocampal slices were maintained at room temperature for at least 1.5 hours to recover before experiments were initiated. Then they were placed in a submerged recording chamber and perfused continuously at a rate of 2 ml/min with ACSF equilibrated with 95% O₂, 5% CO₂ at 31°C. ACSF contained the following (in mM): 120 NaCl, 3.5 KCl, 2.5 CaCl₂, 1.3 MgSO₄, 1.25 NaH₂PO₄, 26 NaHCO₃, and 10 D-glucose. Extracellular recording of field EPSP (fEPSPs) were made in CA1 stratum radiatum with platinum/iridium electrodes (Frederick Haer Company, Bowdoinham, ME). A bipolar Pt/Ir was used to stimulate Schaffer-collateral/commissural afferents with a stimulus duration of 100 μ s. Stimulus response curves were obtained at the beginning of each experiment, 20 minutes after placing the electrodes. LTP was evoked using two different tetani: (i) 100 Hz (1 train of 1 second at 100 Hz) and (ii) 200 Hz (4 trains of 0.5 seconds at 200 Hz every 5 seconds). Both protocols were performed at one-third of the maximum fEPSP. fEPSP measurements were done once per minute. Potentiation was measured as the normalized increase of the mean fEPSP slope for the duration of the baseline. Only stable recordings were included and this judgment was made blind to genotype. Average

LTP was defined as the mean last 10 minutes of the normalized fEPSP slope.

Statistical analysis

All data are presented as means \pm SEM and were tested for normality of distribution using the D'Agostino-Pearson test. If normality of distribution was violated or sample size was too small to determine normality we used the Mann-Whitney U test. In all other cases an appropriate t-test was used to analyze differences between genotypes for spine density, freezing time and LTP induction (based on the average of the last 10 min.). A repeated-measures ANOVA was used to analyze differences between genotypes for fiber volley and fEPSP slope, even when in some cases the distribution was not normal because there is no non-parametric alternative for the repeated-measures ANOVA.

References

1. Elgersma, Y., et al., Inhibitory autophosphorylation of CaMKII controls PSD association, plasticity, and learning. *Neuron*, 2002. 36(3): p. 493-505.
2. Giese, K.P., et al., Autophosphorylation at Thr286 of the alpha calcium-calmodulin kinase II in LTP and learning. *Science*, 1998. 279(5352): p. 870-3.
3. Silva, A.J., et al., Impaired spatial learning in alpha-calcium-calmodulin kinase II mutant mice. *Science*, 1992. 257(5067): p. 206-11.
4. Silva, A.J., et al., Deficient hippocampal long-term potentiation in alpha-calcium-calmodulin kinase II mutant mice. *Science*, 1992. 257(5067): p. 201-6.
5. Bach, M.E., et al., Impairment of spatial but not contextual memory in CaMKII mutant mice with a selective loss of hippocampal LTP in the range of the theta frequency. *Cell*, 1995. 81(6): p. 905-15.
6. Mayford, M., et al., CaMKII regulates the frequency-response function of hippocampal synapses for the production of both LTD and LTP. *Cell*, 1995. 81(6): p. 891-904.
7. Brocke, L., et al., Functional implications of the subunit composition of neuronal CaM kinase II. *J Biol Chem*, 1999. 274(32): p. 22713-22.
8. Hudmon, A. and H. Schulman, Structure-function of the multifunctional Ca²⁺/calmodulin-dependent protein kinase II. *Biochem J*, 2002. 364(Pt 3): p. 593-611.
9. Shen, K., et al., CaMKIIbeta functions as an F-actin targeting module that localizes CaMKIIalpha/beta heterooligomers to dendritic spines. *Neuron*, 1998.

- 21(3): p. 593-606.
10. Shen, K. and T. Meyer, Dynamic control of CaMKII translocation and localization in hippocampal neurons by NMDA receptor stimulation. *Science*, 1999. 284(5411): p. 162-6.
 11. Thiagarajan, T.C., E.S. Piedras-Renteria, and R.W. Tsien, alpha- and betaCaMKII. Inverse regulation by neuronal activity and opposing effects on synaptic strength. *Neuron*, 2002. 36(6): p. 1103-14.
 12. O'Leary, H., E. Lasda, and K.U. Bayer, CaMKIIbeta association with the actin cytoskeleton is regulated by alternative splicing. *Mol Biol Cell*, 2006. 17(11): p. 4656-65.
 13. Okamoto, K., et al., The role of CaMKII as an F-actin-bundling protein crucial for maintenance of dendritic spine structure. *Proc Natl Acad Sci U S A*, 2007. 104(15): p. 6418-23.
 14. Sanabria, H., et al., {beta}CaMKII regulates actin assembly and structure. *J Biol Chem*, 2009. 284(15): p. 9770-80.
 15. Cho, M.H., et al., Dentate gyrus-specific manipulation of beta-Ca²⁺/calmodulin-dependent kinase II disrupts memory consolidation. *Proc Natl Acad Sci U S A*, 2007. 104(41): p. 16317-22.
 16. van Woerden, G.M., et al., betaCaMKII controls the direction of plasticity at parallel fiber-Purkinje cell synapses. *Nat Neurosci*, 2009. 12(7): p. 823-5.
 17. Fink, C.C., et al., Selective regulation of neurite extension and synapse formation by the beta but not the alpha isoform of CaMKII. *Neuron*, 2003. 39(2): p. 283-97.
 18. Lin, Y.C. and L. Redmond, CaMKIIbeta binding to stable F-actin in vivo regulates F-actin filament stability. *Proc Natl Acad Sci U S A*, 2008. 105(41): p. 15791-6.
 19. Okamoto, K., et al., Rapid and persistent modulation of actin dynamics regulates postsynaptic reorganization underlying bidirectional plasticity. *Nat Neurosci*, 2004. 7(10): p. 1104-12.
 20. Allison, D.W., et al., Postsynaptic scaffolds of excitatory and inhibitory synapses in hippocampal neurons: maintenance of core components independent of actin filaments and microtubules. *J Neurosci*, 2000. 20(12): p. 4545-54.
 21. Frankland, P.W., et al., Alpha-CaMKII-dependent plasticity in the cortex is required for permanent memory. *Nature*, 2001. 411(6835): p. 309-13.
 22. Grover, L.M. and T.J. Teyler, Two components of long-term potentiation induced

- by different patterns of afferent activation. *Nature*, 1990. 347(6292): p. 477-9.
23. Lee, S.J., et al., Activation of CaMKII in single dendritic spines during long-term potentiation. *Nature*, 2009. 458(7236): p. 299-304.
 24. De Koninck, P. and H. Schulman, Sensitivity of CaM kinase II to the frequency of Ca²⁺ oscillations. *Science*, 1998. 279(5348): p. 227-30.
 25. Lisman, J., H. Schulman, and H. Cline, The molecular basis of CaMKII function in synaptic and behavioural memory. *Nat Rev Neurosci*, 2002. 3(3): p. 175-90.
 26. Hudmon, A. and H. Schulman, Neuronal CA²⁺/calmodulin-dependent protein kinase II: the role of structure and autoregulation in cellular function. *Annu Rev Biochem*, 2002. 71: p. 473-510.
 27. Colbran, R.J., Targeting of calcium/calmodulin-dependent protein kinase II. *Biochem J*, 2004. 378(Pt 1): p. 1-16.
 28. Bayer, K.U., et al., Developmental expression of the CaM kinase II isoforms: ubiquitous gamma- and delta-CaM kinase II are the early isoforms and most abundant in the developing nervous system. *Brain Res Mol Brain Res*, 1999. 70(1): p. 147-54.
 29. Sahyoun, N., et al., Early postnatal development of calmodulin-dependent protein kinase II in rat brain. *Biochem Biophys Res Commun*, 1985. 132(3): p. 878-84.
 30. Nomura, T., et al., Overexpression of alpha and beta isoforms of Ca²⁺/calmodulin-dependent protein kinase II in neuroblastoma cells -- H-7 promotes neurite outgrowth. *Brain Res*, 1997. 766(1-2): p. 129-41.
 31. Goslin, K. and G. Banker, eds. *Culturing Nerve Cells*. 1991, MIT press: Cambridge, MA. 678.
 32. Jaworski, J., et al., Dynamic microtubules regulate dendritic spine morphology and synaptic plasticity. *Neuron*, 2009. 61(1): p. 85-100.

Chapter 6

Functional requirement of hippocampal CA3 α CaMKII in long-term potentiation

Nils Z. Borgesius*, Mohammad R. Hojjati*, Geeske M. van Woerden, Gabrielle H. S. Buitendijk, Alcino J. Silva and Ype Elgersma

* these authors have contributed equally

Abstract

With a highly unique network architecture, the CA3 region of the hippocampus functions critically in higher-order spatial processing. Specifically, long-term potentiation (LTP) of both the Schaffer-collateral (CA3-CA1) and associational/commissural (CA3-CA3) pathways has been widely proposed as candidate mechanisms for hippocampus-dependent spatial processing. At the molecular level, the alpha isoform of calcium/calmodulin-dependent protein kinase 2 (α CaMKII) is among the most abundant proteins in the hippocampus, and widely demonstrated to function critically in regulating the postsynaptic induction of LTP at the hippocampal Schaffer-collateral CA3-CA1 synapse. However, little is known about the independent presynaptic and postsynaptic requirements for α CaMKII during LTP at the CA3 synapses. Therefore, we investigated the requirement of α CaMKII for Schaffer-collateral (CA3-CA1) and associational/commissural (CA3-CA3) LTP using a selective genetic ablation of *Camk2a* in the CA3 neurons of the hippocampus. Although we confirmed that CA3-CA1 LTP was severely impaired in global *Camk2a* KO mice, CA3-*Camk2a* KO mice showed robust and stable CA3-CA1 LTP. In addition, LTP of the associational/commissural pathway between CA3 neurons was intact in both global *Camk2a* KO and CA3-*Camk2a* KO mice. Taken together, α CaMKII appears to function in a highly specific manner for regulating LTP within hippocampal circuits.

Introduction

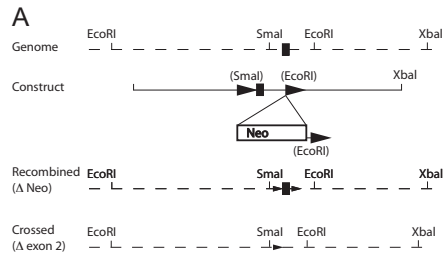
CaMKII is one of the most abundant proteins of the hippocampus, and its role in hippocampal plasticity has been thoroughly investigated by both, pharmacological and genetic approaches (reviewed by [1-4]. The postsynaptic activation of (α) CaMKII has been shown to be critically involved in LTP [5-8]. The role of presynaptic CaMKII in CA3-CA1 LTP is not clear. In contrast, the involvement of (α)CaMKII in neurotransmitter release and its role in short-term plasticity has been well established [9-16]. Using a global α CaMKII knockout, as well as a CA3 specific α CaMKII knockout, it has been shown that presynaptic α CaMKII affects short-term presynaptic plasticity at this synapse [13, 14]. Hence, this could in turn affect the induction of postsynaptic LTP. The possible involvement of presynaptic (CA3) CaMKII has not yet been studied in acute slice preparations, simply because inhibiting presynaptic CaMKII without affecting postsynaptic CaMKII is technically quite difficult as it requires the recording and manipulation of connected pairs of neurons. To get around this problem, organotypic cultures of hippocampal slices have been used to study the requirement of presynaptic CaMKII activity in CA3-CA3 LTP [17]. This study showed that blocking presynaptic CaMKII activity reduced CA3-CA3 LTP induction by 50%. Similar, in a study where dissociated hippocampal neurons were used, inhibition of presynaptic CaMKII activity prevented the induction of LTP between excitatory neurons completely [18]. Hence, these studies indicate a clear role of presynaptic CaMKII activity in LTP between excitatory neurons of the hippocampus. Since the drugs that were used in these studies interfere with the calcium/calmodulin dependent activation of CaMKII, these results further indicate that the activation of presynaptic CaMKII is required for normal potentiation. However, these results are surprising, given that it was shown that the most abundant CaMKII isoform, α CaMKII, plays a structural, rather than an enzymatic role in short-term presynaptic plasticity [14].

To further elucidate the role of presynaptic α CaMKII in LTP of the Schaffer-collateral pathway from CA3 to CA1 neurons, we made use of a genetic ablation of α CaMKII specifically in the CA3 area. Surprisingly, we found no evidence that presynaptic α CaMKII was required for this form of LTP. We also did not find a requirement for presynaptic and postsynaptic α CaMKII in LTP of the associational/commissural pathway between hippocampal CA3-CA3 neurons.

Results

CA3 specific *Camk2a* knockout mouse

To investigate the presynaptic role of α CaMKII in CA3-CA1 LTP *in vivo* we created a mouse with a floxed exon 2 in the *Camk2a* gene using the construct as described in Elgersma et al. [19]. Through Cre recombination we took out the neomycin gene but left



exon 2 flanked by two loxP sites (Figure 1A). We crossed this mouse with a CA3 specific Cre line to generate offspring, which lacks *Camk2a* and thus α CaMKII specifically in the CA3 region (*Camk2a^{flf}Cre*). Indeed, the deletion of α CaMKII is specific for the CA3 region as shown by the immunocytochemistry (Figure 1B). As the two flanking loxP sites by themselves do not affect

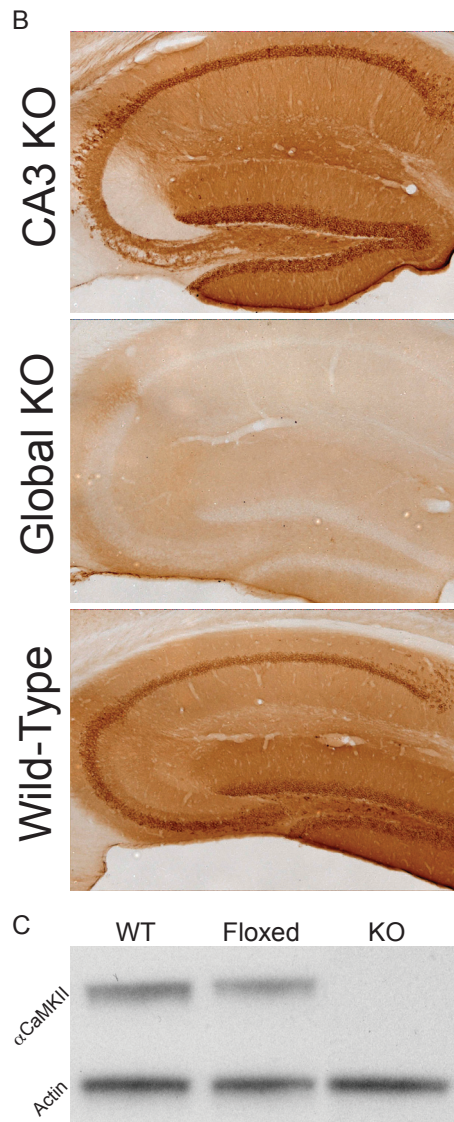


Figure 1. Generation of CA3 specific *Camk2a* knockout mouse. (A) Schematic diagram for the generation of the CA3 specific *Camk2a* knockouts. (Genome) Wild-type *Camk2a* locus with the location of exon 2 depicted as a black box. (Construct) Targeting construct used for introducing the LoxP sites in the *Camk2a* locus. The LoxP sites flanking exon 2 and the neomycin gene are depicted as triangles. (Recombined) Mutant *Camk2a^{flf}* locus after homologous recombination and Cre recombination in ES cells and consequential deletion of the neomycin gene. (Crossed) Mutant *Camk2a^{-/-}* locus after Cre recombination and consequential deletion of exon 2 in CA3 region when crossed with KA1-Cre line. (B) Immunocytochemistry staining using an antibody specific for α CaMKII shows complete deletion of α CaMKII in the CA3 area. *Camk2a^{-/-}* is shown as negative control. *Camk2a^{+/+}* is shown as positive control. (C) Western blot analysis using an antibody specific for α CaMKII shows no reduction of α CaMKII as a consequence of the loxP sites flanking exon 2. *Camk2a^{-/-}* is shown as negative control. Actin is used as a loading control. (WT = *Camk2a^{+/+}*; Floxed = *Camk2a^{flf}*; KO = *Camk2a^{-/-}*)

the expression of α CaMKII as shown by Western blot analysis (Figure 1C) *Camk2a*^{+/+} mice can be used as controls. In most experiments we have also included the other two control groups (*Camk2a*^{fl/fl} and *Camk2a*^{+/+ Cre}). We have thus produced a mouse with a specific deletion of α CaMKII in the CA3 region, which contains the presynaptic neurons of the Schaffer-collateral (CA3-CA1) pathway.

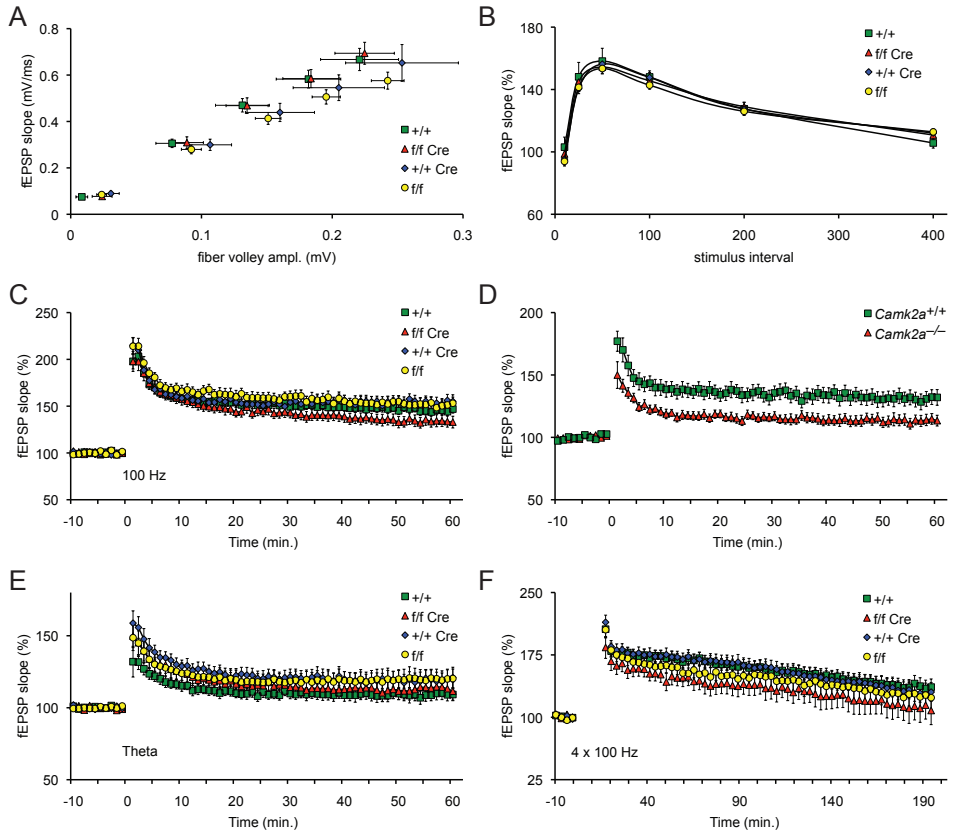


Figure 2. CA3-CA1 LTP is normal in absence of presynaptic α CaMKII.

(A) CA3 specific *Camk2a* knockout mice (*Camk2a*^{fl/fl Cre}) show normal basal synaptic transmission (*Camk2a*^{+/+} n=14, n=36; *Camk2a*^{fl/fl Cre} n=7, n=28; *Camk2a*^{+/+ Cre} n=12, n=24; *Camk2a*^{fl/fl} n=23, n=36 for fiber volley and fEPSP slope respectively) (B) CA3 specific *Camk2a* knockout mice (*Camk2a*^{fl/fl Cre}) show normal PPF (*Camk2a*^{+/+} n=32; *Camk2a*^{fl/fl Cre} n=24; *Camk2a*^{+/+ Cre} n=24; *Camk2a*^{fl/fl} n=32) (C) CA3 specific *Camk2a* knockout mice (*Camk2a*^{fl/fl Cre}) show normal 100 Hz LTP (*Camk2a*^{+/+} n=18; *Camk2a*^{fl/fl Cre} n=14; *Camk2a*^{+/+ Cre} n=13; *Camk2a*^{fl/fl} n=18) (D) Global *Camk2a* knockout mice (*Camk2a*^{-/-}) show impaired 100 Hz LTP (*Camk2a*^{-/-} n=6; *Camk2a*^{+/+} n=12) (E) CA3 specific *Camk2a* knockout mice (*Camk2a*^{fl/fl Cre}) show normal Theta burst LTP (*Camk2a*^{+/+} n=17; *Camk2a*^{fl/fl Cre} n=11; *Camk2a*^{+/+ Cre} n=12; *Camk2a*^{fl/fl} n=18) (F) CA3 specific *Camk2a* knockout mice

(*Camk2 $\alpha^{ff Cre}$*) show normal L-LTP (*Camk2 $\alpha^{+/+}$* n=19; *Camk2 $\alpha^{ff Cre}$* n=11; *Camk2 $\alpha^{+/+ Cre}$* n=20; *Camk2 α^{ff}* n=16)

Presynaptic α CaMKII is not needed for CA3-CA1 LTP in acute hippocampal slices

Before investigating the effect of presynaptic α CaMKII deletion on LTP we confirmed the findings of Hinds, et al. [13] and showed that synaptic transmission and Paired Pulse Facilitation (PPF) were not affected, as fiber volley, fEPSP slope and PPF were similar for all genotypes (Figure 2A-B; $F_{3,52}=11$; $p=0.58$; $F_{3,120}=9.3$; $p=0.48$; $F_{3,104}=5.6$; $p=0.72$; repeated measures ANOVA for fiber volley, fEPSP slope and PPF respectively). However, it has been shown that presynaptic deletion of α CaMKII increases facilitation during trains of high frequency stimuli and enhances synaptic augmentation [13, 14]. This could potentially affect LTP induction.

Surprisingly, 100 Hz LTP was not affected by the presynaptic absence of α CaMKII (Figure 2C; $F_{3,62}=2.3$; $p=0.09$; one-way ANOVA). In contrast, 100 Hz LTP is impaired in the global α CaMKII (Figure 2D; $F_{1,18}=2.7$; $p=0.12$; one-way ANOVA). As different LTP induction protocols rely on slightly different molecular pathways [20-22] and are reported to differ in their dependence on presynaptic α CaMKII [17] we also evoked LTP using a Theta burst protocol. Again, LTP was not affected by the presynaptic absence of α CaMKII (Figure 2E; $F_{3,57}=2.2$; $p=0.10$ one-way ANOVA). Finally, some studies reported a slow onset of the presynaptic component in LTP, i.e. increased vesicle release [23, 24]. As α CaMKII is implicated in vesicle release we wanted to exclude the possibility that we missed the effect of deleting α CaMKII presynaptically by recording only 1 hour after LTP induction. Therefore, we evoked long lasting LTP and recorded for 3 hours. Again, LTP was normal despite the presynaptic absence of α CaMKII (Figure 2F; $F_{3,65}=0.75$; $p=0.53$ one way ANOVA). Taken together, these results strongly suggest that presynaptic α CaMKII is not required for CA3-CA1 LTP in the hippocampus.

α CaMKII is not necessary for CA3-CA3 LTP in acute hippocampal slices

Lu and Hawkins showed both pre- and postsynaptic contribution of α CaMKII in LTP in organotypic hippocampal slices [17]. However, they studied a different synapse, namely the CA3-CA3 synapse. CA3-CA3 and CA3-CA1 connections may differ in their (pre)synaptic molecular mechanisms involved in LTP. Therefore, we also examined the properties of the CA3-CA3 synapse in our CA3 specific knockout.

Pyramidal neurons in the CA3 subfield are innervated by their neighboring CA3 neurons through the commissural pathway and by mossy fibers from the Dentate Gyrus.

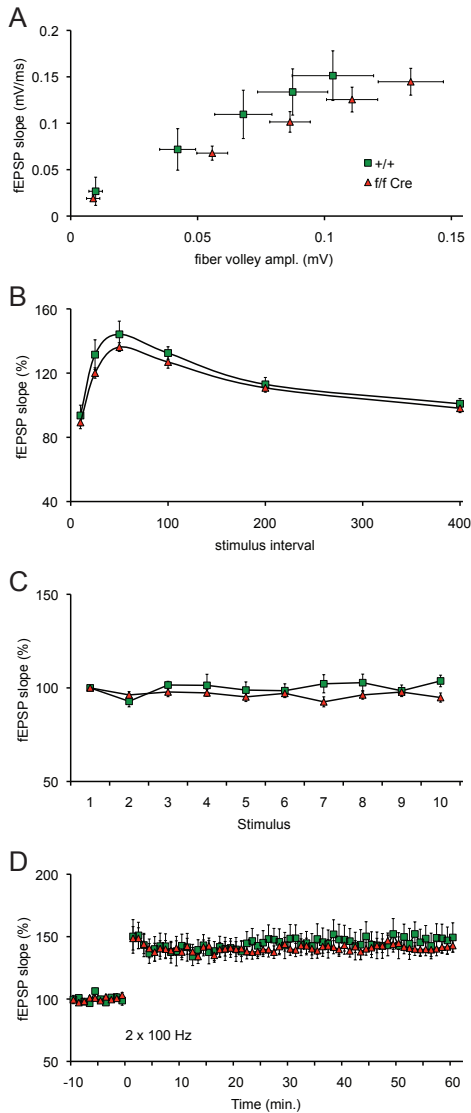


Figure 3. CA3-CA3 LTP is normal in absence of α CaMKII.

(A) CA3 specific *Camk2a* knockout mice (*Camk2a*^{f/f Cre}) show normal basal synaptic transmission (*Camk2a*^{+/+} n=10, n=22; *Camk2a*^{f/f Cre} n=24, n=45 for fiber volley and fEPSP slope respectively) (B) CA3 specific *Camk2a* knockout mice (*Camk2a*^{f/f Cre}) show normal PPF. Both genotypes show no signs of mossy fiber contamination. (*Camk2a*^{+/+} n=18; *Camk2a*^{f/f Cre} n=41) (C) CA3 specific *Camk2a* knockout mice (*Camk2a*^{f/f Cre}) show normal 1 Hz facilitation. Both genotypes show no signs of mossy fiber contamination. (*Camk2a*^{+/+} n=20; *Camk2a*^{f/f Cre} n=45) (D) CA3 specific *Camk2a* knockout mice (*Camk2a*^{f/f Cre}) show normal CA3-CA3 LTP. (*Camk2a*^{+/+} n=16; *Camk2a*^{f/f Cre} n=29)

A possible caveat in fEPSP measurements in the CA3 is distinguishing between these two pathways. Therefore we used PPF and 1 Hz frequency facilitation before each experiment to discriminate these two pathways; afterwards we confirmed this by measuring sensitivity for DCG-IV as described earlier [25]. Mossy fiber transmission shows very strong facilitation ($\pm 215\%$ and $\pm 250\%$ for PPF and 1 Hz respectively). Hence, we excluded all measurements that showed PPF or 1 Hz facilitation exceeding 180% or 130% respectively. Consequently, our recordings show facilitation within the normal range of CA3-CA3 synapses (Figure 3B-C). This strongly suggests that we selectively stimulated commissural fibers without contamination of mossy fibers. Additionally, after each experiment we used DCG-IV to confirm this. As DCG-IV reduces mossy fiber transmission by $\pm 80\%$ [25] and transmission was reduced by less than 20% in our experiments, we are confident that we selectively stimulated CA3-CA3 connections (80.7 ± 3.3 and 80.4 ± 2.6 for *Camk2a*^{+/+}

and *Camk2 $\alpha^{fl/Cre}$* respectively). Finally, there was no effect of genotype on PPF, 1 Hz and DCG-IV (repeated measures ANOVA $F_{1,57}=6.8$; $p=0.25$ and $F_{1,63}=9.2$; $p=0.07$ and unpaired two tailed t-test $p=0.95$, $t=0.06$ respectively).

Basal synaptic transmission was similar between genotypes (Figure 3A-B; $F_{1,32}=10$; $p=0.20$; $F_{1,65}=27$; $p=0.81$; repeated measures ANOVA for fiber volley and fEPSP slope respectively). Next we evoked LTP in CA3-CA3 synapses to investigate the effect of pre- and postsynaptic absence of α CaMKII on CA3-CA3 LTP. Surprisingly, LTP was not affected by the total absence of α CaMKII (unpaired two tailed t-test $p=0.52$, $t=0.65$). To exclude the possibility that these results are caused by side effects the Cre-lox system like incomplete deletion of the *Camk2a* gene, we repeated the experiments in global α CaMKII knockout mice (*Camk2a*^{-/-}). All results were essentially the same. Basal synaptic transmission and LTP were normal in *Camk2a*^{-/-} mice. Moreover, PPF, 1 Hz facilitation and DCG-IV experiments showed no characteristics of mossy fiber stimulation and were not different between genotypes (repeated measures ANOVA: fiber volley $F_{1,21}=9.4$; $p=0.32$, fEPSP slope $F_{1,32}=7.8$; $p=0.58$, PPF $F_{1,28}=5.1$; $p=0.61$ and 1 Hz $F_{1,29}=16$; $p=0.27$; unpaired two tailed t-test: DCG-IV $p=0.11$, $t=1.6$ and LTP $p=0.50$, $t=0.68$). Taken together, these results strongly suggest that CA3-CA3 LTP is independent of both pre- and postsynaptic α CaMKII.

Discussion

Here we describe a specific ablation of the *Camk2a* gene in the CA3 neurons of the hippocampus. We found no evidence that α CaMKII in CA3 neurons is required for LTP of the CA3-CA1 or CA3-CA3 synapse in acute hippocampal preparations. This result was unexpected given the conclusions of previous studies in cultured hippocampal slices or dissociated hippocampal preparations [17, 18]. There are two obvious explanations that can account for these different findings. First, the discrepancy may be caused by the differences in the neuronal preparations that were used. The study of Ninan and Arancio [18] was done in dissociated cultures of mouse neurons. As the authors themselves mention there are important differences between cultured neurons and acute hippocampal slices, e.g. the developing nature of cultures, that might explain incongruities [18]. This same argument may also explain why Lu and Hawkins [17] have different results, despite the use of organotypic slice cultures, which resemble the acute slice more closely. An alternative explanation is that presynaptic CaMKII function was studied previously by pharmacological not genetic manipulations like in our study. Hence, in these studies not only α CaMKII activity was blocked, but also β CaMKII activity. In principle, it could

be that β CaMKII compensates for the loss of α CaMKII in our experimental approach, thereby masking an effect on LTP. However, it should be noted that loss of α CaMKII, both in a global as well as a CA3 specific knockout, is sufficient to cause a marked deficit in short-term presynaptic plasticity [9, 13, 14], indicating that β CaMKII cannot compensate for the loss of presynaptic α CaMKII on these measures. Hence, despite a clear requirement for α CaMKII in presynaptic short-term plasticity, these presynaptic measures have no impact on the induction or maintenance of LTP

It is also surprising that we have found no evidence for involvement of (pre- and postsynaptic) α CaMKII in CA3-CA3 LTP (Figure 3D), since CA3-CA3 LTP shares many characteristics with Schaffer-collateral (CA3-CA1) LTP. Most notably, both CA3-CA3 and CA3-CA1 LTP depend on NMDA receptor activation and a postsynaptic rise in Ca^{2+} [27-34]. Moreover, postsynaptic viral overexpression of α CaMKII that mimics autophosphorylation at T286 results in increased synaptic transmission [30]. However, to our knowledge, no study has yet used genetic deletion of α CaMKII to test its involvement in CA3-CA3 LTP. Furthermore, none of the aforementioned studies used acute hippocampal slices of adult mice. Previous studies using acute hippocampal slice preparations were either using immature guinea pigs or rats [28, 33, 34].

Taken together, our study unexpectedly but intriguingly shows, that α CaMKII in CA3 neurons is not required for either CA3-CA3 as well as CA3-CA1 LTP. Hence, the requirement of α CaMKII in LTP differs markedly between cells of the hippocampus.

Acknowledgements

We greatly appreciate the advice of Heinz Beck on measuring CA3-CA3 fEPSPs and Steven Kushner for discussions and help with the manuscript.

Materials and Methods

Generation of the CA3 Camk2a knockout mice

Camk2a^{ff} mutant ES cells were generated as follows: a genomic clone of approximately 8 Kb encoding the *Camk2a* exon 2 (amino acids 22–53) was isolated by screening a mouse library. The targeting construct was made by inserting a PGK neomycin cassette flanked by LoxP sites into the EcoRI site approximately 1.2 Kbp downstream of exon 2. Another LoxP site was inserted into the SmaI site 60 bp upstream of exon 2. Targeted ES clones (61 out of 130) were identified by Southern blot analysis. PCR analysis revealed that 20 out of these 61 clones contained the additional 5' LoxP site. The PGK neo cassette was removed by transient expression of Cre recombinase (pBS185, Gibco). Some clones

had a deletion only of the neomycin cassette. This results in *Camk2a* exon 2 flanked by LoxP sites. See also [19].

Immunocytochemistry

Immunocytochemistry was performed on free-floating 40 μm thick frozen sections employing a standard avidin-biotin-immunoperoxidase complex method (ABC, Vector Laboratories, USA) with, αCaMKII (MAB3119, 1:10,000; Chemicon) and βCaMKII (CB-b1, 1:2000; Zymed) as the primary antibody and diaminobenzidine (0.05%) as the chromogen (Hansel, 2006).

Western blot

Lysates were prepared by quick dissection of the brain and by homogenization of the brain tissue in lysis buffer (10mM TRIS-HCl 6.8, 2.5% SDS, 2mM EDTA and protease and phosphatase inhibitor cocktails (Sigma). The concentration of the lysates was adjusted to 1 mg/ml. 10 μg was used for Western blot analysis. Western blots were probed with antibodies directed against αCaMKII (MAB3119, 1:10,000; Chemicon) and Actin (MAB1501R, 1:2000; Chemicon). Blots were stained using Enhanced ChemoLuminescence (#32106, Pierce) Western blot quantification was performed using NIH-Image.

Electrophysiology

After the animals had been sacrificed sagittal slices (400 μm) for CA3-CA1 experiments and coronal slices for CA3CA3 experiments were made submerged in ice-cold artificial CSF (ACSF) using a vibratome and hippocampi were dissected out. These hippocampal slices were maintained at room temperature for at least 1.5 hours to recover before experiments were initiated. Then they were placed in a submerged recording chamber and perfused continuously at a rate of 2 ml/min with ACSF equilibrated with 95% O_2 , 5% CO_2 at 31°C. ACSF contained the following (in mM): 120 NaCl, 3.5 KCl, 2.5 CaCl_2 , 1.3 MgSO_4 , 1.25 NaH_2PO_4 , 26 NaHCO_3 , and 10 D-glucose. Extracellular recording of field EPSP (fEPSPs) were made in CA1 or CA3 stratum radiatum with platinum/iridium electrodes (Frederick Haer Companu, Bowdoinham, ME). A bipolar Pt/Ir was used to stimulate Schaffer-collateral/commissural afferents with a stimulus duration of 100 μs . Stimulus response curves were obtained at the beginning of each experiment, 20 minutes after placing the electrodes. PPF experiments were done at one-third of maximum. LTP was evoked using four different tetani: (i) 100 Hz (1 train of 1 second at 100 Hz), (ii)

Theta burst (2 trains of 4 stimuli at 100 Hz 200 ms apart), (iii) L-LTP (4 trains of 1 second at 100 Hz 5 min. apart) and (iv) CA3CA3 LTP (2 trains of 1 second at 100 Hz 10 seconds apart). All protocols were performed at one-third of the maximum fEPSP. fEPSP measurements were done once per minute. Potentiation was measured as the normalized increase of the mean fEPSP slope for the duration of the baseline. Only stable recordings were included and this judgment was made blind to genotype. Average LTP was defined as the mean last 10 minutes of the normalized fEPSP slope.

References

1. Lisman, J., H. Schulman, and H. Cline, *The molecular basis of CaMKII function in synaptic and behavioural memory*. Nat Rev Neurosci, 2002. **3**(3): p. 175-90.
2. Lisman, J.E. and C.C. McIntyre, *Synaptic plasticity: a molecular memory switch*. Curr Biol, 2001. **11**(19): p. R788-91.
3. Elgersma, Y., J.D. Sweatt, and K.P. Giese, *Mouse genetic approaches to investigating calcium/calmodulin-dependent protein kinase II function in plasticity and cognition*. J Neurosci, 2004. **24**(39): p. 8410-5.
4. Griffith, L.C., *Calcium/calmodulin-dependent protein kinase II: an unforgettable kinase*. J Neurosci, 2004. **24**(39): p. 8391-3.
5. Pettit, D.L., S. Perlman, and R. Malinow, *Potentiated transmission and prevention of further LTP by increased CaMKII activity in postsynaptic hippocampal slice neurons*. Science, 1994. **266**(5192): p. 1881-5.
6. Lledo, P.M., et al., *Calcium/calmodulin-dependent kinase II and long-term potentiation enhance synaptic transmission by the same mechanism*. Proc Natl Acad Sci U S A, 1995. **92**(24): p. 11175-9.
7. Hayashi, Y., et al., *Driving AMPA receptors into synapses by LTP and CaMKII: requirement for GluR1 and PDZ domain interaction*. Science, 2000. **287**(5461): p. 2262-7.
8. Pi, H.J., et al., *Autonomous CaMKII can promote either long-term potentiation or long-term depression, depending on the state of T305/T306 phosphorylation*. J Neurosci, 2010. **30**(26): p. 8704-9.
9. Chapman, P.F., et al., *The alpha-Ca²⁺/calmodulin kinase II: a bidirectional modulator of presynaptic plasticity*. Neuron, 1995. **14**(3): p. 591-7.
10. Lin, J.W., et al., *Effects of synapsin I and calcium/calmodulin-dependent protein kinase II on spontaneous neurotransmitter release in the squid giant synapse*. Proc Natl Acad Sci U S A, 1990. **87**(21): p. 8257-61.

11. Llinas, R., et al., *Intraterminal injection of synapsin I or calcium/calmodulin-dependent protein kinase II alters neurotransmitter release at the squid giant synapse*. Proc Natl Acad Sci U S A, 1985. **82**(9): p. 3035-9.
12. Nichols, R.A., et al., *Calcium/calmodulin-dependent protein kinase II increases glutamate and noradrenaline release from synaptosomes*. Nature, 1990. **343**(6259): p. 647-51.
13. Hinds, H.L., et al., *Essential function of alpha-calcium/calmodulin-dependent protein kinase II in neurotransmitter release at a glutamatergic central synapse*. Proc Natl Acad Sci U S A, 2003. **100**(7): p. 4275-80.
14. Hojjati, M.R., et al., *Kinase activity is not required for alphaCaMKII-dependent presynaptic plasticity at CA3-CA1 synapses*. Nat Neurosci, 2007. **10**(9): p. 1125-7.
15. Pang, Z.P., et al., *Calmodulin controls synaptic strength via presynaptic activation of calmodulin kinase II*. J Neurosci, 2010. **30**(11): p. 4132-42.
16. Jiang, X., et al., *Modulation of CaV2.1 channels by Ca²⁺/calmodulin-dependent protein kinase II bound to the C-terminal domain*. Proc Natl Acad Sci U S A, 2008. **105**(1): p. 341-6.
17. Lu, F.M. and R.D. Hawkins, *Presynaptic and postsynaptic Ca(2+) and CamKII contribute to long-term potentiation at synapses between individual CA3 neurons*. Proc Natl Acad Sci U S A, 2006. **103**(11): p. 4264-9.
18. Ninan, I. and O. Arancio, *Presynaptic CaMKII is necessary for synaptic plasticity in cultured hippocampal neurons*. Neuron, 2004. **42**(1): p. 129-41.
19. Elgersma, Y., et al., *Inhibitory autophosphorylation of CaMKII controls PSD association, plasticity, and learning*. Neuron, 2002. **36**(3): p. 493-505.
20. Cavus, I. and T. Teyler, *Two forms of long-term potentiation in area CA1 activate different signal transduction cascades*. J Neurophysiol, 1996. **76**(5): p. 3038-47.
21. Grover, L.M. and T.J. Teyler, *Two components of long-term potentiation induced by different patterns of afferent activation*. Nature, 1990. **347**(6292): p. 477-9.
22. Raymond, C.R. and S.J. Redman, *Different calcium sources are narrowly tuned to the induction of different forms of LTP*. J Neurophysiol, 2002. **88**(1): p. 249-55.
23. Bayazitov, I.T., et al., *Slow presynaptic and fast postsynaptic components of compound long-term potentiation*. J Neurosci, 2007. **27**(43): p. 11510-21.
24. Zakharenko, S.S., L. Zablow, and S.A. Siegelbaum, *Visualization of changes in presynaptic function during long-term synaptic plasticity*. Nat Neurosci, 2001.

- 4(7): p. 711-7.
25. Kirschstein, T., et al., *L-CCG-I activates group III metabotropic glutamate receptors in the hippocampal CA3 region*. *Neuropharmacology*, 2004. **47**(2): p. 157-62.
 26. Jin, I. and R.D. Hawkins, *Presynaptic and postsynaptic mechanisms of a novel form of homosynaptic potentiation at aplysia sensory-motor neuron synapses*. *J Neurosci*, 2003. **23**(19): p. 7288-97.
 27. Bains, J.S., J.M. Longacher, and K.J. Staley, *Reciprocal interactions between CA3 network activity and strength of recurrent collateral synapses*. *Nat Neurosci*, 1999. **2**(8): p. 720-6.
 28. Bradler, J.E. and G. Barrionuevo, *Heterosynaptic correlates of long-term potentiation induction in hippocampal CA3 neurons*. *Neuroscience*, 1990. **35**(2): p. 265-71.
 29. Debanne, D., B.H. Gähwiler, and S.M. Thompson, *Long-term synaptic plasticity between pairs of individual CA3 pyramidal cells in rat hippocampal slice cultures*. *J Physiol*, 1998. **507** (Pt 1): p. 237-47.
 30. Kakegawa, W., et al., *Input- and subunit-specific AMPA receptor trafficking underlying long-term potentiation at hippocampal CA3 synapses*. *Eur J Neurosci*, 2004. **20**(1): p. 101-10.
 31. Debanne, D., B.H. Gähwiler, and S.M. Thompson, *Heterogeneity of synaptic plasticity at unitary CA3-CA1 and CA3-CA3 connections in rat hippocampal slice cultures*. *J Neurosci*, 1999. **19**(24): p. 10664-71.
 32. Pavlidis, P., J. Montgomery, and D.V. Madison, *Presynaptic protein kinase activity supports long-term potentiation at synapses between individual hippocampal neurons*. *J Neurosci*, 2000. **20**(12): p. 4497-505.
 33. Smith, K.L. and J.W. Swann, *Long-term depression of perforant path excitatory postsynaptic potentials following synchronous network bursting in area CA3 of immature hippocampus*. *Neuroscience*, 1999. **89**(3): p. 625-30.
 34. Zalutsky, R.A. and R.A. Nicoll, *Comparison of two forms of long-term potentiation in single hippocampal neurons*. *Science*, 1990. **248**(4963): p. 1619-24.

Chapter 7

General Discussion

The overall aim of the studies described in this thesis is to clarify the role of DNA damage in aging of the nervous system. To this end we analyzed mouse mutants in which we used targeted genetic mutations of the excision repair cross-complementing group 1 (*Ercc1*) gene. As the ERCC1 protein is involved in multiple DNA repair pathways our hypomorph mutations result in more unrepaired DNA damage. We studied the hippocampal, auditory, visual and neuromuscular systems in these mice. Hippocampus-dependent learning and memory has received special attention, as its age-related decline is hard to treat and poses a great threat to personal well-being and society as a whole. To understand how aging affects learning and memory, it is essential to understand the molecular mechanisms of these cognitive processes. Therefore, two studies were directed at the function of CaMKII, a molecule with a pivotal role in learning and memory. Specifically, we investigated for the first time the role of β CaMKII in hippocampus-dependent synaptic plasticity, learning and memory. Furthermore we studied the little explored role of presynaptic α CaMKII in LTP.

7.1 Aging of the nervous system

In chapter 2 we investigated the effect of DNA damage on the hippocampus using a global hypomorph mutant and a neuron specific knockout of the *Ercc1* gene. Using the global mutant we found that DNA damage accumulation causes a progressive increase in pathology indicating stressed and dying neurons. Consequently, there is an age-related reduction of synaptic plasticity, the putative cellular substrate for learning. In addition, we show that the most sensitive cells to DNA damage in the brain are neurons as they are most affected while the hypomorph *Ercc1* mutation is present in all cells. Consistently, when we limit the mutation of *Ercc1* to excitatory neurons in the forebrain we see a similar phenotype. Moreover, we show that DNA damage exclusively in neurons causes impaired learning. Importantly, by restricting the mutation we circumvented any confounding factors such as impaired motor, auditory or visual function (see chapters 2 and 3). Taken together, this strongly suggests that aging of the brain is the result of neuronal DNA damage.

In the hippocampus of the older *Ercc1^{Δ/-}* mice we found very low levels of apoptotic markers and high levels of stress markers. Furthermore, the volume of the brain is not dramatically reduced during aging and there is no reduction in the number and density of dendrites, as indicated by the stable level of MAP2 in the hippocampus. Taken together, this suggests that there is relatively little cell loss in the hippocampus, while there are relatively high numbers of stressed neurons. Furthermore, during the

electrophysiological experiments we found no evidence for neuronal loss, as basal synaptic transmission is normal. Collectively, this strongly suggests that the cause of the impaired function of the hippocampus is reduced functioning of neurons, not loss of them. This is, however, not a universal feature in the aging nervous system.

As we show in chapter 4, contrary to the hippocampus, the spinal cord of *Ercc1^{Δ/-}* mice suffers a significant loss of neurons with increasing age. Moreover, this loss of motoneurons is reflected in disturbed innervation of muscle fibers. Simultaneously an increased number of cells show clear signs of stress. Thus, the reduced motor function is most likely the result of both loss of neurons and reduced functioning of neurons.

It is at present not clear what the relative contributions of reduced neuronal function and loss of neurons are to the age-related loss of hearing and vision we show in chapter 3. While the progressive loss of hearing in the *Ercc1^{Δ/-}* mice is almost certainly caused by functional loss of outer hair cells (OHCs), it is not possible to distinguish between loss of OHCs *per se* or merely loss of their function without proper anatomical and immunohistochemical analyses. In the case of age-related loss of vision in the *Ercc1^{Δ/-}* mice the matter of the relative contribution of optic and neuronal changes has to be resolved before venturing into the discussion whether neuron loss or loss of function contributes more.

Now that we have established that DNA damage can cause an aging-like phenotype by negatively affecting cell function and ultimately cell death, one question remains. How does DNA damage cause this? DNA damage can have three different consequences for the cell: (i) a mutagenic effect causing cancer, (ii) a cytotoxic effect, eventually causing aging through reduced cellular function ultimately resulting in apoptosis or necrosis, or (iii) a cytostatic effect causing aging through senescence, a mechanism which is not applicable to post-mitotic neurons [1]. As we focus on neurons, the cytotoxic effects of DNA damage are most relevant. However, cytotoxicity by itself does not constitute a satisfying answer. Is it always the mutation of the same genes that cause cell death, or is every cell unique in its pattern of DNA damage?

The pathology data show that not all affected neurons exhibit the same (combination of) activated cell stress pathways in the hippocampus and the spinal cord in the older *Ercc1^{Δ/-}* mice. In the spinal cord neurons show different types of Golgi apparatus abnormalities. For example, all ATF3 or p53 positive motoneurons show Golgi abnormalities of one type or another. However, only a minority of the neurons with an abnormal Golgi apparatus was ATF3 or p53 positive. Moreover, there are very

few cells that are positive for both ATF3 and p53. Taken together, this indicates that there are many different patterns of cellular stress within a single cell type as a result of DNA damage. Therefore, we conclude that neurons can die in different ways as a consequence of DNA damage, which fits with the model of stochastic DNA damage perturbing transcription of genes in a random pattern.

Our results are in line with the predictions made by the Disposable Soma theory. The aging phenotype of our mutants is the result of a limitation in repair, the consequential accumulation of molecular damage and this is a stochastic process. However, as the pathology in the spinal cord and the brain are not identical it seems that although the damage is most likely stochastic its results in different effects in different tissues. If the DNA is damaged by ROS we have not tested. However, we can say that all the DNA damage is naturally occurring as we have only impaired its repair and we do not apply any extra extrinsic damage. Hence, our data support the idea that the brain is particularly vulnerable to oxidative stress and DNA damage.

Not all genes are created equal. Some genes are essential for survival of the cell and others for a specific function of a certain cell type, like *Camk2b* in the hippocampus (see chapter 5). Therefore, two questions remain to be answered. First, which genes are damaged in the neurons that show loss of function? Second, damage to which genes results in cell death? However, almost every method available to investigate gene expression can only analyze at tissue-level. When trying to resolve what genes are affected this poses a big problem. When cells are lost the expression pattern of the tissue sample can change if the make up of the cellular population is affected. This would suggest a change of expression within cells, while this is not necessarily so. Moreover, cells will have different changes in their gene expression as a result of stochastic DNA damage. Hence, many changes could be undetectable, as they get lost in the noise of the myriad of random changes that are unique to each cell. A way to solve this conundrum would be to combine whole-cell patch clamping with single cell qPCR. Although very laborious, this combination of techniques would allow one to investigate the expression of a (limited) number of genes in single neurons. If this is combined with characterization of basic electrophysiological properties or even inducing plasticity it might even be possible to relate certain changes in gene expression to electrophysiological phenotypes. Preferably this would be done in an animal with a mosaic deletion of the *Ercc1* gene, as this would allow the side-by-side comparison of affected and unaffected neurons. This could be achieved by injecting a GFP and Cre expressing virus in the brain of the floxed *Ercc1* mouse mutant we used in chapter 2.

An interesting point made by Garinis et al. is that DNA damage stalling RNA polymerase II results in the reduction of the IGF-1 and GH receptors through an unknown mechanism in a cell autonomous fashion, even in post-mitotic neurons [2]. Hence, transcription blocking damage to any transcribed gene in a cell has a similar effect, apart from the consequences of blocking that particular gene. Downregulation of IGF-1 and GH receptors is also seen in normal aging [3-6]. Moreover, caloric restriction, which expands lifespan, reduces IGF-1 signaling [4, 7, 8]. Finally, reducing IGF-1 signaling genetically also expands lifespan [4, 8-10]. Reduced IGF-1 signaling results in a shift from growth to maintenance and stress resistance [4]. Taken together, these findings show that IGF-1 signaling is intimately involved in aging and suggest that downregulation is a protective mechanism [2, 4, 5]. Perhaps this attempt to slow down the aging process has negative side effects, which can explain some of the phenotypes we find in the *Ercc1^{Δ/Δ}* mice and normal aging. Further research is needed to clarify the role of reduced IGF-1 signaling in aging. I would suggest genetic manipulation of the IGF-1 receptor, if possible in a cell specific manner and investigating the consequences on cellular and systems function, i.e. hippocampal synaptic plasticity and hippocampus-dependent learning.

Further and more detailed characterization of the *Ercc1^{Δ/Δ}* mutant will teach us to what extent the aging phenotype is copied in this mutant. For example, whole cell recordings are needed to investigate whether the slow afterhyperpolarization is increased like it is normal aging. With pharmacological experiments it can be unveiled whether the contribution to LTP by L-type VDCC is increased. Our data show that in the hippocampus neurons are mostly affected by DNA damage while in the spinal cord astrocytes and neurons are equally affected. Using the floxed *Ercc1* mutant we can learn more about the relative contributions of different cell types to the aging phenotype at the cellular and the behavioral level. Finally, more elaborate behavioral studies can assist in understanding what systems are affected most by DNA damage.

7.2 Molecular mechanisms of learning and memory

The better one understands a process the better one can understand its failure. If we want to learn more about the effects of DNA damage and aging on hippocampal function we need to understand its underlying molecular mechanisms. Therefore, we investigated the molecular mechanisms of synaptic plasticity in the hippocampus.

In chapter 5 we present the first study on the role of β CaMKII in the hippocampus and show that the kinase function of β CaMKII is dispensable for normal function of the hippocampus. We propose a model in which β CaMKII targets the heteromeric CaMKII holoenzyme to the correct subcellular localization postsynaptically (see figure 1). This finding raises some new questions. The most immediate question is, why does the *Camkb*^{A303R} mutant not have a phenotype? As the current model of synaptic plasticity involves the release of the CaMKII holoenzyme from the actin skeleton and subsequent translocation to the PSD upon calmodulin binding, this is somewhat of a puzzle. Is this translocation not needed or is there another way in which the holoenzyme can be enabled to move to the PSD? Perhaps increased de- and repolymerization of actin during LTP allows the holoenzyme to translocate to the PSD as it is no longer bound when the F-actin is depolymerized. There is also the possibility that the translocation is not essential for LTP. More experiments are needed to clarify this unresolved question.

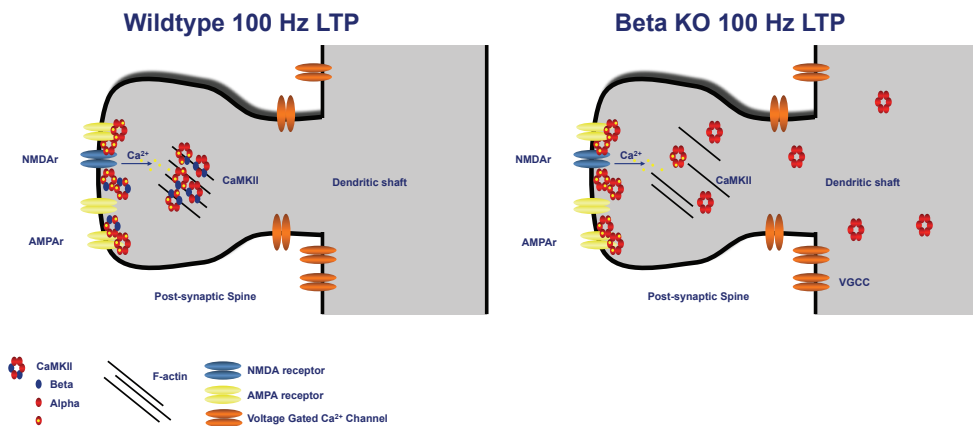


Figure 1. Model for α CaMKII localization in absence of β CaMKII.

In the wildtype spine (left panel) the CaMKII heteromeric holoenzyme is tethered to the actin skeleton through β CaMKII. This places the holoenzyme in the Ca^{2+} nanadomain of the NMDA receptor enabling proper activation during learning and 100 Hz LTP. In absence of β CaMKII in the *Camk2b*^{-/-} mutant (right panel) the distribution of α CaMKII holoenzymes is more dispersed and further away from the Ca^{2+} nanadomain of the NMDA receptor. This results in reduced activation of α CaMKII while the Ca^{2+} influx does not change. The location of the VGCCs explains the normal 200 Hz LTP in the *Camk2b*^{-/-} mutant. When these channels are activated, the not properly localized holoenzymes can still be activated. The *Camk2b*^{A303R} mutant (not shown) cannot be activated by Ca^{2+} /calmodulin but retains its F-actin binding thereby properly targeting the CaMKII holoenzyme to the NMDA receptor Ca^{2+} nanadomain.

During the phase of LTP called L-LTP, which is dependent on protein synthesis, the input specificity is hypothesized to come from a synaptic tag that is produced at the induction of LTP. This tag ‘catches’ the proteins necessary for plasticity that are synthesized elsewhere and transported by diffusion [11]. CaMKII has been shown to be necessary for setting the synaptic tag [12, 13] as is the actin network [14]. β CaMKII could control the access to the spine by crosslinking the actin skeleton in the spine neck, and releasing this when activated [15-17]. Hence, we propose that β CaMKII mediated regulation of access to the spine is the synaptic tag. With our two mutants this theory can be tested. L-LTP in the *Camk2b*^{-/-} mutant would be expected to be less input specific, as the spines are always accessible. In the *Camkb*^{A303R} mutant the spines are likely to be less accessible and L-LTP should be prevented or least of reduced magnitude.

β CaMKII is expressed in both inhibitory and excitatory neurons. Although our model does not incorporate the effects of the β CaMKII mutations in inhibitory cells, it is sufficient to explain our data. For the ultimate test of our model a floxed β CaMKII mutant is needed. This would allow us to restrict the deletion of the β CaMKII gene to the excitatory neurons.

When this floxed β CaMKII mutant becomes available, it would be very interesting to investigate the effects of knocking out *Camk2b* in the inhibitory neurons. As β CaMKII is the only CaMKII that is expressed in GABAergic neurons it would be expected that plasticity of afferent glutamatergic synapses is greatly disturbed. If this were the case, what would be the effect on the network and behavior? A floxed β CaMKII mutant would allow us to test this. Alternatively, the plasticity of these synapses could be tested with whole cell technique. However, this would not allow exploration of the effects on the circuit and behavioral level.

In chapter 6 we present the first *in vivo* study that investigates the presynaptic role of α CaMKII in LTP using genetic targeting. Our findings show that presynaptic α CaMKII is not necessary for LTP in the Schaffer-collateral (CA3-CA1) pathway. Furthermore, our results strongly suggest that CA3-CA3 LTP is completely independent of α CaMKII. This is unexpected as CA3-CA3 LTP shares many characteristics with Schaffer-collateral (CA3-CA1) LTP, such as dependence on NMDA receptor activation and a postsynaptic rise in Ca²⁺ [18-25]. Moreover, viral overexpression of α CaMKII that mimics autophosphorylation at T286 results in increased synaptic transmission [22]. The possibility exists that CA3-CA3 LTP is mediated by β CaMKII and not α CaMKII, although it is hard to imagine how this would work as the two isoforms are thought to

occur in heteromeric holoenzymes. Our recently created *Camk2b*^{-/-} mutant provides us with the opportunity to test this hypothesis.

The question remains why α CaMKII is so abundant in the CA3 region. Behavioral examination of CA3 specific α CaMKII knockout mice would clarify whether α CaMKII in the CA3 is needed for normal hippocampal function, as would be expected. Since short-term presynaptic plasticity is disturbed in absence of α CaMKII [26, 27] any behavioral phenotype would show that short-term plasticity is important on its own merits and not indirectly through an effect on LTP.

Perhaps in future, with increasing knowledge about the molecular mechanisms of both aging and learning and memory, these two fields will show enough overlap to help us preserve our cognitive abilities as we age.

References

1. Mitchell, J.R., J.H. Hoeijmakers, and L.J. Niedernhofer, *Divide and conquer: nucleotide excision repair battles cancer and ageing*. *Curr Opin Cell Biol*, 2003. **15**(2): p. 232-40.
2. Garinis, G.A., et al., *Persistent transcription-blocking DNA lesions trigger somatic growth attenuation associated with longevity*. *Nat Cell Biol*, 2009. **11**(5): p. 604-15.
3. van der Pluijm, I., et al., *Impaired genome maintenance suppresses the growth hormone--insulin-like growth factor 1 axis in mice with Cockayne syndrome*. *PLoS Biol*, 2007. **5**(1): p. e2.
4. Schumacher, B., et al., *Delayed and accelerated aging share common longevity assurance mechanisms*. *PLoS Genet*, 2008. **4**(8): p. e1000161.
5. Niedernhofer, L.J., et al., *A new progeroid syndrome reveals that genotoxic stress suppresses the somatotroph axis*. *Nature*, 2006. **444**(7122): p. 1038-43.
6. van de Ven, M., et al., *Adaptive stress response in segmental progeria resembles long-lived dwarfism and calorie restriction in mice*. *PLoS Genet*, 2006. **2**(12): p. e192.
7. Girard, N., et al., *Long-term calorie restriction protects rat pituitary growth hormone-releasing hormone binding sites from age-related alterations*. *Neuroendocrinology*, 1998. **68**(1): p. 21-9.
8. Holzenberger, M., L. Kappeler, and C. De Magalhaes Filho, *IGF-1 signaling and aging*. *Exp Gerontol*, 2004. **39**(11-12): p. 1761-4.
9. Bartke, A. and H. Brown-Borg, *Life extension in the dwarf mouse*. *Curr Top Dev Biol*, 2004. **63**: p. 189-225.
10. Clancy, D.J., et al., *Extension of life-span by loss of CHICO, a Drosophila insulin receptor substrate protein*. *Science*, 2001. **292**(5514): p. 104-6.
11. Frey, U. and R.G. Morris, *Synaptic tagging and long-term potentiation*. *Nature*, 1997. **385**(6616): p. 533-6.
12. Redondo, R.L., et al., *Synaptic tagging and capture: differential role of distinct calcium/calmodulin kinases in protein synthesis-dependent long-term potentiation*. *J Neurosci*, 2010. **30**(14): p. 4981-9.
13. Sajikumar, S., S. Navakkode, and J.U. Frey, *Identification of compartment- and process-specific molecules required for "synaptic tagging" during long-term potentiation and long-term depression in hippocampal CA1*. *J Neurosci*, 2007.

- 27(19): p. 5068-80.
14. Ramachandran, B. and J.U. Frey, *Interfering with the actin network and its effect on long-term potentiation and synaptic tagging in hippocampal CA1 neurons in slices in vitro*. J Neurosci, 2009. **29**(39): p. 12167-73.
 15. Okamoto, K., et al., *The role of CaMKII as an F-actin-bundling protein crucial for maintenance of dendritic spine structure*. Proc Natl Acad Sci U S A, 2007. **104**(15): p. 6418-23.
 16. Okamoto, K., et al., *Rapid and persistent modulation of actin dynamics regulates postsynaptic reorganization underlying bidirectional plasticity*. Nat Neurosci, 2004. **7**(10): p. 1104-12.
 17. Okamoto, K., M. Bosch, and Y. Hayashi, *The roles of CaMKII and F-actin in the structural plasticity of dendritic spines: a potential molecular identity of a synaptic tag?* Physiology (Bethesda), 2009. **24**: p. 357-66.
 18. Debanne, D., B.H. Gähwiler, and S.M. Thompson, *Heterogeneity of synaptic plasticity at unitary CA3-CA1 and CA3-CA3 connections in rat hippocampal slice cultures*. J Neurosci, 1999. **19**(24): p. 10664-71.
 19. Bains, J.S., J.M. Longacher, and K.J. Staley, *Reciprocal interactions between CA3 network activity and strength of recurrent collateral synapses*. Nat Neurosci, 1999. **2**(8): p. 720-6.
 20. Bradler, J.E. and G. Barrionuevo, *Heterosynaptic correlates of long-term potentiation induction in hippocampal CA3 neurons*. Neuroscience, 1990. **35**(2): p. 265-71.
 21. Debanne, D., B.H. Gähwiler, and S.M. Thompson, *Long-term synaptic plasticity between pairs of individual CA3 pyramidal cells in rat hippocampal slice cultures*. J Physiol, 1998. **507 (Pt 1)**: p. 237-47.
 22. Kakegawa, W., et al., *Input- and subunit-specific AMPA receptor trafficking underlying long-term potentiation at hippocampal CA3 synapses*. Eur J Neurosci, 2004. **20**(1): p. 101-10.
 23. Pavlidis, P., J. Montgomery, and D.V. Madison, *Presynaptic protein kinase activity supports long-term potentiation at synapses between individual hippocampal neurons*. J Neurosci, 2000. **20**(12): p. 4497-505.
 24. Smith, K.L. and J.W. Swann, *Long-term depression of perforant path excitatory postsynaptic potentials following synchronous network bursting in area CA3 of immature hippocampus*. Neuroscience, 1999. **89**(3): p. 625-30.
 25. Zalutsky, R.A. and R.A. Nicoll, *Comparison of two forms of long-term*

- potentiation in single hippocampal neurons*. Science, 1990. **248**(4963): p. 1619-24.
26. Hojjati, M.R., et al., *Kinase activity is not required for alphaCaMKII-dependent presynaptic plasticity at CA3-CA1 synapses*. Nat Neurosci, 2007. **10**(9): p. 1125-7.
27. Hinds, H.L., et al., *Essential function of alpha-calcium/calmodulin-dependent protein kinase II in neurotransmitter release at a glutamatergic central synapse*. Proc Natl Acad Sci U S A, 2003. **100**(7): p. 4275-80.

Addendum

Summary
Samenvatting
Publications
Curriculum vitae
Portfolio
Dankwoord

Summary

The overall aim of the studies described in this thesis is to clarify the role of DNA damage in aging of the nervous system. To this end we analyzed mouse mutants in which we used targeted genetic mutations of the excision repair cross-complementing group 1 (*Ercc1*) gene. As the ERCC1 protein is involved in multiple DNA repair pathways our hypomorph mutations result in more unrepaired DNA damage. We studied the hippocampal, auditory, visual and neuromuscular systems in these mice. Hippocampus-dependent learning and memory has received special attention, as its age-related decline is hard to treat and poses a great threat to personal well-being and society as a whole. To understand how aging affects learning and memory, it is essential to understand the molecular mechanisms of these cognitive processes. Therefore, two studies were directed at the function of CaMKII, a molecule with a pivotal role in learning and memory. Specifically, we investigated for the first time the role of β CaMKII in hippocampus-dependent synaptic plasticity, learning and memory. Furthermore we studied the little explored role of presynaptic α CaMKII in LTP.

In chapter 2 we investigated the effect of DNA damage on the hippocampus using a global hypomorph mutant and a neuron specific knockout of the *Ercc1* gene. Using a global mutant we found that DNA damage accumulation causes a progressive increase in pathology indicating stressed and dying neurons. Simultaneously, there is an age-related reduction of synaptic plasticity, the putative cellular substrate for learning. In addition, we show that the most sensitive cells to DNA damage in the brain are neurons as they are most affected while the hypomorph *Ercc1* mutation is present in all cells. Consistently, when we limit the mutation of *Ercc1* to excitatory neurons in the forebrain we see a similar phenotype. Moreover, we show that DNA damage exclusively in neurons causes impaired learning. Taken together, this strongly suggests that aging of the brain is the result of neuronal DNA damage.

In chapter 3 we describe the effect of unrepaired DNA damage in the global *Ercc1*^{Δ/Δ} mutant mice on hearing and vision. The *Ercc1*^{Δ/Δ} mice show progressively increasing hearing thresholds and reducing otoacoustic emissions. These results suggest that functional loss of outer hair cells in the cochlea is at the basis of the hearing loss. This phenotype is very similar to human age-related hearing loss or presbycusis. Furthermore, the *Ercc1*^{Δ/Δ} mice show progressive loss of contrast sensitivity that is accompanied by thinning of the outer nuclear layer of the eyeball, which suggests loss of photoreceptors. Although, loss of photoreceptors is common to normal aging in humans, rats and mice it

is not clear how relevant this phenomenon is to age-related loss of vision. This suggests that DNA damage could play a causative role in presbycusis and age-related loss of vision.

In chapter 4 we show that, contrary to the hippocampus, the spinal cord of *Ercc1^{Δ/-}* mice suffers a significant loss of neurons with increasing age. Moreover, this loss of motoneurons is reflected in disturbed innervation of muscle fibers. Simultaneously an increased number of cells show clear signs of stress. Thus, the reduced motor function is most likely the result of both loss of neurons and reduced functioning of neurons.

In chapter 5 we present the first study on the role of β CaMKII in the hippocampus. By using two mutants, one where there is no β CaMKII (*Camk2b^{-/-}*) and one where β CaMKII cannot be activated (*Camk2b^{A303R}*), we show that the kinase function of β CaMKII is dispensable for normal function of the hippocampus. We propose a model in which β CaMKII targets the heteromeric CaMKII holoenzyme to the correct subcellular localization postsynaptically through its interaction with F-actin. In chapter 6 we present the first *in vivo* study that investigates the presynaptic role of α CaMKII in LTP using genetic targeting. Our findings show that presynaptic α CaMKII is not necessary for LTP in the Schaffer-collateral (CA3-CA1) pathway. Furthermore, our results strongly suggest that CA3-CA3 LTP is completely independent of α CaMKII.

Samenvatting

Het doel van dit proefschrift is het verduidelijken van de rol van DNA schade in veroudering van het zenuwstelsel. Daartoe hebben wij mutanten geanalyseerd waarin het excision repair cross-complementing group 1 (*Ercc1*) gen gemuteerd is. Aangezien het ERCC1 eiwit deel uitmaakt van meerdere DNA reparatie mechanismen, resulteren de (hypomorphe) mutaties in een toename van niet gerepareerde DNA schade. Wij hebben het functioneren van de hippocampus en de auditieve, visuele en neuromusculaire systemen onderzocht in deze muizen. Het leervermogen en geheugen dat afhankelijk is van de hippocampus heeft extra aandacht gekregen omdat effecten van veroudering daarop een ernstige bedreiging vormen voor het welzijn, zowel voor het individu als voor de gehele samenleving.

Om de effecten van veroudering op leren en geheugen te interpreteren, is het essentieel de moleculaire mechanismen van deze cognitieve processen te begrijpen. Daarom hebben wij ook twee studies gedaan naar de functie van CaMKII, een molecuul met een centrale rol in leren en geheugen. Wij hebben voor het eerst de *in vivo* rol van β CaMKII in de hippocampus onderzocht. Verder hebben wij de tot nog toe weinig onderzochte functie van presynaptische α CaMKII in lange-termijn potentiatie, de algemeen veronderstelde cellulaire basis voor leren, onderzocht.

In hoofdstuk 2 hebben wij het effect van DNA schade op het functioneren van de hippocampus onderzocht met behulp van twee muizen met een mutatie in het *Ercc1* gen. Een muis heeft een mutatie met een verminderde eiwitfunctie in het gehele lichaam tot gevolg, de *Ercc1^{Δ/-}* muis. In de andere muis ontbreekt het gen, en dus het eiwit volledig, maar alleen in bepaalde neuronen. Met de *Ercc1^{Δ/-}* muis hebben wij aangetoond dat DNA schade accumulatie progressieve toename van pathologische kenmerken in de hersenen tot gevolg heeft, die indicatief zijn voor gestreste en stervende neuronen. Tegelijkertijd is er een leeftijdsgelateerde afname van synaptische plasticiteit. Verder laten wij zien dat neuronen in de hersenen het meest gevoelig zijn voor DNA schade, omdat deze het meest zijn aangedaan terwijl de mutatie in alle cellen aanwezig is. Overeenkomstig hiermee treedt er een zelfde fenotype op wanneer wij de mutatie van het *Ercc1* gen beperken tot de exciterende neuronen van het voorbrein. Bovendien tonen wij aan dat DNA schade uitsluitend in neuronen voldoende is om een verminderd leervermogen te veroorzaken. Tezamen is dit een sterke aanwijzing dat neuronale DNA schade een belangrijke oorzaak zou kunnen zijn van veroudering van het brein.

In hoofdstuk 3 beschrijven wij het effect van niet gerepareerde DNA schade

op het gehoor en het gezichtsvermogen in de *Ercc1^{Δ/-}* muis, waarin de functie van het ERCC1 eiwit in het gehele lichaam verminderd is. De gehoordrempels van de *Ercc1^{Δ/-}* muis nemen snel toe. Dit gaat gepaard met een afname van de otoacoustische emissies. Samengenomen suggereert dit gehoorverlies veroorzaakt door het verlies van haarcellen in de cochlea. Dit fenotype is zeer vergelijkbaar met ouderdomsslechthorendheid, ofwel presbycusis, in mensen. Bovendien laat de *Ercc1^{Δ/-}* muis een progressief verlies van contrastgevoeligheid zien, dat gepaard gaat met het dunner worden van de retina door verlies van cellen, wat het verlies van fotoreceptoren suggereert. Hoewel het verlies van fotoreceptoren algemeen wordt waargenomen bij normale veroudering in mensen, ratten en muizen is niet duidelijk hoe relevant dit fenomeen is voor leeftijdsgerelateerd verlies van het gezichtsvermogen. Samengenomen suggereert dit dat DNA schade een rol kan spelen in de oorzaak van presbycusis en ouderdomsgerelateerd verlies van gezichtsvermogen.

In hoofdstuk 4 laten wij zien dat, in tegenstelling tot de hippocampus, in het ruggenmerg van *Ercc1^{Δ/-}* muizen er een aanzienlijk verlies van neuronen met toenemende leeftijd optreedt. Dit verlies van motorneuronen heeft een verstoorde innervatie van de spiervezels tot gevolg. De waargenomen verminderde motoriek is zeer waarschijnlijk het gevolg van zowel het verlies van neuronen als een verminderde werking van neuronen.

In hoofdstuk 5 beschrijven wij onze studie waarin voor het eerst *in vivo* de functie van β CaMKII in de hippocampus is onderzocht. Hiervoor gebruiken wij twee mutanten. Een waarin er geen β CaMKII is (*Camk2b^{-/-}*) en een waarin β CaMKII niet kan worden geactiveerd (*Camk2b^{A303R}*). Wij tonen aan dat de kinase functie van β CaMKII overbodig is voor het normaal functioneren van de hippocampus. Wij stellen een model voor waarin β CaMKII de heteromere CaMKII holoenzymen postsynaptisch op de juiste subcellulaire locatie houdt door middel van zijn interactie met het actine skelet van de cel.

In hoofdstuk 6 presenteren wij onze studie waarin voor het eerst *in vivo* de presynaptische rol van α CaMKII in LTP is onderzocht. Onze bevindingen tonen aan dat presynaptisch α CaMKII niet noodzakelijk is voor het LTP in de Schaffer-collateral zenuwbaan (CA3-CA1). Verder suggereren onze resultaten sterk dat CA3-CA3 LTP volledig onafhankelijk van α CaMKII is.

List of Publications

Spred1 is required for synaptic plasticity and hippocampus-dependent learning

Denayer E, Ahmed T, Brems H, Van Woerden G, **Borgesius NZ**, Callaerts-Vegh Z, Yoshimura A, Hartmann D, Elgersma Y, D'Hooge R, Legius E, Balschun D.
J Neurosci. 2008 Dec 31;28(53):14443-9.

Age-related motor neuron degeneration in DNA repair-deficient *Ercc1* mice

N. Zuiderveen Borgesius*, I. van der Pluijm*, M. de Waard*, L. Comley, E. Haasdijk, Y. Rijksen, Y. Ridwan, G. Zondag, J. Hoeijmakers, Y. Elgersma, T. Gillingwater, D. Jaarsma (*these authors contributed equally)
Acta Neuropathol. 2010 Oct;120(4):461-75. Epub 2010 Jul 4.

β CaMKII plays a non-enzymatic role in hippocampal synaptic plasticity and learning by targeting α CaMKII to synapses

Nils Z. Borgesius, Geeske M. van Woerden, Gabrielle H. S. Buitendijk, Nanda Keijzer, Casper C. Hoogenraad, Dick Jaarsma, Ype Elgersma
Under review

Accelerated age-related cognitive decline and neurodegeneration, caused by deficient DNA repair in *Ercc1*^{Δ/-} mutant mice

Nils Z. Borgesius, Monique C. de Waard, Ingrid van der Pluijm, Azar Omrani, Gerben C. M. Zondag, Gijsbertus T. J. van der Horst, David. W. Melton, Jan H. J. Hoeijmakers, Dick Jaarsma, Ype Elgersma
submitted

Functional requirement of hippocampal CA3 α CaMKII in long-term potentiation

Nils Z. Borgesius*, Mohammad R. Hojjati*, Geeske M. van Woerden, Gabrielle H. S. Buitendijk, Alcino J. Silva, Ype Elgersma (*these authors contributed equally)
In preparation

Age-related loss of hearing and vision in the DNA-repair deficient *Ercc1*^{Δ/-} mouse

Nils Z. Borgesius*, Marcella Spoor*, Bart van Alphen*, Andries P. Nagtegaal*, Yanto Ridwan, Ingrid van der Pluijm, Jan H. J. Hoeijmakers, Maarten A. Frens, Gerard Borst, Ype Elgersma (*these authors contributed equally)
In preparation

Curriculum Vitae

Nils Zuiderveen Borgesius

4-6-1976

Education:

1999 – 2005: Doctorate in Neurobiology, University of Amsterdam, Amsterdam, The Netherlands

1998 – 1999: β - γ propedeeuse: Interdisciplinary Freshman's year aimed at providing insight in into the commonalities and differences of science and humanities.

Working experience:

Year/position: June 2005 – present, PhD student

Department: Neuroscience, Erasmus Medical Centre, Rotterdam, The Netherlands

Supervisor: Prof. Dr. Y. Elgersma

Year/position: September 2004 – March 2005, graduation research Neurobiology

Department: Group Dr. E. Hol, Netherlands Institute for Neuroscience, Amsterdam, The Netherlands

Supervisor: Dr. E. Hol

Year/position: February 2004 – August 2004, graduation research Neurobiology

Department: Integrative Neurophysiology, VU University, Amsterdam, The Netherlands

Supervisor: Prof. Dr. N. Burnashev

PhD Portfolio

Name PhD student: C. H. Zuiderveen Borgesius Erasmus MC Department: Neuroscience Research School: Research School Neurosciences Amsterdam Rotterdam (ONWAR)	PhD period: 2005-2010 Promotor(s): Prof. dr. Ype Elgersma Supervisor: Prof. dr. Ype Elgersma
General courses - Laboratory animal science	2006
(Inter)national conferences - 7 th FENS Forum of European Neuroscience, Amsterdam, The Netherlands (poster) - 40 th Society for Neuroscience annual meeting, Chicago, USA (poster) - Federatie Innovatief Geneesmiddelen Onderzoek Nederland (FIGON), Lunteren, The Netherlands (poster) - IYSM, Heemskerk, The Netherlands (poster) - 39 th Society for Neuroscience annual meeting, Washington DC, USA (poster) - Federatie Innovatief Geneesmiddelen Onderzoek Nederland (FIGON), Lunteren, The Netherlands (oral presentation) - 15 th annual ONWAR PhD meeting, Zeist, The Netherlands (poster) - 7 th Dutch ENP meeting, Doorwerth, The Netherlands (poster) - 14 th annual ONWAR PhD meeting, Zeist, The Netherlands (oral presentation) - 6 th Dutch ENP meeting, Doorwerth, The Netherlands (poster) - 5 th Dutch ENP meeting, Doorwerth, The Netherlands	2010 2009 2009 2009 2008 2008 2008 2008 2008 2007 2006
Other - Organising committee 14 th annual ONWAR PhD meeting	2008
Teaching - Master of Neuroscience - Neuroscience summerschool - Workshop field recording measurements	2006-2009 2006-2009 2008-2010

